UNDERSTANDING OF COUPLED PHYSICOCHEMICAL AND MINERALOGICAL MECHANISMS CONTROLLING SOIL CARBON STORAGE AND PRESERVATION

by

PAVITHRA SAJEEWANI PITUMPE ARACHCHIGE

B.S., University of Peradeniya, Sri Lanka, 2009
M.S., Post Graduate Institute of Agriculture, University of Peradeniya, Sri Lanka 2011

AN ABSTRACT OF A DISSERTATION

submitted in partial fulfillment of the requirements for the degree

DOCTOR OF PHILOSOPHY

Department of Agronomy
College of Agriculture

KANSAS STATE UNIVERSITY
Manhattan, Kansas

2016

Abstract

Soil carbon (C) sequestration has been recognized as one of the most effective potential mitigation options for climate change. Underlying mechanisms of soil C sequestration/preservation is poorly understood, even after decades of soil C research. The main research objectives of this dissertation were three-fold: (1) enhancing our understanding in mineralogical and physicochemical mechanisms of soil C sequestration in microaggregates, (2) understanding the chemistry of organic C sequestered in soil aggregates, and (3) to determine the resilience of C to different temperature-moisture regimes and physical disturbance in a six-month incubation. An integrated approach was used in obtaining a better picture on mechanisms of C preservation. Two long-term agroecosystems located at the North Agronomy Farm, Manhattan, KS (Mollisols) and the Center of Experimentation and Research Fundacep in Cruz Alta-RS, Brazil (Oxisols) were used. Main plots of both systems were till and no-till. Mollisols consisted of three fertilizer treatments; control, manure/compost and urea. Oxisols had three different crop rotations; simple, intermediate, and complex. Submicron level information gathered by spectromicroscopy approaches, identified the direct preservation of OC structures with the original morphology; suggesting that the preservation of OC is a primary mechanism of C sequestration in these soils. Physical protection and organo-mineral associations seemed to also be involved in OC preservation. Manure/compost addition and no-till favored labile C preservation in aggregates of Mollisols. Significant associations observed between reactive minerals and C pools in Mollisols indicated the significance of organo-mineral associations in OC preservation. Large microaggregates exerted strong C preservation through physical protection and organo-mineral associations. Unlike in Mollisols, Oxisols showed a poor correlation between reactive mineral fraction and organic C which indicated the significance of

physical protection over organo-mineral associations. Resilience of sequestred C was significantly affected by temperature across both temperate and tropical soil ecosystems, directly and indirectly. High temperature influenced soil acidity and reactive minerals, ultimately affecting organo-mineral associations. Macromolecular propeties of humic acid fraction showed changes after six months. Overall, direct and indirect evidence from this study suggested that the preservation of SOC is an ecosystem property supporting the newly proposed theories in soil C dynamics.

UNDERSTANDING OF COUPLED PHYSICOCHEMICAL AND MINERALOGICAL MECHANISMS CONTROLLING SOIL CARBON STORAGE AND PRESERVATION

by

PAVITHRA SAJEEWANI PITUMPE ARACHCHIGE

B.S., University of Peradeniya, Sri Lanka, 2009
M.S., Post Graduate Institute of Agriculture, University of Peradeniya, Sri Lanka 2011

A DISSERTATION

submitted in partial fulfillment of the requirements for the degree

DOCTOR OF PHILOSOPHY

Department of Agronomy
College of Agriculture

KANSAS STATE UNIVERSITY
Manhattan, Kansas

2016

Approved by:

Major Professor
Ganga M. Hettiarachchi

Copyright

Abstract

Soil carbon (C) sequestration has been recognized as one of the most effective potential mitigation options for climate change. Underlying mechanisms of soil C sequestration/preservation is poorly understood, even after decades of soil C research. The main research objectives of this dissertation were three-fold: (1) enhancing our understanding in mineralogical and physicochemical mechanisms of soil C sequestration in microaggregates, (2) understanding the chemistry of organic C sequestered in soil aggregates, and (3) to determine the resilience of C to different temperature-moisture regimes and physical disturbance in a six-month incubation. An integrated approach was used in obtaining a better picture on mechanisms of C preservation. Two long-term agroecosystems located at the North Agronomy Farm, Manhattan, KS (Mollisols) and the Center of Experimentation and Research Fundacep in Cruz Alta-RS, Brazil (Oxisols) were used. Main plots of both systems were till and no-till. Mollisols consisted of three fertilizer treatments; control, manure/compost and urea. Oxisols had three different crop rotations; simple, intermediate, and complex. Submicron level information gathered by spectromicroscopy approaches, identified the direct preservation of OC structures with the original morphology; suggesting that the preservation of OC is a primary mechanism of C sequestration in these soils. Physical protection and organo-mineral associations seemed to also be involved in OC preservation. Manure/compost addition and no-till favored labile C preservation in aggregates of Mollisols. Significant associations observed between reactive minerals and C pools in Mollisols indicated the significance of organo-mineral associations in OC preservation. Large microaggregates exerted strong C preservation through physical protection and organo-mineral associations. Unlike in Mollisols, Oxisols showed a poor correlation between reactive mineral fraction and organic C which indicated the significance of

physical protection over organo-mineral associations. Resilience of sequestred C was significantly affected by temperature across both temperate and tropical soil ecosystems, directly and indirectly. High temperature influenced soil acidity and reactive minerals, ultimately affecting organo-mineral associations. Macromolecular propeties of humic acid fraction showed changes after six months. Overall, direct and indirect evidence from this study suggested that the preservation of SOC is an ecosystem property supporting the newly proposed theories in soil C dynamics.

Table of Contents

List of Figures

List of Tables

Acknowledgements

First of all, I would like to express my utmost gratitude to my major advisor Dr. Ganga Hettiarachchi for her excellent guidance, encouragement, patience, care, and immense support throughout my Ph.D. program. She made me a better presenter, a better scientist, and a confident individual. I consider myself so fortunate to be a member of "Hettiarachchi Soil and Environmental Chemistry Lab". On top of that, I'm grateful for the freedom and the friendly environment we had within our research group.

I thank my Ph.D. committee; Dr. Charles Rice, Dr. Michel Ransom, Dr. Stacy Hutchinson and Dr. DeAnn Presley for their valuable inputs and time invested for my research. Also, I am grateful to my outside chair Dr. Mark Hollingsworth.

I wish to extend my deepest gratitude to Dr. Leila Maurmann from the Dept. of Chemistry for her continuous support in analyzing samples and helping with interpretations within last few years. A special thank goes to Dr. Gerard Kluitenberg, Dr. Vara Prasad, and Dr. Rajashekar for assisting with the incubation study. Also, I would like to thank Dr. Chithra Karunakaran, Dr. James Dynes, and Dr. Tom Regier at Canadian Light Source, Saskatoon, Canada. I also wish to extend my gratitude to Dr. David Kilocoyne at Advanced Light Source, Berkeley, CA, USA. I big thank goes to Dr. Yared Aseefa and Nadeesha Mawella for statistical help.

I take this opportunity to thank past and present members of Hettiarachchi Soil and Environmental Chemistry Lab; special thank goes to Dr. Chammi Attanayake, Dorothy Menefee, Dr. Ranju Karna, Dr. Buddhika Galkaduwa, Joy Pierzynski, Dr. Phillip Defoe, and Jay Weeks. Thanks are also extended to past and present members of the Soil Microbiology Lab for their helping hands when ever needed. I greatly appreciate Edwin Akeley and Stuart Watts for

assisting with carbon analysis. I highly acknowledge Oshadhi Athukorala and Caleb Graveson for their immense support with the research. Also, I would like to thank Kasun Dissanayake and Pushpika Munaweera.

My heartiest gratitude is extended to Dr. Srimathie Indraratne and all the professors at the University of Peradeniya, Sri Lanka, for directing me towards higher studies at Kansas State University. Big thanks go to a wonderful group of friends who supported during my studies. I would like to thank National Science Foundation, Kansas State Research and Extension, Department of Agronomy and Provost for research office for providing funds during the Ph.D. program.

Finally, I am very grateful to my loving mother, father, and brother for their continuous encouragement, love, and support. They have sacrificed a lot to make me the person who I am today. I would like to express my appreciation to my mother-in-law and father-in-law for their support. Also, I would like to thank my husband, Pabodha Galgamuwa for being my best friend and standing by me throughout. Lastly, I would like to thank my little angel Methuli, for always cheering me up.

Dedication

Dedicated to my wonderful family…

Chapter 1 - Introduction

Climate change is well-known as one of the grand challenges in the 21st century. Atmospheric and oceanic warming, changes in snow/ice cover, and rising sea levels are the key observations related to climate change (IPCC, 2014). Carbon dioxide (CO_2), methane (CH_4), and nitrous oxide (N_2O) are the key anthropogenic greenhouse gasses (GHGs) which contribute to climate change. The atmospheric concentration of CO_2 is growing at an alarming rate over decades and the current concentration is around 404 ppm as of July 2016, which was reported by the Mauna Loa Observatory in Hawaii (Tans, 2016). There are numerous mitigation routes being proposed to combat increasing atmospheric CO_2. Soils and vegetation were identified by the Intergovernmental Panel on Climate Change (IPCC) with a high mitigation potential and were categorized under the Agriculture, Forestry and Other Land Use (AFOLU) sector (Smith et al., 2014). For the first time, the agriculture sector was nominated as a key segment at the United Nations Climate Change Conference in 2015 (Conference of the Parties/COP21). The goal was set to augment worlds soil organic C (SOC) pool at an annual rate of 0.4% to a depth of 40 cm (16 inches). Management strategies that were brought forward in achieving the set goal were conservation agriculture, mulching, cover cropping, the addition of biochar, and landscape restoration (Lal, 2016). Soil can behave as a sink of atmospheric CO_2 either by reducing heterotrophic soil respiration or improving C addition (Paustian et al., 2000; Lutzov et al., 2006). The potential of global cropping lands in acting as a sink was projected as 88 Gt of C on 1,400 million hectares at a rate of 62 t ha^{-1} (Lal, 2016).

Soil C preservation is attributed to three major mechanisms that are identified as biochemical recalcitrance, chemical stabilization, and physical protection (Sollins et al., 1996). The current understanding is that the persistence of SOC is not only affected by the inherent

properties of SOC; but the surrounding soil environment (Schmidt et al., 2011; Lehmann and Kleber, 2015). The significance of biological and physicochemical mechanisms varies depending on the properties of the agroecosystems. Sequestered C pools are vulnerable to changes in climate which can further increase atmospheric CO_2. Davidson and Janssens (2006) indicated the susceptibility of SOC to any change in temperature/precipitation pattern.

Understanding the potentials of SOC sequestration/preservation with respect to different agricultural management practices is vital. Also, the resilience of sequestered C with changing climate and anthropogenic influence should be studied. Research had been conducted globally on soil C sequestration and storage over decades. Yet, the underlying C preservation mechanisms are not fully revealed. Therefore, this research was designed with the intention of exploring hidden secrets to fill the existing knowledge gap in soil C research and to determine the resilience of SOC as affected by climate and anthropogenic activities.

Studies in this dissertation were based on two contrasting long-term temperate and tropical agroecosystems that were under contrasting management practices. An integrated approach, including traditional and new generation cutting-edge techniques, was followed to overcome the challenges associated with the inherent complexity of SOC. Further, the preservation of *in situ* conditions of soil was taken into the consideration to elucidate the underlying mechanisms with a certainty. Broad objectives of this dissertation research were three-fold.

1) ***Understanding of underlying mineralogical and physicochemical mechanisms of soil C preservation in microaggregates using scanning transmission X-ray microscopy coupled with near edge X-ray absorption fine structure spectroscopy (STXM-NEXAFS) (Chapters 03-Tropical Agroecosystem and 04-Temperate Agroecosystem)***

Microaggregates from both agroecosystems were used for this experiment. Two-fold specific research goals were aimed to recognize soil C preservation mechanisms in intact soil microaggregate thin sections. Carbon and relevant elemental distributions (calcium, nitrogen, iron, aluminum, and silicon) were analyzed to study submicron scale organo-mineral associations and interactions; thus providing insight into the complexity of the underlying mechanisms of SOC preservation. The second objective was to combine STXM-NEXAFS data with relevant bulk chemical analysis to support the elucidations and outspread the results beyond.

2) Understanding the chemistry of OC preserved in soil aggregates (chapter 05)

This study was conducted for both agroecosystems, however, the tropical agroecosystem study is not included in the dissertation. Specific goals of this research were to follow an integrative approach (new generation and traditional techniques) to understand the effect of long-term agricultural management strategies on SOC chemistry and mechanisms of SOC preservation in four different aggregate size fractions. Moreover, organo-mineral associations were assessed.

3) Determining the contribution of mineralogical/physicochemical mechanisms on C preservation and the resilience of sequestered C to different temperature-moisture regimes and physical disturbance (chapter 06)

For this six-month long incubation study, two soils (two different management practices) from each agroecosystem were selected based on the highest C input to the system. The specific objectives were to determine soil heterotrophic respiration rates subjected to different environmental/anthropogenic scenarios (temperature, moisture, and physical disturbance) and to assess the temporal dynamics of SOC. Moreover, changes in the chemistry of humic acid (HA),

pH, and the amorphous iron were examined. Microbial community shifts and adaptations as a response to changing temperature-moisture regimes and physical disturbance were assessed as a complementary study (Menefee, 2016).

Organization of the dissertation:

Chapter 02: *Literature review*

Chapter 03: *Preservation of Organic Carbon in Oxisol Soil Microaggregates: Insight from STXM-NEXAFS Spectroscopy*

Chapter 04: *Exploring Secrets Behind Carbon Preservation in Soil Microaggregates from a Temperate Ecosystem*

Chapter 05: *Assessing Soil Carbon Preservation in a Long-term Temperate Agroecosystem: An Integrated Approach*

Chapter 06: *Evaluation of Resilience of Sequestered Soil Organic Carbon to Environmental and Anthropogenic Influences*

Chapter 07: *Summary and Recommendations*

References

Davidson, E.A. and I.A. Janssens. 2006. Temperature sensitivity of soil carbon decomposition and feedbacks to climate change. Nature. 440:165-173.

Intergovernmental Panel on Climate Change (IPCC). 2014. Climate change 2013: The physical science basis: Working group I contribution to the fifth assessment report of the intergovernmental panel on climate change. Cambridge University Press.

Lal, R. 2016. Beyond COP 21: Potential and challenges of the "4 per thousand" initiative. J. Soil Water Conserv. 71:20A-25A.

Lehmann, J. and M. Kleber. 2015. The contentious nature of soil organic matter. Nature. 528:60-68.

Lützow, M.v., I. Kögel-Knabner, K. Ekschmitt, E. Matzner, G. Guggenberger, B. Marschner and H. Flessa. 2006. Stabilization of organic matter in temperate soils: Mechanisms and their relevance under different soil conditions–a review. Eur. J. Soil Sci. 57:426-445.

Menefee, D. 2016. Anthropogenic Influences on Soil Microbial Properties. MS diss. Kansas State University, Manhattan.

Paustian, K., J. Six, E. Elliott and H. Hunt. 2000. Management options for reducing CO2 emissions from agricultural soils. Biogeochemistry. 48:147-163.

Schmidt, M.W., M.S. Torn, S. Abiven, T. Dittmar, G. Guggenberger, I.A. Janssens, M. Kleber, I. Kögel-Knabner, J. Lehmann and D.A. Manning. 2011. Persistence of soil organic matter as an ecosystem property. Nature. 478:49-56.

Smith, P., H. Clark, H. Dong, E. Elsiddig, H. Haberl, R. Harper, J. House, M. Jafari, O. Masera and C. Mbow. 2014. Agriculture, forestry and other land use (AFOLU).

Sollins, P., P. Homann and B.A. Caldwell. 1996. Stabilization and destabilization of soil organic matter: Mechanisms and controls. Geoderma. 74:65-105.

Tans, P. 2016. NOAA/ESRL (http://www.esrl.noaa.gov/gmd/ccgg/trends/), earth system research laboratory. Global Monitoring Division. (accessed August 11, 2016).

Chapter 2 - Review of Literature

Climate Change Overview

Climate change is identified as one of the global pressing calamities in the 21st century. It can be defined as an identifiable alteration of the climate which lasts for prolonged time periods by deviating the mean or its properties such as frequency, length, trend, and magnitude (Cubasch et al., 2013). In climate systems, significant alterations that have gained attentions include warming the atmosphere and oceans, changes in snow/ice cover and rising sea levels (IPCC, 2014). There are contradictory arguments on the existence of climate change. Due to restrictions in research methods and observational data, the real reasons for climate change are still not fully revealed (Mao et al., 2015). A plethora of research is being conducted on various aspects of climate change in solving hidden mysteries. At a regional scale, changes in atmosphere and ocean circulations seem to be the major factor that triggers climate change (Mao et al., 2015).

In 1827, Jean-Baptiste Joseph Fourier, a French mathematician first brought forward the idea of the "greenhouse effect", which is the warming of the earth surface and lower atmosphere. This occurs as a result of the presence of radiatively active gases, also known as greenhouse gases (GHGs). Earth's major GHGs are water vapor (gaseous H_2O), carbon dioxide (CO_2), nitrous oxide (N_2O), methane (CH_4), and ozone (O_3). Non-greenhouse effects also play a role in climate change scenario which is mainly related to the Milankovitch variation and albedo properties of ice caps (Cowie, 2012). Throughout the era of 1880 to 2012, the increase in temperature was 0.85 ºC when the global land and ocean surface temperature data were considered (IPCC, 2014). Since the mid-20th century, the principal cause of the observed warming is recognized as anthropogenic activities (IPCC, 2014) that have enhanced the earth's radiative properties. The atmospheric concentrations of CO_2, N_2O, and CH_4 demonstrated a

significant increasing trend since the pre-industrial era (IPCC, 2014) with a capacity of enhancing earth's radiative properties. Fossil fuel usage (CO_2), cement industry (CO_2), deforestation (CO_2 and N_2O), biomass burning (CO_2, CO, CH_4 and N_2O), plowing (CO_2), fertilizer use (N_2O), manure application (CH_4 and N_2O), and drainage (CO_2) are examples of anthropogenic activities which introduce GHGs. In the context of soil inorganic C (SIC) dynamics, irrigation that brings carbonates to the surface and fertilizer additions/liming which form caliche, can be listed (Lal, 2009).

In 1992, at the Earth Summit held in Rio de Janeiro, United Nations Framework Convention on Climate Change (UNFCCC) concentrated on scientific evidence on dangers of GHGs (Sands, 1992). In 1997, at the Conference of the Parties (COP3) held in Kyoto, Japan, the "Kyoto Protocol" was accepted with the intention of reducing GHG emission from developed countries (Wigley, 1998). The key message at COP15 held in Copenhagen, Denmark in 2009, was to reduce GHG emission to hold the global average temperature below 2 ºC above the pre-industrial level. Joshi et al. (2011) stated that high GHG emissions might cause the global average temperature to be increased by 2 ºC by 2060 whereas, at low emission scenarios, the threshold could be delayed by several decades. The COP21 held in Paris in December 2015, identified agriculture as a significant component for the first time in the history. A proposal called "4 per thousand" was brought forward which targets to enhance soil organic carbon (SOC) content of world soils to a depth of 40 cm (16 inches) at a rate of 0.4% per year. Strategies such as conservation agriculture, mulching, cover cropping, the addition of biochar, and landscape restoration were stated in the proposal (Lal, 2015).

Global carbon cycle

Carbon is one of the vital elements associated with life. In the global C cycle, two domains can be identified as slow and fast. Fast domain behaves with massive exchange fluxes and rapid turnovers which consist of C pools in the atmosphere, oceans, sediments, vegetation, soils, and freshwaters. Slow domains represent sinks such as rocks and sediments with turnover times greater than 10,000 years (Ciais et al., 2013).

Atmospheric C

Major C bearing gas in the atmosphere is CO_2. Its concentration is being increased at an alarming rate over decades, and the current concentration is about 406 ppm as of June 2015, measured at the Mauna Loa Laboratory, Hawaii (Tans et al., 2016). The atmospheric masses of CO_2, CH_4, and CO are approximately around 828, 3.7 and 0.2 Pg C, respectively (Ciais et al., 2013). Through photosynthetic reactions, CO_2 is consumed and fixed into plant biomass. Consecutively, through reactions of respiration and ecosystem functions (i.e., natural fires), C is emitted back to the atmosphere which leads in an increment of the atmospheric concentrations.

Oceanic C

Atmospheric CO_2 interacts with the ocean. Main C pools in the oceanic ecosystem are dissolved inorganic C, carbonic acid, bicarbonate, carbonate, dissolved organic C, and marine biota. Carbon pool associated with phytoplankton and microbial community (3 Pg) turns over rapidly within days to few weeks (Ciais et al., 2013). Carbon circulates in the oceanic ecosystems via three pathways such as the solubility pump in the means of CO_2 dissolution, biological pump and marine carbonate pump (Ciais et al., 2013).

Terrestrial C

Terrestrial C pool can be subdivided into vegetation, soil/litter associated dead organic matter (OM), C in wetland and permafrost-associated C (Table 2-1). The total C pool in the world's land area was reported as 2,157-2,293 Pg in the top 100 cm layer, excluding litter and charcoal. Estimated OC in the upper 30 cm and 100 cm were reported as 684-724 Pg and 1,462-1,548 Pg, respectively (Batjes, 2014).

A combination of a meta-analysis with data assimilation revealed an increase of C input (+19.8 %) and turnover (+16.5%) due to an enrichment of atmospheric CO_2 (Groenigen et al., 2014). Also, they stated that the turnover leads to a lower equilibrium in soil C stocks. Warming can behave in two different ways. It can involve in the enhancement of C input through the increment of above and belowground biomass (net primary production) due to enhanced photosynthesis. Simultaneously, a rapid turnover of C can take place due to high decomposition exerted by soil microorganisms at warmer temperatures.

Carbon sequestration

Carbon sequestration is the net transfer of atmospheric C into solid and/or liquid associated forms reducing the concentration of C in the atmosphere. Carbon sequestration is governed by biotic and abiotic factors. Abiotic C sequestration has a greater potential to sequester CO_2 than biotic C sequestration (Lal, 2008). Capturing CO_2 by oceanic and geologic aspects is mainly encompassed in the abiotic C sequestration scenario via injection. Oceanic injection is needed to be done at deeper depths to prevent outgassing. Geological injection links with coal seams, old oil wells, stable rocks, and saline aquifers. Injection of industrial based CO_2 into saline aquifers leads in the formation of carbonates by reacting with other dissolved salts. There are processes (i.e. scrubbing and mineral carbonation) which can be used to transfer the

industrial based CO_2 (by-products) to thermodynamically and geologically stable carbonates such as calcium and magnesium carbonate (Lal, 2008).

Biotic C sequestration mainly employs higher plants and microorganisms to remove atmospheric CO_2. Oceanic sequestration is the enhancement of photosynthesis in phytoplankton population (Rivkin and Legendre, 2001). The produced particulate organic matter (POM) tends to deposit in the ocean bottom that ultimately contributes to mitigating the increasing atmospheric CO_2 concentration. The transformation of atmospheric CO_2 either into biogenic or pedogenic pools is known as terrestrial C sequestration. As in oceans, photosynthesis by biotic community improves above and below ground biomass. Forest ecosystems play a significant role in uptaking atmospheric CO_2. Since the terrestrial NPP is under saturated, an enhancement of atmospheric CO_2 can exert a fertilization effect (Lal, 2008). Biofuel production is another option to enhance C sequestration through growing biofuel crops in marginal lands and converting atmospheric biofuels into biomass-based biofuels (Lal, 2008).

Soil carbon sequestration

As agriculturists, soil C sequestration is vital in mitigating increasing atmospheric CO_2. The degree of C sequestration depends on climatic as well as management practices exerted by anthropogenic involvement. Soil C storage is primarily governed by inputs associated with NPP and its decomposition rate (Lutzov et al., 2006). Soil C stabilization is mediated by biological and physicochemical factors as well as anthropogenic involvement. Reports indicate that saturation of C in soil systems is driven by affiliated physicochemical properties (Six et al., 2002). The increase of the density of SOC, depth distribution and improvement of physical protection through soil aggregation (Lal, 2004) include in the technical approach to soil C stabilization. With the projected climate change, moisture and temperature regimes will be

altered impacting the soil microbial community structure, and NPP, which can ultimately alter the sequestration of soil C.

Wetlands, peatlands, and permafrost are OC-rich soils in comparison to the mineral soils (Davidson and Janssens, 2006). Undisturbed wetland soils are known as net sinks of CO_2. Disturbance-related to anthropogenic involvements such as draining and cultivation, converts wetlands into significant net sources of CO_2. Moreover, soil C sequestration occurs in inorganic forms such as secondary carbonates which are found in various forms such as films, threads, concretions, and pedants. At higher temperatures, these products can be relatively recalcitrant (Dalias et al., 2001) slowing down the dissolution process. Loss of SOC due to climatic variations is severe in Boreal, Tundra and Polar regions compared to mid-latitudes (Lal, 2004). Soil C sequestration related to agriculture will be further elaborated in following sections.

Anthropogenic influence on soil carbon

Global cropping lands have the potential to sequester approximately 88 Gt of C on 1,400 million hectares at a rate of 62 t ha^{-1} (Lal, 2016). Kuchaick et al., (2001) highlighted the significance of managing ecosystems. A variety of agricultural management practices are identified as key contributors in improving soil C sequestration such as conservation tillage/no-tillage, the addition of organic amendments, crop rotation, and crop intensification. Conversely, there are opposing thoughts and discrepancies on the link between different management strategies and soil C sequestration. Particularly, there are arguments on how management practices could affect climate change mitigation. For the exposure of management and environment-induced changes in SOC, mineralizable C seems to be the most reliable indicator due to its relatively lower variability (Ladoni et al., 2015).

Tillage

From 1999 to 2009, world wide areas under no-till were extended at a growth rate of six million ha per annum (Derpsch et al., 2010). Even though most researchers agree on benefits of no-till on climate change mitigation, contradictory concepts are emerging. Recently, VandenBygaart (2016) reported the effect of no-till on climate change as a myth. Furthermore, Powlson et al. (2014) emphasized the uncertainty of the benefits of no-till management in mitigating climate change, although it possesses indirect advantages such as improvement of soil quality which facilitates crop growth. Vitro et al. (2012) reported that 30% of the variability of SOC storage is significantly and positively correlated with the crop production in no-till systems in comparison with the tilled systems. Most of the tillage experiments consider only the top soil fraction and the deep soil research is scarce. Baker et al. (2007) stated the influence of conventional tillage on soil C sequestration in deeper layers that might have hidden due to sampling protocols adapted by researchers, which only focus up to a maximum depth of 30 cm. Lengthy roots in cropping systems aid in sequestering C in deeper layers. No-till soils exhibit lower heat flux and high albedo which can hinder root growth, than conventionally tilled soils. Moreover, no-till soils can impede root growth due to soil compaction which impacts on the deeper soil C loading. An experiment confirmed a significant higher root growth in 0-5 cm depth in no-till soils while exhibiting a deeper root growth in tilled soils (Qin et al., 2004).

Additionally, tillage operations facilitate heterotrophic soil respiration through breaking soil aggregates and exposing interior C to the surrounding environment (Six et al., 2000). Conservation tillage with residue application improves C held by small and large macroaggregates in the top soil compared to the conventionally tilled soils (Fuentes et al., 2012).

Reduced tillage and green manure addition together found to be effective in improving soil C sequestration. That is because the reduced tillage incorporates C into the soil, facilitating the aggregate formation which ultimately intensifies the physical protection mechanisms (Garia-Franco et al., 2015). Additionally, no-till managed lands tend to preserve more labile C, which was evident due to the abundance of O-alkyl C implying a lesser degree of humification compared to the tilled systems where alkyl C tends to be the dominated fraction (Shrestha et al., 2015). Effect of tillage on soil biological properties will be discussed in the following sections.

Cover cropping

Cover cropping could be considered as a useful approach towards the target of the "4 per thousand" proposal suggested by the COP21 (Lal, 2015). Incorporation of cover crops in a rotation cycle can enhance soil C sequestration due to high C input. Through a meta-analysis, cover crop input based annual C sequestration rate was assessed as 0.12±0.03 Pg C (excluding N_2O emissions and albedo) which accounts in compensating 8% of the annual GHG emissions (Poeplau and Don, 2015). Moreover, cover crops facilitate the abundance of microbes as well as the storage of C and N where additions of inorganic N is not needed (Mbuthia et al., 2015).

Organic amendments

There are various types of organic amendments such as manure, compost, crop residues, biochar, and bio solids which are commonly used by farmers worldwide. A quantitative meta-analysis by Gattinger et al. (2012) stated the potential of manure addition in improving soil C sequestration. Opposing to the statement on benefits, Leifeld et al. (2013) argued stating the inability of using manure addition as a best option in mitigating climate change since it cannot be considered as net transfer of C from the atmosphere to the soil. Moreover, they emphasized on relatively lower crop yields in OF systems which lead to low inputs to the soil system. Even

though the manure addition is a spatial transfer, the affiliated benefits such as microbial community shifts and soil aggregation indirectly contribute to the soil C sequestration/stabilization. Biochar addition as a soil amendment has gained attention in the last decade, and it can persist in soil systems on a centennial scale which substantially improves soil C sequestration and SOM dynamics (Wang et al., 2015). Biochar is a material which possesses a negative emission potential with minimum drastic impacts on land, water, cost, energy, albedo, and nutrients (Smith, 2016). Production of biochar is carried out by a process called pyrolysis which involves heating of biomass slowly at higher temperatures in an oxygen-free atmosphere which leads to an increase of the C content by two-fold (Lehmann, 2007). Its stability depends on the temperature during the pyrolysis process. The ratio of aromatic C seems to be increasing at temperatures greater than 800 ºC as the condensation of aromatic rings proceeds with the carbonization process (Nishimiya et al., 1998). The addition of biochar is a long lasting strategy due to its restrict susceptibility in converting into a source of CO_2 as related to forest fires, geological C leakages, and tillage operations in no-till farms (Lehmann, 2007).

Liming

Incorporation of liming materials has long been adopted, especially in acidic soils. The benefits associated with liming on C sequestration are not intensely studied (Paradelo et al., 2015). Moreover, Paradelo et al. (2015) linked the net effect of liming on soil C sequestration with the enhancement of the biological community, soil structure, and NPP. All these processes can impact on soil C sequestration/stabilization either directly or indirectly. Liming can improve biomass production due to changes in pH (especially in acidic soils) and provision of nutrients. Surface liming enhances particulate organic C (POC) and mineral associated OC in Oxisols (Briedis et al., 2012). A long-term no-till experiment in southern Brazil (medium textured

Oxisol) exhibited stability and protection of intra-aggregate C due to surface application of lime (Briedis et al., 2012). This links with the cationic bridging between kaolinite in the clay fraction and OC, with the aid of Ca^{2+} cations.

Influence of the biological community

Microorganisms take part in an essential role in the decomposition process of SOM whereas it is less affected by other soil organisms (10-15%) and abiotic processes (<15%) (Wolters, 2000; Lavelle et al., 1993). Microbial communities have a significant effect on the C sequestration in soils where the outcome can either be negative or positive on C dynamics. Microbes can produce recalcitrant forms of C such as amino sugar and glomalin related soil proteins (Zhang et al., 2013). Higher bacterial populations correspond to a high degree of decomposition which lowers the net accumulation of soil C (Wardle et al., 2004). Among most of the fungi species, the arbuscular mycorrhizal fungi (AMF) play a significant role in the ecosystem through their symbiotic relationships with plant species. Arbuscular mycorrhizal fungi aid plants in receiving scarce and immobile soil nutrients; especially phosphorus (P) where they receive C in return. It's reported that AMF can act as a net source of CO_2 due to the encouragement of SOC decomposition by supplying labile C to other microbes. Therefore, the growth and development of microorganisms get enhanced, leading to decompose native OC sources (Kowalchuk, 2012). This is known as the priming effect. Furthermore, a study indicated the inability of AMF in soil C storage at elevated CO_2. In an atmosphere with elevated CO_2, the decomposition of C in AMF active zones seems to be contributing to increasing CO_2 emission (Cheng et al., 2012). Additionally, they observed a transfer of mycorrhizal N from organic debris to host plants at elevated CO_2. Elevated CO_2 leads to stimulate the priming effect by leading saprotrophs towards new organic debris as a result of lowered labile C by AM fungi and release

of metabolic suppression by providing NH_4^+. Moreover, AMF fungi are the most significant facilitators in soil aggregation which is necessary for protecting C, especially via physical protection. Fungi population involve in physical entanglement and incorporation of extracellular polysaccharides/hydrophobic components (Cosentino et al., 2006). Aggregation is facilitated by a glycoprotein called glomalin, produced by AMF fungi (Wright et al., 2006). It is found that the aggregate stability and glomalin correlate well with each other (Wright and Upadhyaya, 1998).

Helgason et al. (2010) reported on the influences of tillage management on microbial diversity. No-till promoted a higher microbial biomass, indicating 32% more in comparison to the aggregates from tilled systems. No-till systems indicated greater than 40-60% of AMF in aggregates compared to tilled systems. Modeling using the structural equation representing conservation tillage systems revealed that the higher abundance of AMF population, leading to a higher C retention in aggregates which are >1 mm. Gram-positive bacteria tends to increase C in <1 mm sized aggregates (Zhang et al., 2013). Gram-negative bacteria exhibited a high C accumulation and turnover rates, implying the assimilation of newly formed photosynthesized root C input in the soil (Treonis et al., 2004). Dehydrogenase activity is linked with the OM decomposition whereas phenol oxidase activity is linked with the lignin depolymerization. Both enzymatic activities were found as strong signs of soil quality in agricultural fields (Veum et al., 2014).

Earthworms have a greater influence on the formation of soil aggregates and C pools associated with soil aggregates. The proportion of large macroaggregates is significantly high in the presence of earthworms and are enriched with total C (TC) and residue derived C (Bossuyt et al., 2005). Moreover, they observed a significantly higher pool of C enriched with newly added C in microaggregates encapsulated within macroaggregates.

Influence of mineralogy

Mineralogy plays a vital role in mediating chemical stabilization and physical protection mechanisms. The influence of mineralogy on C preservation can vary with the ecosystem properties. Physicochemical mechanisms involving C preservation will be evaluated in depth in the following sections.

Carbon stabilization mechanisms

Soil C stabilization is vital in the perspective of soil C sequestration which is recognized as a robust element in climate change mitigation. There are three primary mechanisms contributing to soil C preservation and they are known as biochemical recalcitrance, physical protection, and chemical stabilization (Stevenson, 1994). Biochemical recalcitrance is attributed to the inherent molecular characteristics of the SOM whereas the chemical stabilization is linked with the involvement of the soil mineral matrix. Krull et al. (2003) suggested that the biochemical recalcitrance is the only mechanism which stabilizes SOM for longer periods whereas the other two mechanisms are only responsible for retarding the decomposition process. Physical protection addresses the physical disconnection between SOM and microbial community which leads to lengthy turnover times, even for labile C compounds. Stabilization of SOC occurs due to the contribution of all three mechanisms. The current understanding is that the persistence of SOM as a property of the ecosystem (Schmidt et al., 2011). Soil moisture, temperature, oxygen diffusion, pH, nutrients, clay content, and soil mineralogy are the governing factors of OM dynamics in soil (Batjes, 1998). Even after decades of soil C research, underlying mechanisms of soil C stabilization are not entirely understood. In 2004, Blanco-Canqui and Lal highlighted the need of focusing on the mechanisms accountable for the dynamics of soil aggregates and their contribution to sequestered SOC. Moreover, studies which focusing on

understanding SOC sequestration and preservation mechanisms in soil aggregates using preserved natural conditions and aggregate architecture are scarcer.

Biochemical recalcitrance

Biochemical recalcitrance is related to the inherent characteristics of SOM and complexing reactions such as condensation, which makes SOM highly heterogeneous in nature. It can be categorized as primary and secondary recalcitrance. Primary recalcitrance is linked with the plant litter and rhizodeposition whereas secondary recalcitrance is related with the microbial/faunal products, extracellular neoformations, and charcoal formation (Lutzov et al., 2006). Microbial synthesized products are known to be recalcitrant due to its highly aromatic nature. Microbial byproducts such as murein, chitin, lipids, and melanin pigments have slower decomposition rates attributed due to their complex aromatic structure. Plant litter and rhizodeposits represent a major channel of natural OM input. Major constitutes of plant materials are polysaccharides, lignin, protein, chlorophyll, cutin, suberin, lipids, and waxes. High lignin/polyphenol content, high ratios of lignin:N, and C:N directly link with lower decomposition rates (Kleber, 2010). Lignin:cellulose ratio is identified as an important predictor of the exponential decay constant (Aber et al., 1990). Macromolecular substances with hydrolytic bonds exhibit low turnover times which is attributed to the availability of degrading enzymes such as cellulose, glucosidase, amidase, protease, chitinase, pectinase, and xylanase. They have the capability in hydrolyzing ether, ester-glycoside, peptide, and C-N bonds (Lutzov et al., 2006). The rate of decomposition is associated with characteristics of the molecules such as the size, polarity, ether-bridges, quaternary C atoms, phenyl- and heterocyclic B groups, hydrophobicity, and three-fold substituted N-linkages (Ottow, 1997). Transformation and decomposition pathways of lignin biopolymers are poorly understood due to the heterogeneous

buildup of phenolic monomers with contrasting kinetics of decomposition (Bahri et al., 2006). As an example, Bahri et al. (2006) reported that syringyl and cinnamyl phenols from maize possess higher turnover kinetics in comparison to the vanillyl.

Physicochemical Mechanisms

As described above, biochemical recalcitrance, chemical stabilization, and physical protection play a vital role in soil C stabilization. Geochemical influence is significant in predicting soil C storage and turnover which is proven using model-based researches (Doetterl et al., 2015). Carbon stabilization in soil is attributed mainly due to physicochemical processes which could be categorized into two;

1. Creation of a physical barrier by means of aggregation which limits the entry of biota, enzymes, oxygen, and nutrients

2. Associations with metallic ions and soil mineral surfaces (Von Lützow et al., 2006)

Mineral-associated SOM is hard to separate from mineral surfaces which resemble a highly stable nature and relative resistance to decomposition (Kalbitz et al., 2005; Schneider et al., 2010). In the short term SOC dynamics, the inherent recalcitrance of SOC and inaccessibility due to aggregation can perform a significant role. Conversely, chemical stabilization due to organomineral associations is the most powerful mechanism in the long run (Kögel-Knabner et al., 2008). Mineral-associated SOC fractions tend to have a longer turnover time compared with other physical fractions of SOC (Li et al., 2013). The current concept is that physicochemical processes are much more important in stabilizing soil C in comparison to the inherent recalcitrance of SOC (Han et al., 2016; Schmidt et al., 2011). Underlying physicochemical mechanisms which govern the C stabilization are still unknown (Wen et al., 2014). To fill the existing gap in the research knowledge, in-depth studies focusing on understanding these

mechanisms have gained more attention among soil science researchers. Significant mechanisms related to some soil orders are displayed in the Table 2.2.

Minerals and soil carbon

Soil C associate with mineral matrix employing a broad array of complex mechanisms. In general, on average, 20.5±7.8% of TOC is associated with Fe minerals (Lalonde et al., 2012). Physicochemical mechanisms hugely vary depending upon the soil properties. Interaction with mineral surfaces and formations of organo-mineral complexes are known to be the primary mechanisms that control the stabilized nature of SOC (Mikutta et al., 2009; Schmidt et al., 2011). The interactions between mineral phases and organic molecules differ depending upon the properties of the minerals and SOC. Type, distribution, charge, size, shape, topography, and involvement of particle aggregation are some of the key features that influence on the efficacy of the binding mechanisms (Kleber et al., 2015).

Factors mediating interactions of C with soil minerals

Soil composition and mineral characteristics

Soil texture cannot be solely used as the universal predictor in estimating soil C sequestration (Plante et al., 2006). The stabilization and the rate of decomposition of SOC are heavily varied depending upon the texture of soil (Bationo and Buerkert, 2001). Mostly, the earlier research addressed the role of phyllosilicates on the sorption of C whereas, in recent, the attention is mostly towards the amorphous mineral fraction, especially Fe and Al (oxy) hydroxides (Torn et al., 1997). The surface area and the reactivity of soil minerals govern the capacity of soil C stabilization (Kiem et al., 2002) as well as soil aggregation. Topographical variability with surface defects is favorable in creating robust and stable organomineral associations (Cutting et al., 2006). Particle size is also identified as a matter of soil C sorption

which enhances with the decrease in the size of soil grains (Anderson, 1988; Oades, 1988). The smaller particle size of minerals with a high specific surface area (SSA) is beneficial in providing an extensive surface area for organic molecule binding. The sorption of SOC to mineral surfaces tends to lower the specific surface area at varying levels depending on the mineralogy (Kaiser and Guggenberger, 2003). Lowering the SSA can ultimately saturate the mineral surfaces and are not capable of further accepting C loadings, efficiently. Saturation of soils with respect to C loadings can vary depending on the properties of soil. Kaiser and Guggenberger (2003) brought forward that the reduction in SSA in different minerals as a factor of an extent of C loading with further explanations. When sorbing smaller loadings, C molecules tends to spread out which allow maximum amounts of ligands to attach to the sorbing surface. Moreover, with bigger C loadings, organic C molecules may not solely sorb to mineral surfaces. Instead, they might be sorbing to already sorbed organic molecules via chemical bonding mechanisms. Additionally, large C inputs lead to the formation of multiple attachments (low stretching and unfolding) of molecules which can reduce the SSA, either by clogging of micropores or reducing the surface roughness. Significant reduction of micropore surface area was found in ferrihydrites and amorphous gibbsites. Furthermore, the porosity of minerals behaves successfully in retaining organic molecules retarding the transport process in the soil solution (Kleber et al., 2015). Surface functional groups are important in ligand exchange between mineral matter and SOC. Three major surface functional sites which interact with SOM are;

1) Single coordinated hydroxyl groups (Fe/Al oxides, allophane, imogolite, and edges of layer silicates)

2) Siloxane surfaces with layer charge (vermiculite, illite, and smectite) and,

3) Siloxane surfaces without layer charge (pyrophyllite and kaolinite) (Kögel-Knabner et al., 2008).

Metal oxides, phyllosilicates, and short range order (SRO) aluminosilicates are the three most important groups of soil minerals which participate in the formation of organomineral assemblages.

Metal oxides

Lalonde et al. (2012) named active Fe minerals as "rusty sink" and highlighted their tremendous ability in binding C which involve in the long-term C storage. Moreover, when minerals coat with goethite, the sorption capacity tends to increase. Among coatings of goethite, hematite, and ferrihydrite, ferrihydrite-coated illite shows the maximum sorption potential. Hydrous oxides do interact with SOM and clay fraction to form clay-organomineral associations (Tombacz et al., 2004). The stability of OC sorbed to clay-oxide associations depend on the net charge from negatively charged clays and positively charged oxyhydroxides (Saidy et al., 2015). In a study, which was designed to evaluate the capacity of minerals in protecting OC, revealed that the amorphous Al is more capable of preserving SOC compared to amorphous Fe mineral pool (Xiao et al., 2015). Furthermore, they observed a dense portion of organic biopolymers such as proteins, polysaccharides, and lipids in association with the mineral pool.

Phyllosilicates

There are variations in charge densities in phyllosilicate mineral fraction which can alter the sorption capacity of SOC. Sorption of SOM onto clay minerals contribute to C stabilization (Basile-Doelsch et al., 2007). Mineral and SOM association is mainly reported as an effect of ligand exchange between Al-OH groups in minerals and the carboxyl group of HA (Basile-Doelsch et al., 2007). Greater surface area attributed to higher clay content promotes to create

interactions with DOC (Jardine et al., 2006; Sutton and Sposito, 2006). Kaolinites are relatively large with a low negative charge in comparison to the smectitic clays. Therefore, low active minerals like kaolinite have the lower tendency in protecting SOM from microbial attacks (Richter et al., 1999). A sorption experiment (Saidy et al., 2013) indicated that smectite minerals tend to sorb more DOC compared with kaolinite and illite.

Short range order aluminosilicates

Short range order mineral pool significantly aids in the protection of soil C. Most of the world wide soil classes representing a broad range of climates and parent materials bear even a small quantity of amorphous minerals which play beneficial roles, interacting with C (Kramer et al., 2012). Volcanic soils are the foremost domains which are rich with amorphous minerals. It was found that the OM associated with SRO minerals possess a lesser rate of C mineralization compared with the OM, associated with 1:1 and 2:1 phyllosilicate (Rasmussen et al., 2006). Non-crystalline nano minerals (imogolite and allophane) are formed as a result of an association between organic ligands (-OH and Si-O) and Al^{3+} (Wen et al., 2014) and possess an inherent potential of holding a significantly higher amount of OC attributed to their hydrolytic property, greater SSA and higher amount of variable charge, and the availability of large number of hydroxyl groups (Kramer et al., 2012; Saidy et al., 2015). Organic ligands such as low molecular weight organic acids and HA hinder the crystallization via incorporating into the mineral network of amorphous nano minerals (Xu et al., 2010). The crystallization is inhibited by hydrolytic and polymeric reactions.

Furthermore, the physical protection is governed by the encapsulation of SOM into nano/micropores and soil aggregation. Soil aggregation plays a key role in separating SOC and microbial community, acting as a physical barrier. The texture and mineralogy play an important

role in the protection where clay aids in encapsulating SOM inside micropores (Baldock and Skjemstad, 2000). The crystalline nature of soil minerals, pH, size, ionic composition, and the presence of organic molecules in soil solution are the factors which affect the soil aggregation process (Duiker et al., 2003). Highly weathered soils, dominated with kaolinite and sesquioxides have a greater potential in aggregation which is mainly attributed due to the electrostatic attractions between the positively charged oxides and the negatively charged clay surfaces (Pinheiro-Dick and Schwertmann, 1996). The smaller crystal size of Fe oxides is very important in soil aggregation (Fontes, 1992). Aggregates are classified into two sections; those are macroaggregate (>250 μm) and microaggregates (<250 μm) (Sollins et al., 1996). The most labile C fraction is protected by >250 μm; but easily decomposable after mechanical disturbances (Gulde et al., 2008). Mineral-associated C in microaggregates and mass of water stable microaggregates in a Mediterranean semi-arid soil indicated the significance of the physical protection (Blanco-Moure et al., 2016). Soil C associated with smaller aggregates tend to have longer turnover rates (John et al., 2005; Monreal et al., 1997; Li et al., 2013) and still the reason of C preservation of C in microaggregates remain a mystery (Han et al., 2016). The degree of physical protection exerted by free microaggregates (Balesdent et al., 2000) and microaggregates protected inside macroaggregates (Denef et al., 2001) is high compared to macroaggregates (Beare et al., 1994; Elliot, 1986). Pores less than 0.2 μm prevent microorganisms entering into microaggregates and around 52% of the soil porosity is inaccessible to microbes in clay soils (Chenu et al., 2002). Involving ^{13}C-natural abundance technique, Jastrow et al. (1996) reported that the turnover rate of C associated with free stable microaggregates (412 years) is three times slower compared with the C associated with

macroaggregates (140 years). They reported that this effect was attributed due to the physical protection and the recalcitrant nature of C associated with microaggregate-derived C.

In-depth assessment of factors affecting carbon stabilization mechanisms

Characteristics of OM

Characteristics of SOM hugely vary depending upon the inherent properties and environmental influences. Oxidative processes can enhance the solubility and chemical reactivity. Coupled oxidative reactions with enzymatic depolymerization facilitate the organo-mineral associations, solubility, and chemical reactivity (Kleber et al., 2015). Hydrophobicity is related to the aliphatic C and with the increase of hydrophobicity, the degradation becomes slower due to the low solubility (Laudicina et al., 2015). The stability of DOC is governed by the chemical properties of sorbate molecules (Jagadamma et al., 2012). It is reported that the hydrophobic nature of OC aids effectively in sorbing on to mineral surfaces due to the high molecular weight, mechanisms of interaction, the arrangement of functional groups, and favorable ligand exchange mechanism attributed to the availability of larger amount of hydroxyl benzoic structures. The presence of organic molecules can enhance soil aggregation forming inner-sphere complexes on Fe(oxy)hydroxides (Cornell and Schwertmann, 1996). Newly formed HSs have a higher tendency in associating with smectite clays (Gonzalez and Laird, 2003). Furthermore, it is reported that aromatic functionalities and SRO minerals have a higher tendency in associating with each other (Kramer et al., 2012). The current belief suggests that lignin is not preserved selectively in soil where the mineral associated SOC (even labile C) which accounts for a huge fraction of SOM pool is stabilized as proved by an isotopic study (Haddix et al., 2016)

Soil solution composition

Humic acid and fulvic acid (FA) are complex molecules which are rich in carboxyl and hydroxyl functional groups. They are capable of forming stable complexes with metallic/hydroxyl-metallic compounds in the order of $Fe^{3+}>Al^{3+}>Pb^{2+}>Ca^{2+}>Mn^{2+}>Mg^{2+}$ etc. (Gu et al., 1994; Lutzov et al., 2007). Availability of Ca^{2+} ions involves in binding HA to mineral surfaces forming cationic bridges between mineral surfaces and HA where Ca^{2+} is found to be efficient compared with K^{+} (Shaker et al., 2012). Ionic strength in soil solution can have a significant influence on the HA adsorption where an enhancement of adsorption onto kaolinite and hematite was observed with the rise of the ionic strength (IS) (Shaker et al., 2012). Humic acid sorption to goethite is found to be stimulated by the increase in IS (Weng et al., 2007). This occurs as a result of a decrease in the molecular size which increases the competitive ability for sorption onto the surface sites. This finding was explained by a reduction of the volume of HA due to coagulation mechanisms which are related to the less electrostatic repulsing nature and fast diffusion of HA. Increasing IS leads to the enhancement of OC sorption where Ca^{2+} involvement was found to be significantly higher compared with Na^{+} (Feng et al., 2005).

pH

Soil pH is considered as a major determinant in the sorption of DOC (Mayes et al., 2012) and it influences on the properties of the adsorbent and adsorbate. Lowering pH tends to increase the anion exchange capacity (Feng et al., 2005). Phyllosilicates are negatively charged at the normal range of pH whereas Fe oxides tend to be positively charged. Filius et al. (2000) reported that the sorption of FA by goethite is strongly dependent on pH where protons involve in protonating FA, surfaces of goethite mineral, and proton co-adsorption/desorption upon FA adsorption. A modeling approach revealed that in acidic conditions, inner-sphere coordination of

carboxylic groups of FA plays a significant role whereas at alkaline condition outer-sphere complexes are more important. The point of zero charge (PZC) of Fe oxides stays around pH ranges between 7 to 9 (Borggaard, 1983). Natural OM adsorption to Fe oxides surfaces is mainly due to the ligand exchange mechanisms at least at pH below the ZPC of Fe oxides (Gu et al., 1994). Iron oxides tend to sorb the highest amount of DOC around pH 3-4 whereas the sorption decreases with the increasing pH. With the drop of pH, clays and variable charged minerals increase their surface positive charges which facilitate the sorption. Moreover, with decreasing pH, aqueous species become more positive which lead to facilitate the ligand exchange and anion exchange (Gu et al., 1994). The formation of aggregation with the involvement of clay and Fe(oxy)hydroxides depends on the soil pH where it requires a pH below the PZC (Goldberg, 1989). A reduction in the pH of soil enhances the adsorption of HA to hematite and kaolinite (Hur and Schlautman, 2004; Shaket et al., 2012) due to the creation of less negative charges associated with carboxylic C functional groups (Arnarson and Keil, 2000). The increment in pH tends to uplift the negative sites in the OM molecules and minerals through rising the pH-dependent charges (Oste et al., 2002). Increasing negativity is the precursor of the increasing repulsion between HA and soil minerals which leads to poor sorption.

Anthropogenic influence

The incorporation of the organic fertilizers indirectly involves in the soil C stabilization/sequestration. Amorphous Fe and Al (oxy)hydroxides fraction builds up with long-term addition of manure which is linked with the transformation of crystalline fraction into amorphous pool (Abdala et al., 2015; Huang et al., 2016; Wen et al., 2014; Yu et al., 2012; Zhang et al., 2013). Additionally, Yu et al. (2012) suggested the formation of amorphous aluminosilicate microparticles (i.e. allophane and imogolite) associated with the long-term

application of manure which contributes to the improvement of C status in soils. Not only organic fertilizers do create a favorable atmosphere for C stabilization. Phosphate and lime addition enhances the SOC stabilization especially in Oxisols (Batjes and Sombroek, 1997). Chemical characteristics including the structure and hydrophilic/hydrophobic nature of the SOM are significantly influenced by agricultural management practices such as tillage and cropping (Cosentino et al., 2006; Simon et al., 2009). Moreover, they found that the no-till and crop rotation have a tendency in enhancing hydrophobicity whereas tillage directs towards aromaticity where the microbial decomposition gets slower. Aromaticity and hydrophobicity of SOM are negatively correlated.

Soil C analytical tools

There are quantitative, semi-quantitative, and qualitative methods of determining SOC. Quantification of SOC is mainly based on destructive methods (either using chemicals or heat), where C is oxidized to CO_2. The method of quantification is based on gravimetric, volumetric, spectrophotometric or chromatographic methods. For the determination of TOC, either wet chemical extractions or dry combustion can be employed, but dry combustion method is considered superior to wet chemical methods. Qualitative methods include ^{13}C-Nuclear Magnetic Resonance (^{13}C-NMR), Diffuse Reflectance Infrared Fourier Transform (DRIFT), synchrotron-based techniques (i.e. bulk-NEXAFS, STXM-NEXAFS, etc.), nano Secondary Ion Mass Spectrometry (nanoSIMS), etc. Furthermore, the analytical approaches can be categorized as bulk, imaging, and synchrotron/neutron-based.

Modern science concentrates on new generation techniques which capture important information with minimum damages to the original condition of the soil samples. Synchrotron x-ray based technologies are one of the most promising fields which have generated a great hope and interest

in the soil and environmental scisence research world. Electrons traveling at velocities, closer to the speed of light are subjected to change their direction under a magnetic field. This produces an electromagnetic radiation which is known as the synchrotron light with unique properties such as high brightness, broad energy spectrum, greater polarization, and time structured emission (Lombi and Susini, 2009). When focusing on spatially resolved features less than 1 μm, the spectroscopy measurements are known as spectromicroscopy. An integrated approach to SOC determination is always preferred to overcome the weaknesses and complications associated with the complexity of natural samples such as soils.

Bulk approaches

Soil pH, ionic strength, the point of zero charge, and specific surface area are some of the parameters that can be studied to observe insights on the mechanisms and strength of organo-mineral associations (Mikutta et al., 2007). Thermogravimetric analysis (TG) combined with Differential Scanning Calorimetry (DSC), Fourier Transform Infrared spectroscopy (FTIR) and stable isotopes are some of the bulk approaches which are useful in studying organo-mineral associations. Thermal analysis techniques coupled with DSC are widely used to determine the stability, chemical composition, and molecular structure of SOC (Plante et al., 2009; Peltre et al., 2013). The energy required for thermal oxidation gives clues on the resistance of SOM decomposition and energy stored in a soil sample. This can be related to the energy yield obtained by microbial populations during the SOM degradation process (Peltre et al., 2013). The energy associated with organo-mineral associations can be studied using the TG-DSC where the soil is heated, and the corresponding energy absorption/release is recorded as a function of the temperature. The absence of a pretreatment, little sample preparation, and analysis of C even at a low C concentration are some of the advantages tied with the thermal analysis technique.

Contrasting results were observed by researchers on thermal and biological stability even though it is believed that the relatively recalcitrant C corresponds to a higher thermal stability (Strezov et al., 2004; Lopez-Capel et al., 2005).

Fourier transform infra-red spectroscopy can either be used alone or with a microscope to obtain spatially resolved information and it is related to the vibrations of the different bonds of the OC functional groups upon absorption of the infra-red radiation. The traditional FTIR spectroscopy is based on the KBr pelleting. There are two other sample preparation techniques named as Attenuated Total Reflection (ATR) and Diffuse Reflectance Infrared Fourier Transform (DRIFT). These methods are cheap and quick which allow obtaining information of SOM characterization.

Furthermore, stable isotopic techniques can be used to examine transformation mechanisms of organic C which have the capability in identifying the changes without fully resolving the chemical nature of the OM (Kleber et al., 2015).

Nuclear magnetic resonance provides information on quantitative and semi-quantitative aspects. Both solid-state and liquid-state NMR are used to characterize SOC where as solid state cross polarization and magic angle spinning NMR (CPMAS-NMR) is widely used. When using liquid state-NMR, usually HA fraction is extracted for the analysis whereas the whole soil is considered for the solid state-NMR. There are drawbacks associated with this ^{13}C-NMR such as line broadening due to paramagnetic ions (i.e. Fe, Mn, Cu, etc.), poor representation of SOC pool (Elliott et al., 1986) and possible alterations of HA during the extraction process. Furthermore, HA is an operationally defined fraction of soil C.

Imaging techniques

Imaging techniques can be used to obtain spatial information on organo-mineral associations which can be incorporated when developing conceptual models. Electron-based Scanning Electron Microscopy (SEM) and Transmission Electron Microscopy (TEM) are widely used to obtain information on the arrangement of organo-mineral associations. Those two approaches are not chemically sensitive. Using electron dispersive X-ray microscopy or d-spacing obtained from TEM, mineral phases can be studied.

Atomic Force Microscopy (AFM) is another source where information on the topography of surfaces, bond strengths, and mechanical properties can be obtained (Kleber et al., 2015). Atomic Force Microscopy coupled with nano thermal analysis (AFM-nTA) is used to distinct microscale and nanoscale heterogeneity of complex soil samples.

NanoSIMS is a surface sensitive destructive technique which physically detach ions from the surface and send to the detector. This method can be used to obtain elemental and isotopic maps of mineral-associated SOM to acquire evidence on organo-mineral associations. The spatial resolution of this technique is less than 100 nm where the information gathered represents only the surface with a collection depth of about few tens of nanometer. The region of interest (ROI) should be about 500 nm in diameter to obtain a decent counting statistics. There can be inferences depending upon the charging and surface topography. When analyzing soils, the charging issue attributed to the presence of quartz grains lowers the signal intensity (Remusat et al., 2012).

Synchrotron-based technique

Data collection of NEXAFS technique is usually conducted based on the sample characteristics and the objectives of the study. Different modes such as transmission,

fluorescence, and electron yield can be employed in the data acquisition process. In the transmission mode, electrons are transmitted through the sample. In the fluorescence mode, fluorescent x-rays are generated as a result of the absorption of incident x-rays by the sample. During the electron yield process, photo-emitted electrons are generated from the sample. Scanning microscopy techniques such as scanning transmission x-ray microscopy (STXM) and scanning photoemission microscopy (SPEM) can be used to obtain spatial information on elemental distribution.

The NEXAFS technique first established in the 1980s with the intention of studying low Z organic molecules containing C, N, O, and F (Stohr, 2013). When an atom is excited with an x-ray photon, it emits a core electron from a K (1s) or L (2p) shell to an unoccupied discrete energy level, leading to a core hole. This is followed by filling the core hole with an electron from a higher energy level which leads to release excess energy, either as fluorescence photons or auger electrons. Spectra are obtained by measuring the electron or fluorescence yield as a function of the incident photon energy. Low Z molecules such as C, N, and O, yield a much higher augur electron yield compared to the fluorescence yield (Winick and Doniach , 2012). These measurements illustrate the existence of the core hole and are a measure of the absorption of the cross section (Hahner, 2006). Bulk-NEXAFS technique provides insights of the bulk SOC chemistry with minimum alterations to its original conditions.

Scanning Transmission x-ray microscopy is another powerful technique which uses soft, high flux of x-ray photons (~100 to 2000 eV) generated by a synchrotron light source. It allows mapping of micrometer-sized environmental samples with nanometer spatial resolution (Jacobsen et al., 2000). When coupled with NEXAFS, it can be used in fingerprinting fine structures. Therefore, STXM-NEXAFS is considered as a powerful technique which can be used

to map thin environmental specimens at a nanometer scale spatial resolution and to identify the chemical speciation (Schumacher et al., 2005). In recent soil science research, STXM-NEXAFS has been used in investigating organo-mineral associations at nanometer scale spatial resolution (Chen and Sparks, 2015; Kinyangi et al., 2006; Lehmann et al., 2008; Solomon et al., 2012). This technique generates element-specific component maps for a wide range of biologically important elements (C, N, O, P and S), alkaline metals as well as first-row transition metals at a greater spatial resolution (<25 nm) (Dynes et al., 2015). Beamlines with STXM-NEXAFS facilities are mostly optimized for studies on C whereas flux is lacking for imaging Ca, Fe, Al, and Si. Furthermore, studies on management induced changes and clues on biogeochemical cycle on soil C can be carefully examined using this technique (Solomon et al., 2009).

Synchrotron-based FTIR another technique that can reveal information about organo-mineral associations which possess the ability to analyze both phases (i.e. organic and mineral) at the same time. It makes it difficult in identifying to the exact feature associated with a particular resonance (Kleber et al., 2015).

Future needs for the advancement of C research

Soil OM is the least known and most complex piece in soil (Magdoff and Weil, 2004). The incredibly complex, heterogeneous nature of SOM creates challenges in SOC research. Apart from the inherent molecular complexity, the associations with the mineral matter and other organic molecules, escalate these challenges. Moreover, contradictory arguments addressing issues related to SOM are being brought forward. Most of the fine details related to soil C are remaining as mysteries. This is mainly because of the lack of proper analytical tools. Most of the analytical tools do not preserve the natural conditions of the SOM.

Furthermore, C based research addressing environmental challenges are scanty. Hartemink et al. (2014) highlighted the necessity of directing researchers towards global human and environmental challenges linking food and fiber production, water, energy, climate change, waste recycling, and environmental degradation. They categorized the research needs under three themes named soil C in space and time, soil C properties and processes, and soil C depletion and management. Under the C in space and time, measurement and monitoring across landscapes, depth distribution, watersheds, and larger extents were identified. The monitoring programs should be carefully designed and maintained in the long-run. Soil OC research about rapid land use changes, climatic variations, peat, and permafrost soils are needed.

Under the second theme, the main highlights were the interactions of mineral surfaces with SOC, effect of mineralogy on SOC storage, biologically mediated SOC sequestration, turnover rates of SOC, the contribution of roots and microbes in SOC sequestration, erosion processes, dynamics of inorganic C, molecular scales investigations, and micro scale determinations. Moreover, an integrated approach combining remote sensing, modeling, and molecular/submicron scale investigations are needed.

The third theme indicated the ways of rising g SOC pool, management induced changes in SOC pool or the root zone, the depth distribution of SOC pool related to conservation agriculture, residue management, etc. Furthermore, an efficient analysis of samples and method standardization are needed more attention. Cover crop based research should focus on species, N_2O emission and albedo due to cultivation processes (Poeplau and Don, 2015).

Prediction of the resilience of OM to rising temperatures is challenging due to lack of knowledge in mechanisms (Kleber, 2010). Soil OM research on different ecosystems, the effect of SOC on soil quality and agronomic productivity, effects of crop residue removal in bioethanol

production, use of biochar, erosion induced SOC movements, effects of nutrients in increasing SOC, modeling for tropical ecosystems and trading C credits are required (Lal, 2009).

Han et al. (2016) highlighted some research areas on soil C research to fill the existing knowledge gap. In brief, those points were the evaluation of the decomposition of coal-derived OC, turnover of pyrogenic HA, identification of the relationship between mineralogy and the characteristics of black C, dynamics of Fe oxides in soils, further studies on associations of microbial C and soil minerals, studies on nanometer to micrometer sized soil microaggregates as SOC preservation sites, evaluation of mechanisms responsible for the persistence of SOC, and studies on SOC in deep horizons.

Lehmann and Kleber (2015) stated the necessity revealing the mysteries between detailed and fine-scale mechanistic research at the plant-soil interface as well as field-scale research. Moreover, they emphasized on evaluating how soil C behaves at different levels of warming, soil fertility, and water quality. The importance of proper coordination between modelers and biochemists was also highlighted as a significant need in the soil C research world for the growth and development which will narrow the gap between knowns and unknowns in soil C world.

Tables

Table 2-1 Terrestrial carbon pool

Terrestrial C pools	Size (Pg)	References
Vegetation	450-650	Prentice et al., 2001
Soil/litter associated dead OM	1,500-2,400	Batjes, 1996
Wetland	300-700	Bridgham et al., 2006
Permafrost	1,700	Tarnocai et al., 2009

Table 2-2 Soil carbon stabilization mechanisms in different soil orders

Soil Order	Characterization	Mineral properties	Mechanisms	References
Andisols	Rich in allophane, imogolite and ferrihydrite Relative high mean residence time of C	High surface areas of allophane and immogolite (700-1500 m^2g^{-1}) , ferrihydrite (200-500 m^2g^{-1}) Variable surface charge properties Nanoaggregate formations and wall perforations	Humus complexation and precipitation with Al^{3+} Organic C encapsulation inside nanopores Physical adsorption of SOC Sorption of C into micropores	Hochella et al., 2008; Parfitt, 2009; Nierop et al., 2007; Churchman, 2000; Dahlgren et al., 2004

Oxisols	Poorly crystalline Fe/Al oxides goethite and hematite Kaolinites	Minute crystals Surface covered with OH^- Large surface area, poorly ordered	Inner sphere complexation pH dependent charges Aggregation into microaggregates of goethite and hematite [2]electrostatic attractions between kaolinite and oxides aid in aggregation [3]High flocculation capacity in kaolinites	Schwertmann, 2008 [2]Denef et al., 2002 [3]Dixon, 1989
Ultisols	Poorly crystalline and crystalline Fe oxides Clay content		Aggregation into microaggrgates of goethite and hematite	Schwertmann, 2008
Inceptisols		Sorption to clay minerals Increasing capacity of SOC		Paul et al.,2008

Mollisols	2:1 clay minerals	[1]pH dependent electrostatic attraction involving anion exchange	[1]Mayes et al., 2012
Alfisols	[2] Mixed mineralogy (vermiculite, kaolinite and oxides)	[1]pH dependent electrostatic attraction involving anion exchange [2]high binding capacity of vermiculites with SOM Oxides and kaolinites form aggregates	[1]Mayes et al., 2012 Denef et al., 2002

Reference

Abdala, D.B., I.R. da Silva, L. Vergütz and D.L. Sparks. 2015. Long-term manure application effects on phosphorus speciation, kinetics and distribution in highly weathered agricultural soils. Chemosphere 119:504-514.

Aber, J.D., J.M. Melillo and C.A. McClaugherty. 1990. Predicting long-term patterns of mass loss, nitrogen dynamics, and soil organic matter formation from initial fine litter chemistry in temperate forest ecosystems. Canadian Journal of Botany 68:2201-2208.

Anderson, D. 1988. The effect of parent material and soil development on nutrient cycling in temperate ecosystems. Biogeochemistry 5:71-97.

Arnarson, T.S. and R.G. Keil. 2000. Mechanisms of pore water organic matter adsorption to montmorillonite. Mar. Chem. 71:309-320.

Bahri, H., M. Dignac, C. Rumpel, D.P. Rasse, C. Chenu and A. Mariotti. 2006. Lignin turnover kinetics in an agricultural soil is monomer specific. Soil Biol. Biochem. 38:1977-1988.

Baker, J.M., T.E. Ochsner, R.T. Venterea and T.J. Griffis. 2007. Tillage and soil carbon sequestration—What do we really know? Agric. Ecosyst. Environ. 118:1-5.

Baldock, J.A. and J. Skjemstad. 2000. Role of the soil matrix and minerals in protecting natural organic materials against biological attack. Org. Geochem. 31:697-710.

Balesdent, J., C. Chenu and M. Balabane. 2000. Relationship of soil organic matter dynamics to physical protection and tillage. Soil Tillage Res. 53:215-230.

Basile-Doelsch, I., R. Amundson, W. Stone, D. Borschneck, J. Bottero, S. Moustier, F. Masin and F. Colin. 2007. Mineral control of carbon pools in a volcanic soil horizon. Geoderma 137:477-489.

Bationo, A. and A. Buerkert. 2001. Soil organic carbon management for sustainable land use in sudano-sahelian west africa. Nutr. Cycling Agroecosyst. 61:131-142.

Batjes, N. 1998. Mitigation of atmospheric CO2 concentrations by increased carbon sequestration in the soil. Biol. Fertility Soils 27:230-235.

Batjes, N. 2014. Total carbon and nitrogen in the soils of the world. Eur. J. Soil Sci. 65:10-21.

Batjes, N. and W. Sombroek. 1997. Possibilities for carbon sequestration in tropical and subtropical soils. Global Change Biol. 3:161-173.

Batjes, N.H. 1996. Total carbon and nitrogen in the soils of the world. Eur. J. Soil Sci. 47:151-163.

Beare, M., P. Hendrix, M. Cabrera and D. Coleman. 1994. Aggregate-protected and unprotected organic matter pools in conventional-and no-tillage soils. Soil Sci. Soc. Am. J. 58:787-795.

Blanco-Canqui, H. and R. Lal. 2004. Mechanisms of carbon sequestration in soil aggregates. Crit. Rev. Plant Sci. 23:481-504.

Blanco-Moure, N., R. Gracia, A.C. Bielsa and M.V. López. 2016. Soil organic matter fractions as affected by tillage and soil texture under semiarid mediterranean conditions. Soil Tillage Res. 155:381-389.

Borggaard, O. 1983. Effects of surface area and mineralogy of iron oxides on their surface charge and anion-adsorption properties. Clays Clay Miner. 31:230-232.

Bossuyt, H., J. Six and P.F. Hendrix. 2005. Protection of soil carbon by microaggregates within earthworm casts. Soil Biol. Biochem. 37:251-258.

Bridgham, S.D., J.P. Megonigal, J.K. Keller, N.B. Bliss and C. Trettin. 2006. The carbon balance of north american wetlands. Wetlands 26:889-916.

Briedis, C., de Moraes Sá, João Carlos, E.F. Caires, J. de Fátima Navarro, T.M. Inagaki, A. Boer, A. de Oliveira Ferreira, C.Q. Neto, L.B. Canalli and J. Bürkner dos Santos. 2012. Changes in organic matter pools and increases in carbon sequestration in response to surface liming in an oxisol under long-term no-till. Soil Sci. Soc. Am. J. 76:151-160.

Chen, C. and D.L. Sparks. 2015. Multi-elemental scanning transmission X-ray microscopy–near edge X-ray absorption fine structure spectroscopy assessment of organo–mineral associations in soils from reduced environments. Environmental Chemistry 12:64-73.

Cheng, L., F.L. Booker, C. Tu, K.O. Burkey, L. Zhou, H.D. Shew, T.W. Rufty and S. Hu. 2012. Arbuscular mycorrhizal fungi increase organic carbon decomposition under elevated CO2. Science 337:1084-1087.

Chenu, C., G. Stotzky, P. Huang, J. Bollag and N. Sensi. 2002. Interactions between microorganisms and soil particles: An overview. Interactions between Soil Particles and Microorganisms: Impact on the Terrestrial Ecosystem.IUPAC.John Wiley & Sons, Ltd., Manchester, UK1-40.

Churchman, G. 2000. The alteration and formation of soil minerals by weathering. Handbook of Soil ScienceF3-F76.

Ciais, P., C. Sabine, G. Bala, L. Bopp, V. Brovkin, J. Canadell, A. Chhabra, R. DeFries, J. Galloway and M. Heimann. 2014. Carbon and other biogeochemical cycles. p. 465-570. *In* Climate change 2013: The physical science basis. contribution of working group I to the fifth assessment report of the intergovernmental panel on climate change. Cambridge University Press.

Cornell, R. and U. Schwertmann. 1996. The iron oxide. VCH, New York 377.

Cosentino, D., C. Chenu and Y. Le Bissonnais. 2006. Aggregate stability and microbial community dynamics under drying–wetting cycles in a silt loam soil. Soil Biol. Biochem. 38:2053-2062.

Cowie, J. 2012. Climate change: Biological and human aspects. Cambridge University Press.

Cubasch, U., Wuebbles, D., Chen, D., Facchini, M.C., Frame, D., Mahowald, N., & Winther, J. G. (2013). Introduction. In: Climate Change 2013: The Physical Science Basis. Contribution of Working Group I to the Fifth Assessment Report of the Intergovernmental Panel on Climate Change. Stocker, T.F., D. Qin, G.-K. Plattner, M. Tignor, S.K. Allen, J. Boschung, A. Nauels, Y. Xia, V. Bex and P.M. Midgley (Ed.). Cambridge University Press, Cambridge, United Kingdom and New York, NY, USA.

Cutting, R.S., C.A. Muryn, G. Thornton and D.J. Vaughan. 2006. Molecular scale investigations of the reactivity of magnetite with formic acid, pyridine, and carbon tetrachloride. Geochim. Cosmochim. Acta 70:3593-3612.

Dahlgren, R., M. Saigusa and F. Ugolini. 2004. The nature, properties and management of volcanic soils. Adv. Agron. 82:113-182.

Dalias, P., J.M. Anderson, P. Bottner and M. Coûteaux. 2001. Temperature responses of carbon mineralization in conifer forest soils from different regional climates incubated under standard laboratory conditions. Global Change Biol. 7:181-192.

Davidson, E.A. and I.A. Janssens. 2006. Temperature sensitivity of soil carbon decomposition and feedbacks to climate change. Nature 440:165-173.

Denef, K., J. Six, H. Bossuyt, S.D. Frey, E.T. Elliott, R. Merckx and K. Paustian. 2001. Influence of dry–wet cycles on the interrelationship between aggregate, particulate organic matter, and microbial community dynamics. Soil Biol. Biochem. 33:1599-1611.

Denef, K., J. Six, R. Merckx and K. Paustian. 2002. Short-term effects of biological and physical forces on aggregate formation in soils with different clay mineralogy. Plant Soil 246:185-200.

Derpsch, R., T. Friedrich, A. Kassam and H. Li. 2010. Current status of adoption of no-till farming in the world and some of its main benefits. International Journal of Agricultural and Biological Engineering 3:1-25.

Dixon, J. 1989. Kaolin and serpentine group minerals. Minerals in Soil Environments. 467-525.

Doetterl, S., A. Stevens, J. Six, R. Merckx, K. Van Oost, M.C. Pinto, A. Casanova-Katny, C. Muñoz, M. Boudin and E.Z. Venegas. 2015. Soil carbon storage controlled by interactions between geochemistry and climate. Nature Geoscience 8:780-783.

Duiker, S.W., F.E. Rhoton, J. Torrent, N.E. Smeck and R. Lal. 2003. Iron (hydr) oxide crystallinity effects on soil aggregation. Soil Sci. Soc. Am. J. 67:606-611.

Dynes, J.J., T.Z. Regier, I. Snape, S.D. Siciliano and D. Peak. 2015. Validating the scalability of soft X-ray spectromicroscopy for quantitative soil ecology and biogeochemistry research. Environ. Sci. Technol. 49:1035-1042.

Elliott, E. 1986. Aggregate structure and carbon, nitrogen, and phosphorus in native and cultivated soils. Soil Sci. Soc. Am. J. 50:627-633.

Feng, X., A.J. Simpson and M.J. Simpson. 2005. Chemical and mineralogical controls on humic acid sorption to clay mineral surfaces. Org. Geochem. 36:1553-1566.

Filius, J.D., D.G. Lumsdon, J.C. Meeussen, T. Hiemstra and W.H. Van Riemsdijk. 2000. Adsorption of fulvic acid on goethite. Geochim. Cosmochim. Acta 64:51-60.

Fontes, M.F. 1992. Iron oxide-clay mineral association in brazilian oxisols: A magnetic separation study. Clays Clay Miner. 40:175-179.

Fuentes, M., C. Hidalgo, J. Etchevers, F. De León, A. Guerrero, L. Dendooven, N. Verhulst and B. Govaerts. 2012. Conservation agriculture, increased organic carbon in the top-soil macro-aggregates and reduced soil CO2 emissions. Plant Soil 355:183-197.

Garcia-Franco, N., J. Albaladejo, M. Almagro and M. Martínez-Mena. 2015. Beneficial effects of reduced tillage and green manure on soil aggregation and stabilization of organic carbon in a mediterranean agroecosystem. Soil Tillage Res. 153:66-75.

Gattinger, A., A. Muller, M. Haeni, C. Skinner, A. Fliessbach, N. Buchmann, P. Mader, M. Stolze, P. Smith, N. Scialabba and U. Niggli. 2012. Enhanced top soil carbon stocks under organic farming. Proc. Natl. Acad. Sci. U. S. A. 109:18226-18231.

Goldberg, S. 1989. Interaction of aluminum and iron oxides and clay minerals and their effect on soil physical properties: A review. Commun. Soil Sci. Plant Anal. 20:1181-1207.

Gonzalez, J.M. and D.A. Laird. 2003. Carbon sequestration in clay mineral fractions from C-labeled plant residues. Soil Sci. Soc. Am. J. 67:1715-1720.

Groenigen, K.J., X. Qi, C.W. Osenberg, Y. Luo and B.A. Hungate. 2014. Faster decomposition under increased atmospheric CO(2) limits soil carbon storage. Science 344:508-509.

Gu, B., J. Schmitt, Z. Chen, L. Liang and J.F. McCarthy. 1994. Adsorption and desorption of natural organic matter on iron oxide: Mechanisms and models. Environ. Sci. Technol. 28:38-46.

Gulde, S., H. Chung, W. Amelung, C. Chang and J. Six. 2008. Soil carbon saturation controls labile and stable carbon pool dynamics. Soil Sci. Soc. Am. J. 72:605-612.

Haddix, M.L., E.A. Paul and M.F. Cotrufo. 2016. Dual, differential isotope labeling shows the preferential movement of labile plant constituents into mineral-bonded soil organic matter. Global Change Biol.

Hahner, G. 2006. Near edge X-ray absorption fine structure spectroscopy as a tool to probe electronic and structural properties of thin organic films and liquids. Chem. Soc. Rev. 35:1244-1255.

Han, L., K. Sun, J. Jin and B. Xing. 2016. Some concepts of soil organic carbon characteristics and mineral interaction from a review of literature. Soil Biol. Biochem. 94:107-121.

Hartemink, A.E., R. Lal, M.H. Gerzabek, B. Jama, A. McBratney, J. Six and C.G. Tornquist. 2014. Soil carbon research and global environmental challenges. Peerj Preprints 2: e366v1.

Helgason, B., F. Walley and J. Germida. 2010. No-till soil management increases microbial biomass and alters community profiles in soil aggregates. Applied Soil Ecology 46:390-397.

Hochella, M.F.,Jr, S.K. Lower, P.A. Maurice, R.L. Penn, N. Sahai, D.L. Sparks and B.S. Twining. 2008. Nanominerals, mineral nanoparticles, and earth systems. Science 319:1631-1635.

Huang, C., S. Liu, R. Li, F. Sun, Y. Zhou and G. Yu. 2016. Spectroscopic evidence of the improvement of reactive iron mineral content in red soil by long-term application of swine manure. PloS One 11.

Hur, J. and M.A. Schlautman. 2004. Effects of pH and phosphate on the adsorptive fractionation of purified aldrich humic acid on kaolinite and hematite. J. Colloid Interface Sci. 277:264-270.

Intergovernmental Panel on Climate Change (IPCC). 2014. Climate change 2013: The physical science basis: Working group I contribution to the fifth assessment report of the intergovernmental panel on climate change. Cambridge University Press.

Jacobsen, C., S. Wirick, G. Flynn and C. Zimba. 2000. Soft X-ray spectroscopy from image sequences with sub-100 nm spatial resolution. J. Microsc. 197:173-184.

Jagadamma, S., M.A. Mayes and J.R. Phillips. 2012. Selective sorption of dissolved organic carbon compounds by temperate soils. PloS One 7:e50434.

Jardine, P.M., M. Mayes, P.J. Mulholland, P.J. Hanson, J. Tarver, R.J. Luxmoore, J.F. McCarthy and G. Wilson. 2006. Vadose zone flow and transport of dissolved organic carbon at multiple scales in humid regimes. Vadose Zone Journal 5:140-152.

Jastrow, J. 1996. Soil aggregate formation and the accrual of particulate and mineral-associated organic matter. Soil Biol. Biochem. 28:665-676.

John, B., T. Yamashita, B. Ludwig and H. Flessa. 2005. Storage of organic carbon in aggregate and density fractions of silty soils under different types of land use. Geoderma 128:63-79.

Joshi, M., E. Hawkins, R. Sutton, J. Lowe and D. Frame. 2011. Projections of when temperature change will exceed 2 [deg] C above pre-industrial levels. Nature Climate Change 1:407-412.

Kaiser, K. and G. Guggenberger. 2003. Mineral surfaces and soil organic matter. Eur. J. Soil Sci. 54:219-236.

Kalbitz, K., D. Schwesig, J. Rethemeyer and E. Matzner. 2005. Stabilization of dissolved organic matter by sorption to the mineral soil. Soil Biol. Biochem. 37:1319-1331.

Kiem, R., H. Knicker and I. Kögel-Knabner. 2002. Refractory organic carbon in particle-size fractions of arable soils I: Distribution of refractory carbon between the size fractions. Org. Geochem. 33:1683-1697.

Kinyangi, J., D. Solomon, B. Liang, M. Lerotic, S. Wirick and J. Lehmann. 2006. Nanoscale biogeocomplexity of the organomineral assemblage in soil. Soil Sci. Soc. Am. J. 70:1708-1718.

Kleber, M. 2010. What is recalcitrant soil organic matter? Environmental Chemistry 7:320-332.

Kleber, M., K. Eusterhues, M. Keiluweit, C. Mikutta, R. Mikutta and P.S. Nico. 2015. Chapter one-Mineral–Organic associations: Formation, properties, and relevance in soil environments. Adv. Agron. 130:1-140.

Kögel-Knabner, I., G. Guggenberger, M. Kleber, E. Kandeler, K. Kalbitz, S. Scheu, K. Eusterhues and P. Leinweber. 2008. Organo-mineral associations in temperate soils: Integrating biology, mineralogy, and organic matter chemistry. Journal of Plant Nutrition and Soil Science 171:61-82.

Kowalchuk, G.A. 2012. Bad news for soil carbon sequestration. Science 337:1049-1050.

Kramer, M.G., J. Sanderman, O.A. Chadwick, J. Chorover and P.M. Vitousek. 2012. Long-term carbon storage through retention of dissolved aromatic acids by reactive particles in soil. Global Change Biol. 18:2594-2605.

Krull, E.S., J.A. Baldock and J.O. Skjemstad. 2003. Importance of mechanisms and processes of the stabilisation of soil organic matter for modelling carbon turnover. Functional Plant Biology 30:207-222.

Kucharik, C.J., K.R. Brye, J.M. Norman, J.A. Foley, S.T. Gower and L.G. Bundy. 2001. Measurements and modeling of carbon and nitrogen cycling in agroecosystems of southern wisconsin: Potential for SOC sequestration during the next 50 years. Ecosystems 4:237-258.

Ladoni, M., A. Basir and A. Kravchenko. 2015. Which soil carbon fraction is the best for assessing management differences? A statistical power perspective. Soil Sci. Soc. Am. J. 79:848-857.

Lal, R. 2004. Soil carbon sequestration to mitigate climate change. Geoderma 123:1-22.

Lal, R. 2008. Carbon sequestration. Philos. Trans. R. Soc. Lond. B. Biol. Sci. 363:815-830.

Lal, R. 2009. Sequestering atmospheric carbon dioxide. Critical Reviews in Plant Science 28:90-96.

Lal, R. 2015. Cover cropping and the “4 per thousand” proposal. J. Soil Water Conserv. 70:141A-141A.

Lal, R. 2016. Beyond COP 21: Potential and challenges of the “4 per thousand” initiative. J. Soil Water Conserv. 71:20A-25A.

Lalonde, K., A. Mucci, A. Ouellet and Y. Gélinas. 2012. Preservation of organic matter in sediments promoted by iron. Nature 483:198-200.

Laudicina, V.A., A. Novara, V. Barbera, M. Egli and L. Badalucco. 2015. Long-Term tillage and cropping system effects on chemical and biochemical characteristics of soil organic matter in a mediterranean semiarid environment. Land Degrad. Dev. 26:45-53.

Lavelle, P., E. Blanchart, A. Martin, S. Martin and A. Spain. 1993. A hierarchical model for decomposition in terrestrial ecosystems: Application to soils of the humid tropics. Biotropica130-150.

Lehmann, J. 2007. A handful of carbon. Nature 447:143-144.

Lehmann, J. and M. Kleber. 2015. The contentious nature of soil organic matter. Nature 528:60-68.

Lehmann, J., D. Solomon, J. Kinyangi, L. Dathe, S. Wirick and C. Jacobsen. 2008. Spatial complexity of soil organic matter forms at nanometre scales. Nature Geoscience 1:238-242.

Leifeld, J., D.A. Angers, C. Chenu, J. Fuhrer, T. Katterer and D.S. Powlson. 2013. Organic farming gives no climate change benefit through soil carbon sequestration. Proc. Natl. Acad. Sci. U. S. A. 110:E984.

Li, J., G.K. Evanylo, K. Xia and J. Mao. 2013. Soil carbon characterization 10 to 15 years after organic residual application: Carbon (1s) K-edge near-edge X-ray absorption fine-structure spectroscopy study. Soil Sci. 178:453-464.

Lombi, E. and J. Susini. 2009. Synchrotron-based techniques for plant and soil science: Opportunities, challenges and future perspectives. Plant Soil 320:1-35.

Lopez-Capel, E., S.P. Sohi, J.L. Gaunt and D.A. Manning. 2005. Use of thermogravimetry–differential scanning calorimetry to characterize modelable soil organic matter fractions. Soil Sci. Soc. Am. J. 69:136-140.

Lützow, M., I. Kögel-Knabner, K. Ekschmitt, H. Flessa, G. Guggenberger, E. Matzner and B. Marschner. 2007. SOM fractionation methods: Relevance to functional pools and to stabilization mechanisms. Soil Biol. Biochem. 39:2183-2207.

Lützow, M.v., I. Kögel-Knabner, K. Ekschmitt, E. Matzner, G. Guggenberger, B. Marschner and H. Flessa. 2006. Stabilization of organic matter in temperate soils: Mechanisms and their relevance under different soil conditions–a review. Eur. J. Soil Sci. 57:426-445.

Magdoff, F. and R.R. Weil. 2004. Soil organic matter in sustainable agriculture. CRC Press.

Mao, K., Y. Ma, T. Xu, Q. Liu, X. Shen, T. He, J. Han and L. Xia. 2015. A new perspective about climate change. Scientific Journal of Earth Science 5.

Mayes, M.A., K.R. Heal, C.C. Brandt, J.R. Phillips and P.M. Jardine. 2012. Relation between soil order and sorption of dissolved organic carbon in temperate subsoils. Soil Sci. Soc. Am. J. 76:1027-1037.

Mbuthia, L.W., V. Acosta-Martínez, J. Debryun, S. Schaeffer, D. Tyler, E. Odoi, M. Mpheshea, F. Walker and N. Eash. 2015. Long term tillage, cover crop, and fertilization effects on microbial community structure, activity: Implications for soil quality. Soil Biol. Biochem. 89:24-34.

Mikutta, R., C. Mikutta, K. Kalbitz, T. Scheel, K. Kaiser and R. Jahn. 2007. Biodegradation of forest floor organic matter bound to minerals via different binding mechanisms. Geochim. Cosmochim. Acta 71:2569-2590.

Mikutta, R., G.E. Schaumann, D. Gildemeister, S. Bonneville, M.G. Kramer, J. Chorover, O.A. Chadwick and G. Guggenberger. 2009. Biogeochemistry of mineral–organic associations across a long-term mineralogical soil gradient (0.3–4100kyr), hawaiian islands. Geochim. Cosmochim. Acta 73:2034-2060.

Monreal, C., H. Schulten and H. Kodama. 1997. Age, turnover and molecular diversity of soil organic matter in aggregates of a gleysol. Can. J. Soil Sci. 77:379-388.

Nierop, K.G., F.H. Tonneijck, B. Jansen and J.M. Verstraten. 2007. Organic matter in volcanic ash soils under forest and páramo along an ecuadorian altitudinal transect. Soil Sci. Soc. Am. J. 71:1119-1127.

Nishimiya, K., T. Hata, Y. Imamura and S. Ishihara. 1998. Analysis of chemical structure of wood charcoal by X-ray photoelectron spectroscopy. Journal of Wood Science 44:56-61.

Oades, J. 1988. The retention of organic matter in soils. Biogeochemistry 5:35-70.

Oste, L., E. Temminghoff and W.V. Riemsdijk. 2002. Solid-solution partitioning of organic matter in soils as influenced by an increase in pH or ca concentration. Environ. Sci. Technol. 36:208-214.

Ottow, J. 1997. Abbaukinetik und persistenz von fremdstoffen in böden. Umweltbiotechnologie. 97-138.

Paradelo, R., I. Virto and C. Chenu. 2015. Net effect of liming on soil organic carbon stocks: A review. Agric., Ecosyst. Environ. 202:98-107.

Parfitt, R. 2009. Allophane and imogolite: Role in soil biogeochemical processes. Clay Miner. 44:135-155.

Paul, S., H. Flessa, E. Veldkamp and M. López-Ulloa. 2008. Stabilization of recent soil carbon in the humid tropics following land use changes: Evidence from aggregate fractionation and stable isotope analyses. Biogeochemistry 87:247-263.

Peltre, C., J.M. Fernández, J.M. Craine and A.F. Plante. 2013. Relationships between biological and thermal indices of soil organic matter stability differ with soil organic carbon level. Soil Sci. Soc. Am. J. 77:2020-2028.

Pinheiro-Dick, D. and U. Schwertmann. 1996. Microaggregates from oxisols and inceptisols: Dispersion through selective dissolutions and physicochemical treatments. Geoderma 74:49-63.

Plante, A.F., J.M. Fernández and J. Leifeld. 2009. Application of thermal analysis techniques in soil science. Geoderma 153:1-10.

Plante, A.F., R.T. Conant, C.E. Stewart, K. Paustian and J. Six. 2006. Impact of soil texture on the distribution of soil organic matter in physical and chemical fractions. Soil Sci. Soc. Am. J. 70:287-296.

Poeplau, C. and A. Don. 2015. Carbon sequestration in agricultural soils via cultivation of cover crops–A meta-analysis. Agric. Ecosyst. Environ. 200:33-41.

Powlson, D.S., C.M. Stirling, M. Jat, B.G. Gerard, C.A. Palm, P.A. Sanchez and K.G. Cassman. 2014. Limited potential of no-till agriculture for climate change mitigation. Nature Climate Change 4:678-683.

Prentice, I.C., G. Farquhar, M. Fasham, M. Goulden, M. Heimann, V. Jaramillo, H. Kheshgi, C. Le Quéré, R.J.B. Scholes and D.W. Wallace. 2001. The carbon cycle and atmospheric carbon dioxide. Cambridge University Press.

Qin, R., P. Stamp and W. Richner. 2004. Impact of tillage on root systems of winter wheat. Agron. J. 96:1523-1530.

Rasmussen, C., R.J. Southard and W.R. Horwath. 2006. Mineral control of organic carbon mineralization in a range of temperate conifer forest soils. Global Change Biol. 12:834-847.

Remusat, L., P. Hatton, P.S. Nico, B. Zeller, M. Kleber and D. Derrien. 2012. NanoSIMS study of organic matter associated with soil aggregates: Advantages, limitations, and combination with STXM. Environ. Sci. Technol. 46:3943-3949.

Richter, D.D., D. Markewitz, S.E. Trumbore and C.G. Wells. 1999. Rapid accumulation and turnover of soil carbon in a re-establishing forest. Nature 400:56-58.

Rivkin, R.B. and L. Legendre. 2001. Biogenic carbon cycling in the upper ocean: Effects of microbial respiration. Science 291:2398-2400.

Saidy, A., R. Smernik, J. Baldock, K. Kaiser and J. Sanderman. 2015. Microbial degradation of organic carbon sorbed to phyllosilicate clays with and without hydrous iron oxide coating. Eur. J. Soil Sci. 66:83-94.

Saidy, A., R. Smernik, J.A. Baldock, K. Kaiser and J. Sanderman. 2013. The sorption of organic carbon onto differing clay minerals in the presence and absence of hydrous iron oxide. Geoderma 209:15-21.

Sands, P. 1992. The united nations framework convention on climate change. Review of European Community & International Environmental Law 1:270-277.

Schmidt, M.W., M.S. Torn, S. Abiven, T. Dittmar, G. Guggenberger, I.A. Janssens, M. Kleber, I. Kögel-Knabner, J. Lehmann and D.A. Manning. 2011. Persistence of soil organic matter as an ecosystem property. Nature 478:49-56.

Schneider, M., T. Scheel, R. Mikutta, P. Van Hees, K. Kaiser and K. Kalbitz. 2010. Sorptive stabilization of organic matter by amorphous al hydroxide. Geochim. Cosmochim. Acta 74:1606-1619.

Schumacher, M., I. Christl, A.C. Scheinost, C. Jacobsen and R. Kretzschmar. 2005. Chemical heterogeneity of organic soil colloids investigated by scanning transmission X-ray microscopy and C-1s NEXAFS microspectroscopy. Environ. Sci. Technol. 39:9094-9100.

Schwertmann, U. 2008. Iron oxides. p. 363-369. *In* Encyclopedia of soil science. Springer.

Shaker, A.M., Z.R. Komy, S.E. Heggy and M.E. El-Sayed. 2012. Kinetic study for adsorption humic acid on soil minerals. The Journal of Physical Chemistry A. 116:10889-10896.

Shrestha, B., B. Singh, C. Forte and G. Certini. 2015. Long-term effects of tillage, nutrient application and crop rotation on soil organic matter quality assessed by NMR spectroscopy. Soil use Manage. 31:358-366.

Šimon, T., M. Javůrek, O. Mikanova and M. Vach. 2009. The influence of tillage systems on soil organic matter and soil hydrophobicity. Soil Tillage Res. 105:44-48.

Six, J., E. Elliott and K. Paustian. 2000. Soil macroaggregate turnover and microaggregate formation: A mechanism for C sequestration under no-tillage agriculture. Soil Biol. Biochem. 32:2099-2103.

Six, J., R. Conant, E.A. Paul and K. Paustian. 2002. Stabilization mechanisms of soil organic matter: Implications for C-saturation of soils. Plant Soil 241:155-176.

Smith, P. 2016. Soil carbon sequestration and biochar as negative emission technologies. Global Change Biol.

Sollins, P., P. Homann and B.A. Caldwell. 1996. Stabilization and destabilization of soil organic matter: Mechanisms and controls. Geoderma 74:65-105.

Solomon, D., J. Lehmann, J. Harden, J. Wang, J. Kinyangi, K. Heymann, C. Karunakaran, Y. Lu, S. Wirick and C. Jacobsen. 2012. Micro-and nano-environments of carbon sequestration: Multi-element STXM–NEXAFS spectromicroscopy assessment of microbial carbon and mineral associations. Chem. Geol. 329:53-73.

Solomon, D., J. Lehmann, J. Kinyangi, B. Liang, K. Heymann, L. Dathe, K. Hanley, S. Wirick and C. Jacobsen. 2009. Carbon (1s) NEXAFS spectroscopy of biogeochemically relevant reference organic compounds. Soil Sci. Soc. Am. J. 73:1817-1830.

Stevenson, F.J. 1994. Humus chemistry: Genesis, composition, reactions. John Wiley & Sons.

Stöhr, J. 2013. NEXAFS spectroscopy. Springer Science & Business Media.

Strezov, V., B. Moghtaderi and J.A. Lucas. 2004. Computational calorimetric investigation of the reactions during thermal conversion of wood biomass. Biomass Bioenergy 27:459-465.

Sutton, R. and G. Sposito. 2006. Molecular simulation of humic substance–Ca-montmorillonite complexes. Geochim. Cosmochim. Acta 70:3566-3581.

Tans, P. 2016. NOAA/ESRL (http://www.esrl.noaa.gov/gmd/ccgg/trends/), earth system research laboratory. Global Monitoring Division. (accessed August 11, 2016).

Tarnocai, C., J. Canadell, E. Schuur, P. Kuhry, G. Mazhitova and S. Zimov. 2009. Soil organic carbon pools in the northern circumpolar permafrost region. Global Biogeochem. Cycles 23.

Tombacz, E., Z. Libor, E. Illes, A. Majzik and E. Klumpp. 2004. The role of reactive surface sites and complexation by humic acids in the interaction of clay mineral and iron oxide particles. Org. Geochem. 35:257-267.

Torn, M.S., S.E. Trumbore, O.A. Chadwick, P.M. Vitousek and D.M. Hendricks. 1997. Mineral control of soil organic carbon storage and turnover. Nature 389:170-173.

Treonis, A.M., N.J. Ostle, A.W. Stott, R. Primrose, S.J. Grayston and P. Ineson. 2004. Identification of groups of metabolically-active rhizosphere microorganisms by stable isotope probing of PLFAs. Soil Biol. Biochem. 36:533-537.

VandenBygaart, A. 2016. The myth that no-till can mitigate global climate change. Agric, Ecosyst. Environ. 216:98-99.

Veum, K.S., K.W. Goyne, R.J. Kremer, R.J. Miles and K.A. Sudduth. 2014. Biological indicators of soil quality and soil organic matter characteristics in an agricultural management continuum. Biogeochemistry 117:81-99.

Virto, I., P. Barré, A. Burlot and C. Chenu. 2012. Carbon input differences as the main factor explaining the variability in soil organic C storage in no-tilled compared to inversion tilled agrosystems. Biogeochemistry 108:17-26.

Wang, J., Z. Xiong and Y. Kuzyakov. 2015. Biochar stability in soil: Meta-analysis of decomposition and priming effects. GCB Bioenergy.

Wardle, D.A., R.D. Bardgett, J.N. Klironomos, H. Setala, W.H. van der Putten and D.H. Wall. 2004. Ecological linkages between aboveground and belowground biota. Science 304:1629-1633.

Wen, Y., H. Li, J. Xiao, C. Wang, Q. Shen, W. Ran, X. He, Q. Zhou and G. Yu. 2014. Insights into complexation of dissolved organic matter and al (III) and nanominerals formation in soils under contrasting fertilizations using two-dimensional correlation spectroscopy and high resolution-transmission electron microscopy techniques. Chemosphere 111:441-449.

Weng, L., W.H. Van Riemsdijk and T. Hiemstra. 2007. Adsorption of humic acids onto goethite: Effects of molar mass, pH and ionic strength. J. Colloid Interface Sci. 314:107-118.

Wigley, T.M. 1998. The kyoto protocol: CO2 CH4 and climate implications. Geophys. Res. Lett. 25:2285-2288.

Winick, H. and S. Doniach. 2012. Synchrotron radiation research. Springer Science & Business Media.

Wolters, V. 2000. Invertebrate control of soil organic matter stability. Biol. Fertility Soils 31:1-19.

Wright, S. and A. Upadhyaya. 1998. A survey of soils for aggregate stability and glomalin, a glycoprotein produced by hyphae of arbuscular mycorrhizal fungi. Plant Soil 198:97-107.

Wright, S., K. Nichols and W. Schmidt. 2006. Comparison of efficacy of three extractants to solubilize glomalin on hyphae and in soil. Chemosphere 64:1219-1224.

Xiao, J., Y. Wen, H. Li, J. Hao, Q. Shen, W. Ran, X. Mei, X. He and G. Yu. 2015. In situ visualisation and characterisation of the capacity of highly reactive minerals to preserve soil organic matter (SOM) in colloids at submicron scale. Chemosphere 138:225-232.

Xu, R., Y. Hu, J. Dynes, A. Zhao, R. Blyth, L. Kozak and P. Huang. 2010. Coordination nature of aluminum (oxy) hydroxides formed under the influence of low molecular weight organic acids and a soil humic acid studied by X-ray absorption spectroscopy. Geochim. Cosmochim. Acta 74:6422-6435.

Yu, G., M. Wu, G. Wei, Y. Luo, W. Ran, B. Wang, J.c. Zhang and Q. Shen. 2012. Binding of organic ligands with al (III) in dissolved organic matter from soil: Implications for soil organic carbon storage. Environ. Sci. Technol. 46:6102-6109.

Zhang, J., L. Zhang, P. Wang, Q. Huang, G. Yu, D. Li, Q. Shen and W. Ran. 2013. The role of non-crystalline fe in the increase of SOC after long-term organic manure application to the red soil of southern china. Eur. J. Soil Sci. 64:797-804.

Chapter 3 - Preservation of Organic Carbon in Oxisol Soil Microaggregates: Insight from STXM-NEXAFS Spectroscopy

Abstract

Traditional views of soil organic carbon (SOC) preservation need to be re-examined and newly proposed theories should be assessed with direct evidence. The research goal was to identify soil C preservation mechanisms in microaggregates with preserved aggregate architecture, using a spectromicroscopy approach and support the findings with relevant bulk chemical analyses. Free stable microaggregates were collected from a long-term tropical agroecosystem from Cruz Alta, Brazil. The experiment had two tillage systems (till and no-till) with a complex crop rotation. Findings provided direct evidence on the preservation of SOC sources with the original morphology indicating that the preservation is not purely related to the substrate chemistry. Submicron scale findings showed evidence on organo-mineral associations. Bulk analyses provided limited evidence on chemical stabilization mechanisms. Relatively high accumulation of OC was observed in no-till microaggregates. The primary mechanism cooperative in soil C sequestration in microaggregates is the direct preservation of OC sources with the involvement of mineral matter. The findings of this spectromicroscopy approach supported the newly proposed concepts on the SOC preservation by providing direct evidence. Microscale revelations on soil C preservation are useful in building mechanistic models with a better certainty.

Introduction

Increasing carbon dioxide (CO_2) in the atmosphere urges the necessity of employing mitigation options to reduce climate change. Carbon (C) sequestration in soils/vegetation has a significant potential in the agriculture, forestry and other land use (AFOLU) sector to reduce atmospheric CO_2 (Smith et al., 2014) as proposed by the Intergovernmental Panel on Climate Change (IPCC). Agriculture affects anthropogenic C by intervening uptake, emission, fixation, and relocation of C in various pools (Lal, 2004). With appropriate agricultural management practices such as reduced/no-till, increased cropping intensity, incorporation of soil amendments, cover cropping, and crop rotation, soil can serve as a sink of atmospheric CO_2, either by reducing heterotrophic soil respiration or enhancing C input (Paustian et al., 2000). Soils capacity to serve as a sink of C depends on the initial level of soil organic C (SOC), soil characteristics, climate, and soil management practices (Lal, 2004). Soil C preservation occurs through biochemical recalcitrance, chemical stabilization, and physical protection (Sollins et al., 1996).

Researchers have been focusing on understanding the ways of enhancing SOC sequestration/preservation and soil aggregation over decades. However, studies which focus on providing insights into the underlying mechanisms with direct evidences are limited. Investigations with preserved soil aggregate architecture are even scarcer (Solomon et al., 2012; Lehmann et al., 2008). The current understanding is that the persistence of SOC is influenced by its intrinsic properties and surrounding environment (Schmidt et al., 2011). Blanco-Canqui and Lal (2004) highlighted the requisite of focusing on mechanisms accountable for aggregate dynamics and their contribution to sequester SOC. Han et al. (2016) stressed the need for future research on the sites of SOC preservation in nanometer- to micrometer-sized microaggregates. In addition, Lehmann and Kleber (2015) argued supporting a soil continuum model (SCM)

emphasizing on the inaccessibility of microbiota and the contribution of soil minerals in preserving SOC. Therefore, direct evidence-based approaches are necessary to evaluate newly proposed theories on SOC storage.

Scanning transmission X-ray microscopy coupled with near edge X-ray absorption fine structure spectroscopy (STXM-NEXAFS) is a very powerful technique which creates the ability to image micrometer-sized soil samples at nanometer scale resolution with minimal disturbances to the specimen. This technique generates element-specific component maps for a broad range of biologically important elements (i.e. C, N, O, P and S), alkaline metals (i.e. Na, Ca, K, Mg), first row transition metals (i.e., Mn, and Ti), Al, and Si at a greater spatial resolution (<25 nm) (Dynes et al., 2015).

With the goal of filling gaps in scientific knowledge on mechanisms of SOC preservation, we focused on minimal disturbance to the original aggregate architecture. To the best of our knowledge, there is no published research studies focused on understanding the mechanisms of C preservation in long-term agroecosystems with preserved aggregate architecture. The specific objectives of this study were two-fold. The first objective was to understand mechanisms of soil C preservation in intact soil microaggregates by imaging C and relevant elemental distributions to study submicron scale associations and interactions. The second objective was to combine STXM-NEXAFS data with appropriate bulk chemical analyses to strengthen the spectromicroscopy findings and to extend the results into macroscopic levels.

Materials and methods

Soil samples were collected from a long-term agricultural experiment (established in 1985) located in Cruz Alta, Rio Grande do Sul, Brazil (28º 33’ S 53º 40’W, 409 m of altitude). The mean annual rainfall was recorded as 1,774 mm and the mean annual temperature was 19.2

˚C. The soil type was a clayey, kaolinitic, thermic Rhodic Hapludox enriched with kaolinites and iron (Fe) oxides (Campos et al., 2011). The experiment had two tillage systems (no-till (NT) and conventional till (CT)) and a complex crop rotation (R2) (summer and winter crop rotation: wheat/soybean/black oat/soybean/black oat + common vetch/maize/forage radish). These plots were amended with dolomitic lime in 1985 prior to the initiation of the study and repeated in 1995 and in 2011 at a rate of 5 Mg ha^{-1}. Soils were sampled to a depth of 0-5 cm in December 2012. Moist soils were packed carefully in polypropylene bags to minimize physical damages to aggregates and shipped to Kansas State University, Manhattan, KS, USA. A subfraction was separated and kept frozen at -4^{o}C until further use.

Preparation of 100 and 800 nm thin sections

For the preparation of thin sections, the method followed Solomon et al. (2012). The frozen soil was thawed and passed through a 250 μm sieve and trapped on a 150 μm sieve. Free stable microaggregates (150-250 μm) with minimal damage to the outer edges were identified under a light microscope (x40). Using a needle (BD microlance needle, Fisher Scientific, USA), microaggregates were carefully placed on a glass fiber filter (Whatman GF/A, 90 nm diameter, Sigma-Aldrich, USA) positioned on a 7.5 cm diameter sieve. Microaggregates were saturated with ultra-pure water for 16-18 hrs using a cold mist humidifier (Vicks® Ultrasonic humidifier, Kaz USA, Inc., USA) with an attached glass chimney to direct cold mist to the filter paper. Once microaggregates were saturated, excess droplets of water were drained. Microaggregates were flash frozen using liquid nitrogen (LN_2) after placing the microaggregate on a specimen carrier with concentric rings. A drop of water on the sample carrier aided in gluing the microaggregate when flash frozen.

Microaggregate thin sections were obtained using a cryo-ultramicrotome (EM UC7/EM FC7, Leica Microsystems Inc, Bannockburn, Illinois, USA) at -55 ˚C as described below. For C, calcium (Ca), nitrogen (N) and iron (Fe) analysis, 100 nm thin sections were used and additionally 800 nm thin sections were used for aluminum (Al) and silicon (Si) analyses. Initially, a trimming knife (Cryotrim 20, Diatome Ltd., Biel, Switzerland) was used to create a flat smooth surface on the microaggregate and final cutting was accomplished with a diamond knife (Cryo 35˚, Diatome Ltd., Biel, Switzerland) at a cutting speed of 1.2 mm s^{-1} and a cutting angle of 6°. An eyelash probe was used to transfer thin sections on to C free copper (Cu) transmission electron microscopy (TEM) grids which were impregnated with silicon monoxide (SiO) (200 meshes, No. 53002, Ladd Research, Williston, Vermont, USA). Sample specimens were stored in helium (He) atmosphere to prevent possible oxidation reactions. See details in supporting information (SI) of Appendix A.

Spectromicroscopy data acquisition and analysis

Data collection was conducted at the Advanced Light Source, Berkeley, USA (ALS) at beamline 5.3.2.2 (polymer STXM) and Canadian Light Source, Saskatoon, Canada (CLS) at SM (10ID-1) beamline. The beamline at ALS (250-780 eV) used a bending magnet with an energy resolution of $(E/\Delta E) \leq 5{,}000$ and the CLS had a wide energy range (130-2700 eV) which originated from a 75 mm generalized Apple II elliptically Polarizing Undulator (EPU) with a $E/\Delta E$ of 3000-10,000. Data on thin section representing CTR (conventional till, complex crop rotation) were collected at the ALS in 2014 while NTR (no-till, complex crop rotation) data were acquired at the CLS in 2015. The energy range of the two beamlines allowed examination of the K-edge of C and N as well as L-edge of Ca and Fe. In addition to those elemental analyses, wide energy range at SM beamline at CLS had the capability of collecting information on Al and Si.

The monochromators at both beamlines were calibrated using CO_2. The major drawback of C spectromicroscopy is that it identifies areas as C free when C is associated with thick mineral matter. This is due to poor X-ray transmission (Wan et al., 2007). So, small areas of thin sections were selected considering thickness, the presence of morphologically interesting preserved features (root hairs, coagulated OC sources etc.) and less disturbed nature of the thin section (i.e., lesser empty spaces). High resolution scans were conducted in the selected area at nanometer scale resolutions and the dwell time was modified according to the necessity at particular energy ranges, considering the absorption edges of interested elements.

Individual images collected at all energy levels were built into a stack using Stack Analyze 2.6.1 software (Jacobsen et al., 2000). Images with uneven intensities were removed from the stack and stack alignment was performed. Cluster analysis was performed to identify areas with similar spectral regions using PCA GUI 1.1.1 program (Lerotic et al., 2004). Cluster analysis aided in identifying natural groupings of data with related spectral properties and thickness which is established as an efficacious analysis technique in recognizing chemically distinct regions (Lerotic et al., 2004). Based on eigen spectra, eigen values, and eigen images (Lehmann et al., 2008), components and clusters were selected for further analysis. Spectra were normalized and smoothened using ATHENA software (Ravel and Newville, 2005). Peaks of C-NEXAFS sepctra were identified by published literature (Table 3.1). Linear combination fitting (LCF) was carried out using mineral standards for Ca and Fe using ATHENA software. Furthermore, Gaussian peak fitting was used to determine the relative proportion of C functional groups represented by each of the C spectra corresponding to individual cluster images using ATHENA software. An arctangent function for the ionization step at 292 eV and four Gaussian peaks representing aromatic, aliphatic, carboxylic, and carbonyl/carbonate were used for

deconvolution (Table 3-1 and 4-1). An arctangent function and Gaussian peaks were fixed at 1.5 eV and 0.4 eV of full width at half maximum (FWHM), respectively (Mukome et al., 2014). The relative percentages of C functional groups representing each transition were determined by setting the area under the Gaussian curve to 100%. R-factor was considered to obtain the best fit. The amplitude represented the area under the curve since the peak shapes are being unit normalized. Contrast maps were generated by averaging images around the interested peak of the NEXAFS spectrum. For statistical analysis on elemental correlations, contrast maps were cropped to focus only on a region of interest. The correlation of C functional groups with Fe/Ca was determined using SAS 9.4 statistical software (SAS Institute Inc, Cary, NC).

Bulk soil analysis

With the intention of relating submicron scale interpretations to bulk scale, analyses were carried out using the microaggregate fraction (150-250 µm). Collected microaggregates were ground and humic acid (HA) was extracted following the International Humic Substances Society (IHSS) method with some modifications (Swift, 1996). Humic acid dissolved in NaOH extractant was passed twice through 0.2 µm nylon filters and once through an amberlite (Amberlite IR120 hydrogen form, Sigma-Aldrich, USA) column (2.5 g amberlite per 50 mL of NaOH extractant) with gaseous N_2 pressure to remove paramagnetic ions (Kelleher and Simpson, 2006). Approximately 20 mg of HA were dissolved in 0.4 mL of 0.3 *M* NaOD/D_2O solution and mixed well with a vortex and centrifuged at 3300 rpm (Dou et al., 2008). Dialysis was performed to remove salts and chloride ions in HA extractant before freeze drying. Solution state ^{13}C-NMR of the freeze dried HA was conducted on a Varian Mercury Spectrometer (400 MHz) working at 100.58 MHz on ^{13}C using a 5 mm SW probe. Spectra were obtained by proton broad band decoupling and samples were run with a 45^{o} pulse and interpulse delay of 0.5 s.

Spectral width was set to 30,000 Hz and 200,000 transients were recorded. Sample temperature was kept at 25 ºC. Fourier transform of the resulting data were zero filled to 8,192 data points and a line broadening of 200 Hz was applied to all spectra. Tetramethylsilane (TMS) was used as an external chemical shift reference.

Additionally, hydrophilic (HIL) and hydrophobic (HOB) properties were determined with a liquid chromatograph Gilson system, with DAD detector. Separation was carried out using an Atlantis T3 column (5 µm, 250 x 4.6 mm, 100 A). The mobile phase of deionized water and acetonitrile (flow rate 1 mL min^{-1}) used a gradient elution program. Humic acid samples were digested in 0.01 *M* NaOH at a concentration of 2g L^{-1} for 24 hrs. A 50 µL sample was injected into the column. Chromatograms were analyzed at 254 nm (Debska and Gonet, 2007).

Total OC and amorphous Fe were determined in the microaggregate fraction of each treatment. Organic C was determined by dry combustion using Carlo Erba C/N analyzer (Carlo Erba instruments, Milan, Italy) (Nelson et al., 1996). Amorphous Fe was extracted according to the ammonium oxalate in dark method (Loeppert and Inskeep, 1996) and analyzed using a Varian 720-ES Inductive coupled plasma-optical emission spectrometer (ICP-OES).

Results and Discussion

The use of free microaggregates for this study was based on their potential in bearing preserved C. Carbon associated with free microaggregates possesses a slower turnover rate compared to C in macroaggregates (Jastrow, 1996). Moreover, free microaggregates tend to stay relatively intact compared to macroaggregates during tillage operations (Denef et al., 2001) where the strength is attributed to associations with resistant binding agents (Bossuyt et al., 2002). Cluster indices maps (Fig. 3-1) illustrated nano- and micro- scale variations in the elemental distribution corresponding to the area of interest. In CTR, C and Ca cluster indices

maps recognized two distinct regions showing a unique C and Ca chemistry (Fig. 3-1, cluster indices map a and b) whereas the NTR identified a preserved feature with unique C, Ca, and Fe chemistry (Fig. 3-1, cluster d, e and g). Of two identified structures in CTR, one had a unique Fe composition (Fig. 3-1, cluster indices map c).

Carbon spectromicroscopy

Spectromicroscopy analysis of C revealed the spatial heterogeneity in both thin sections, representing conventional till and no-till systems. Soil OC was scattered (Fig. 3-2, cluster indices maps a and d), and appeared to be located inside protective micro- and nano- pores in microaggregates. Thin sections exhibited resonance peaks representing aromatic ring structures (284.9-285.5 eV), phenols and ketones (286.5-287.1 eV), and carboxylic C (287.7-288.8 eV). In addition, a shoulder occurred representing aliphatic C and imidazol ring structures (287.1-287.8 eV). None of the thin sections indicated a peak representing carbonate (290.3 eV) implying the absence of inorganic C (Kleber and Johnson., 2010; Brandes et al., 2010). Gaussian peak fitting indicated a relative dominance of carboxylic C in both thin sections compared to other C functional groups (Table 3-2, 3-3). Aromatic C ranged from 11.6% to 35.9% and 4.1% to 12.5% in each individual cluster, representing CTR and NTR, respectively. Aliphatic C in CTR was negligible, indicating a high degree of humification. The spectra representing NTR showed aliphatic C shoulders accounting for 10.4% to 39.6% of total C (Table 3-3). The ratio between aliphatic and aromatic C (AL/AR) implies the degree of humification. Aromatic C is known to be relatively stable in comparison to the aliphatic C. With further humification, humic substances become highly aromatic due to the formation of polycondensed rings (Xing and Chen, 1999). Thus a decrease in AL/AR ratio coincides with advanced humification (Aranda et al., 2015).

Preserved structures with noticeable morphology were identified in both CTR (Fig. 3-2, cluster f) and NTR (Fig. 3-3, cluster e) with a unique C chemistry. The OC structures represented by cluster f in NTR (Fig 3-5) could be a root hair. The preserved structures in both clusters showed the carboxylic C peak around 288.5 eV, indicating the plant-derived nature. Resonance shifts towards the lower energy when amide type C is linked to carboxylic C (Lawrence et al., 2003). Peak around 288.2 eV indicates carboxylic C with amide type features, and it resembles microbial-derived C (Keiluweit et al., 2012). Cluster g (Fig. 3-3) of NTR identified the carboxylic C peak around 288.2 eV which clued its microbial origin. Gaussian peak fitting illustrated that the preserved structures in CTR (Table 3-2, cluster f) were relatively rich in aromatic C (**Error! Reference source not found.**). Cluster e and g from NTR (Fig. 3-3) i ndicated the lowest aliphatic C proportion relative to the surrounding. In NTR, all the clusters showed a negligible proportion of aromatic C, except in cluster g which resembled a microbial origin and cluster e which represented a root hair (**Error! Reference source not found.**). The p resence of phenols/ketones and phenolic C functional groups in both thin sections was an indication of plant-derived C from lignin degradation (Chen and Sparks, 2015).

Calcium spectromicroscopy

Calcium distribution in both thin sections showed a heterogeneous scattering similar to C. The incorporation of dolomitic lime could have impacted the enrichment of Ca. In Ca-NEXAFS spectra, two well-resolved peaks (349.2 eV and 359.2 eV) were observed with less intense crystal field peaks (Fig. 3-4, 3-5, 3-6). Multiple peaks were due to crystal field arising from the symmetry of the atoms surrounding Ca^{2+} in the first coordination sphere (Naftel et al., 2001). Less intense crystal field peaks were observed in both thin sections indicating the amorphous nature of Ca minerals (Politi et al., 2008). Amorphous Ca minerals are more efficient in building

organo-mineral complexes than crystalline minerals (Schlesinger, 2005). Linear combination fitting (LCF) indicated the occurrence of aragonite, Ca adsorbed to extracellular polymeric substances (EPS) and hydrous calcium dihydrogen phosphate like minerals in both thin sections (Table 3-4 and 3-5). Interestingly, the cluster analysis identified a unique Ca composition in preserved structures. Most of the Ca spectra corresponding to the identified clusters of NTR showed associations of aragonite like minerals and hydrous calcium dihydrogen phosphate/Ca adsorbed to EPS. The presence of aragonite like minerals (from LCF) was reaffirmed by comparing spectra of aragonite, calcite, and amorphous Ca (Ca adsorbed to EPS). Findings indicated the role of Ca minerals in protecting OC inside microaggregates. In NTR, the cluster f (Fig. 3-5) indicated a lining with a unique Ca chemistry around the root hair. The relatively high proportion of hydrous calcium dihydrogen phosphate was found in preserved structures in both thin sections. Additionally, a 800 nm thin section was analyzed (Fig. 3-6) and LCF indicated the presence of aragonite, hydrous calcium dihydrogen phosphate and Ca adsorbed to EPS (Table 3-6). This is similar to the findings from 100 nm thin section of NTR.

Nitrogen spectromicroscopy

Nitrogen NEXAFS spectromicroscopy of CTR exhibited weak signals, partly attributed to the lower concentration of N in soil. The chemistry of organic N is poorly understood, and 1/3 to 1/2 of N is usually categorized into the "unknown" group (Stevenson, 1994). Analysis of NTR (Fig. 3-7) showed how the N was distributed in different forms all over the thin section. Unlike other cluster indices maps (C, Ca, and Fe) of NTR, N cluster indices map did not recognize any special feature with a unique N chemistry (Fig. 3-7). Peaks were identified at 401.2, 401.9, 402.5, 405.2, and 405.7 eV. Spectral features within the range from 398.6 to 405 represents 1s–π* transitions whereas 1s–σ* transitions usually occur >405 eV (Leinweber et al., 2007). Resonance

around 401.2 eV and 402.5 eV could be attributed to the presence of different amino acids, amines, amides as well as heterocyclic N compounds associated with pyrimidine and purine structures that are microbial-derived (Solomon et al., 2012). Cluster d of NTR (Fig. 3-7) indicated peaks around 401 eV and 412 eV showing the occurrence of ammonium compounds (Leinweber et al., 2007). Additionally, the absorption band near 405.7 eV could be a reflectance of amino acids and heterocyclic N (Leinweber et al., 2007).

Iron spectromicroscopy

Iron (Fig. 3-8, 3-9 and 3-10) was distributed heterogeneously in the thin sections similarly to other elements. Iron NEXAFS spectra showed multiple peaks at Fe L3- (708.1 and 709.6 eV) and L2- (721.1 and 722.5 eV) edges (Fig. 3-8, 3-9 and 3-10). The shape of the Fe L3 2P3/2 signal determined the Fe oxidation status. Peaks at 708.1 eV and 709.6 eV illustrated the presence of $Fe^{2+}$and Fe^{3+}, respectively (Dynes et al., 2006; Hitchcock et al., 2009). Iron spectromicroscopy indicated the presence of Fe^{2+}/ Fe^{3+} mixed minerals (Ferrihydrite, maghemite, magnetite, iron(II) hydroxycarbonate, ferric phosphate, and goethite) where Fe^{3+} was the dominant form. The preserved structures indicated a unique Fe chemistry in both thin sections (Fig. 3-8, cluster c and Fig. 3-9, cluster g) and LCF indicated the presence of iron(II) hydroxycarbonate (Table 3-7, 3-8). Thicker sections (800 nm) of NTR showed a unique Fe chemistry associated with preserved structures as displayed in cluster d (Fig. 3-10). The NTR (800 nm) showed an abundance of maghemite and ferric phosphate like minerals (Table 3-9) and the maghemite was the most abundant Fe mineral species. Moreover, preserved C sources of this thin section identified a higher percentage of ferric phosphate compared to the surrounding. In CTR, only the preserved structures identified the presence of ferric phosphate agreeing to the findings of NTR (800 nm).

Aluminum and silicon spectromicroscopy

Thin sections of 100 nm are not ideal for the data acquisition of Al and Si. Those were mainly used to obtain information on the spatial distribution of Al/Si using contrast maps. Aluminum K-edge cluster indices maps (100 and 800 nm) of NTR indicated the heterogeneous distribution of Al. Aluminum NEXAFS spectra of 100 nm thin sections seemed to be noisy except in the first two clusters (Fig. 3-11). None of the spectra identified a better fit from LCF due to the unavailability of a reasonable set of standard spectra. Aluminum K-edge NEXAFS can be used to differentiate four and six-fold coordination (Hu et al., 2008). Four-fold coordinated Al mineral species possess a strong, single-edge maxima at 1565.4 eV, 1566.8 eV, and 1566.4 eV with poorly defined features at higher energy levels (Ildefonse et al.,1998). Six-fold coordinated gibbsite and kaolinite display two main maxima at 1567.8±0.4 eV and 1571.7±0.5 eV (Ildefonse et al., 1998). Shapes of the spectra in both thin sections (100 and 800 nm) indicated the dominance of kaolinite and gibbsite-like minerals (Ildefonse et al., 1998). The cluster e of NTR (800 nm) showed a resonance at 1571.3 eV implying the presence of short range ordered (SRO) minerals (Fig. 3-11). In the 800 nm thin section, an individual cluster map showed a unique Al composition in preserved structures. The lining of the preserved structures exhibited a separate unique Al chemistry. This could be an indication of efficient accumulation of plant-derived C by kaolinite (Neurath et al., 2015).

Silicon NEXAFS spectra can be in different shapes and the positioning of the absorption maximum varies depending on the oxidation status (0 or +4), coordination number, polymerization of silicate, Si-O bond distances, and valences, tetrahedral and octahedral sheet chemical substitution etc. (Hitchcock et al., 2009). Linear combination fitting did not indicate better fits due to the unavailability of a reasonable set of standard spectra, suitable for Oxisols. In

NTR (800 nm), a lining with a unique Si chemistry was identified around the preserved structures. Some Al and Si clusters demonstrated the spatial comparability with preserved C structures and exhibited a unique Al/Si chemistry.

Elemental correlations

Contrast maps provided information on the spatial distribution of interested elements and co-existence. Contrast maps of C indicated a high concentration in preserved structures than surrounding areas (Fig. 3-12 3-13 and 3-14). Visual observations of the correlation maps clearly indicated the co-existence of C and Ca. Contrast maps of Ca (Fig. 3-12 d/e, 3-13 f/g and 3-14 b) for L3 edge indicated the Ca-rich nature in preserved structures. The co-existence of C and Ca was not an indication of the presence of $CaCO_3$ which was confirmed by data analyses. Nitrogen contrast maps did not show a distinct pattern of distribution in NTR (100 nm). Iron contrast maps (Fig. 3-12 h/i, 3-13 hand 3-14 c) indicated a heterogeneous distribution and the concentration was high in certain areas of the thin section. Preserved structures and some other areas of thin sections showed a poor concentration of Fe and C. Nitrogen and Fe/Al/Si co-existed to a certain extent. Preserved structures in CTR (Fig. 3-12 f/g) indicated statistically significant correlations between carboxyl/aromatic/phenol and ketone and Ca ($p<0.0001$). Correlation between carboxylic functional groups and Fe^{3+} was statistically significant ($p<0.0001$) in the selected area of CTR (Fig. 3-12 j). For the same area, Fe and aromatic C were not significantly correlated. In NTR (800 nm), the contrast map of Si showed coagulated Si minerals at a high concentration in certain areas of the thin section. The Si concentration was lower in organic structures (Fig. 3-14 d).

Bulk chemical analysis

The SOC of the microaggregates from NTR and CTR was 3.2% and 1.8%, respectively. The high C concentration in no-till can be attributed to strong protection mechanisms and less disturbance. Selected microaggregate fractions from CTR and NTR were not correlated with amorphous Fe/ammonium oxalate extractable-Al. This suggested that the organo-mineral associations were not the primary mechanism in protecting OC as was observed in temperate agroecosystem (see Chapter 4 for more details).

^{13}C-NMR of the HA extracted from the microaggregates (150-250 μm) indicated intense peaks of aliphatic C, amino acid C, carboxylic C, aromatic C, carbohydrate C, and carboxylic C. Carbohydrate peak (61-83 ppm) and amino acid (47-60 ppm) peaks were identified according to Albers et al. (2008) and both thin sections showed the presence of carbohydrate C and amino acid C. The amino acid peak was relatively more intense in NTR compared to the carbohydrate. Nitrogen NEXAFS spectra also identified amino acid compounds in the NTR thin section. The existence of easily degradable organic C and N components indicated the strength of C preservation mechanisms. The ratio of AL/AR indicated that the HA in NTR was relatively more humified compared with CTR. The HIL/HOB ratio, however, conflicted with the ^{13}C-NMR in that NTR was less humified.

Highlights on the story of soil carbon preservation

Carbon spectromicroscopy indicated that C was located inside nano- and micropores within microaggregates exerting a physical protection (Krull et al., 2003; Six et al., 2004). Heterogeneity of SOC could be attributed to the nature of different C inputs over the time as well as climate that influence on different degrees of decomposition (Kogel-Knabner et al., 1988). Studied agroecosystem has favorable climatic conditions for high microbial activities throughout

the year which leads to a lower capacity of preserved SOC (Six et al., 2004). The presence of preserved structures even with the original morphology and unique C chemistry, exemplify the strength of preservation mechanisms inside microaggregates. Therefore, evidence on the direct preservation of OC illustrated the contribution on C sequestration even at nanometer scale resolution. Preservation is most likely achieved through creating spatial and kinetic constraints (McCarthy et al., 2008). Restricted accessibility of C by microorganisms and exoenzymes as well as reduced flow of water, air, and nutrients increase the residence time of OC. Pores less than 0.2 μm prevent microorganisms entering into microaggregates and 52% of the soil porosity is inaccessible to microbes in clay soils (Chenu et al., 2002). High clay content (52%) and abundance of Fe/Al oxyhydroxides in Oxisol create strong aggregate stability. Microbes/microbial by-products are usually found to be physically protected inside microaggregates contributing to the preservation of C in no-till systems (Plaza et al., 2013).

The percentage of aromatic C (stable) was significantly greater in tilled soils (CTR) whereas no-till soils (NTR) had a higher proportion of aliphatic C (labile C). This suggested the advanced decomposition in tilled soils. The labile C preservation could be linked with numerous chemical stabilization mechanisms apart from physical protection. Most of the aliphatic C may end up in hydrophobic termini which may influence the formation of hydrophobic bonding with metals cations (Chen et al., 2014) leading them to be preserved. Moreover, aliphatic C is commonly found in association with SRO minerals (Kramer et al., 2012). Carboxyl amide and aromatic C are usually microbial-derived (i.e. protein, DNA, and RNA) whereas aliphatic C is mainly plant-derived (Chen and Sparks, 2015). Carbonyl C is relatively labile and mediated by microbial communities (Ng et al., 2014). Therefore, the presence of labile C pool clued the existence of strong C preservation mechanisms. Carbonyl C rich microbial metabolites release as

neutral/acidic sugars and are strongly sorbed onto clay minerals (Golchin et al., 1996). Moreover, carboxylic and carbonyl C functional groups form strong polyvalent cation bridges with Fe^{3+} to make them chemically stabilized (Lutzow et al., 2006). Iron phosphate minerals identified from LC fitting could be an indicative of phosphorus involvement in C preservation.

High surface area and small size of amorphous Ca minerals are beneficial on organo-mineral associations. Preserved structures (in NTR and CTR) indicated the occurrence of aragonite and hydrous calcium dihydrogen phosphate. In addition, the root hair in NTR indicated the occurrence of Ca adsorbed to EPS. The presence of aragonite-like SRO minerals represents a transient precursor phase of calcite precipitation that is mediated by cyanobacterial communities (Obst et al., 2009). Within tightly-bound EPS produced by cyanobacteria closer to the cell wall, the nucleation of amorphous aragonite like minerals can be occurred (Obst et al., 2009). Biofilms adsorbed to root surfaces produce EPS and Ca acts as cation bridges to stabilize OC compounds. The co-existence of C and Ca suggested the chemical stabilization by a way of electrostatic cation bridges and complexation with metallic/hydroxyl metallic compounds (Gu et al., 1994; Lutzow et al., 2007). Hitchcock et al. (2009) reported that Ca act as a cation bridge between negatively charged C functional groups such as $COOH^-$ and OH^-.

Furthermore, the presence of easily degradable amino acid based compounds suggested the contribution of preservation mechanisms as opposed to chemical stabilization inside soil microaggregates. Co-existence of N with Fe/Al and Si indicated a way of preserving N inside microaggregates. Amino acids could have adsorbed to crystalline minerals like kaolinite and goethite or to poorly crystalline metal oxyhydroxides such as ferrihydrite (Kaiser and Zech, 2000; Mikutta et al., 2010). Mineralogy of Oxisol, dominated with kaolinite and Fe/Al

oxyhydroxides, is favorable for adsorption mechanisms. Amines and heterocyclic N are protected due to anion exchange mechanisms and H bonding (Lutzow, 2006).

Studies have implied the importance of poorly crystalline minerals on OC preservation, resulting a significant correlation with amorphous Fe and Al fraction (Mikutta et al., 2005). Due to the large surface area and high density of surface functional groups, SRO metal oxides are more important than aluminosilicate minerals in C preservation. Reduced forms of Fe could be linked with the availability of root exudates as they have the ability to reduce and solubilize Fe^{3+} minerals (Pédrot et al., 2011). Since the studied soils were designed with a complex crop rotation, a variety of root exudates were added continuously. Moreover, O_2-depleted microsites in microaggregates may have form metastable Fe(II) hydroxycarbonate (chukanovite) which then transform to common Fe oxide minerals with time (Taylor, 1980). Microbial activity creates O_2-depleted microsites in soil (Rappoldt and Crawford, 1999). The presence of ferrihydrite was found in both thin sections. High molecular weight humic substances stabilize poorly crystalline Fe precipitates (Colombo et al., 2014; Eusterhues et al., 2010). Moreover, ferrihydrite accumulates plant-based C, slowing down the biodegradation process (Neurath et al., 2015). Aging of HA co-precipitated with Fe^{2+} involves in the disturbance of Fe hydroxyl sheets, promoting the formation of ferrihydrite around pH of 5 (Colombo et al., 2015). The Oxisol has a favorable pH for the formation of ferrihydrite. Eusterhues et al., (2014) indicated that polysaccharide-rich compounds become resistant for biodegradation whereas lignin degradation is inhibited when associated with ferrihydrites. Iron and Al^{3+} form strong coordination complexes with organic compounds efficiently compared to Ca^{2+} (Lutzow et al., 2006). Also, the bonding efficiency though ligand exchange is greater than the cation bridging between SOC and phyllosilicate minerals (Kaiser and Zech, 2000). Kaolinite like minerals can participate in

accumulating plant-derived C which was proven with isotopic tracing (^{13}C) (Neurath et al., 2015). Correlation between elements and OC provided information on the involvement of mineralogy in C preservation. Ligand exchange, polyvalent cation bridges, and weak interactions (hydrophobic interactions, Van der Waals forces and H bonding) contribute to preserve SOC in soils.

Summary

This study revealed the potential of using a non-invasive spectromicroscopy approach to unravel the submicron level information on soil C preservation. Results indicated both biotic and abiotic involvement on C preservation in microaggregates. Findings provided direct evidence on the preservation of OC structures even with the original morphology, indicating that preservation is not purely related to substrate chemistry. Furthermore, the presence of relatively labile C inside microaggregates reaffirmed our understanding of C preservation as an ecosystem property. Direct evidence on co-existence indicated a variety of organo-mineral associations. Overall, the preservation of OC in microaggregates is attributed as a result of a large array of physicochemical and biological involvements. Based on the evidence provided by spectromicroscopy, we propose that one of the primary mechanisms contributing to soil C sequestration in this soil is the direct preservation of C sources inside pores spaces, which then are protected due to inaccessibility to microbiota and formation of organo-mineral associations. Microscale findings and direct evidence in soil C preservation are useful in building mechanistic models on soil C preservation with a better certainty. The findings of this spectromicroscopy approach support the concepts brought forward by the Schimidt et al. (2011) and Lehmann and Kleber (2015) by providing direct submicron-scale level evidence.

References

Albers, C.N., G.T. Banta, O. Jacobsen and P.E. Hansen. 2008. Characterization and structural modelling of humic substances in field soil displaying significant differences from previously proposed structures. Eur. J. Soil Sci. 59:693-705.

Aranda, V. and F. Comino. 2014. Soil organic matter quality in three mediterranean environments (a first barrier against desertification in europe). Journal of Soil Science and Plant Nutrition. 14:743-760.

Blanco-Canqui, H. and R. Lal. 2004. Mechanisms of carbon sequestration in soil aggregates. Crit. Rev. Plant Sci. 23:481-504.

Bossuyt, H., J. Six and P.F. Hendrix. 2002. Aggregate-protected carbon in no-tillage and conventional tillage agroecosystems using carbon-14 labeled plant residue. Soil Sci. Soc. Am. J. 66:1965-1973.

Brandes, J.A., C. Lee, S. Wakeham, M. Peterson, C. Jacobsen, S. Wirick and G. Cody. 2004. Examining marine particulate organic matter at sub-micron scales using scanning transmission X-ray microscopy and carbon X-ray absorption near edge structure spectroscopy. Mar. Chem. 92:107-121.

Brandes, J.A., S. Wirick and C. Jacobsen. 2010. Carbon K-edge spectra of carbonate minerals. Journal of Synchrotron Radiation. 17:676-682.

Braun, A., F. Huggins, N. Shah, Y. Chen, S. Wirick, S. Mun, C. Jacobsen and G. Huffman. 2005. Advantages of soft X-ray absorption over TEM-EELS for solid carbon studies—a comparative study on diesel soot with EELS and NEXAFS. Carbon, 43:117-124.

Campos, B.H.C.D., T.J.C. Amado, C. Bayer, R.d.S. Nicoloso and J.E. Fiorin. 2011. Carbon stock and its compartments in a subtropical oxisol under long-term tillage and crop rotation systems. Revista Brasileira De Ciência do Solo. 35:805-817.

Chen, C. and D.L. Sparks. 2015. Multi-elemental scanning transmission X-ray microscopy–near edge X-ray absorption fine structure spectroscopy assessment of organo–mineral associations in soils from reduced environments. Environmental Chemistry. 12:64-73.

Chen, R., M. Senbayram, S. Blagodatsky, O. Myachina, K. Dittert, X. Lin, E. Blagodatskaya and Y. Kuzyakov. 2014. Soil C and N availability determine the priming effect: Microbial N mining and stoichiometric decomposition theories. Global Change Biol. 20:2356-2367.

Chenu, C., G. Stotzky, P. Huang, J. Bollag and N. Sensi. 2002. Interactions between microorganisms and soil particles: An overview. Interactions between Soil Particles and Microorganisms: Impact on the Terrestrial Ecosystem.IUPAC.John Wiley & Sons, Ltd., Manchester, UK1-40.

Cody, G., H. Ade, S. Wirick, G. Mitchell and A. Davis. 1998. Determination of chemical-structural changes in vitrinite accompanying luminescence alteration using C-NEXAFS analysis. Org. Geochem. 28:441-455.

Colombo, C., G. Palumbo, J. He, R. Pinton and S. Cesco. 2014. Review on iron availability in soil: Interaction of fe minerals, plants, and microbes. Journal of Soils and Sediments. 14:538-548.

Colombo, C., G. Palumbo, V.M. Sellitto, H.G. Cho, C. Amalfitano and P. Adamo. 2015. Stability of coprecipitated natural humic acid and ferrous iron under oxidative conditions. J. Geochem. Explor. 151:50-56.

Debska, B. and I. Gonet. 2007. Share of hydrophilic and hydrophobic fractions in humic acids formed as a result of post-harvest residue decomposition. Pol. J. Soil Sci. 40:57-65.

Denef, K., J. Six, H. Bossuyt, S.D. Frey, E.T. Elliott, R. Merckx and K. Paustian. 2001. Influence of dry–wet cycles on the interrelationship between aggregate, particulate organic matter, and microbial community dynamics. Soil Biol. Biochem. 33:1599-1611.

Dou, S., J. Zhang and K. Li. 2008. Effect of organic matter applications on 13C-NMR spectra of humic acids of soil. Eur. J. Soil Sci. 59:532-539.

Dynes, J.J., T. Tyliszczak, T. Araki, J.R. Lawrence, G.D. Swerhone, G.G. Leppard and A.P. Hitchcock. 2006. Speciation and quantitative mapping of metal species in microbial biofilms using scanning transmission X-ray microscopy. Environ. Sci. Technol. 40:1556-1565.

Dynes, J.J., T.Z. Regier, I. Snape, S.D. Siciliano and D. Peak. 2015. Validating the scalability of soft X-ray spectromicroscopy for quantitative soil ecology and biogeochemistry research. Environ. Sci. Technol. 49:1035-1042.

Eusterhues, K., J. Neidhardt, A. Hädrich, K. Küsel and K.U. Totsche. 2014. Biodegradation of ferrihydrite-associated organic matter. Biogeochemistry. 119:45-50.

Eusterhues, K., T. Rennert, H. Knicker, I. Kögel-Knabner, K.U. Totsche and U. Schwertmann. 2010. Fractionation of organic matter due to reaction with ferrihydrite: Coprecipitation versus adsorption. Environ. Sci. Technol. 45:527-533.

Golchin, A., P. Clarke and J. Oades. 1996. The heterogeneous nature of microbial products as shown by solid-state13C CP/MAS NMR spectroscopy. Biogeochemistry. 34:71-97.

Gu, B., J. Schmitt, Z. Chen, L. Liang and J.F. McCarthy. 1994. Adsorption and desorption of natural organic matter on iron oxide: Mechanisms and models. Environ. Sci. Technol. 28:38-46.

Han, L., K. Sun, J. Jin and B. Xing. 2016. Some concepts of soil organic carbon characteristics and mineral interaction from a review of literature. Soil Biol. Biochem. 94:107-121.

Hitchcock, A., J. Dynes, J. Lawrence, M. Obst, G. Swerhone, D. Korber and G. Leppard. 2009. Soft X-ray spectromicroscopy of nickel sorption in a natural river biofilm. Geobiology. 7:432-453.

Hitchcock, A.P., H.D. Stöver, L.M. Croll and R.F. Childs. 2005. Chemical mapping of polymer microstructure using soft X-ray spectromicroscopy. Aust. J. Chem. 58:423-432.

Hu, Y., R. Xu, J. Dynes, R. Blyth, G. Yu, L. Kozak and P. Huang. 2008. Coordination nature of aluminum (oxy) hydroxides formed under the influence of tannic acid studied by X-ray absorption spectroscopy. Geochim. Cosmochim. Acta. 72:1959-1969.

Ildefonse, P., D. Cabaret, P. Sainctavit, G. Calas, A. Flank and P. Lagarde. 1998. Aluminium X-ray absorption near edge structure in model compounds and Earth's surface minerals. Physics and Chemistry of Minerals. 25:112-121.

Jacobsen, C., S. Wirick, G. Flynn and C. Zimba. 2000. Soft X-ray spectroscopy from image sequences with sub-100 nm spatial resolution. J. Microsc. 197:173-184.

Jastrow, J. 1996. Soil aggregate formation and the accrual of particulate and mineral-associated organic matter. Soil Biol. Biochem. 28:665-676.

Kaiser, K. and W. Zech. 2000. Dissolved organic matter sorption by mineral constituents of subsoil clay fractions. Journal of Plant Nutrition and Soil Science. 163:531-535.

Keiluweit, M., J.J. Bougoure, L.H. Zeglin, D.D. Myrold, P.K. Weber, J. Pett-Ridge, M. Kleber and P.S. Nico. 2012. Nano-scale investigation of the association of microbial nitrogen residues with iron (hydr) oxides in a forest soil O-horizon. Geochim. Cosmochim. Acta. 95:213-226.

Kelleher, B.P. and A.J. Simpson. 2006. Humic substances in soils: Are they really chemically distinct? Environ. Sci. Technol. 40:4605-4611.

Kleber, M. and M.G. Johnson. 2010. Advances in understanding the molecular structure of soil organic matter: Implications for interactions in the environment. Adv. Agron. 106:77-142.

Kögel-Knabner, I., W. Zech and P.G. Hatcher. 1988. Chemical composition of the organic matter in forest soils: The humus layer. Zeitschrift Für Pflanzenernährung Und Bodenkunde. 151:331-340.

Kramer, M.G., J. Sanderman, O.A. Chadwick, J. Chorover and P.M. Vitousek. 2012. Long-term carbon storage through retention of dissolved aromatic acids by reactive particles in soil. Global Change Biol. 18:2594-2605.

Krull, E.S., J.A. Baldock and J.O. Skjemstad. 2003. Importance of mechanisms and processes of the stabilisation of soil organic matter for modelling carbon turnover. Functional Plant Biology. 30:207-222.

Lal, R. 2004. Soil carbon sequestration to mitigate climate change. Geoderma. 123:1-22.

Lawrence, J.R., G.D. Swerhone, G.G. Leppard, T. Araki, X. Zhang, M.M. West and A.P. Hitchcock. 2003. Scanning transmission X-ray, laser scanning, and transmission electron microscopy mapping of the exopolymeric matrix of microbial biofilms. Appl. Environ. Microbiol. 69:5543-5554.

Lehmann, J. and M. Kleber. 2015. The contentious nature of soil organic matter. Nature. 528:60-68.

Lehmann, J., D. Liang, M. Solomon, F. Lerotic, J. Luizão, T. Kinyangi, S. Schäfer, C. Wirick and Jacobsen. 2005. Near-edge X-ray absorption fine structure (NEXAFS) spectroscopy for mapping nano-scale distribution of organic carbon forms in soil: Application to black carbon particles. Global Biogeochem. Cycles. 19.

Lehmann, J., D. Solomon, J. Kinyangi, L. Dathe, S. Wirick and C. Jacobsen. 2008. Spatial complexity of soil organic matter forms at nanometre scales. Nature Geoscience. 1:238-242.

Leinweber, P., J. Kruse, F.L. Walley, A. Gillespie, K. Eckhardt, R.I. Blyth and T. Regier. 2007. Nitrogen K-edge XANES-an overview of reference compounds used to identifyunknown'organic nitrogen in environmental samples. Journal of Synchrotron Radiation. 14:500-511.

Lerotic, M., C. Jacobsen, T. Schäfer and S. Vogt. 2004. Cluster analysis of soft X-ray spectromicroscopy data. Ultramicroscopy. 100:35-57.

Li, F., X. Cao, L. Zhao, J. Wang and Z. Ding. 2014. Effects of mineral additives on biochar formation: Carbon retention, stability, and properties. Environ. Sci. Technol. 48:11211-11217.

Loeppert, R. and W. Inskeep. 1996. Iron. P 639-664. Methods of Soil Analysis, Part 3.

Lützow, M., I. Kögel-Knabner, K. Ekschmitt, H. Flessa, G. Guggenberger, E. Matzner and B. Marschner. 2007. SOM fractionation methods: Relevance to functional pools and to stabilization mechanisms. Soil Biol. Biochem. 39:2183-2207.

Lützow, M.v., I. Kögel-Knabner, K. Ekschmitt, E. Matzner, G. Guggenberger, B. Marschner and H. Flessa. 2006. Stabilization of organic matter in temperate soils: Mechanisms and their relevance under different soil conditions–a review. Eur. J. Soil Sci. 57:426-445.

McCarthy, J.F., J. Ilavsky, J.D. Jastrow, L.M. Mayer, E. Perfect and J. Zhuang. 2008. Protection of organic carbon in soil microaggregates via restructuring of aggregate porosity and filling of pores with accumulating organic matter. Geochim. Cosmochim. Acta. 72:4725-4744.

Mikutta, R., K. Kaiser, N. Dörr, A. Vollmer, O.A. Chadwick, J. Chorover, M.G. Kramer and G. Guggenberger. 2010. Mineralogical impact on organic nitrogen across a long-term soil chronosequence (0.3–4100kyr). Geochim. Cosmochim. Acta. 74:2142-2164.

Mikutta, R., M. Kleber and R. Jahn. 2005. Poorly crystalline minerals protect organic carbon in clay subfractions from acid subsoil horizons. Geoderma. 128:106-115.

Mukome, F.N., A.L. Kilcoyne and S.J. Parikh. 2014. Alteration of biochar carbon chemistry during soil incubations: SR-FTIR and NEXAFS investigation. Soil Sci. Soc. Am. J. 78:1632-1640.Naftel, S., T. Sham, Y. Yiu and B. Yates. 2001. Calcium L-edge XANES study of some calcium compounds. Journal of Synchrotron Radiation. 8:255-257.

Naftel, S., T. Sham, Y. Yiu and B. Yates. 2001. Calcium L-edge XANES study of some calcium compounds. Journal of Synchrotron Radiation. 8:255-257.

Nelson, D.W., L.E. Sommers, D. Sparks, A. Page, P. Helmke, R. Loeppert, P. Soltanpour, M. Tabatabai, C. Johnston and M. Sumner. 1996. Total carbon, organic carbon, and organic matter. Methods of Soil Analysis.Part 3-Chemical Methods. 961-1010.

Neurath, R., M. Keiluweit, J. Pett-Ridge, P. Nico and M. Firestone. 2015. 61. tracing the influence of mineralogy, microbiology, and exudate chemistry on the stabilization of root-derived carbon. p. 83. *In* 61. tracing the influence of mineralogy, microbiology, and exudate chemistry on the stabilization of root-derived carbon. Genomic science Contractors–Grantees meeting XIII, 2015.

Ng, E., A. Patti, M. Rose, C. Schefe, K. Wilkinson, R. Smernik and T. Cavagnaro. 2014. Does the chemical nature of soil carbon drive the structure and functioning of soil microbial communities? Soil Biol. Biochem. 70:54-61.

Obst, M., J. Dynes, J. Lawrence, G. Swerhone, K. Benzerara, C. Karunakaran, K. Kaznatcheev, T. Tyliszczak and A. Hitchcock. 2009. Precipitation of amorphous CaCO 3 (aragonite-like) by cyanobacteria: A STXM study of the influence of EPS on the nucleation process. Geochim. Cosmochim. Acta. 73:4180-4198.

Paustian, K., J. Six, E. Elliott and H. Hunt. 2000. Management options for reducing CO2 emissions from agricultural soils. Biogeochemistry. 48:147-163.

Pédrot, M., A. Le Boudec, M. Davranche, A. Dia and O. Henin. 2011. How does organic matter constrain the nature, size and availability of fe nanoparticles for biological reduction? J. Colloid Interface Sci. 359:75-85.

Plaza, C., D. Courtier-Murias, J.M. Fernández, A. Polo and A.J. Simpson. 2013. Physical, chemical, and biochemical mechanisms of soil organic matter stabilization under conservation tillage systems: A central role for microbes and microbial by-products in C sequestration. Soil Biol. Biochem. 57:124-134.

Politi, Y., R.A. Metzler, M. Abrecht, B. Gilbert, F.H. Wilt, I. Sagi, L. Addadi, S. Weiner and P.U. Gilbert. 2008. Transformation mechanism of amorphous calcium carbonate into calcite in the sea urchin larval spicule. Proc. Natl. Acad. Sci. U. S. A. 105:17362-17366.

Rappoldt, C. and J.W. Crawford. 1999. The distribution of anoxic volume in a fractal model of soil. Geoderma. 88:329-347.

Ravel, B. and M. Newville. 2005. ATHENA, ARTEMIS, HEPHAESTUS: Data analysis for X-ray absorption spectroscopy using IFEFFIT. Journal of Synchrotron Radiation. 12:537-541.

Schlesinger, W.H. 2005. Biogeochemistry. Gulf Professional Publishing.

Schmidt, M.W., M.S. Torn, S. Abiven, T. Dittmar, G. Guggenberger, I.A. Janssens, M. Kleber, I. Kögel-Knabner, J. Lehmann and D.A. Manning. 2011. Persistence of soil organic matter as an ecosystem property. Nature. 478:49-56.

Six, J., H. Bossuyt, S. Degryze and K. Denef. 2004. A history of research on the link between (micro) aggregates, soil biota, and soil organic matter dynamics. Soil Tillage Res. 79:7-31.

Smith, P., M. Bustamante, H. Ahammad, H. Clark, H. Dong, E.A. Elsiddig, H. Haberl, R. Harper, J. House and M. Jafari. 2014. Agriculture, forestry and other land use (AFOLU). Climate Change. 811-922.

Sollins, P., P. Homann and B.A. Caldwell. 1996. Stabilization and destabilization of soil organic matter: Mechanisms and controls. Geoderma. 74:65-105.

Solomon, D., J. Lehmann, J. Harden, J. Wang, J. Kinyangi, K. Heymann, C. Karunakaran, Y. Lu, S. Wirick and C. Jacobsen. 2012. Micro-and nano-environments of carbon sequestration: Multi-element STXM–NEXAFS spectromicroscopy assessment of microbial carbon and mineral associations. Chem. Geol. 329:53-73.

Stevenson, F.J. 1994. Humus chemistry: Genesis, composition, reactions. John Wiley & Sons.

Swift, R.S., D. Sparks, A. Page, P. Helmke, R. Loeppert, P. Soltanpour, M. Tabatabai, C. Johnston and M. Sumner. 1996. Organic matter characterization. Methods of Soil Analysis.Part 3-Chemical Methods.1011-1069.

Taylor, R. 1980. Formation and properties of fe (II) fe (III) hydroxy-carbonate and its possible significance in soil formation. Clay Miner. 15:369-382.

Wan, J., T.K. Tyliszczak and Tokunaga. 2007. Organic carbon distribution, speciation, and elemental correlations within soil microaggregates: Applications of STXM and NEXAFS spectroscopy. Geochim. Cosmochim. Acta. 71:5439-5449.

Xing, B. and Z. Chen. 1999. Spectroscopic evidence for condensed domains in soil organic matter. Soil Sci. 164:40-47.

Figures

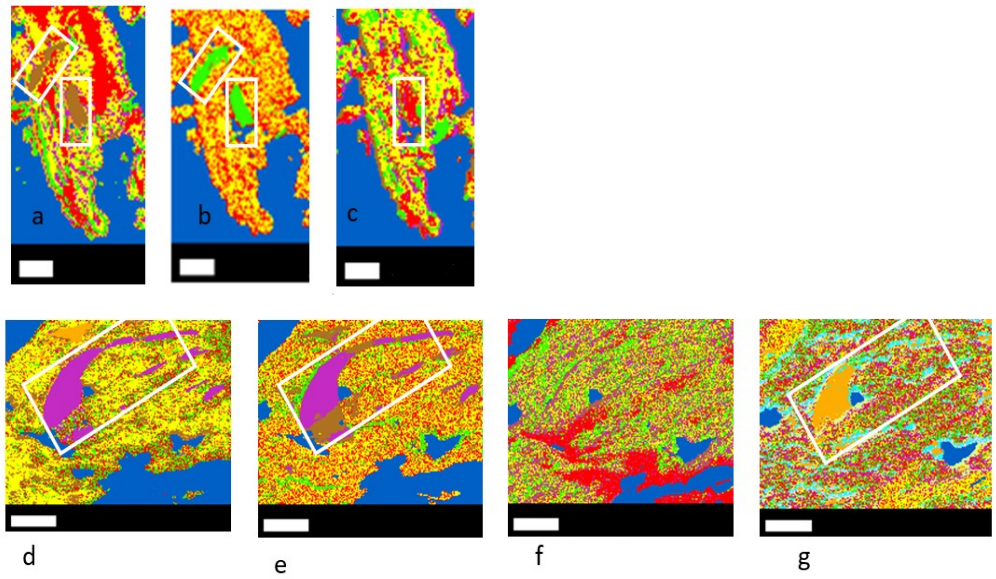

Figure 3-1 Cluster indices maps of carbon (a), calcium (b) and iron (c) of a 20 µm x 8 µm selected area of CTR-100 nm thin section and cluster indices maps of carbon (d), calcium (e), nitrogen (f) and iron (g) of a 20 µm x 15 µm selected area of NTR-100 nm thin section. NTR represents no-till, complex crop rotation. CTR represents conventional till, complex crop rotation.

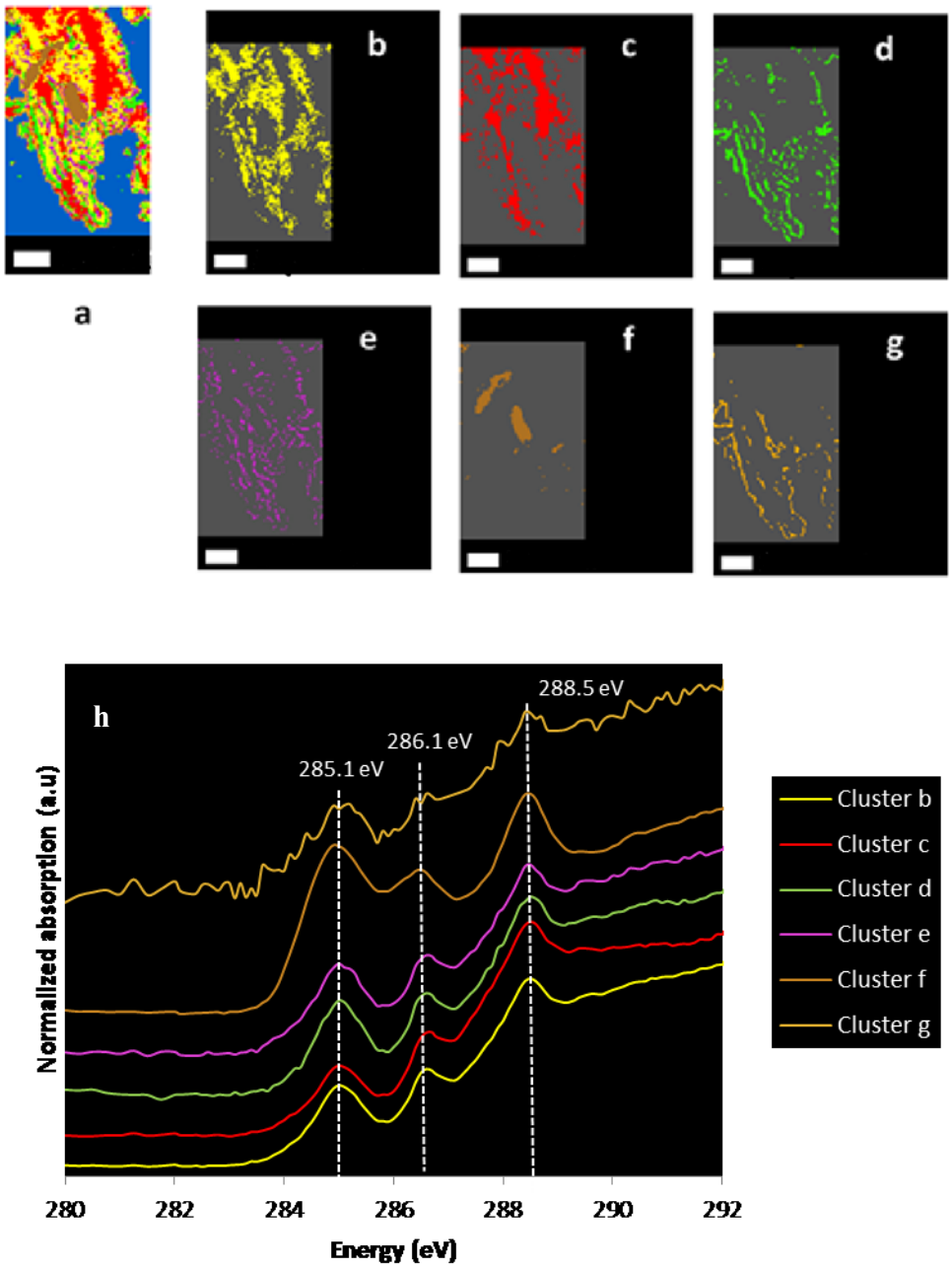

Figure 3-2 Cluster indices map of carbon (a), individual cluster images of (b-g) and carbon NEXAFS spectra (h) representing individual cluster images of CTR-100 nm thin section. CTR represents conventional till, complex crop rotation.

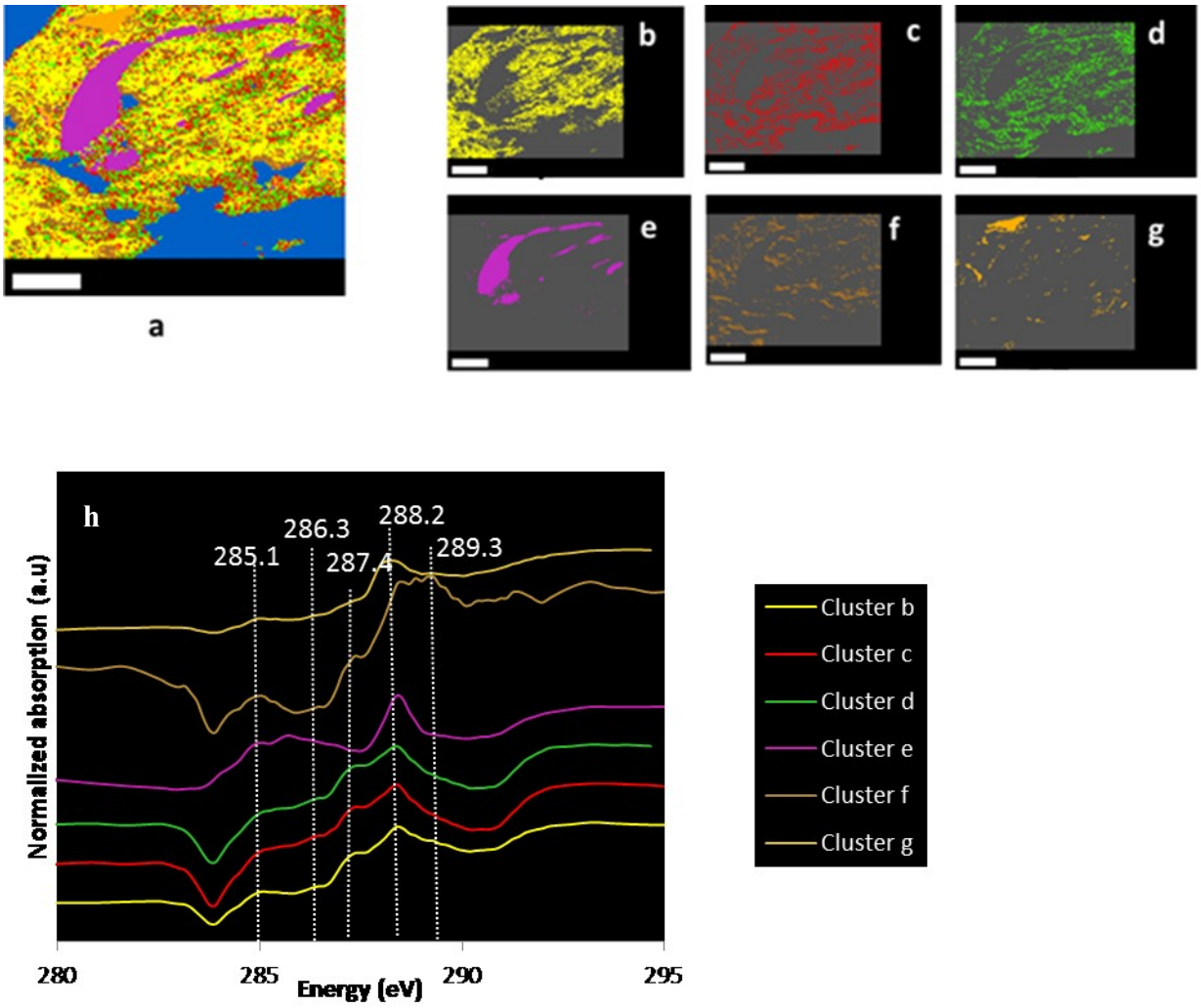

Figure 3-3 Cluster indices map of carbon (a), individual cluster images (b-g) and carbon NEXAFS spectra (h) representing individual cluster images of NTR-100 nm thin section. NTR represents no-till, complex crop rotation.

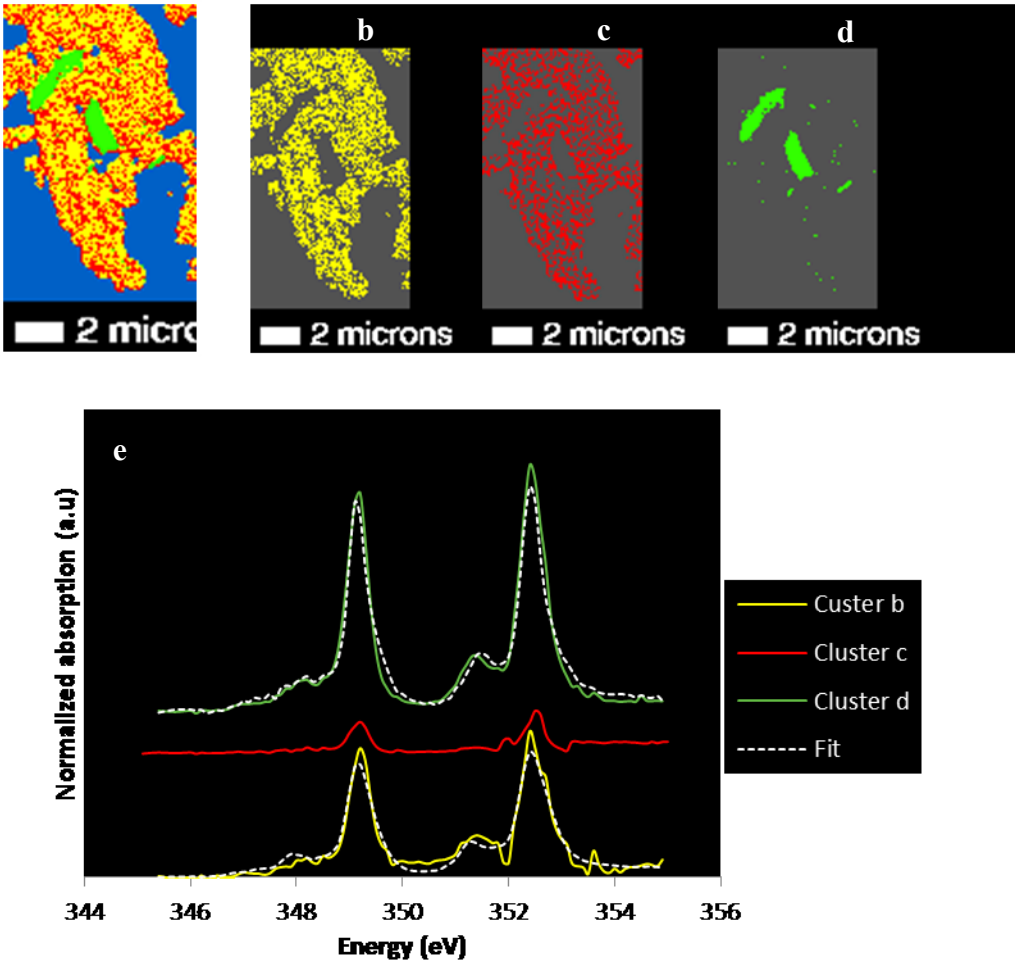

Figure 3-4 Cluster indices map of calcium (a), individual cluster images of (b-d) and calcium NEXAFS spectra (e) representing individual cluster images of CTR-100 nm thin section. CTR represents conventional till, complex crop rotation. Cluster c did not show an acceptable fit.

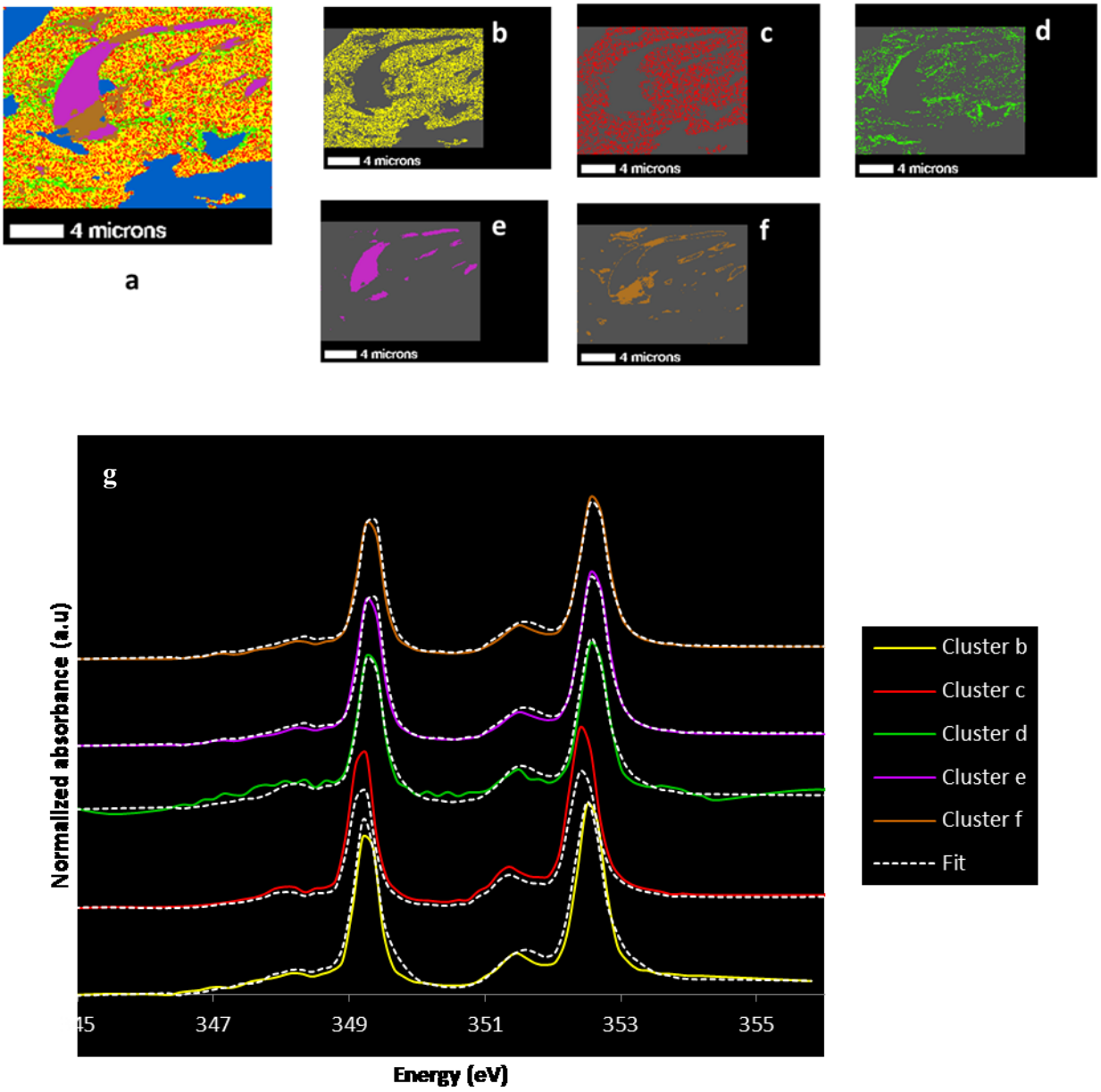

Figure 3-5 Cluster indices map of calcium (a), individual cluster images (b-f) and calcium NEXAFS spectra (g) representing individual cluster images of NTR-100 nm thin section. NTR represents no-till, complex crop rotation.

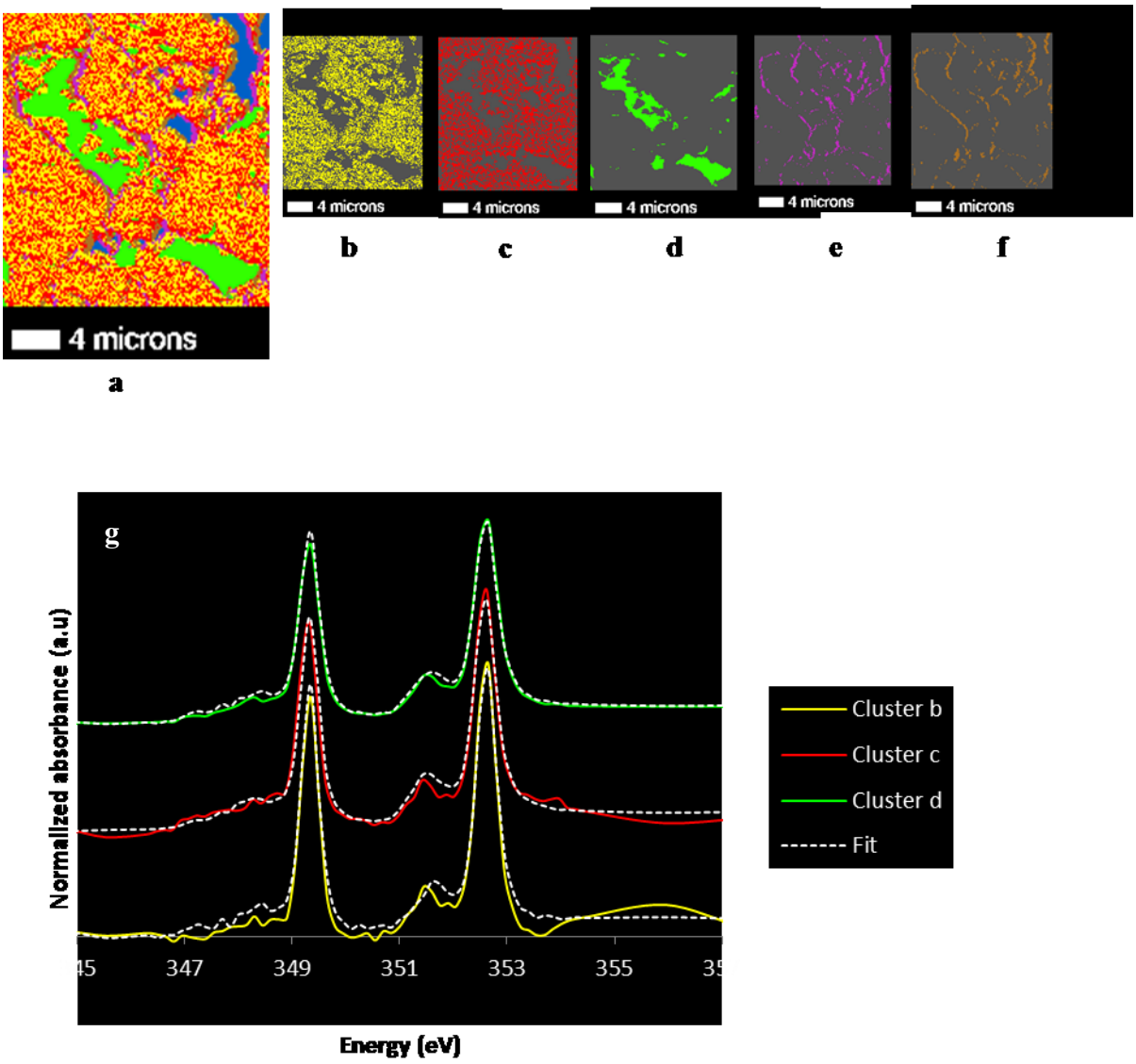

Figure 3-6 Cluster indices map of calcium (a), individual cluster images (b-f) and calcium NEXAFS spectra (g) representing individual cluster images of NTR-800 nm thin section. NTR represents no-till, complex crop rotation.

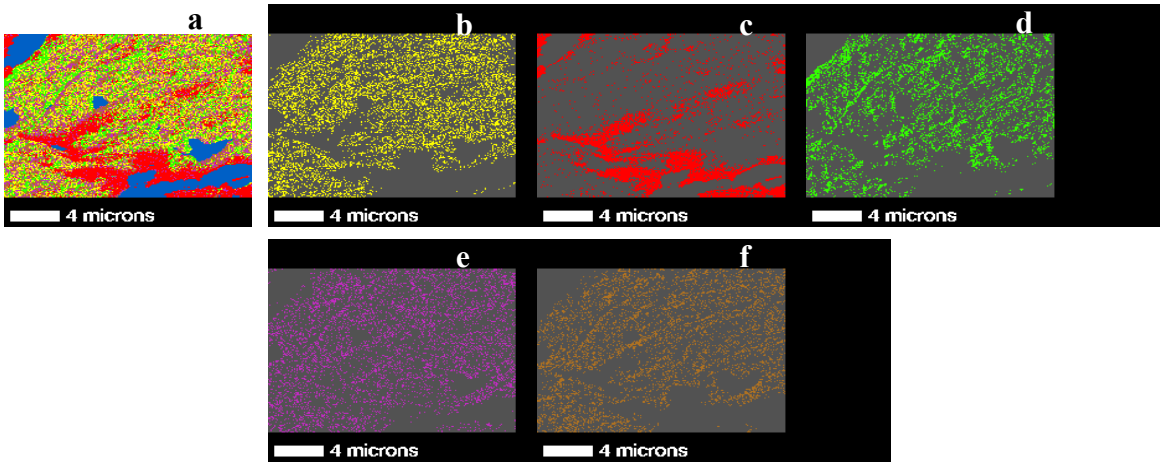

Figure 3-7 Cluster indices map of nitrogen (a) and individual cluster images (b-f) of NTR-100 nm thin section.

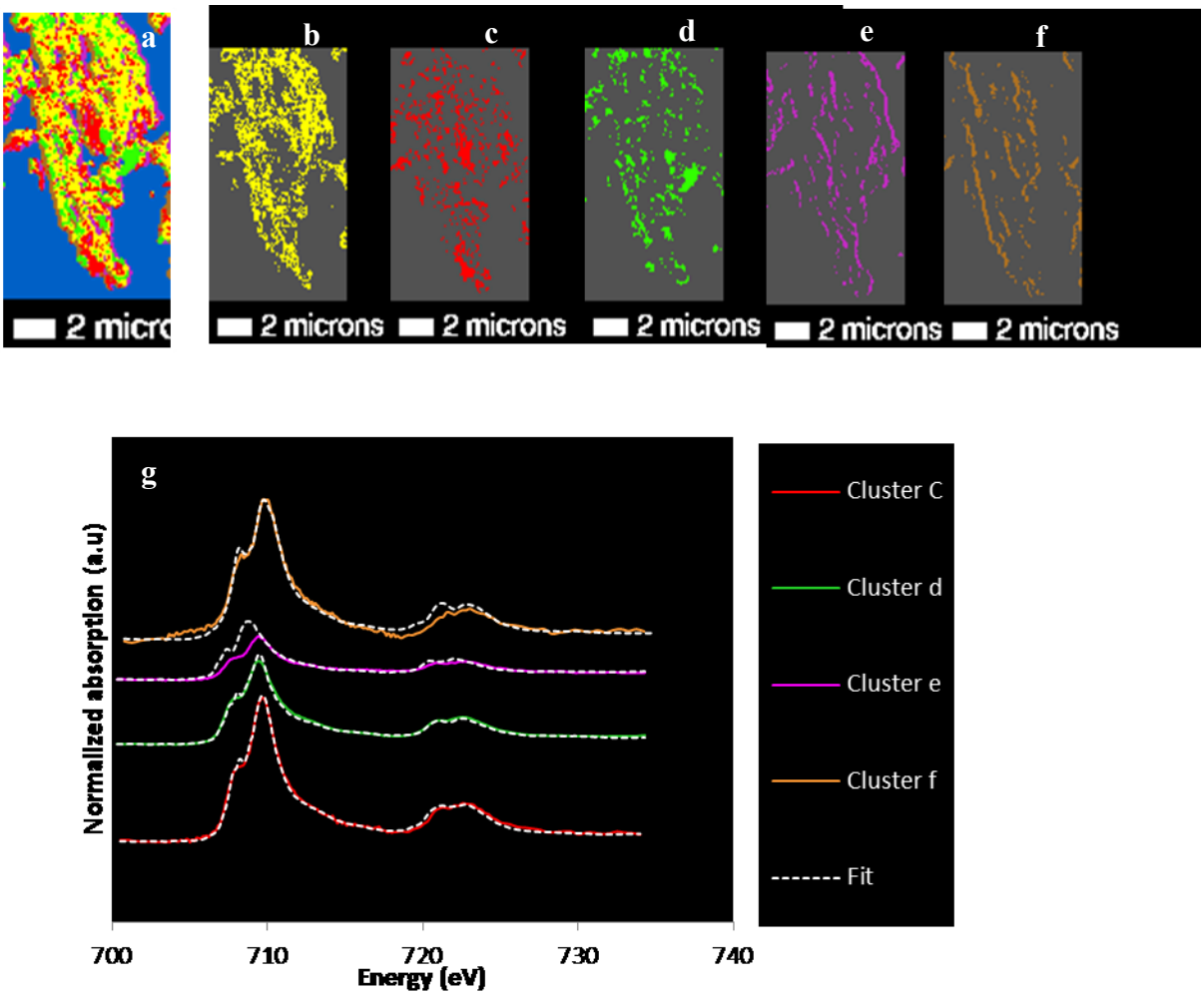

Figure 3-8 Cluster indices map of iron (a), individual cluster images (b-f) and linear combination fitting (LCF) of iron NEXAFS spectra (g) representing CTR-100 nm thin section. CTR represents conventional-till, complex crop rotation. Only the spectra with significant fits are shown.

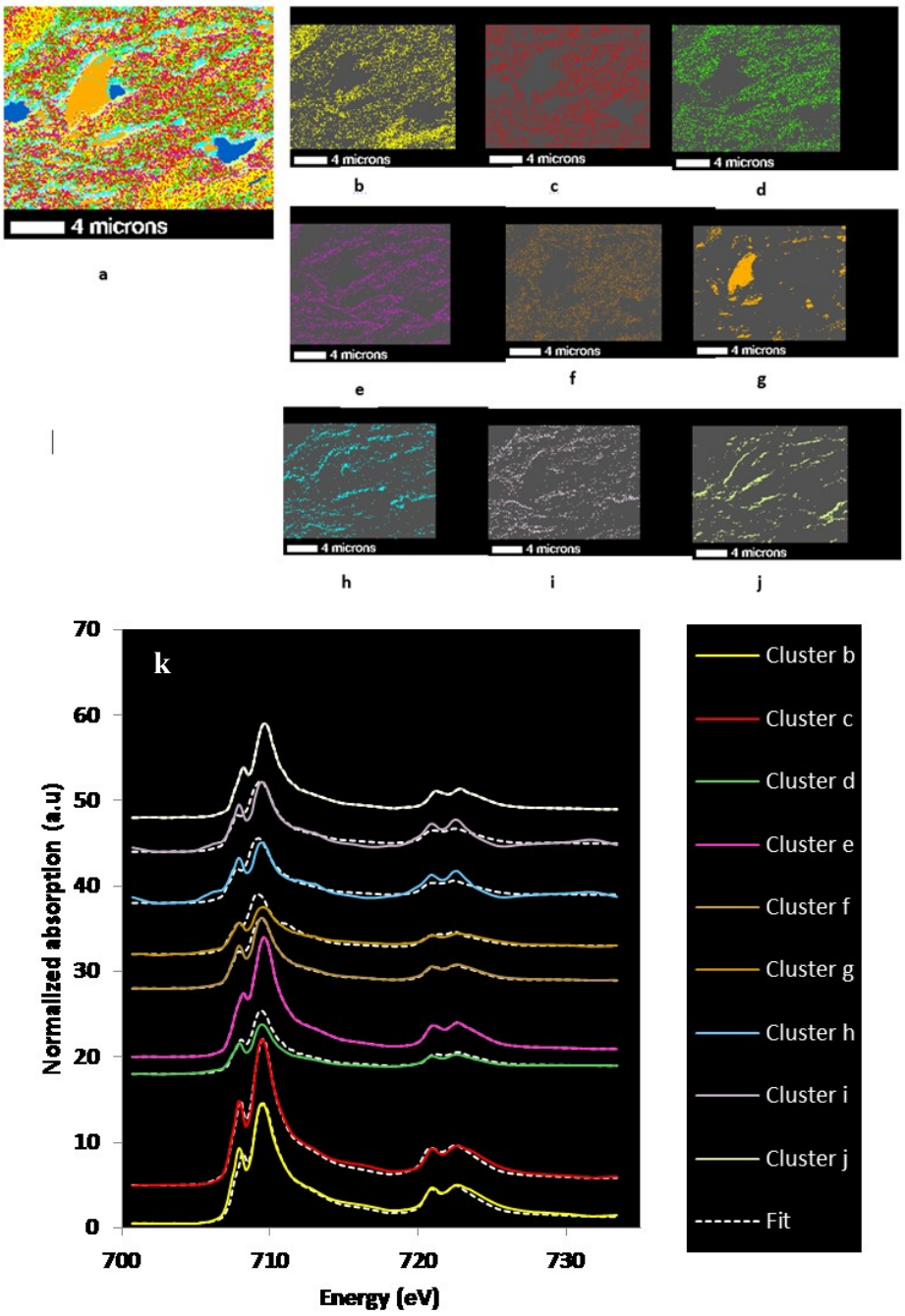

Figure 3-9 Cluster indices map of iron (a), individual cluster images (b-j) and linear combination fitting (LCF) of iron NEXAFS spectra (k) representing NTR-100 nm thin section. NTR represents no-till, complex crop rotation. Only the spectra with significant fits are shown.

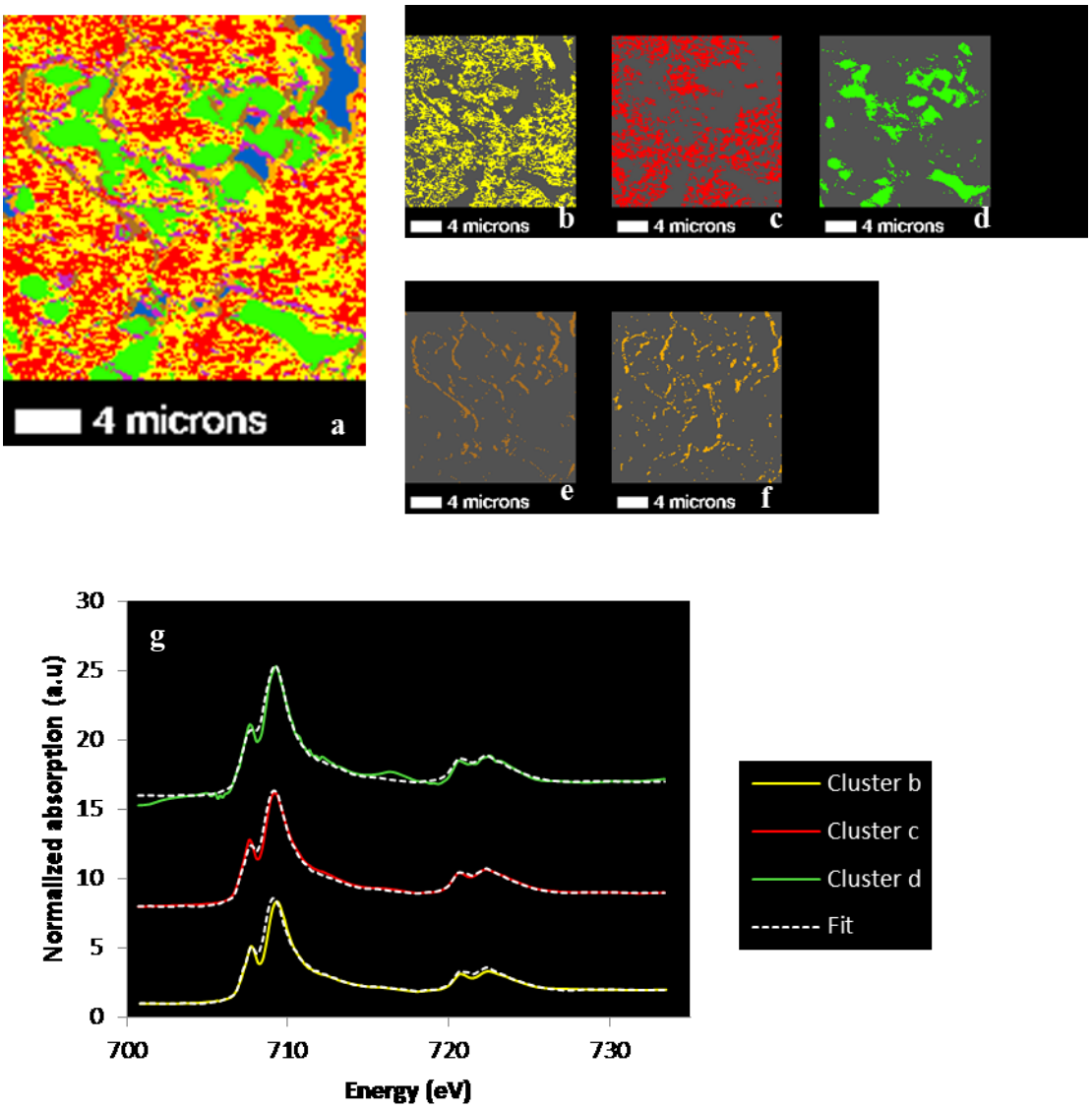

Figure 3-10 Cluster indices map of iron (a), individual cluster images (b-f) and linear combination fitting (LCF) of iron NEXAFS spectra (g) representing NTR-800 nm thin section. NTR represents no-till, complex crop rotation. Only the spectra with significant fits are shown.

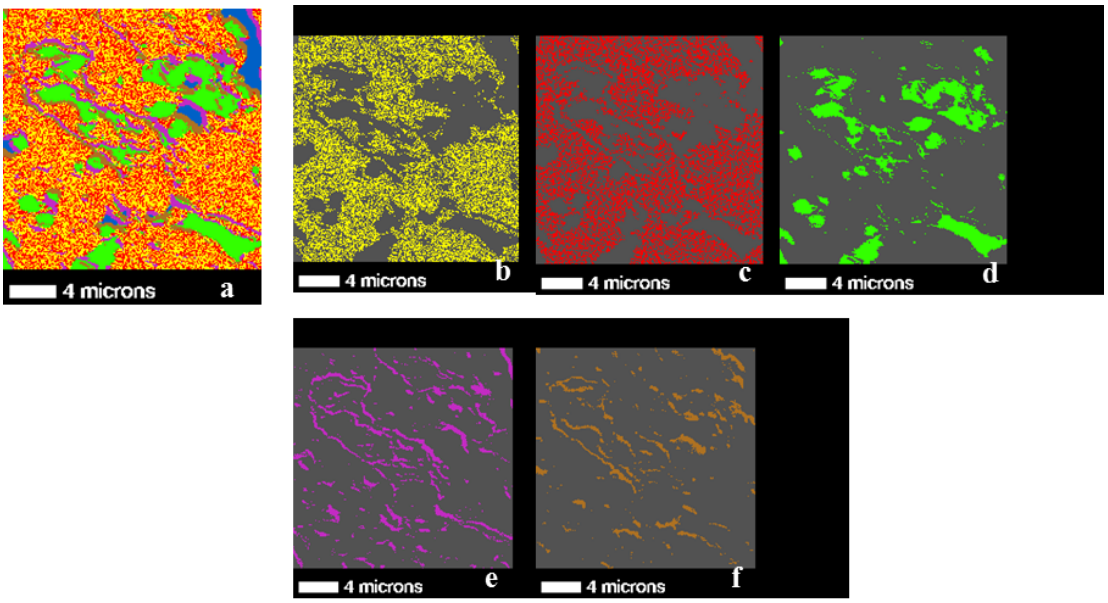

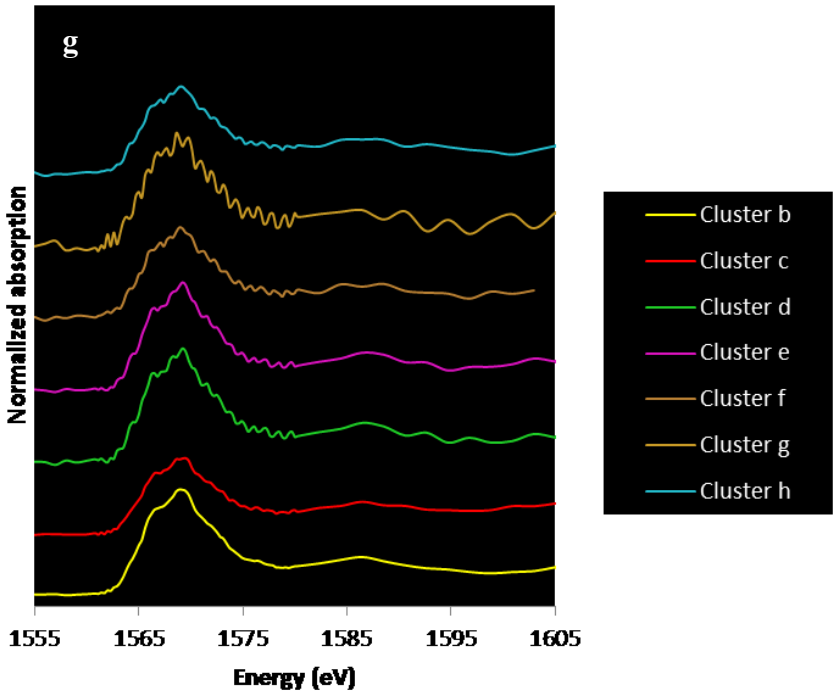

Figure 3-11 Cluster indices map of aluminum (a) individual cluster images (b-f) of NTR and aluminum NEXAFS spectra (g) representing NTR-100 nm thin section. NTR represents no-till, complex crop rotation.

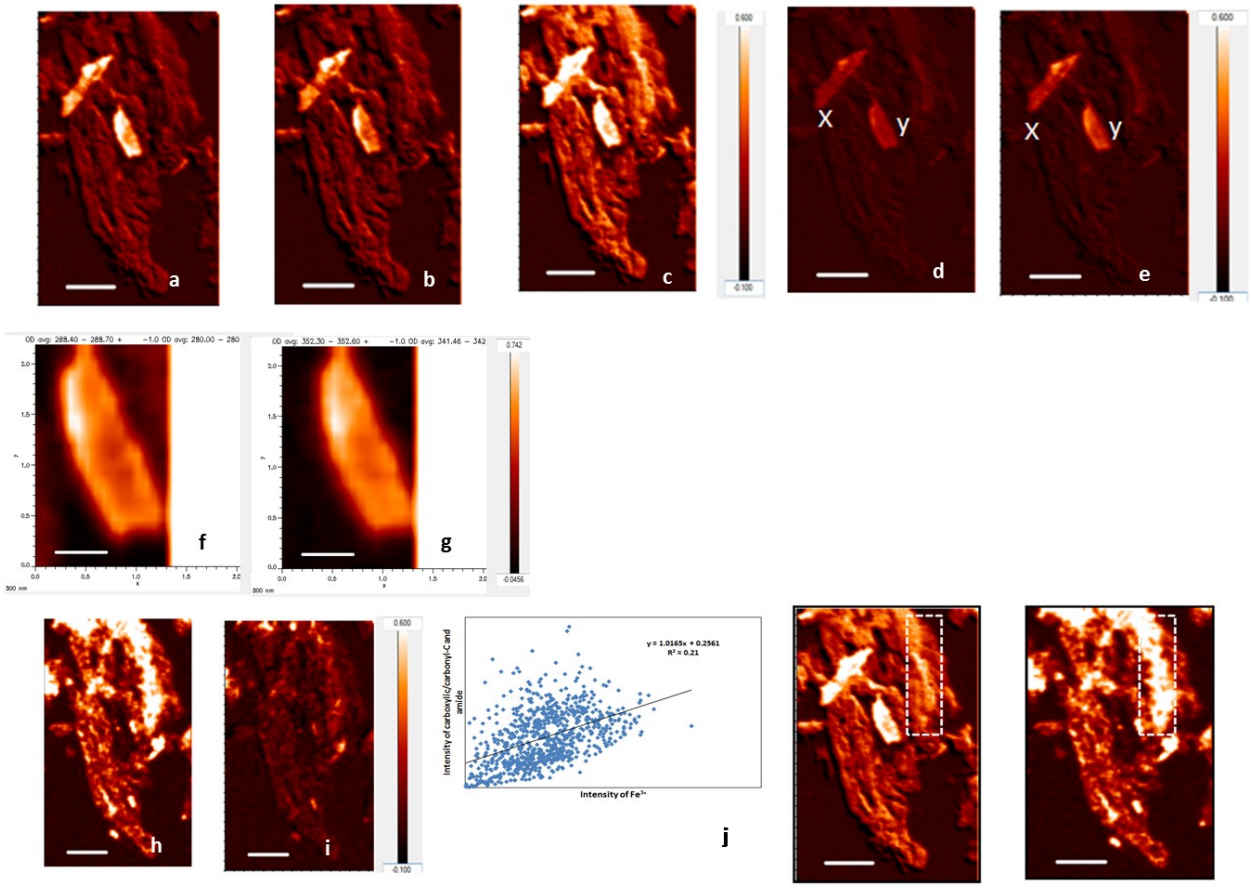

Figure 3-12 Contrast maps of CTR-100 nm thin section. Aromatic C (a), phenols/ketones (b), carboxylic C (c), and calcium contrast maps (L3- (d) and L2- (e) edges). Preserved structures are denoted with x and y. Carbon (f) and calcium (g) contrast maps of the selected preserved area y. Iron contrast maps (L3- (h) and L2- (i) edge). An elemental correlation plot of Fe and carboxylic C in the selected area (j). Dotted box (j) exhibits the selected area of the organo-mineral assemblage of carbon (left) and Fe (right) contrast maps. CTR represents conventional-till, complex crop rotation.

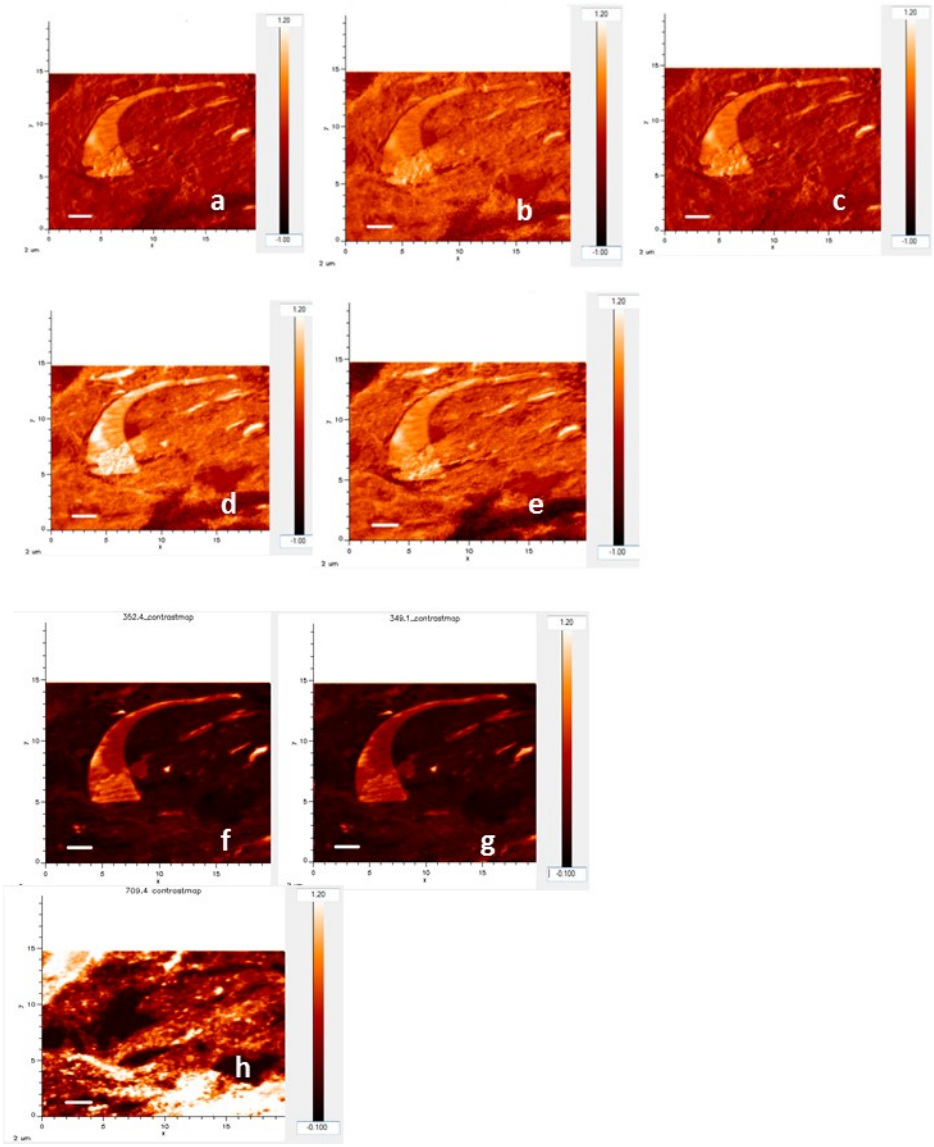

Figure 3-13 Contrast maps of NTR-100 nm thin section. Aromatic C (a), aliphatic (b), phenols/ketones (c), carboxylic C (d), and carbonyl C (e). Calcium contrast maps (L3- (f) and L2- (g) edge. Iron contrast map of L3- edge (h). NTR represents no-till, complex crop rotation.

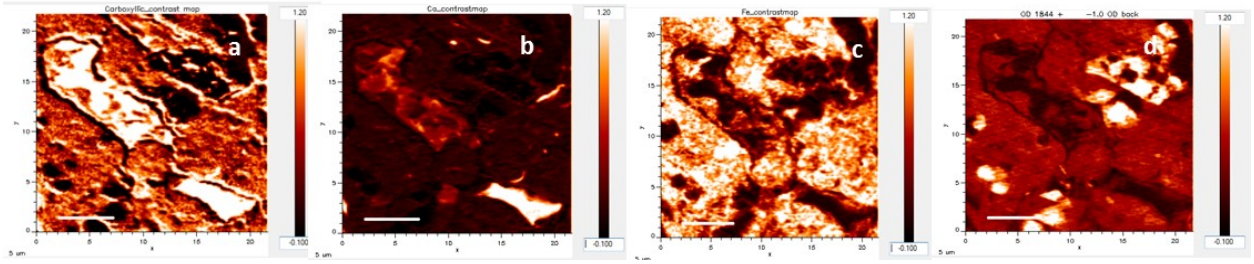

Figure 3-14 Contrast maps of NTR-800 nm thin section. Carboxylic C (a), calcium (b) contrast maps (L3 edge). Iron contrast map L3 edge (c). Silicon contrast map (d). NTR represents no-till, complex crop rotation.

Tables

Table 3-1 Peak assignment for carbon K-edge near edge X-ray absorption fine structure spectroscopy (C-NEXAFS)

Form of C	Transition	Peak energy (eV)	References
Alkylated to carbonyl-substituted aromatic C	1s-π*	284.9-285.5	Brandes et al. (2004); Braun et al. (2005)
Phenolic OH, Ketonic O-C-O		286.5-287.1	Cody et al. (1998) Hitchcock et al. (2005); Lehmann et al. (2005)
Aliphatic C-H	1s-3p/σ*	287.1-287.8	Lehmann et al., 2005
Carboxylic C	1s-π*	287.7-288.6	Lehmann et al., 2005
Carbonyl C	1s-3p, σ *	289.3-289.8	Hitchcock et al. (2005); Lehmann et al. (2005)
Carboxylic C		288.98	Li et al., 2014
Carboxylic substituted aromatic, carbonyl C=O, carbonates		290-290.5	Kleber et al., 2010 Brandes et al., 2010

Table 3-2 Percentages (%) of different carbon functional groups (based on Gaussian peak fitting) of individual clusters (b-g) representing CTR-100 nm thin section (conventional-till, complex crop rotation).

	b	c	d	e	f[#]	g
Aromatic	35.9	11.6	19	19.3	32.3	20.1
Phenol/ketones	24.5	19.5	19.2	20.1	25.2	19.8
Carboxylic	39.5	47.8	42.4	40.2	33.3	41.3
Carbonyl	-	21.1	19.4	20	9.2	18.8

[#] Preserved structure

Table 3-3 Percentages (%) of different carbon functional groups (based on Gaussian peak fitting) of individual clusters (b-g) representing NTR-100 nm thin section (no-till, complex crop rotation).

	b	c	d	e [#]	f [$]	g
Aromatic	-	-	-	12.5	-	4.1
Phenol/ketones	-	-	-	10.9	-	7.7
Aliphatic	29.4	39.6	36.3	-	17.3	10.4
Carboxylic	47	39.9	41.3	51	42.6	45.1
Carbonyl	23.5	20.5	22.3	25.6	40.1	32.6
AL/AR ratio	-	-	-			3.1

[#] Preserved structure

[$] Microbial derived

Table 3-4 Linear combination fitting of Ca-NEXAFS spectra representing individual cluster images of CTR-100nm thin section (conventional-till, complex crop rotation)

Cluster	Composition	R-factor
b	Adsorbed Ca_eps: 41.2 %; Hydrous calcium dihydrogen phosphate: 21.7 %; Calcite: 14.6%; Calcium sulphate:22.5%	0.020
d [#]	Aragonite: 6.2 %; Hydrous calcium dihydrogen phosphate:64.8% Calcium sulphate:25.4%	0.015

[#]Preserved structure

Table 3-5 Linear combination fitting of Ca-NEXAFS spectra representing individual cluster images of NTR-100 nm thin section (no-till, complex crop rotation)

Cluster	Composition	R-factor
b	Aragonite: 59.3 %;	0.08
	Hydrous calcium dihydrogen phosphate: 40.7 %	
c	Aragonite: 74.8 %;	0.2
	Hydrous calcium dihydrogen phosphate: 25.2 %	
d	Aragonite: 84.7 %; Adsorbed Ca_eps: 15.3 %	0.1
e [#]	Aragonite: 19.4 %; Adsorbed Ca_eps: 24.1 **%**	0.004
	Hydrous calcium dihydrogen phosphate: 56.5 %	
f	Adsorbed Ca_eps: 11.8 %	0.012
	Hydrous calcium dihydrogen phosphate: 88.2	

[#]Preserved structure

Table 3-6 Linear combination fitting of Ca-NEXAFS spectra representing individual cluster images of NTR-800nm thin section (no-till, complex crop rotation)

Cluster	Composition	R-factor
b	Aragonite: 12.8% Hydrous calcium dihydrogen phosphate: 87.2 % 	0.022
c	Aragonite: 33.9 % Hydrous calcium dihydrogen phosphate: 53.2 % Adsorbed Ca_eps: 12.9 %;	0.012
d [#]	Aragonite: 45.3 % Hydrous calcium dihydrogen phosphate: 17.2 % Adsorbed Ca_eps: 35.5 %;	0.004

[#]Preserved structure

Table 3-7 Linear combination fitting of Fe-NEXAFS spectra representing individual cluster images of CTR-100nm thin section (conventional-till, complex crop rotation)

Cluster	Composition	R-factor
c	Ferrihydrite 30.6%; Fe(II) hydroxycarbonate 13.2%; Ferric phosphate 45.3%; Magnetite 10.9%	0.002
d	Geothite 17.2%; Maghemite 82.8%;	0.004
e	Ferrihydrite 9.1%; Maghemite 90.9%	0.18
f	Ferrihydrite 20.2 %; Geothite 32.5%; Magnetite 45.4%; Siderite 1.9%	0.01

Table 3-8 Linear combination fitting of Fe-NEXAFS spectra representing individual cluster images of NTR-100nm thin section (No-till, complex crop rotation)

Cluster	Composition	R factor
b	Ferrihydrite 54.9 % ; Maghemite 45.1%	0.008
c	Ferrihydrite 48.7 % ; Fe(II) hydroxycarbonate 14.1% Ferric phosphate 27.8 % ; Maghemite 9.4%	0.002
d	Fe(II) hydroxycarbonate 1.6% ; Maghemite 98.4%	0.068
e	Ferrihydrite 19.7 %; Ferric phosphate 25.6 % ; Maghemite 54.7%	0.008
f	Geothite 3.9%; Ferric Phosphate 2.7 %; Maghematite 93.4 %	0.009
g	Fe(II) hydroxycarbonate 27.6%; Maghemite 72.4%	0.061
h	Fe(II) hydroxycarbonate 6.2%; Ferric phosphate 4.7% Maghemite 89.1%	0.047
i	Ferric phosphate 11.8%; Maghemite 88.2%	0.026
j	Ferric Phosphate 13.7 % Maghematite 86.3 %	0.044

Table 3-9 Linear combination fitting of Fe-NEXAFS spectra representing individual cluster images of NTR-800 nm thin section (no-till, complex crop rotation)

Cluster	Composition	R-factor
b	Maghemite 98.7%; Ferric phosphate 1.3%	0.018
c	Maghemite 88.6%; Ferric phosphate 11.4%	0.005
d [#]	Maghemite 78.3%; Ferric phosphate 21.7%	0.008

[#]Preserved structures

Chapter 4 - Exploring Secrets behind Carbon Preservation in Soil Microaggregates from a Temperate Agroecosystem

Abstract

Carbon (C) is the most complex piece in soil, where most of the underlying mechanisms remain hidden even after decades of soil C research. Research goals aimed to recognize soil C preservation mechanisms in microaggregates with preserved aggregate architecture, using a spectromicroscopy approach. Additionally, bulk chemical analyses were used to support submicron scale level findings. Free microaggregates were collected from a long-term corn system (Manhattan, KS, USA), which had been under no-till with fertilizer additions for 22 years. One hundred-nanometer thin sections were obtained from microaggregates using a cryo-ultramicrotome. Spectromicroscopy study provided evidence on direct preservation of organic C, probably inside soil micropores, which ultimately contributed to soil C sequestration. The presence of relatively labile C inside the microaggregates substantiated that the preservation is not purely related to substrate chemistry. Both bulk and spectromicroscopy approach provided information on organo-mineral associations. Bulk analyses of microaggregates indicated the involvement of manure/compost addition in the enhancement of soil C, reactive minerals, and preservation of macromolecular C of humic acid. Overall, organic C dynamics inside microaggregates is influenced by a large array of biotic and abiotic processes.

We suggest the primary mechanism in C sequestration as the direct preservation of OC sources inside microspores. Restricting the entry of microbes and organo-mineral associations also play a major role in further preservation of the OC sources. This study supports the recent claims that the soil organic C preservation is an ecosystem property.

Introduction

Increasing atmospheric carbon dioxide (CO_2) is one of the global challenges in the 21st century. Enhancing the removal and minimizing the emission of atmospheric greenhouse gases could be achieved through management strategies as brought forward by the Agriculture, Forestry, and Other Land Use (AFOLU) sector (Smith et al., 2014). Soil, the largest terrestrial carbon (C) pool can serve as a sink and/or a source of anthropogenic CO_2. With reduced/no-till, increased cropping intensity, incorporation of soil amendments, cover cropping, and crop rotation, soil can serve as a sink of atmospheric CO_2, either reducing heterotrophic soil respiration or enhancing C input (Paustian et al., 2000).

Carbon is the most complex piece in soil. It is necessary to reveal the underlying processes to justify the benefits of soil organic C (SOC) sequestration (Kong et al., 2005). The key mechanisms of C preservation are related to the inherent nature of OC (i.e. biochemical recalcitrance) and physicochemical mechanisms such as chemical stabilization and physical protection (Sollins et al., 1996). The current understanding states that the persistence of C is governed not only by its recalcitrant nature; also by the influence from the surrounding (Schmidt et al., 2011). In addition, Lehmann and Kleber (2015) proposed the soil continuum model (SCM) highlighting the inaccessibility of microbiota and the contribution of soil minerals in preserving C. There exists a knowledge gap on mechanisms of C preservation, urging the necessity for more in-depth studies. Further, Han et al. (2016) highlighted the significance of researching OC preservation mechanisms in nanometer to micrometer-sized microaggregates.

The microaggregate fraction (20-250 μm) contains a highly stable C pool (Beare et al., 1994; Elliot, 1986; Balesdent et al., 2000). Jastrow et al. (1996) stated that the turnover rate of C associated with free stable microaggregates, is three times slower than the C associated with

macroaggregates. Associations of bacterial residues/hyphal debris and primary particles/clay microstructures form silt-sized microaggregates (20-53 μm) while fungal and plant debris form large microaggregates (Wilson et al., 2009).

Scanning transmission X-ray microscopy coupled with near edge X-ray absorption fine structure spectroscopy (STXM-NEXAFS) aids in imaging micrometer-sized specimens at nanometer scale spatial resolution with minimum damage. In recent soil science research, STXM-NEXAFS was successfully used in investigating organo-mineral associations (Chen and Sparks, 2015; Kinyangi et al., 2006; Lehmann et al., 2008; Solomon et al., 2012). Element-specific component maps for a wide range of biologically significant elements (i.e. C, N, O, P, S), alkaline metals (i.e. Na, Ca, K, Mg), first row transition metals (i.e. Fe, Mn, Ti), Al, and Si can be generated at a high spatial resolution (<25 nm) (Dynes et al., 2015).

There are no published studies focused on *in situ* analysis of microaggregates from long-term temperate agroecosystems with preserved aggregate architecture using spectromicroscopy. This chapter follows a companion study of Chapter 3 that was based on a tropical agroecosystem. In this study, the objectives were to understand soil C preservation mechanisms in soil microaggregates with *in situ* natural conditions by imaging C and relevant elements, and to perform bulk chemical analyses to better elucidate submicron scale organo-mineral findings.

Materials and Methods

Soil sampling and sample preparation

The experiment was a long-term (established in 1990) continuous corn system (*Zea mays L.*), located at the North Agronomy Farm, Manhattan, Kansas, USA (39º 12’42” N, 96º 35’ 39” W). The soil was a moderately well-drained Kennebec silt loam (fine-silty, mixed superactive, mesic Cumulic Hapludolls) with sand, silt, and clay content of 9%, 69%, and 22%, respectively

(Mikha et al., 2005). The clay fraction was dominated with 2:1 layer silicates (montmorillonite). The sampling plots represented no-till and three different fertilizer treatments; control (NTC), (manure/compost-NTM), and fertilizer (NTF). With the basis of supplying 168 kg ha^{-1} yr^{-1} of N, two sources of N (urea or manure/compost) were added. Fresh cattle manure was added in the first ten years and compost was applied since 2000. The soil was collected from 0-5 cm depth in February 2012 for this study.

Sample preparation and analysis

Preparation of intact ultrathin sections, spectromicroscopy data acquisition, and data analysis were conducted following the methodology described in Chapter 3. The NTM thin section was analyzed at the Advanced Light Source (ALS), Berkeley, USA at beamline 5.3.2.2 (polymer STXM). Other two thin sections (NTF and NTC) were analyzed at the Canadian Light Source (CLS), Saskatoon, Canada at SM (10ID-1) beamline. Cluster analysis, which is proven as a successful method for recognizing chemically distinct regions of biological samples, was used to assemble the areas into groups considering similar spectral properties and thickness (Lerotic et al., 2004). Bulk chemical analyses were also conducted for the microaggregate fraction as described in Chapter 3.

Results and Discussion

Carbon spectromicroscopy

The spectromicroscopy analysis exhibited a complex and heterogeneous spatial distribution of OC (Fig. 4-1, 4-2 and 4-3). Uneven spatial distribution of OC suggested the preservation of C in micro- and nanopores. The cluster analysis identified distinct coagulated C-rich areas sharing similar spectral properties (Fig. 4-1, cluster d; Fig. 4-2, cluster d). Individual cluster map d of NTC (Fig. 4-1) recognized a C-rich area (approximately 2 μmx3 μm), which

could be a reflectance of preserved OC with a distorted morphology. The complex nature of OC could be linked with the continuous incorporation of C. All soils received corn crop residues since their establishment in 1990, in addition to the fertilizer additions.

The resonance peaks of C-NEXAFS spectra were identified by published literature (Table 4-1). Peaks representing aromatic ring structures (284.9-285.5 eV), shoulder representing aliphatic C and imidazole ring structures (287.1-287.8 eV), carboxylic C (287.7 -288.8 eV) and carbonyl/carbonate C (290-290.5 eV) were identified. The peak around 285.1 eV corresponded to the π* of atoms in unsaturated aromatic ring structures reflecting aromatic protein macromolecules, amino acids with aromatic side chains and nucleobases (Solomon et al., 2012). Cluster c of NTC (Fig. 4-1) showed a shift of the carboxylic C peak towards the lower energy (288.2 eV), indicating carboxylic and amide type C associations (Lawrence et al., 2003). Carboxylic C with amide features was an indicative of microbial-derived C (Keiluweit et al., 2012). Moreover, Benzerara et al. (2006) attributed a peak at 288.2 eV to microbial cells. They observed the peptide bonds of microbial cells get excited approximately around 288.2 eV. All other C-NEXAFS spectra denoted resonances representing carboxylic C at 288.4 eV, implying the plant-derived nature. Gaussian peak fitting was done for each normalized spectra to obtain the relative proportions of C functional groups. The peak fitting indicated a high proportion of carboxylic C (38.7%-97.5%) in all thin sections (Table 4-2, 4-3 and 4-4). Microaggregates representing NTF and NTC indicated a greater proportion of carboxylic C than NTM. Instead, NTM showed a high proportion of aliphatic and aromatic C. The presence a high proportion of labile aliphatic C in NTM could be an indication of robust organic C protection mechanisms.

Calcium spectromicroscopy

Heterogeneous distribution of Ca was observed (Fig. 4-4, 4-5, and 4-6). The spectromicroscopy analysis identified two well-resolved peaks (349.2 eV and 359.2 eV) with less intense crystal field peaks. The less intense crystal field peaks can be due to the amorphous nature of Ca minerals (Politi et al., 2008) which can be re-precipitates or new microbial-derived mineral precipitates. Short range order (SRO) amorphous minerals are highly active and possess high surface area and hydroxyl groups (Kramer et al., 2012; Schlesinger, 2005). The linear combination fitting (LCF) indicated the presence of aragonite, Ca adsorbed to extracellular polysaccharides (EPS), hydrous calcium dihydrogen phosphate, calcium sulfate, and calcite (Table 4-5, 4-6 and 4-7). The presence of aragonite like mineral species represents transient precursors of calcite precipitation that is mediated by cyanobacterial communities (Obst et al., 2009). Moreover, researchers have observed the nucleation of amorphous aragonite like minerals associated with EPS (Obst et al., 2009). Amorphous calcium carbonate transforms into crystalline calcite through a series of reactions involving dehydration, dissolution, and re-precipitation (Rodriguez-Blanco, 2011) and therefore, the presence of aragonite and amorphous carbonate indicates biologically and chemically active soil aggregates.

Nitrogen spectromicroscopy

The chemistry of organic N is poorly understood and a significant portion of N is classified as “unknown” (Stevenson, 1994). Nitrogen NEXAFS of NTC and NTF identified peaks around 401.4, 405.2, 411, 412, 414, and 420 eV (Fig. 4-7 and 4-8). Both thin sections (NTC and NTF) exhibited spectral features within the range from 398.6 to 405 eV. This represented 1s–π* and 1s–σ* transitions that occur at energies >405 eV (Leinweber et al., 2007). Ammonium compounds exhibits π* and 1s–σ* resonances around 401 eV and 412 eV,

respectively (Leinweber et al., 2007). A peak at 401.2 eV indicated the presence of microbial-originated amino acids, amines, amides, and heterocyclic N compounds (Solomon et al., 2012). A distinct sharp peak was noted in cluster g of NTC at 405.2 eV corresponding to NO_2 π* resonance (La et al., 2003). The peaks appeared at 412 and 420 eV resembled σ*(N-C) excitations (Polzonetti et al., 2004).

Iron spectromicroscopy

Iron NEXAFS spectra corresponding each individual cluster exhibited multiple Fe L3- (708.1 and 709.6 eV) and L2- (721.1 and 722.5 eV) edges. The shape of the Fe L3 2P3/2 signal indicates the oxidation status of Fe. Peaks at 708.1 and 709.6 eV illustrate the presence of $Fe^{2+}$and Fe^{3+}, respectively (Dynes et al., 2006; Hitchcock et al., 2009). Linear combination fitting identified the presence of ferrihydrite, maghemite, goethite, iron(II) hydroxycarbonate, and siderite like minerals. Good fits (as indicated by chi-square statistics) were obtained only for some spectra of NTC and NTF (Table 4-8 and 4-9). Maghemite and goethite like minerals were the most abundant forms of Fe minerals found in NTC and NTF. Reduced forms of Fe minerals that were found in some clusters reflected the biotic and abiotic processes. Common Fe^{2+} minerals such as siderite, green rust (iron(II)hydroxycarbonate/chukanovite), and magnetite-like minerals were also identified (Peretyazhko and Sposito, 2005). In addition, root exudates are capable of reductive dissolution of Fe^{3+} minerals (Pédrot et al., 2011).

Aluminum spectromicroscopy

Aluminum NEXAFS differentiates four and six-fold coordinated Al minerals (Hu et al., 2008). Four-fold coordinated Al minerals possess strong single edge maxima at 1565.4 eV, 1566.8 eV, and 1566.4 eV with poorly defined features at high energy levels (Ildefonse et al., 1998). Six-fold coordinated Al species such as gibbsite and kaolinite display two main maxima

at 1567.8±0.4 eV and 1571.7±0.5 eV (Ildefonse et al., 1998). Thin sections of NTC and NTF showed well-resolved, distinct features within the energy range from 1566 to 1588 eV. Linear combination fitting of Al-NEXAFS spectra identified the presence of kaolinite, montmorillonite, muscovite, and illite like minerals. Kaolinite and muscovite appeared to be the dominant mineral species in NTC and NTF (Table 4-10 and 4-11). The cluster d of NTF indicated a peak at 1565.9 eV corresponding to four-fold aluminum phosphate (Hu et al., 2008). Some clusters had a peak around 1571.3 eV, indicating the presence of SRO minerals.

Contrast maps of the studied areas

Visual observations of contrast maps showed intimate associations of C and Ca, indicating a significant involvement of Ca-based minerals in C preservation (Fig. 4-9, 4-10 and 4-11). The contrast maps showed clear associations of Ca and carboxylic C indicating polyvalent cation bridging (Lutzow et al., 2006). Associations between Fe and OC were evident in some areas of the thin section. In NTC, the distribution of Fe and N had distinct spatial similarities, providing evidence for association between N and Fe compounds in the soil aggregate (Fig. 4-12). In NTF, C, Ca, Fe, and Al indicated co-existence to a certain extent (Fig. 4-10 and 4-13). Iron contrast maps of NTM indicated the presence of a strong lining of Fe outside the thin section (Fig. 4-14). An area of NTC was clipped to concentrate on a selected small area as displayed in Fig. 4-9 e. The statistical analysis of the selected area indicated significant correlations ($p<0.0001$) between C functional groups and Ca and the relationship between the carboxylic C and Ca was the strongest. None of the C functional groups showed a statistically significant correlation with Fe for the clipped area.

Bulk chemical analysis

Microaggregates from manure/compost added soils (NTM) indicated significantly high TOC than other treatments (NTF and NTC) (Fig. 4-15 a). Moreover, NTM showed a higher reactive mineral fraction (amorphous Fe and ammonium oxalate extractable-Al/Si) in comparison to NTC and NTF (Fig. 4-15 b). Significant strong correlations were observed for OC and reactive mineral fraction, providing evidence on chemical stabilization (Fig. 4-15 c). It has been found that the recalcitrant C pool possesses a strong correlation with the active mineral fraction (Mikutta et al., 2005; Torn et al., 2007).

Moreover, the macromolecular chemistry of HA indicated treatment effects. In high performance liquid chromatography (HPLC) study, peaks appeared during the times of 3-4, 4-5.3, 14.5-17.5, and 19-21 min. Hydrophilic (HIL) and hydrophobic (HOB) portions were calculated during the times from 3-6 min and 11-22 min, respectively. The HOB and HIL nature of the HA determine the solubility, susceptibility to degradation, and the sorption potential (Debska and Gornet, 2007). The increase in the HIL nature corresponded to a high maturity; thus a high degree of humification (Debska and Gornet, 2007). The highest and the lowest ratios of HIL/HOB were obtained for NTC and NTM, respectively (Fig. 4-15 d). The low degree of humification in manure/compost added microaggregates (NTM) may be an indicative of C preservation due to enhanced formation of organo-mineral associations, attributed to high content of reactive minerals. Except in NTC microaggregates, the ratios of aromatic/aliphatic C (AR/AL) obtained from ^{13}C-NMR (Fig. 4-15 e) were in agreement with HIL/HOB ratio from HPLC (Fig. 4-15 d). Both techniques showed that the HA from NTM was less humified than the HA from NTF.

Highlights on soil C preservation

Carbon spectromicroscopy illustrated coagulated OC inside soil pores that were protected against decomposition (Krull et al., 2003; Six et al., 2004). Exerted physical protection over spatial and kinetic constraints prevents the microbial degradation in temperate soils (McCarthy et al., 2008). Moreover, they elaborated the benefit of encapsulation of OC in soil pores over chemical stabilization. The presence of high content of soil OM is beneficial in stabilizing aggregates in the studied soil (Mollisols), dominated with 2:1 layer silicates (Oades and Waters, 1991; Six et al., 2000).

The peak at 290.2/290.3 eV reflects either carbonyl C (Kleber et al., 2011; Brandes et al., 2010) or carbonate C (Karunakaran et al., 2015; Benzerara et al., 2006). The less intense nature of the peak at 290.3/290.2 eV, and the weak correlation observed between Ca and C suggested the absence of $CaCO_3$ (Wan et al., 2007; Benzerara et al., 2006). Additionally, the less strong correlation observed between Ca and C indirectly indicated the non-existence of $CaCO_3$.Coversely, Ca-NEXAFS identified the presence of $CaCO_3$ minerals to a certain extent. Therefore, the peak could be attributed to carbonyl C or carbonate. The presence of carbonyl C that is abundant in organic acids/proteins resembled microbial activities inside microaggregates (Ng et al., 2014). A relatively high proportion of carboxylic C was observed in comparison to other C functional groups in all the thin sections. Ligand exchange reactions between hydroxyl groups of mineral surfaces and carboxylic C associated with SOC leads in the chemical stabilization (Gu et al., 1994). Cluster c of NTC (Fig. 4-13) indicated the presence of microbial-derived C implying the biotic involvement. The AL/AR ratio of C-NEXAFS spectra (Table 4-2, cluster b, c, and g; Table 4-3, cluster e and f; Table 4-4, cluster b, c, d, and e) indicated the degree of humification, reflecting the proportion of relatively labile and stable C (Ceccanti et al.,

2007; Marinari et al., 2007a). With further humification, the aromaticity of humic substances gets enhanced due to the formation of polycondensed rings (Xing and Chen, 1999; Chen and Pawluk, 1995; Ding et al., 2002). The spatially varied AL/AR ratio in cluster maps indicated a spatial variability in humification. The unevenness of humification can be attributed to the clear sub-micron level variability in physicochemical and biological contribution inside the microaggregate.

In NTC, the spatial distribution of Ca in cluster b (Fig. 4-4) resembled the distribution of C in cluster c (Fig. 4-1) to a certain extent. Carboxylic C of cluster c was found to be microbial-originated (carboxylic peak at 288.2 eV) and the Ca-NEXAFS identified the presence of aragonite and Ca adsorbed to EPS (Table 4-4). From these observations, microbial-mediated processes occur inside microaggregates in intervening C budgets were evident. Calcium ions participate in cation bridging with EPS (Hitchcock et al., 2009). Moreover, the mineral and EPS associations were found to be the precursors of organo-mineral complexes in soil (Chenu and Stotzky, 2002). The high specific surface area corresponding to the amorphous nature of Ca minerals favors chemical stabilization. The presence of amorphous $CaCO_3$ and aragonite could be related to the inhibitory effect imposed by organic molecules in hindering further crystallization (Manoli et al., 2002). Additionally, organic molecules promote nucleation sites to form amorphous Ca minerals (Grassmann and Lobmann, 2004). In the studied site, the long-term addition of manure/compost may have promoted the formation of Ca/Si nanoparticles (Wang et al., 2016) that are effective in accumulating SOC (Wang et al., 2016). Nitrogen compounds with microbial origin were observed indicating that these compounds could be protected in soil pores, minimizing the pathways of microbial accessibility. Furthermore, the co-existence of N with Al/Fe was observed in contrast maps most likely indicating the N sequestration by Fe oxides and

clay minerals (Vogel et al., 2015) which occurs through cation exchange and ionic, covalent, hydrophobic, and hydrogen bonding as well as Van der Waals forces (Solomon et al., 2012). Abundant montmorillonite in the studied soil might have been beneficial in fixing ammonium ions (Cavalli et al., 2015).

The co-existence of C and Fe in particular areas illustrated C preservation through chemical stabilization. Iron minerals with reduced Fe^{2+} (i.e., metastable ferrihydrite like minerals) were found in microaggregates. The occurrence of ferrihydrite is favorable in accumulating plant-based C compounds and retarding the biodegradation (Neurath et al., 2015). Anaerobic microsites inside microaggregates slow down the microbial activities. Eusterhues et al. (2014) reported the potential of ferrihydrite in lowering the biodegradation of polysaccharides and inhibition of lignin degradation upon association. Short range ordered Al (oxy)hydroxides are vital in C storage and preservation (Torn et al., 1997; Rasmussen et al., 2005). The presence of an assortment of Ca, Al, and Fe minerals provide a range of polyvalent cations, hydroxyl surface functional groups and edges that possess the tendency to attract microbial biopolymers (Solomon et al., 2012).

Bulk chemical analysis hinted on chemical stabilization mechanisms showing strong significant correlations between the reactive mineral fraction and OC. This supported the submicron scale level observation witnessed in contrast maps. Enhancement of amorphous Fe in manure/compost added soils link with the ligand-promoted dissolution of crystalline Fe minerals or the blocking of crystallization of amorphous Fe minerals (Abdala et al., 2015). Moreover, manure addition incorporates additional Fe to soil. Chemistry of macromolecular HA highlighted the nature of sequestrated recalcitrant C. The HA of NTM suggested a slow degree of humification, signifying the benefits of manure/compost addition. In contrast to Oxisols (Chapter

3 and 5), which showed that the preservation of SOC predominately due to physical protection by minerals, in Mollisols chemical stabilization mechanisms were appeared to be more significant.

Summary

This study revealed the potential of using a non-invasive spectromicroscopy approach to unravel the submicron level information of soil C preservation. Furthermore, this study provided evidence on direct preservation of OC in microaggregates. A variety of biotic and abiotic processes contributing to SOC stabilization was apparent. Submicron level information and bulk analyses provided useful insight on soil organo-mineral associations. Moreover, bulk data highlighted the importance of manure/compost addition on enhancing stored C concentrations, reactive minerals and the preservation of macromolecular C of HA.

We propose the primary mechanisms of soil C sequestration in studied Mollisols are: direct preservation of OC sources inside pores of microaggregates by restricting the entry of microbes; and the organo-mineral associations. The findings support the concepts proposed by the Schimidt et al. (2011) and Lehmann and Kleber (2015) by providing submicron scale level evidence.

References

Abdala, D.B., I.R. da Silva, L. Vergütz and D.L. Sparks. 2015. Long-term manure application effects on phosphorus speciation, kinetics and distribution in highly weathered agricultural soils. Chemosphere 119:504-514.

Balesdent, J., C. Chenu and M. Balabane. 2000. Relationship of soil organic matter dynamics to physical protection and tillage. Soil Tillage Res. 53:215-230.

Beare, M., P. Hendrix, M. Cabrera and D. Coleman. 1994. Aggregate-protected and unprotected organic matter pools in conventional-and no-tillage soils. Soil Sci. Soc. Am. J. 58:787-795.

Benzerara, K., N. Menguy, P. Lopez-Garcia, T.H. Yoon, J. Kazmierczak, T. Tyliszczak, F. Guyot and G.E. Brown Jr. 2006. Nanoscale detection of organic signatures in carbonate microbialites. Proc. Natl. Acad. Sci. U. S. A. 103:9440-9445.

Brandes, J.A., C. Lee, S. Wakeham, M. Peterson, C. Jacobsen, S. Wirick and G. Cody. 2004. Examining marine particulate organic matter at sub-micron scales using scanning transmission X-ray microscopy and carbon X-ray absorption near edge structure spectroscopy. Mar. Chem. 92:107-121.

Brandes, J.A., S. Wirick and C. Jacobsen. 2010. Carbon K-edge spectra of carbonate minerals. Journal of Synchrotron Radiation 17:676-682.

Braun, A., F. Huggins, N. Shah, Y. Chen, S. Wirick, S. Mun, C. Jacobsen and G. Huffman. 2005. Advantages of soft X-ray absorption over TEM-EELS for solid carbon studies—a comparative study on diesel soot with EELS and NEXAFS. Carbon 43:117-124.

Cavalli, D., G. Consolati, P. Marino and L. Bechini. 2015. Measurement and simulation of soluble, exchangeable, and non-exchangeable ammonium in three soils. Geoderma 259:116-125.

Ceccanti, B., G. Masciandaro and C. Macci. 2007. Pyrolysis-gas chromatography to evaluate the organic matter quality of a mulched soil. Soil Tillage Res. 97:71-78.

Chen, C. and D.L. Sparks. 2015. Multi-elemental scanning transmission X-ray microscopy–near edge X-ray absorption fine structure spectroscopy assessment of organo–mineral associations in soils from reduced environments. Environmental Chemistry 12:64-73.

Chen, Z. and S. Pawluk. 1995. Structural variations of humic acids in two sola of alberta mollisols. Geoderma 65:173-193.

Chenu, C., G. Stotzky, P. Huang, J. Bollag and N. Sensi. 2002. Interactions between microorganisms and soil particles: An overview. Interactions between Soil Particles and Microorganisms: Impact on the Terrestrial Ecosystem.IUPAC.John Wiley & Sons, Ltd., Manchester, UK1-40.

Cody, G., H. Ade, S. Wirick, G. Mitchell and A. Davis. 1998. Determination of chemical-structural changes in vitrinite accompanying luminescence alteration using C-NEXAFS analysis. Org. Geochem. 28:441-455.

Debska, B. and I. Gonet. 2007. Share of hydrophilic and hydrophobic fractions in humic acids formed as a result of post-harvest residue decomposition. Pol. J. Soil Sci. 40:57-65.

Ding, G., J. Novak, D. Amarasiriwardena, P. Hunt and B. Xing. 2002. Soil organic matter characteristics as affected by tillage management. Soil Sci. Soc. Am. J. 66:421-429.

Dynes, J.J., T. Tyliszczak, T. Araki, J.R. Lawrence, G.D. Swerhone, G.G. Leppard and A.P. Hitchcock. 2006. Speciation and quantitative mapping of metal species in microbial biofilms using scanning transmission X-ray microscopy. Environ. Sci. Technol. 40:1556-1565.

Dynes, J.J., T.Z. Regier, I. Snape, S.D. Siciliano and D. Peak. 2015. Validating the scalability of soft X-ray spectromicroscopy for quantitative soil ecology and biogeochemistry research. Environ. Sci. Technol. 49:1035-1042.

Elliott, E. 1986. Aggregate structure and carbon, nitrogen, and phosphorus in native and cultivated soils. Soil Sci. Soc. Am. J. 50:627-633.

Eusterhues, K., J. Neidhardt, A. Hädrich, K. Küsel and K.U. Totsche. 2014. Biodegradation of ferrihydrite-associated organic matter. Biogeochemistry. 119:45-50.

Grassmann, O. and P. Löbmann. 2004. Biomimetic nucleation and growth of CaCO 3 in hydrogels incorporating carboxylate groups. Biomaterials 25:277-282.

Gu, B., J. Schmitt, Z. Chen, L. Liang and J.F. McCarthy. 1994. Adsorption and desorption of natural organic matter on iron oxide: Mechanisms and models. Environ. Sci. Technol. 28:38-46.

Han, L., K. Sun, J. Jin and B. Xing. 2016. Some concepts of soil organic carbon characteristics and mineral interaction from a review of literature. Soil Biol. Biochem. 94:107-121.

Hitchcock, A., J. Dynes, J. Lawrence, M. Obst, G. Swerhone, D. Korber and G. Leppard. 2009. Soft X-ray spectromicroscopy of nickel sorption in a natural river biofilm. Geobiology 7:432-453.

Hitchcock, A.P., H.D. Stöver, L.M. Croll and R.F. Childs. 2005. Chemical mapping of polymer microstructure using soft X-ray spectromicroscopy. Aust. J. Chem. 58:423-432.

Hu, Y., R. Xu, J. Dynes, R. Blyth, G. Yu, L. Kozak and P. Huang. 2008. Coordination nature of aluminum (oxy) hydroxides formed under the influence of tannic acid studied by X-ray absorption spectroscopy. Geochim. Cosmochim. Acta 72:1959-1969.

Ildefonse, P., D. Cabaret, P. Sainctavit, G. Calas, A. Flank and P. Lagarde. 1998. Aluminium X-ray absorption near edge structure in model compounds and Earth's surface minerals. Physics and Chemistry of Minerals 25:112-121.

Jastrow, J., R. Miller and T. Boutton. 1996. Carbon dynamics of aggregate-associated organic matter estimated by carbon-13 natural abundance. Soil Sci. Soc. Am. J. 60:801-807.

Karunakaran, C., C.R. Christensen, C. Gaillard, R. Lahlali, L.M. Blair, V. Perumal, S.S. Miller and A.P. Hitchcock. 2015. Introduction of soft X-ray spectromicroscopy as an advanced technique for plant biopolymers research. PloS One 10: e0122959.

Keiluweit, M., J.J. Bougoure, L.H. Zeglin, D.D. Myrold, P.K. Weber, J. Pett-Ridge, M. Kleber and P.S. Nico. 2012. Nano-scale investigation of the association of microbial nitrogen residues with iron (hydr) oxides in a forest soil O-horizon. Geochim. Cosmochim. Acta 95:213-226.

Kinyangi, J., D. Solomon, B. Liang, M. Lerotic, S. Wirick and J. Lehmann. 2006. Nanoscale biogeocomplexity of the organomineral assemblage in soil. Soil Sci. Soc. Am. J. 70:1708-1718.

Kleber, M., P.S. Nico, A. Plante, T. Filley, M. Kramer, C. Swanston and P. Sollins. 2011. Old and stable soil organic matter is not necessarily chemically recalcitrant: Implications for modeling concepts and temperature sensitivity. Global Change Biol. 17:1097-1107.

Kong, A.Y., J. Six, D.C. Bryant, R.F. Denison and C. Van Kessel. 2005. The relationship between carbon input, aggregation, and soil organic carbon stabilization in sustainable cropping systems. Soil Sci. Soc. Am. J. 69:1078-1085.

Kramer, M.G., J. Sanderman, O.A. Chadwick, J. Chorover and P.M. Vitousek. 2012. Long-term carbon storage through retention of dissolved aromatic acids by reactive particles in soil. Global Change Biol. 18:2594-2605.

Krull, E.S., J.A. Baldock and J.O. Skjemstad. 2003. Importance of mechanisms and processes of the stabilisation of soil organic matter for modelling carbon turnover. Functional Plant Biology 30:207-222.

La, Y., Y.J. Jung, T. Kang, K. Ihm, K. Kim, B. Kim and J.W. Park. 2003. NEXAFS studies on the soft X-ray induced chemical transformation of a 4-nitrobenzaldimine monolayer. Langmuir 19:9984-9987.

Lawrence, J.R., G.D. Swerhone, G.G. Leppard, T. Araki, X. Zhang, M.M. West and A.P. Hitchcock. 2003. Scanning transmission X-ray, laser scanning, and transmission electron microscopy mapping of the exopolymeric matrix of microbial biofilms. Appl. Environ. Microbiol. 69:5543-5554.

Lehmann, J. and M. Kleber. 2015. The contentious nature of soil organic matter. Nature 528:60-68.

Lehmann, J., D. Liang, M. Solomon, F. Lerotic, J. Luizão, T. Kinyangi, S. Schäfer, C. Wirick and Jacobsen. 2005. Near-edge X-ray absorption fine structure (NEXAFS) spectroscopy for mapping nano-scale distribution of organic carbon forms in soil: Application to black carbon particles. Global Biogeochem. Cycles 19.

Lehmann, J., D. Solomon, J. Kinyangi, L. Dathe, S. Wirick and C. Jacobsen. 2008. Spatial complexity of soil organic matter forms at nanometre scales. Nature Geoscience 1:238-242.

Leinweber, P., J. Kruse, F.L. Walley, A. Gillespie, K. Eckhardt, R.I. Blyth and T. Regier. 2007. Nitrogen K-edge XANES-an overview of reference compounds used to

identifyunknown'organic nitrogen in environmental samples. Journal of Synchrotron Radiation 14:500-511.

Lerotic, M., C. Jacobsen, T. Schäfer and S. Vogt. 2004. Cluster analysis of soft X-ray spectromicroscopy data. Ultramicroscopy 100:35-57.

Manoli, F., J. Kanakis, P. Malkaj and E. Dalas. 2002. The effect of aminoacids on the crystal growth of calcium carbonate. J. Cryst. Growth 236:363-370.

Marinari, S., K. Liburdi, G. Masciandaro, B. Ceccanti and S. Grego. 2007. Humification-mineralization pyrolytic indices and carbon fractions of soil under organic and conventional management in central italy. Soil Tillage Res. 92:10-17.

McCarthy, J.F., J. Ilavsky, J.D. Jastrow, L.M. Mayer, E. Perfect and J. Zhuang. 2008. Protection of organic carbon in soil microaggregates via restructuring of aggregate porosity and filling of pores with accumulating organic matter. Geochim. Cosmochim. Acta 72:4725-4744.

Mikha, M.M., C.W. Rice and G.A. Milliken. 2005. Carbon and nitrogen mineralization as affected by drying and wetting cycles. Soil Biol. Biochem. 37:339-347.

Mikutta, R., M. Kleber and R. Jahn. 2005. Poorly crystalline minerals protect organic carbon in clay subfractions from acid subsoil horizons. Geoderma 128:106-115.

Neurath, R., M. Keiluweit, J. Pett-Ridge, P. Nico and M. Firestone. 2015. 61. tracing the influence of mineralogy, microbiology, and exudate chemistry on the stabilization of root-derived carbon. p. 83. *In* 61. tracing the influence of mineralogy, microbiology, and exudate chemistry on the stabilization of root-derived carbon. Genomic science Contractors–Grantees meeting XIII, 2015.

Ng, E., A. Patti, M. Rose, C. Schefe, K. Wilkinson, R. Smernik and T. Cavagnaro. 2014. Does the chemical nature of soil carbon drive the structure and functioning of soil microbial communities? Soil Biol. Biochem. 70:54-61.

Oades, J. and A. Waters. 1991. Aggregate hierarchy in soils. Soil Research 29:815-828.

Obst, M., J. Dynes, J. Lawrence, G. Swerhone, K. Benzerara, C. Karunakaran, K. Kaznatcheev, T. Tyliszczak and A. Hitchcock. 2009. Precipitation of amorphous CaCO 3 (aragonite-like) by cyanobacteria: A STXM study of the influence of EPS on the nucleation process. Geochim. Cosmochim. Acta 73:4180-4198.

Pal, D., P. Srivastava and T. Bhattacharyya. 2003. Clay illuviation in calcareous soils of the semiarid part of the indo-gangetic plains, india. Geoderma 115:177-192.

Paustian, K., J. Six, E. Elliott and H. Hunt. 2000. Management options for reducing CO2 emissions from agricultural soils. Biogeochemistry 48:147-163.

Pédrot, M., A. Le Boudec, M. Davranche, A. Dia and O. Henin. 2011. How does organic matter constrain the nature, size and availability of fe nanoparticles for biological reduction? J. Colloid Interface Sci. 359:75-85.

Peretyazhko, T. and G. Sposito. 2005. Iron (III) reduction and phosphorous solubilization in humid tropical forest soils. Geochim. Cosmochim. Acta 69:3643-3652.

Politi, Y., R.A. Metzler, M. Abrecht, B. Gilbert, F.H. Wilt, I. Sagi, L. Addadi, S. Weiner and P.U. Gilbert. 2008. Transformation mechanism of amorphous calcium carbonate into calcite in the sea urchin larval spicule. Proc. Natl. Acad. Sci. U. S. A. 105:17362-17366.

Polzonetti, G., V. Carravetta, G. Iucci, A. Ferri, G. Paolucci, A. Goldoni, P. Parent, C. Laffon and M. Russo. 2004. Electronic structure of platinum complex/Zn-porphyrinato assembled

macrosystems, related precursors and model molecules, as probed by X-ray absorption spectroscopy (NEXAFS): Theory and experiment. Chem. Phys. 296:87-100.

Rasmussen, C., M.S. Torn and R.J. Southard. 2005. Mineral assemblage and aggregates control carbon dynamics in a california conifer forest. Soil Sci. Soc. Am. J. 69:1711-1721.

Rodriguez-Blanco, J.D., S. Shaw and L.G. Benning. 2011. The kinetics and mechanisms of amorphous calcium carbonate (ACC) crystallization to calcite, via vaterite. Nanoscale 3:265-271.

Schlesinger, W.H. 2005. Biogeochemistry. Gulf Professional Publishing.

Schmidt, M.W., M.S. Torn, S. Abiven, T. Dittmar, G. Guggenberger, I.A. Janssens, M. Kleber, I. Kögel-Knabner, J. Lehmann and D.A. Manning. 2011. Persistence of soil organic matter as an ecosystem property. Nature 478:49-56.

Six, J., H. Bossuyt, S. Degryze and K. Denef. 2004. A history of research on the link between (micro) aggregates, soil biota, and soil organic matter dynamics. Soil Tillage Res. 79:7-31.

Six, J., K. Paustian, E. Elliott and C. Combrink. 2000. Soil structure and organic matter I. distribution of aggregate-size classes and aggregate-associated carbon. Soil Sci. Soc. Am. J. 64:681-689.

Smith, P., M. Bustamante, H. Ahammad, H. Clark, H. Dong, E.A. Elsiddig, H. Haberl, R. Harper, J. House and M. Jafari. 2014. Agriculture, forestry and other land use (AFOLU). Climate Change. 811-922.

Sollins, P., P. Homann and B.A. Caldwell. 1996. Stabilization and destabilization of soil organic matter: Mechanisms and controls. Geoderma 74:65-105.

Solomon, D., J. Lehmann, J. Harden, J. Wang, J. Kinyangi, K. Heymann, C. Karunakaran, Y. Lu, S. Wirick and C. Jacobsen. 2012. Micro-and nano-environments of carbon sequestration:

Multi-element STXM–NEXAFS spectromicroscopy assessment of microbial carbon and mineral associations. Chem. Geol. 329:53-73.

Stevenson, F.J. 1994. Humus chemistry: Genesis, composition, reactions. John Wiley & Sons.

Torn, M.S., S.E. Trumbore, O.A. Chadwick, P.M. Vitousek and D.M. Hendricks. 1997. Mineral control of soil organic carbon storage and turnover. Nature 389:170-173.

Vogel, C., K. Heister, F. Buegger, I. Tanuwidjaja, S. Haug, M. Schloter and I. Kögel-Knabner. 2015. Clay mineral composition modifies decomposition and sequestration of organic carbon and nitrogen in fine soil fractions. Biol. Fertility Soils 51:427-442.

Wan, J., T.K. Tyliszczak and Tokunaga. 2007. Organic carbon distribution, speciation, and elemental correlations within soil microaggregates: Applications of STXM and NEXAFS spectroscopy. Geochim. Cosmochim. Acta 71:5439-5449.

Wang, P., Y. Ma, X. Wang, H. Jiang, H. Liu, W. Ran and Q. Shen. 2016. Spectral exploration of calcium accumulation in organic matter in gray desert soil from northwest china. PLoS One 11: e0145054.

Wilson, G.W., C.W. Rice, M.C. Rillig, A. Springer and D.C. Hartnett. 2009. Soil aggregation and carbon sequestration are tightly correlated with the abundance of arbuscular mycorrhizal fungi: Results from long-term field experiments. Ecol. Lett. 12:452-461.

Xing, B. and Z. Chen. 1999. Spectroscopic evidence for condensed domains in soil organic matter. Soil Sci. 164:40-47.

Figures

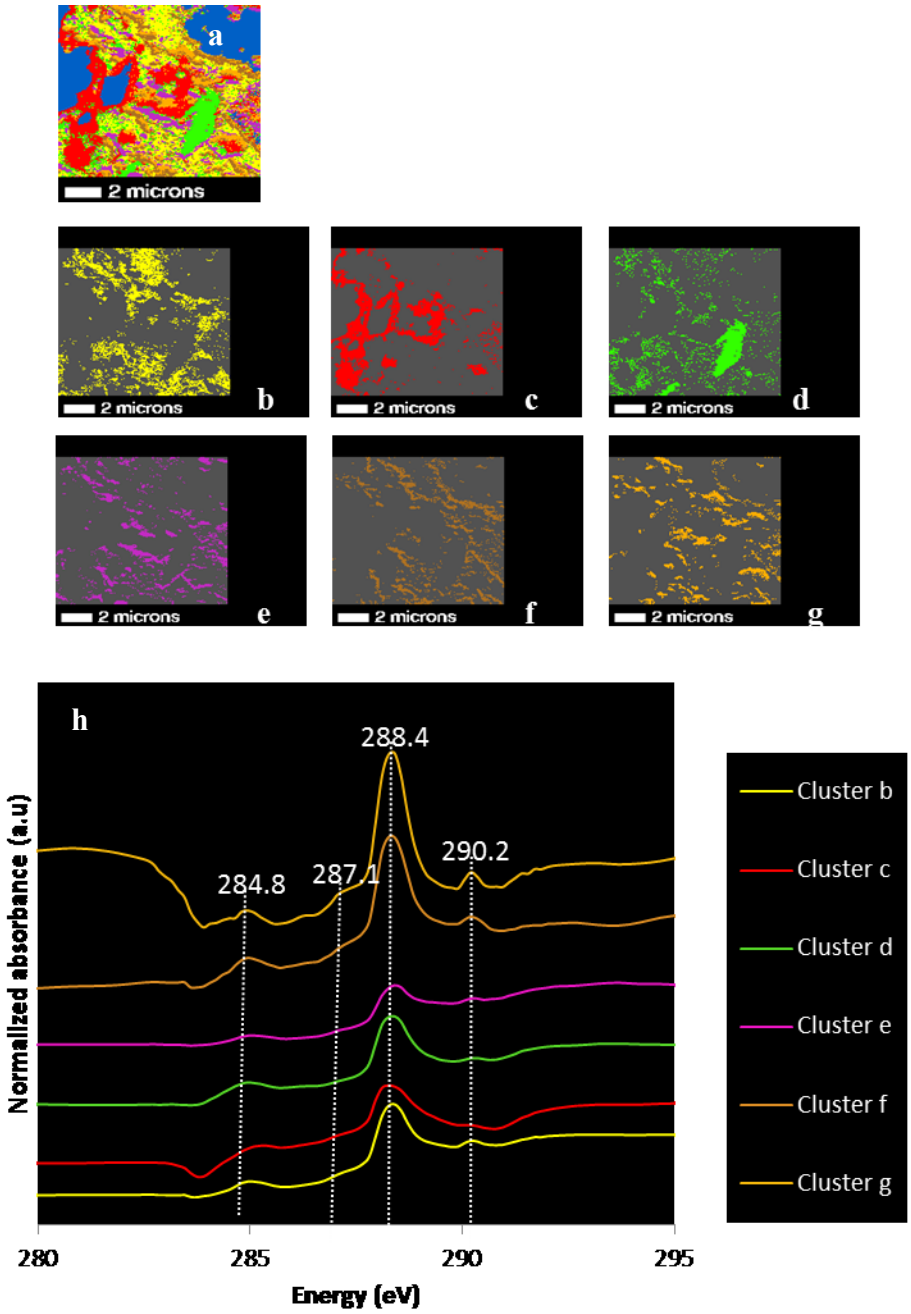

Figure 4-1 Cluster indices map of C (a), individual cluster images (b-g) and C-NEXAFS spectra (h) representing each individual cluster images of NTC (no-till, control) thin section.

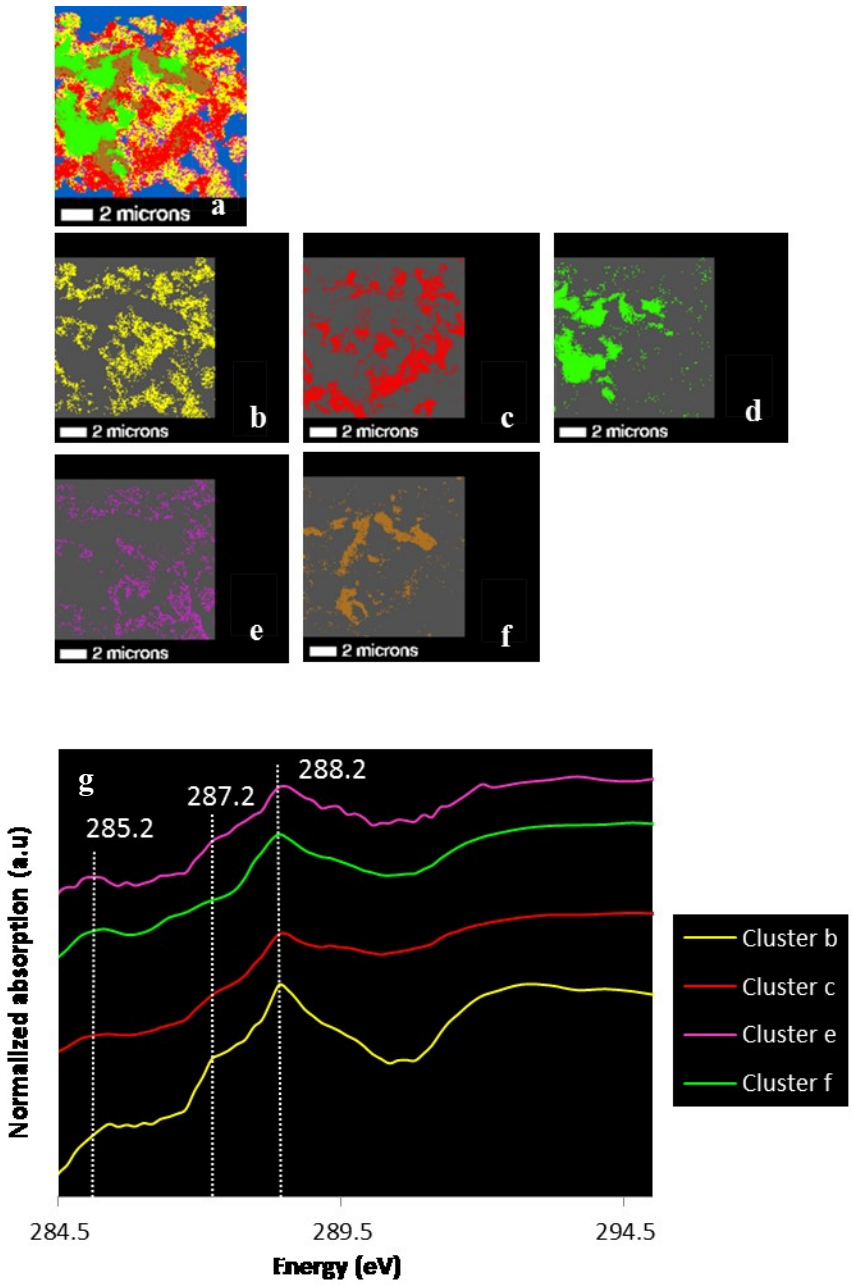

Figure 4-2 Cluster indices map of C (a), individual cluster images (b-f) and C-NEXAFS spectra (g) representing each individual cluster images of NTF (no-till, urea) thin section.

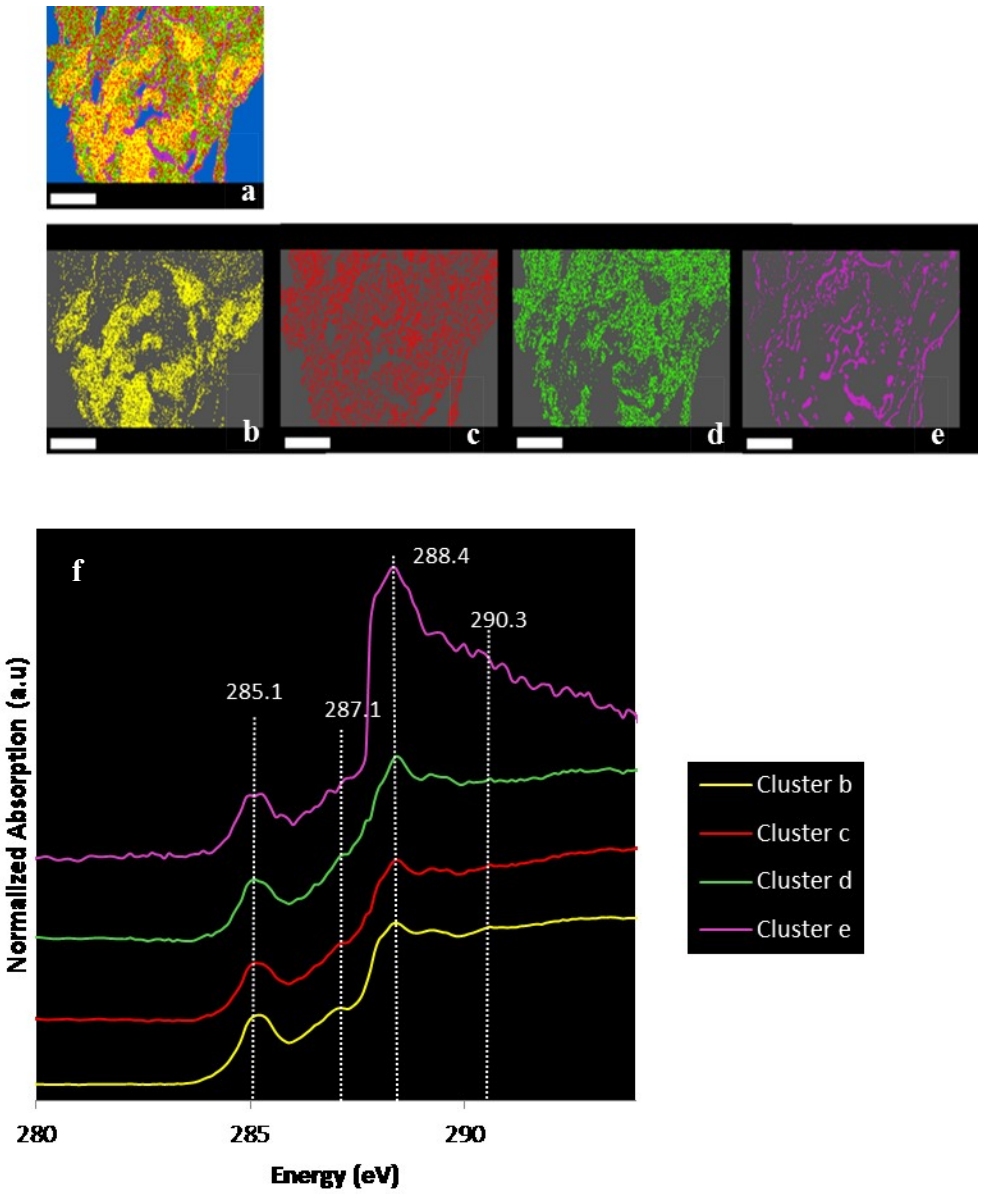

Figure 4-3 Cluster indices map of C (a), individual cluster images (b-e) and C-NEXAFS spectra (f) representing each individual cluster images of NTM (no-till, manure/compost) thin section.

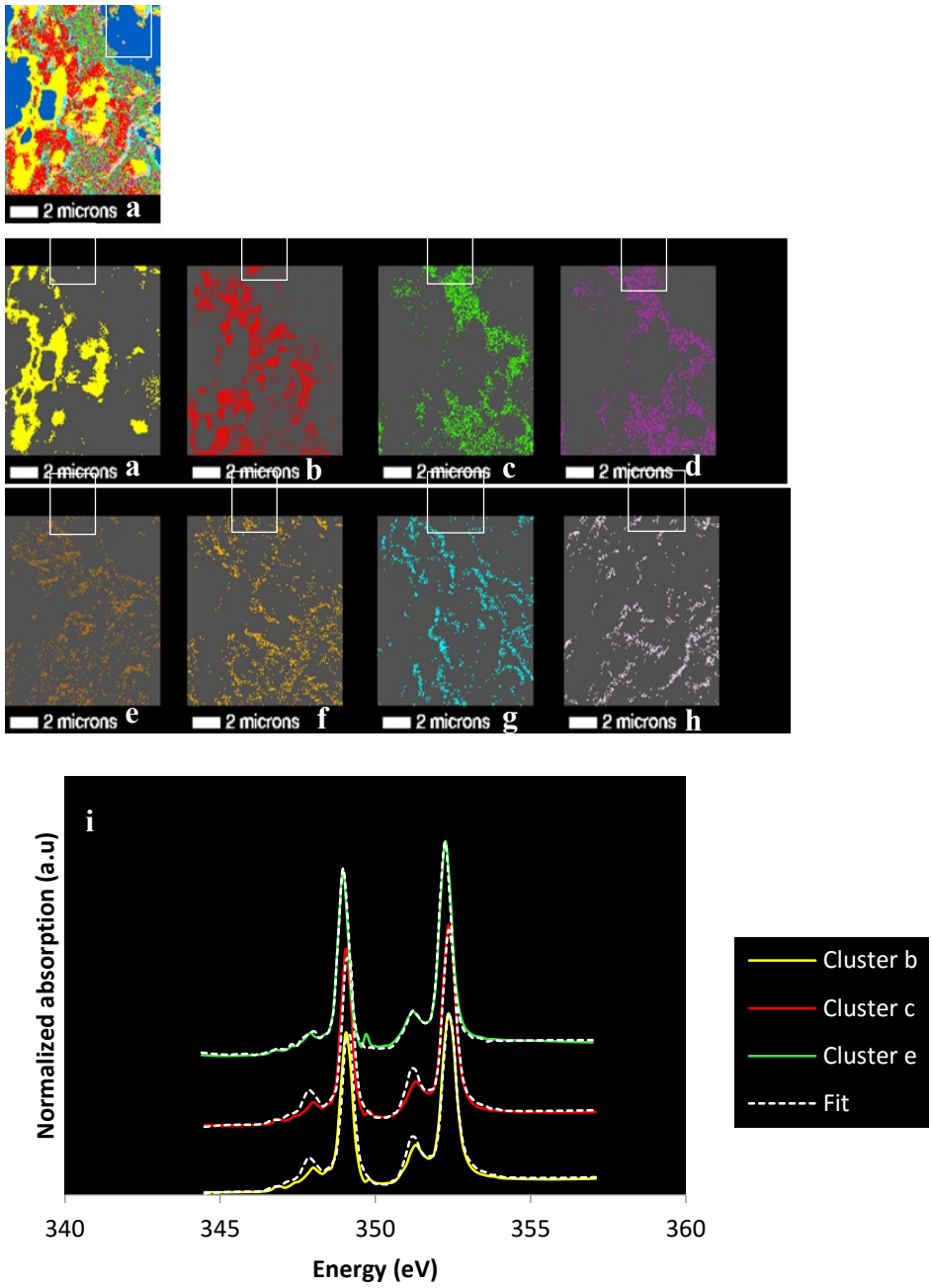

Figure 4-4 Cluster indices map of Ca (a), individual cluster images (b-i) and Ca linear combination fitting (i) representing some individual cluster images of the NTC (no-till, control) thin section (Only spectra with a significant LC fitting are shown).

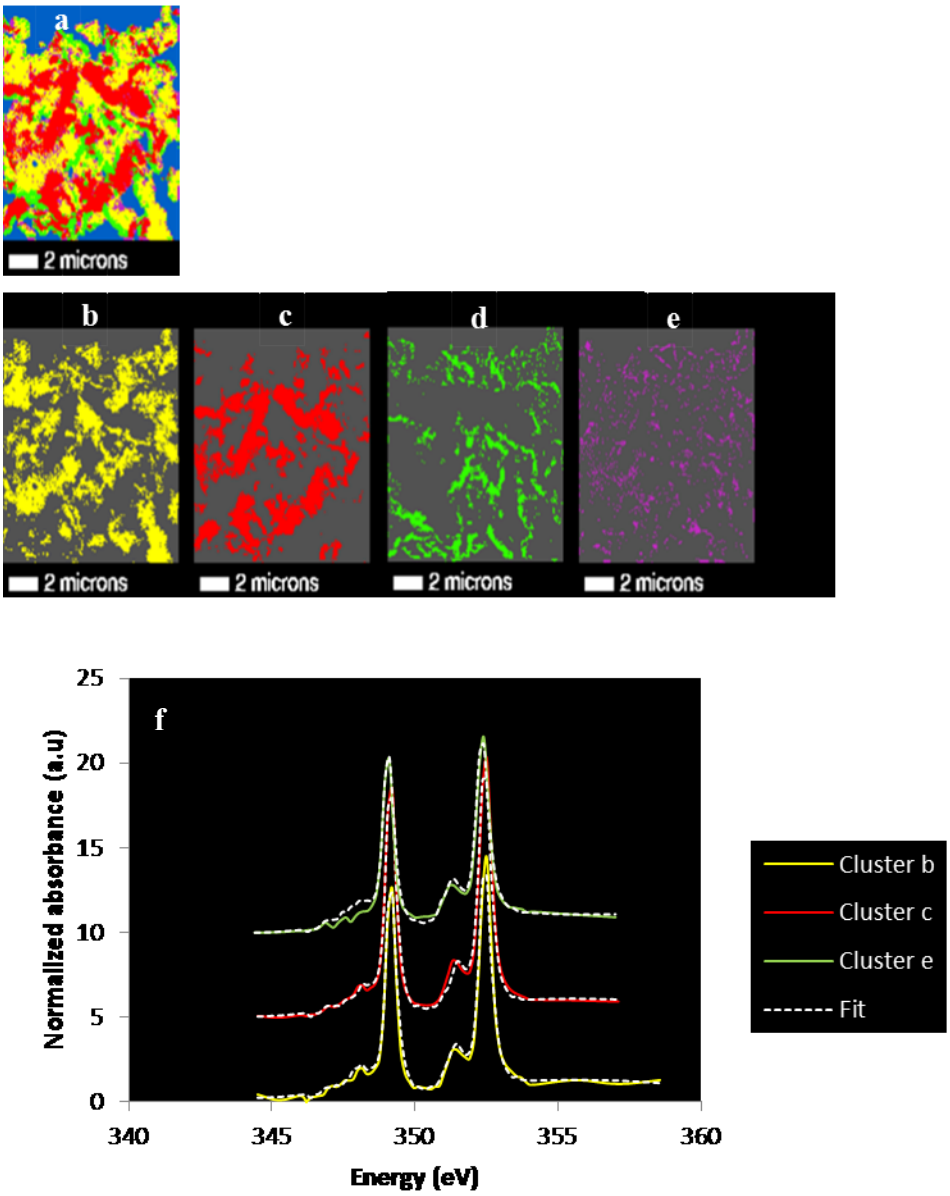

Figure 4-5 Cluster indices map of Ca (a), individual cluster images (b-e) and Ca linear combination fitting (f) representing some individual cluster images of the NTF (no-till, urea) thin section (Only spectra with a significant LC fitting are shown).

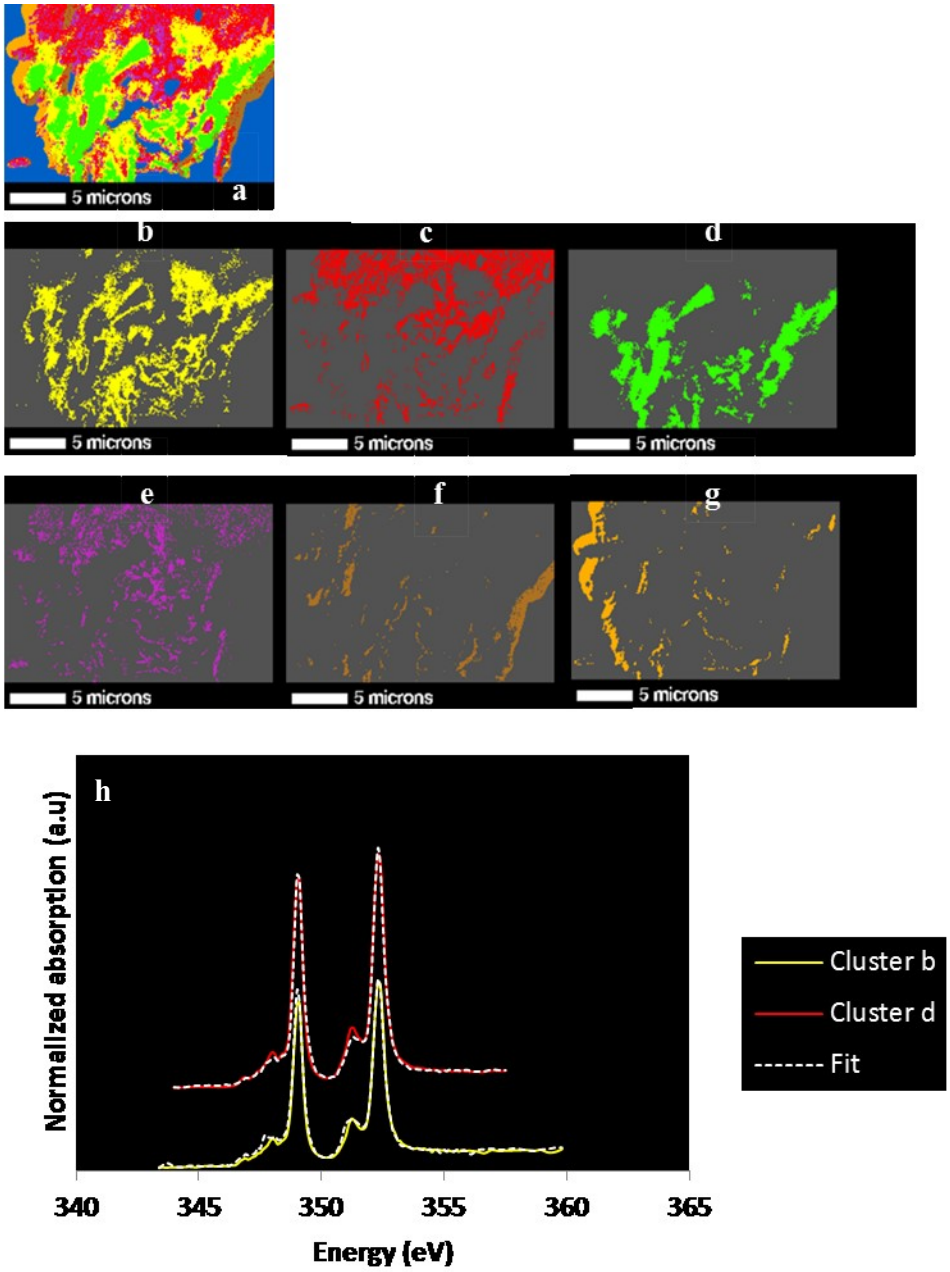

Figure 4-6 Cluster indices map of Ca (a), individual cluster images (b-g) and Ca linear combination fitting (h) representing some individual cluster images of the NTM (no-till, manure/compost) thin section (Only spectra with a significant LC fitting are shown).

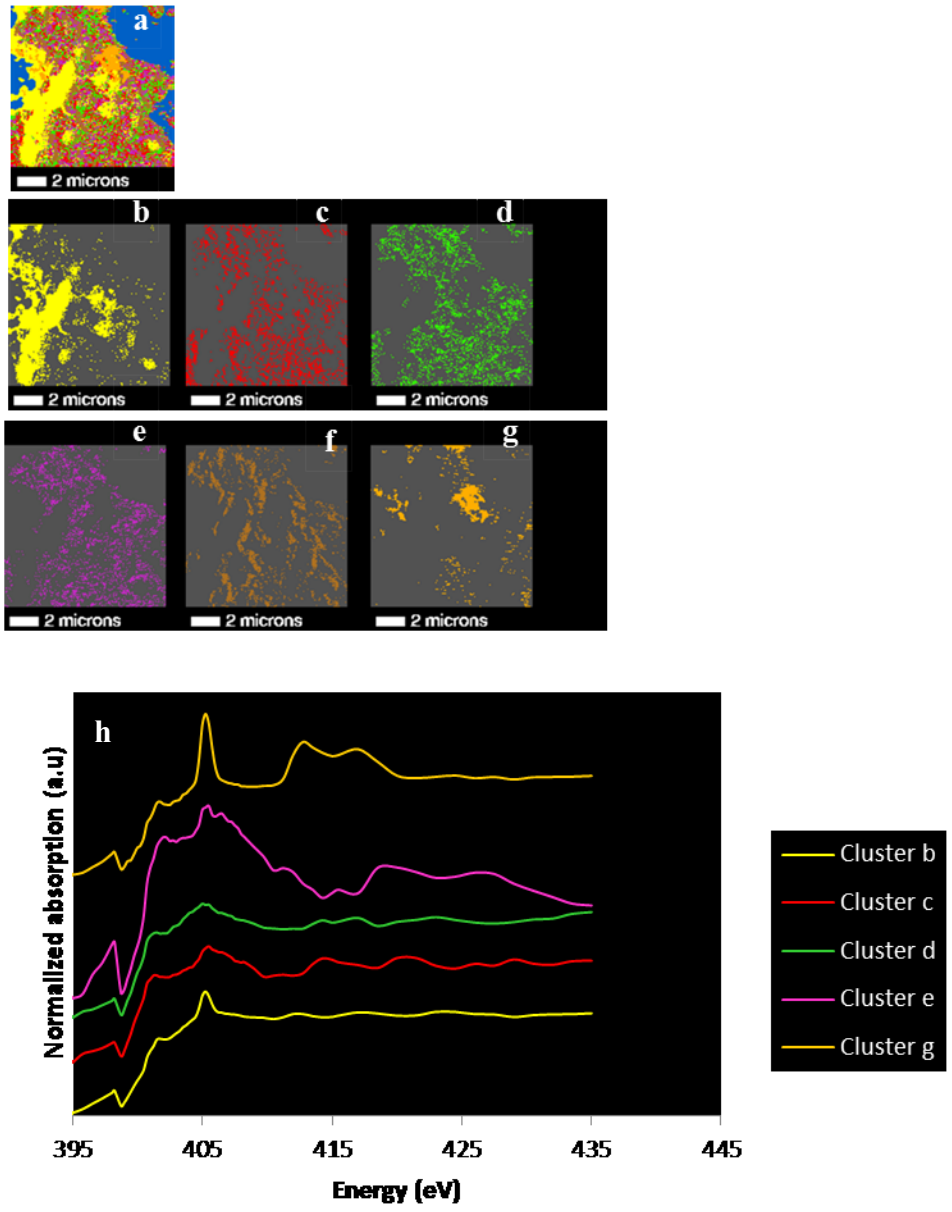

Figure 4-7Cluster indices map of N (a), individual cluster images (b-g) and N-NEXAFS spectra (h) representing each individual cluster images of NTC (no-till, control) thin section.

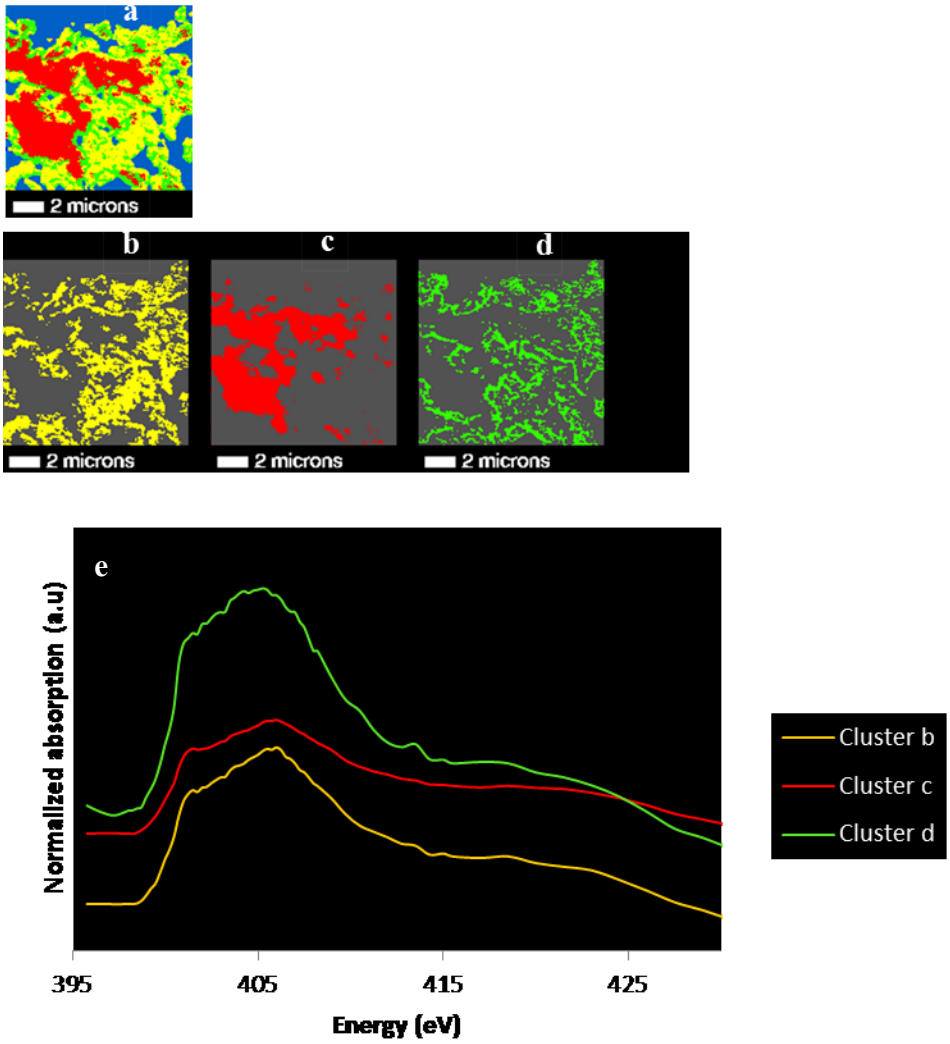

Figure 4-8 Cluster indices map of N (a), individual cluster images (b-d) and spectra of N-NEXAFS spectra (e) representing individual cluster images of NTF (no-till, urea) thin section.

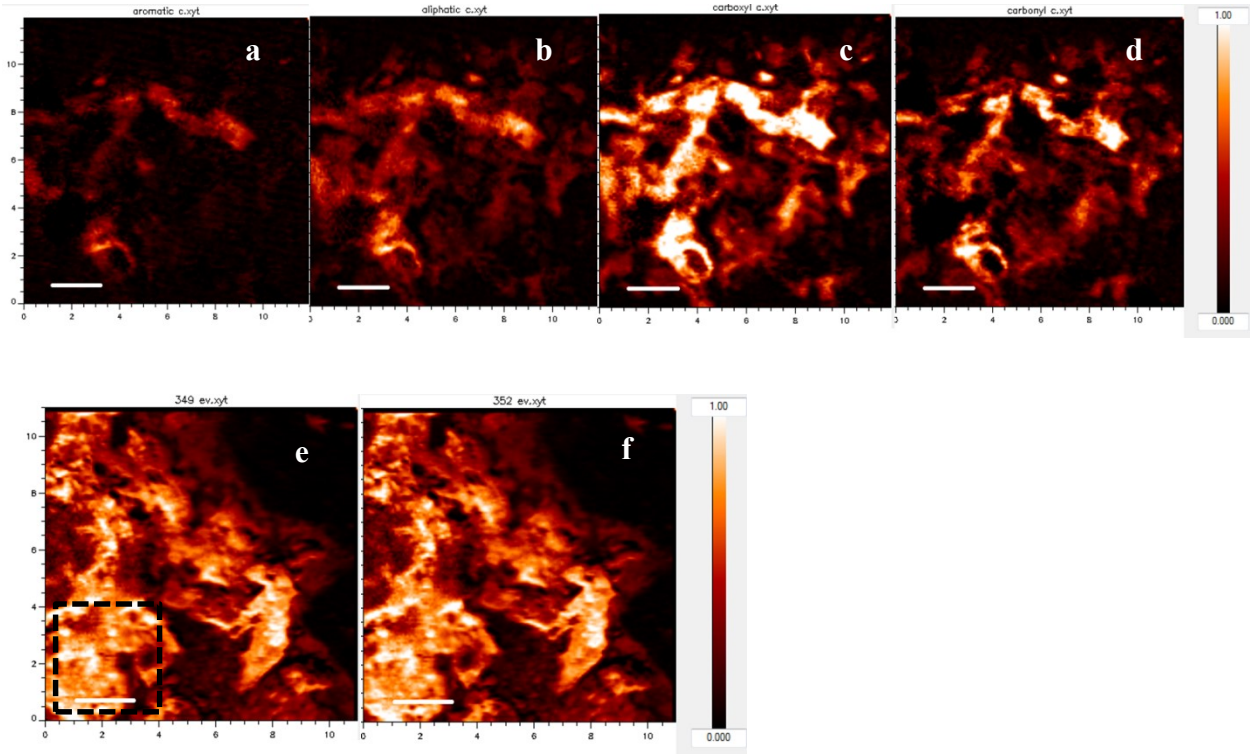

Figure 4-9 Carbon contrast maps representing aliphatic (a) aromatic (b) carboxylic (c) carbonyl (d) and calcium contrast maps (e and f) of NTC (no-till, control) thin section. Clipped area for the statistical analysis is displayed in figure e.

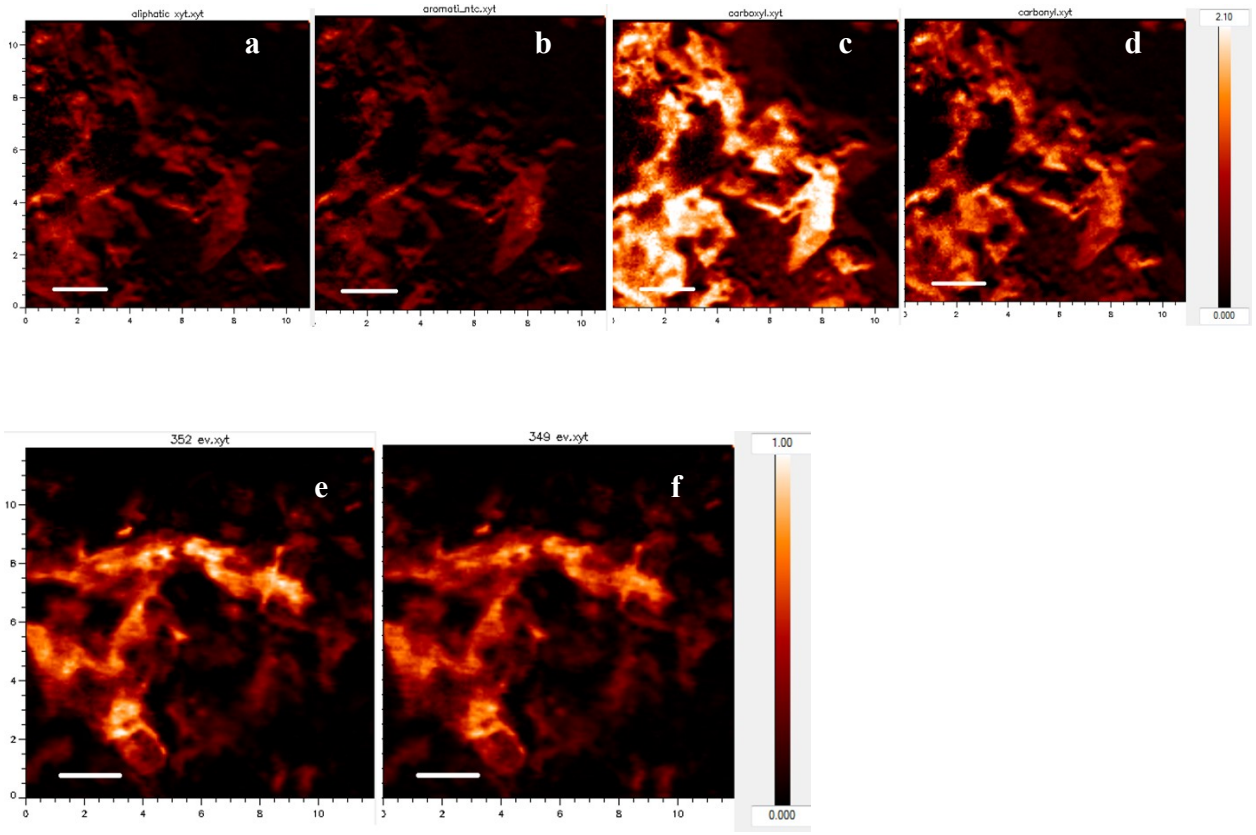

Figure 4-10 Carbon contrast maps representing aliphatic (a) aromatic (b) carboxylic (c) carbonyl (d) and calcium contrast map (e and f) of NTF (no-till, urea) thin section.

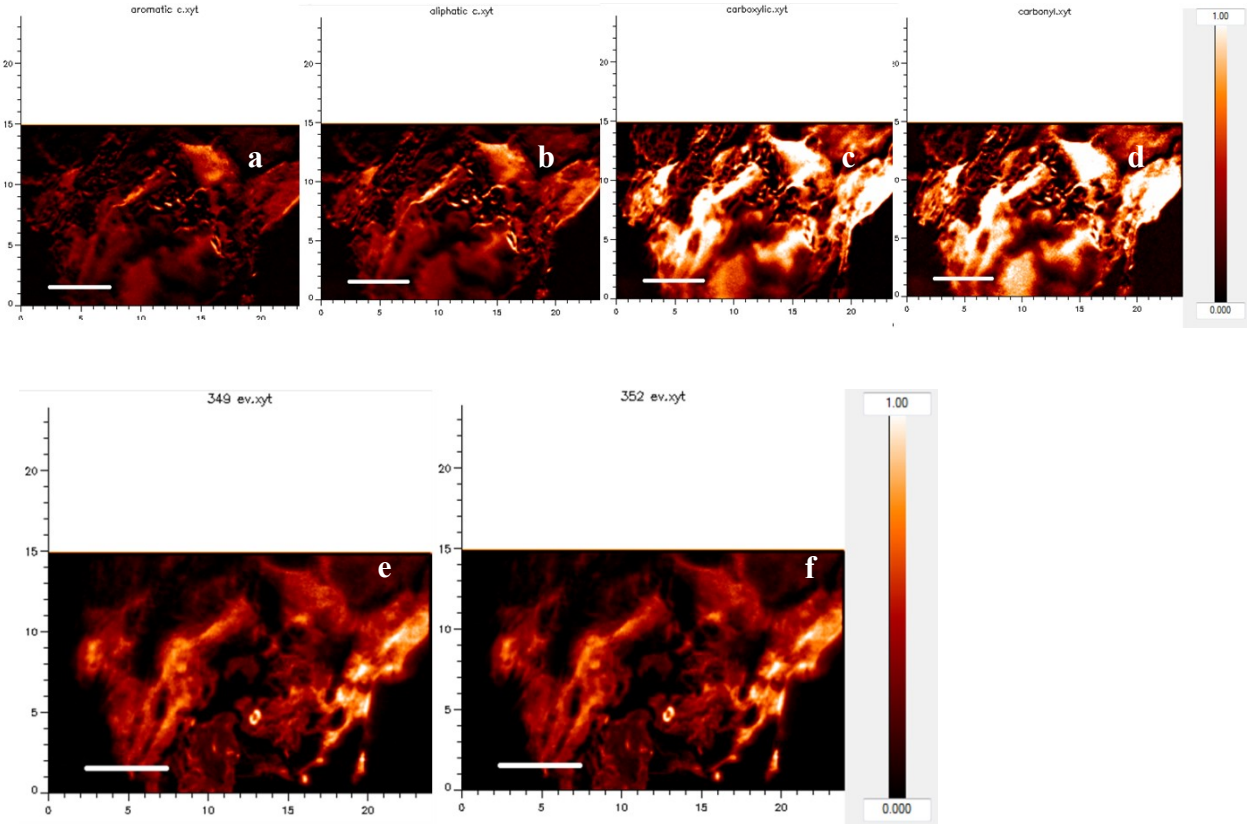

Figure 4-11 Carbon contrast maps representing aliphatic (a) aromatic (b) carboxylic (c) carbonyl (d) and calcium contrast maps (e and f) of NTM (no-till, manure/compost) thin section.

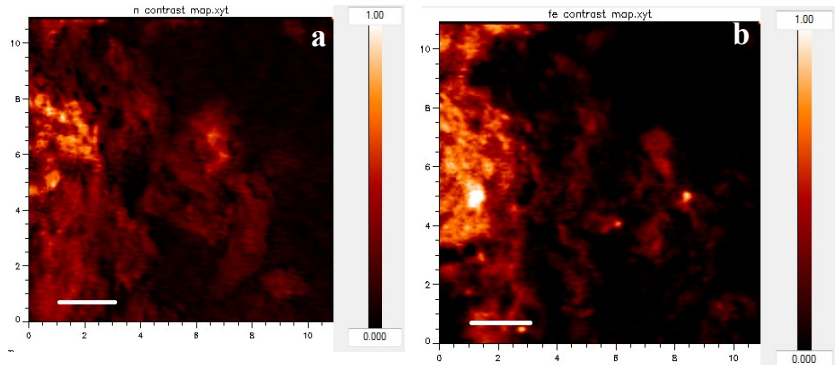

Figure 4-12 Nitrogen (a) and iron (b) contrast maps of NTC (no-till, control) thin section.

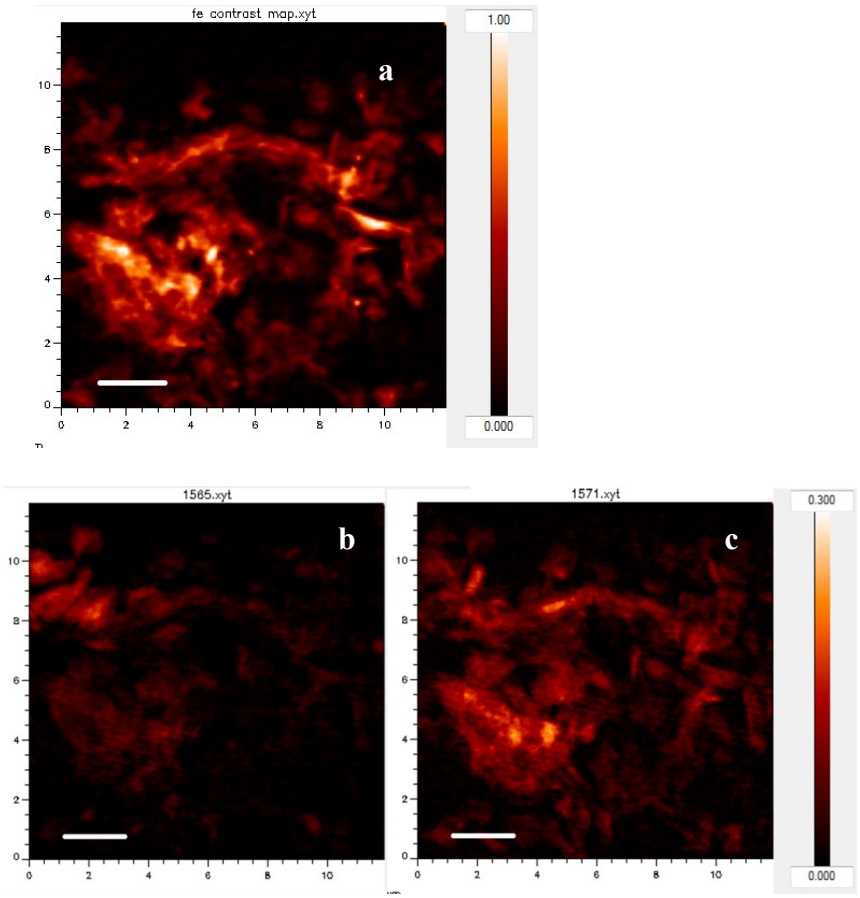

Figure 4-13 Iron (a) and aluminum contrast maps (b and c) of NTF (no-till, urea) thin section. Figure b represents aluminum phosphates contrast map.

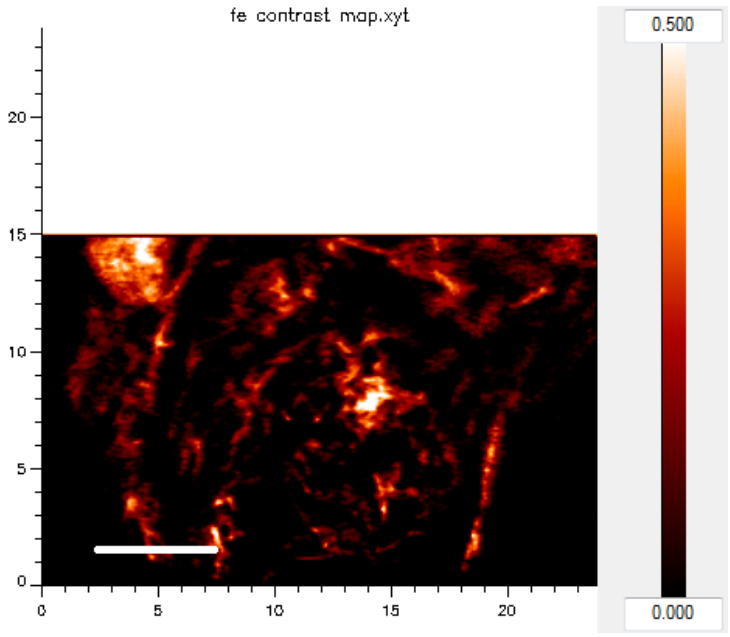

Figure 4-14 Iron contrast maps of NTM (no-till, manure/compost) thin section.

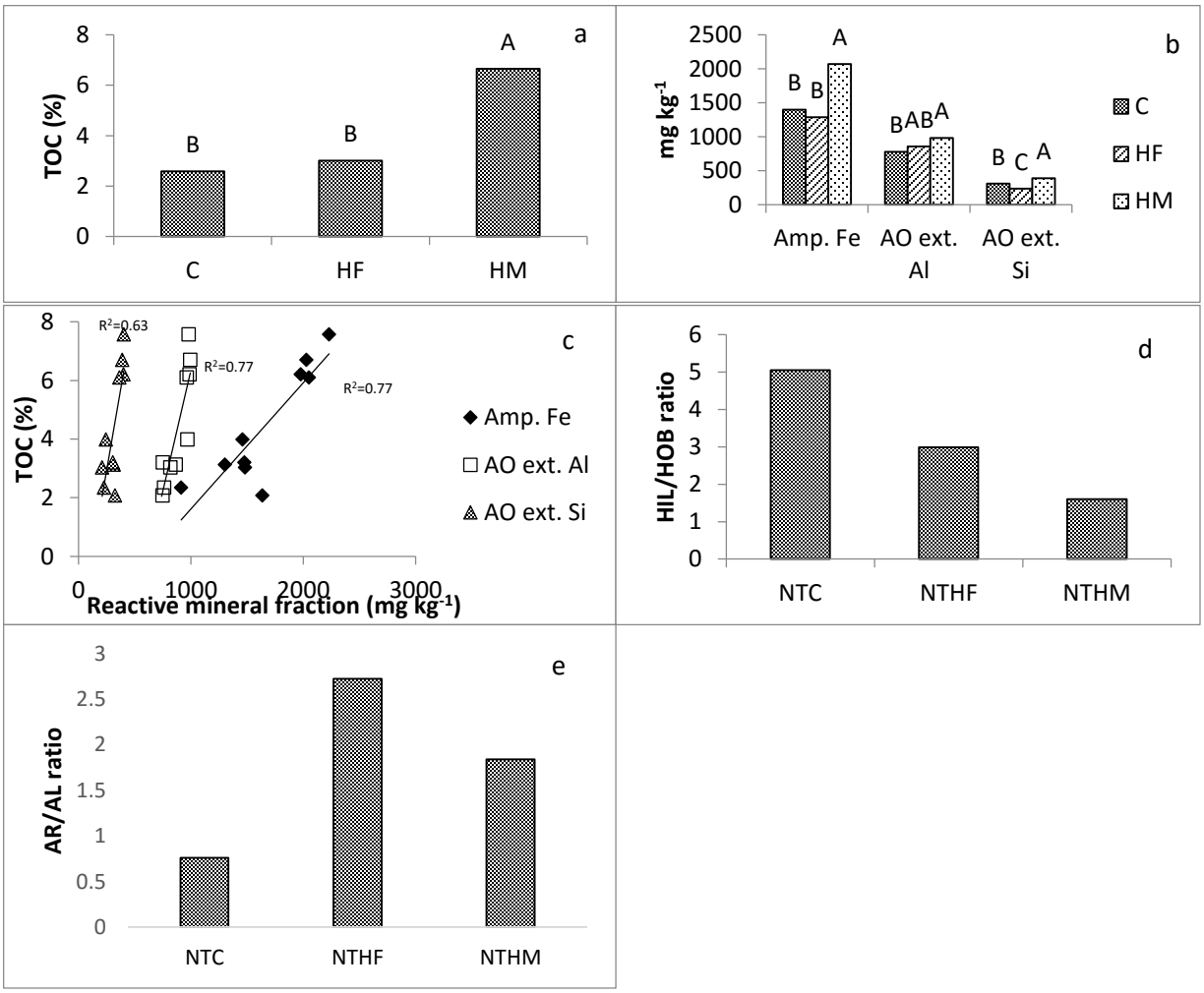

Figure 4-15 Percentage of TOC of free microaggregates (a), Concentration of reactive mineral fraction (b), Correlation between reactive minerals and TOC (c), HIL/HOB ratio (HPLC) of humic acid (d) and AR/AL ratio (^{13}C-NMR) representing different fertilizer treatments representing different fertilizer treatments (e).

Tables

Table 4-1 Peak assignment of C-NEXAFS spectra

Form of C	Peak energy (eV)	References
Alkylated to carbonyl-substituted aromatic C	284.9-285.5	Brandes et al. (2004); Braun et al. (2005)
Phenolic OH and Ketonic O-C-O	286.5-287.1	Cody et al. (1998) Hitchcock et al. (2005); Lehmann et al. (2005)
Aliphatic C-H	287.1-287.8	Lehmann et al., 2005
Carboxylic C	287.7-288.6	Lehmann et al., 2005
Carboxylic substituted aromatic, carbonyl C=O, carbonates	290-290.5	Kleber et al., 2011 Brandes et al., 2010

Table 4-2 Gaussian peak fitting for the identified clusters displayed in Fig. 4-1 representing NTC (no-till, control)

	b	c	d	e	f	g
Aromatic	6.7	3.4	7.5	-	5.5	-
Aliphatic	11.3	7.2	-	-	6.2	2.8
Carboxylic	68	72.4	74.3	75.6	69.3	83.7
Carbonate/aromatic substituted carboxyl	14	17	18.2	24.4	19	13.5
Al/AR ratio	1.7	2.1	-	-	1.3	-

Table 4-3 Gaussian peak fitting for identified clusters displayed in Fig. 4-2 representing NTF (no-till, urea) thin section

	b	e	f
Aromatic	-	1.7	6.5
Aliphatic	2.5	0.7	10.8
Carboxylic	97.5	87.5	82.7
Al/AR ratio	-	0.41	1.66

Table 4-4 Gaussian peak fitting for identified clusters displayed in Fig. 4-3 representing NTM (no-till, manure/compost) thin section

	b	c	d	e
Aromatic	16.6	13.3	12.2	9
Aliphatic	17.5	18	17.1	8.4
Carboxylic	38.7	40.3	41.8	51.7
Carbonate/aromatic substituted carboxyl	27.2	28.4	28.9	30.9
Al/AR ratio	1	1.4	1.4	0.9

Table 4-5 Linear combination fitting of Ca-NEXAFS spectra representing individual cluster images of NTC (no-till, control) thin section

Cluster	Composition	R-factor
b	Adsorbed Ca_EPS: 58 %; Aragonite: 12.5 %, Calcite: 29.5%	0.020
c	Adsorbed Ca_EPS: 68.7 %; Calcite 31.3 %	0.025
e	Adsorbed Ca_EPS: 26.6 %; Hydrous calcium dihydrogen phosphate: 73.4 %	0.005

Only the significant fits are displayed.

Table 4-6 Linear combination fitting of Ca-NEXAFS spectra representing individual cluster images of NTF (no-till, urea) thin section

Cluster	Composition	R-factor
b	Calcium sulfate: 21.3 %; Calcite: 16.6 %;	0.008
	Hydrous calcium dihydrogen phosphate: 62.1 %	
c	Hydrous calcium dihydrogen phosphate 63.5 %;	0.009
	Calcium sulfate: 36.5 %	
e	Aragonite: 43.5 %; Ca adsorbed_EPS: 22.7 %;	0.010
	Hydrous calcium dihydrogen phosphate: 33.8%	

Only the significant fits are displayed.

Table 4-7 Linear combination fitting of Ca-NEXAFS spectra representing individual cluster images of NTM (no-till, manure/compost) thin section

Cluster	Composition	R-factor
b	Aragonite: 17.2%; Calcium sulfate: 6.3 %; Calcite: 27.5 %; Hydrous calcium dihydrogen phosphate: 49 %	0.006
d	Hydrous calcium dihydrogen phosphate: 25.3 %; Calcium sulfate: 18.5%; Ca adsorbed_EPS: 56.2 %	0.005

Only the significant fits are displayed.

Table 4-8 Linear combination fitting of Fe-NEXAFS spectra representing individual cluster images of NTC (no-till, control) thin section

Cluster	Composition	R-factor
b	Goethite: 25.6%; Fe(II) hydroxycarbonate: 9.6%	0.04
	Maghemite: 64.8 %	
e	Ferric phosphate: 57.9 %	0.052
	Maghemite: 42.1%	

Only the significant fits are displayed

Table 4-9 Linear combination fitting of Fe-NEXAFS spectra representing individual cluster images of NTF (no-till, urea) thin section

Cluster	Composition	R-factor
b	Fe(II) hydroxycarbonate: 23.2 %; Maghemite: 76.8 %	0.057
c	Ferrihydrite: 11.1 %; Goethite: 81.1 %	0.008
	Siderite 22.8 %	

Only the significant fits are displayed.

Table 4-10 Linear combination fitting of Al-NEXAFS spectra representing individual cluster images of NTC (no-till, control) thin section

Cluster	Composition	R-factor
c	Kaolinite: 20.5 %; Muscovite: 79.5 %	0.033
e	Kaolinite: 98.7%; Illite: 8.3%	0.024
f	Kaolinite: 54.2%; Muscovite: 30.8%; Montmorillonite: 15%	0.050

Only the significant fits are displayed.

Table 4-11 Linear combination fitting of Al-NEXAFS spectra representing individual cluster images of NTF (no-till, urea) thin section

Cluster	Composition	R-factor
b	Montmorillonite: 29.6 %; Muscovite: 70.4 %	0.013
c	Kaolinite: 65.6%; Illite: 34.4%	0.073
d	Aluminum Phosphate	-

Only the significant fits are displayed.

Chapter 5 - Assessing Soil Carbon Preservation in a Long-term Temperate Agroecosystem: *An Integrated Approach*

Abstract

Researching the mechanisms governing the persistence of soil organic carbon (SOC) is vital to identify agricultural management strategies to improve soil C sequestration. Two-fold research goals of this study were to use an integrative approach to understand the effect of long-term agricultural management strategies on SOC chemistry and mechanisms of SOC sequestration/preservation in four different water stable aggregate fractions. Secondly, the data from different approaches were evaluated. Soils were collected from a long-term continuous corn system (>22 years) which consisted of three fertilizer treatments (control, manure/compost, and fertilizer) and two tillage treatments (conventional till and no-till). Soil sampling was done from 0-5 cm depth. Bulk C near edge X-ray absorption fine structure spectroscopy (C-NEXAFS), ^{13}C-nuclear magnetic resonance (^{13}C-NMR), total organic carbon (TOC), permanganate oxidizable C (POXC) and reactive minerals were measured. Manure/compost addition enhanced the labile C stabilization and concentrations of TOC and reactive minerals in soils. No-till promoted labile C preservation in macroaggregates. Significant organo-mineral associations were observed. Large microaggregates exerted a strong labile C preservation through physical protection and chemical stabilization. This study revealed that the preservation of C is heavily influenced by the surrounding environment. Overall, this study provided insight into the how the soil management practices affecting SOC sequestration and preservation, and the significance of soil management practices on climate change mitigation potential of agricultural soils.

Introduction

Agriculture is profoundly influenced by climate change while, simultaneously, it significantly contributes to the greenhouse gas (GHG) emission (IPCC, 2014). With much evidence and agreement, it was reported that climate change mitigation potential of Agriculture, Forestry, and Other Land Use (AFOLU) sector is based on enhancing removals and lowering the emission of GHGs (Smith et al., 2014). For the first time in the history, "The 2015 United Nations Climate Change Conference" considered the agriculture as a significant component and brought forward a target to enhance world's soil organic carbon (SOC) to a depth of 40 cm at a rate of 0.4% per year. Management strategies proposed in achieving the target were conservation agriculture, mulching, cover cropping, the addition of biochar, and landscape restoration (Lal, 2016). With diverse strategies of improving soil C sequestration, agricultural lands obtain a new SOC equilibrium with the time (Wiesmeier et al., 2014) and ultimately to a point of saturation.

Climate change influences soil C storage either negatively or positively. Negative impacts are linked with SOC decomposition at high temperatures and low inputs due to shortening of crops life cycles (Rosenzweig and Tubiello, 2007). Conversely, elevated CO_2 and lengthening of growing cycles enhance the above and below ground biomass. Furthermore, it was reported that elevated CO_2 stimulate the priming effect and decompose native soil C (Kowalchuk, 2012; Cheng et al., 2012).

Biochemical recalcitrance, chemical stabilization, and physical protection are three mechanisms for SOC preservation (Sollins et al., 1996). Molecular characteristics of SOC do not solely govern the turnover rate. Interactions with the surrounding environment (mineral associations, occlusions within soil aggregates, and microbial composition) exert a significant influence on the persistence of stored C (Han et al., 2016). Simple labile compounds like sugars

can exist in soils for decades if the preservation mechanisms stand against microbial decomposition (Schmidt et al., 2011).

Soil aggregation plays a significant role in protecting SOC by restricting the entrance of microbes, enzymes, nutrients, and gas. In soils dominated with 2:1 layer silicates, SOC plays a major role in aggregation since polyvalent OC complexes create electrostatic cation bridges with negatively charged clay particles (Six et al., 2000). Soil biotas (Bossuyt et al., 2001; Lynch and Bragg, 1985; Oades and Waters, 1991) and management practices influence on aggregation and thus SOC preservation.

Research has focused on understanding agricultural management strategies to improve soil C. However, studies offering insights into the mechanisms of soil C preservation are lacking. Han et al. (2016) highlighted the significance of researching the mechanisms of SOC preservation using an integrated approach. They illustrated the contribution of molecular structure and minerals on SOC preservation that can be hidden depending on dissimilar climates, mineralogy, and land uses patterns. Due to the complexity of soil C, proper understanding could be achieved only through an integrative approach involving new generation techniques, in addition to the traditional laboratory-based analyses. Lack of suitable non-invasive analytical tools is a major drawback in understanding the mechanisms of C preservation at micro- and nano- scale level (Solomon et al., 2012). Therefore, we followed an integrated approach to understand underlying mechanisms of C preservation. The main goals of this research were to 1) follow an integrative approach (new generation and traditional techniques) to understand the effect of long-term agricultural management strategies on OC chemistry and mechanisms of soil C preservation, 2) assessment of organo-mineral associations, and 3) evaluation of data from different approaches to comprehend the agreement with each other.

Materials and methods

Soil sampling and sample preparation

In February 2012, soils were collected from a long-term (established in 1990) continuous corn system (*Zea mays L.*) located in the North Agronomy Farm, Manhattan, Kansas, USA (39º 12'42" N, 96º 35' 39" W). The soil was characterized as moderately well-drained Kennebec silt loam (fine-silty, mixed superactive, mesic Cumulic Hapludolls), and the sand, silt, and clay contents were 9%, 69% and 22%, respectively (Mikha et al., 2005). Soil mineralogy was dominated by 2:1 layer silicates (montmorillonite). The field experiment was designed as a split-plot randomized complete-block design with four blocks. Main plots represented tillage (conventional/CT and no-till/NT) and sub plots were three different fertilizer treatments, control (no manure or fertilizer-C), manure (manure/compost-HM), and fertilizer (urea-HF). Manure and fertilizer were added on the basis of supplying 168 kg ha^{-1} yr^{-1} of N. Fresh cattle manure was added in the first 10 years and compost was added lately.

Soils were sampled from 0-5 cm depth using a 2-cm diameter soil sampling probe randomly from 10-15 locations of each plot. Samples were collected in polypropylene bags and stored at 5°C with minimum disturbance to soil aggregates. Soils were slightly air dried for few hours and passed through a 8 mm sieve onto a 4 mm sieve. Larger aggregates (4-8 mm) were separated into four different sizes of water stable aggregates (WSA) (Mikha and Rice, 2004). Aggregate sizes were >2000 µm (macroaggregates), 250-2000 µm (mesoaggregates), 53-250 µm (large microaggregates) and, <53 µm (small microaggregates plus clay and silt) fractions. Large soil aggregates (50 g) were placed on 2 mm sieve which was stacked on a 250 µm sieve. The sieves were attached to the wet-sieving apparatus and the top of the 2 mm sieve was submerged in distilled water for 5 min followed by 2 min oscillation at a frequency of 30 cycles per min.

Another sieve (53 μm) was used to separate the latter two fractions. All the aggregate fractions were oven dried at 40-45 ˚C and stored at 5˚C, until further use. For qualitative analysis (NEXAFS and ^{13}C-NMR), all four field replicates representing each treatment combination and aggregate fraction were combined for a composite sample.

Sample analysis

Chemical characterization of SOC was done using near edge X-ray fine structure spectroscopy (NEXAFS) at beamline SGM 11 ID-1 at the Canadian Light Source (CLS), Saskatoon, Canada. Finely ground samples were mixed with e-pure water to form slurries and placed on gold sputtered silicon (Si) wafers (0.5 cm x0.5 cm) to create thin, uniform soil layers. The monochromator was calibrated using citric acid. Approximately 40-75 fast scans of 20 seconds were collected in the energy range from 270 to 310 eV. Slew scanning mode was used with continuous scanning to minimize sample damage through X-ray exposure with a beam spot size of 1000 μmx100 μm (Regier et al., 2007a,b). Multiple (approximately 40-75 scans per sample) fast scans for C-NEXAFS were obtained on fresh sample spots for the energy range from 270 to 310 eV by moving the sample stage on x and/or y direction. A silicon photodiode for flux normalization was used to avoid contamination of beamline optics. This was carried out by measuring the beam intensity with a photodiode between sample scans (Gillespie et al., 2014). Data processing was performed using IGOR PRO (Wavemetrics, Lake Oswego, Oregon, USA), AXIS 2000 (Hitchcock, 2008) and ATHENA software (Ravel and Newville, 2005).

Carbon NEXAFS speciation occurs in the range of 284-290 eV of the main energy transitions (1s-π*) in the fine structure region. Gaussian peak fitting (Fig. 5-1) was conducted to the energy range of 282-292 eV to get proportions of different C functional groups. Spectra were pre and post edge normalized to minimize the influences associated with total C content

(Jablonski et al., 2003). Therefore, spectra were useful in obtaining clues on changes in C chemistry. An arctangent function for the ionization step at 292 eV and six Gaussian peaks (286, 286.7, 287.6, 288.4, 288.98, and 290.1eV) were used for deconvolution (Table 5-1). Arctangent function was fixed 1eV full width at half maximum (FWHM), and six Gaussian peaks with FWHM set at 0.4 eV were used (Mukome et al., 2014). Percentage of each C functional group representing each transition was determined by setting the area under the Gaussian curve to 100%. Amplitude represented the area under the peak since the peak shapes were unit normalized. The R- factor was considered to obtain a best fit.

In addition to using non-invasive, new generation approaches, traditional laboratory-based analyses such as liquid-state ^{13}C-nuclear magnetic resonance (^{13}C-NMR) were used. Humic acid (HA) of composite soils were analyzed with liquid state ^{13}C-NMR to characterize HA linking with management strategies. Extraction of HA was done following International Humic Society Substance (IHSS) method with some modifications (Swift et al., 1996). Refer to the Chapter 03 for more details.

Some wet chemical analyses such as total organic carbon (TOC), amorphous iron (Fe), ammonium oxalate extractable aluminum (Al) and silicon (Si) were done for composite and non-composite soils. Permanganate oxidizable C (POXC) was determined only in composite soils. Amorphous iron (Fe), ammonium oxalate extractable aluminum (Al) and silicon (Si) were considered as a representation of the reactive mineral fraction. For TOC, ground soils (<150 μm) were directly combusted using Carlo Erba C/N analyzer (Carlo Erba instruments, Milan, Italy) after treating with 1*N* phosphoric acid to remove inorganic C. Permanganate oxidizable C was determined following Weil et al. (2003). Amorphous Fe was determined using ammonium oxalate in dark method (Loeppert and Inskeep, 1996). Ammonium oxalate extractable Al and Si

were also measured from the same extractants. Sample analysis was conducted using Varian 720-ES Inductive couple plasma-optical emission spectrometer (ICP-OES).

Analysis of variance (ANOVA) was performed by means of PROC MIXED using SAS 9.4 (SAS Institute Inc., 2013). Results were considered statistically significant at $p<0.05$. Means were compared using the Tukey test ($p<0.05$). Linear regression analysis was performed using SAS 9.4 to determine the significance ($p<0.05$) of different relationships.

Results and Discussion

Total organic carbon

Total OC concentration was significantly affected by tillage-aggregate interaction and fertilizer treatment. Manure added soils had higher TOC than other treatments (Fig.5-2 a). There was no effect of tillage on TOC at each aggregate size except for mesoaggregates. In comparison to no-till soils, conventionally tilled soils contained a significantly lower amount of TOC in the mesoaggregate fraction (Fig. 5-2 b). The lowest TOC was found in the <53 μm fraction. The extent of aggregate distribution gives an idea on OC stocks in soils with respect to each aggregate fraction. A study on the same site showed high proportion of large microaggregates and <53 μm fractions (<250 μm) in tilled soils compared to no-till soils (Nicoloso, 2008). Macroaggregates (>250 μm) were significantly high in no-till compared to tilled soils (30% and 10% in no-till and tilled soils, respectively). Therefore, the distribution of aggregates revealed the existence of large OC stocks in macroaggregates of no-till soils while tilled soils contained a high amount of OC in association with microaggregates.

Reactive mineral fraction

The amorphous Fe oxides (i.e. ferrihydrite and ferrihydrite like minerals) are very active due to smaller (2-5 nm) crystal size (Blume et al., 2010) and high surface area (Cornelis et al.,

2008). Amorphous Fe was significantly affected by the treatment-tillage interaction and aggregate size (Fig.5-3 a). No-till manure/compost amended soils had a high concentration of amorphous Fe. Amorphous Fe was higher in macroaggregates (>250 μm) than in microaggregates (Fig.5-3 b). Ammonium oxalate extractable Al and Si were not affected by treatments. The addition of manure/compost builds up amorphous Fe and Al (oxy)hydroxides which is mainly attributed to the transformation of the crystalline minerals into an amorphous pool due to high C content (Abdala et al., 2015; Zhang et al., 2013). Amorphous minerals provide an extensive surface area and chelation capacity to form metastable and intermediate organo-mineral complexes (Berhe et al., 2012). Yu et al. (2012) suggested the formation of amorphous alumino silicate micro particles (i.e. allophane and imogolite) due to manure addition which enhances the formation of organo-mineral associations. Moreover, tillage created a dilution effect due to the mixing of soil up to a depth of 20 cm, leading to low amorphous Fe in the top layer of tilled soils.

Correlations between soil C pool and reactive mineral fraction

Amorphous Fe and Al oxides have the capability in preserving SOC (Kleber et al., 2004; Schwertmann et al., 2005). Non-composite soils (i.e., soil collected from four field treatment replicates) indicated a significant positive correlation (R^2=0.48, $p<0.0001$) between TOC and amorphous Fe (Fig. 5-4 a). All aggregates showed significant positive correlations between amorphous Fe and TOC. The strongest correlations were observed in large microaggergate (R^2=0.66) and <53 μm fractions (R^2=0.61) (Fig. 5-4 b and c). Ammonium oxalate extractable Al and Si did not show any significant correlation with TOC in non-composite soils.

In addition to the non-composite samples, relationships were studied for composite soils as they were used for qualitative analyses (^{13}C-NMR and NEXAFS). Composite soils showed a

significant correlation between reactive minerals and TOC (Fig. 5-5 a)/ POXC (Fig. 5-5 b). The correlation with amorphous Fe was the strongest. Large microaggregate fraction illustrated strong correlations between amorphous Fe and TOC/POXC, implying the strength of chemical stabilization (Fig. 5-5 c and 5-5 d).

^{13}C-Nuclear magnetic resonance (composite soil samples)

The spectra (Fig. 5-6) were divided into four regions: carboxyl C (220-160 ppm), aromatic C (160-100 ppm), O-alkyl C (110-45 ppm), and alkyl-C (45-10 ppm) (Mathers et al., 2003; Zhang et al., 2013). Peaks were integrated and the percentages of each C functional group were calculated. Alkyl-C is preferentially resistant for degradation compared with O-alkyl C (Pisani et al., 2016). Lipids, cutin, and suberin are composed mainly of alkyl-C whereas carbohydrates, hemicellulose and cellulose contain O-alkyl C. Plant-derived alkyl C preserve in soils with minimum alterations and ultimately incorporate into the humic C fraction (Almendros et al., 1996; Zech et al., 1997). In tilled soil, alkyl-C was more prominent in manure/compost added soil.

The ratio of O-alkyl C to alkyl-C reflects the degree of SOC decomposition (Baldock et al., 1995). A high ratio indicates the preservation of labile C (Cusack et al., 2012). General trend illustrated the preservation of O-alkyl C (most labile fraction) with the decrease of the aggregate sizes (Fig. 5-7 a). This could be linked with physical protection in soil aggregates (Lutzow et al., 2006) and chemical stabilization through organo-mineral associations (Kleber et al., 2004; Schoning et al., 2005).

In some aggregates, a noticeable carbohydrate peak around 61-83 ppm (Albers et al., 2008) appeared, especially in manure/compost added soils compared with other treatments (Fig. 5-6). This implied the HA-bound carbohydrate fraction (Wershaw, 1986). Carbohydrates involve

in soil aggregation (Piccolo and Mbagwu, 1999) and tend to be physically protected when located inside pores.

The ratio of aliphatic to aromatic C (AL/AR) indicated the degree of humification and it implied the quotient between labile and stable C which is considered as an "energetic reservoir" in extremely poor soils (Ceccanti et al., 2007; Marinari et al., 2007). Decrease in AL/AR ratio corresponds to an advanced humification (Aranda et al., 2015). With further humification, AL/AR ratio decreases (Aranda et al., 2015) as humic substances become highly aromatic due to the formation of polycondensed rings (Xing and Chen, 1999; Hsu and Lo, 1999; Chen and Pawluk, 1995; Ding et al., 2002). Except in NTHM, the large macroaggregates had the lowest AL/AR ratio (Fig. 5-7 b), implying an advanced humification. Humification was found to be lowest in microaggregates in all soils except in manure/compost added soils. Tillage effect was observed only in macroaggregates and was clear in control and manure/compost added soils.

Bulk carbon near edge X-ray absorption fine structure spectroscopy (composite soil samples)

Bulk C-NEXAFS is a new generation powerful and non-invasive technique. It can be used to fingerprint SOC and to determine the effect of management strategies in terrestrial ecosystems (Li et al., 2013). Low concentration and complexity of soil C are the main challenges associated with C-NEXAFS (Lehmann and Solomon, 2010). However, when integrated with the information collected with other techniques, the C-NEXAFS can be quite powerful and insightful.

Data analysis identified a complex pool of C consisted with unsaturated aromatic C, phenolic OH, ketonic O-C-O, aliphatic C-H, carboxylic C and carboxylic substituted aromatic,

carbonyl C=O/carbonates. The aliphatic C was the abundant form of C (35% to 45%). This was contradictory to the findings from ^{13}C-NMR which indicated the dominance of aromatic C.

In each tillage system, a high proportion of aliphatic C, which is the labile pool (Margenot et al., 2015) was found in macro- and mesoaggregates of manure/compost added soils (Fig. 5-8). This trend was observed in both tillage systems. Large aggregates (macro- and mesoaggregate) had relatively lower AL/AR ratios suggesting an advanced humification than smaller aggregates (<250 μm). Moreover, large microaggregates of manure/compost and fertilizer added soils had the highest AL/AR ratio implying the lowest degree of humification. In control, except in the <53 μm fraction, all other aggregate sizes illustrated an advanced humification in tilled soils than in no-till. Large microaggregates showed high humification in control compared to urea added soils.

In no-till, macroaggregates in control and manure/compost added soils showed an enrichment of labile C compared to their counterpart tilled-soils. The <53 μm fraction of control showed less humification in tilled soils. This implied that small microaggregates (53-20 μm) were least affected by tillage. Tillage brings up deeper C and enhances interactions with minerals, facilitating the formation of organo-mineral associations. Moreover, SOC might have tightly bound to clay inferring a strong chemical stabilization.

The presence of relatively labile C in manure/compost added soils indicated chemical stabilization of C through organo-mineral associations, attributed to the high content of reactive minerals (Abdala et al., 2015; Zhang et al., 2013). The selective preservation of labile C in large microaggregates can be explained by associations with reactive minerals (Fig. 5-5 c and d) and strong physical protection. Organic C encapsulated in microaggregates possesses strong preservation mechanisms due to spatial and kinetic constraints, preventing the microbial

degradation (McCarthy et al., 2008). The water stable microaggregate fraction represented free microaggregates and microaggregates inside macroaggregates which were released during wet sieving. Free microaggregates (Balesdent et al., 2000) and microaggregates protected inside macroaggregates (Denef et al., 2001) exert a strong physical barrier compared to macroaggregates (Beare et al., 1994; Elliot, 1986). Moreover, Jastrow et al. (1996) reported that the turnover rate of C associated with free stable microaggregates (412 yrs) is three times slower compared to C in macroaggregates (140 yrs). Microaggregates inside macroaggregates possess a superior physical protection restricting the entry of microbes and enzymes as well as oxygen diffusion. Pores less than 0.2 μm prevent the entry of microorganisms (Chenu et al., 2002). Moreover, they elaborated that the encapsulation of OC in porous structures is much stronger than preservation due to organo-mineral associations.

Near edge X-ray absorption fine structure spectroscopy and ^{13}C-nuclear magnetic resonance

To determine if the macromolecular chemistry of HA (^{13}C-NMR) is related to the chemistry of whole soil C (NEXAFS), a correlation was determined between aliphatic and aromatic C proportions obtained from each approach. Aromatic and aliphatic C proportions were not in agreement with each other and could be due to differences in C pools (HA and whole soil C). There are discrepancies between each approach and each technique possesses its own disadvantages. A significant negative correlation was observed for aliphatic C obtained from both approaches representing all aggregates in control soil (R^2=0.66).

The ratio of AL/AR obtained from NEXAFS and ^{13}C-NMR in each aggregate fraction did not resemble any significant correlation. The mesoaggregate fraction demonstrated a significant positive correlation (Fig. 5-9 b). Large microaggregates exhibited a negative

correlation for AL/AR ratio obtained from each approach (R^2=0.34). In large microaggregates, NEXAFS indicated highly humified nature in whole soil C in control. Conversely, ^{13}C-NMR indicated a less humified nature in control than two fertilizer treatments. The manure/compost added soil showed highly humified nature of HA and less humified nature in whole soil C in large microaggregates. This indicated the accumulation of labile C as a result of manure/compost addition in large microaggaregates which might have protected as a result of a complex array C preservation mechanisms.

Permanganate oxidizable carbon vs near edge x-ray absorption fine structure spectroscopy/ ^{13}C-nuclear magnetic resonance

The proportion of labile C obtained from each approach was used to examine the correlation of each approach. Permanganate oxidizable C pool is often referred to as the active/labile C pool in soil (Blair et al., 1995; Rudrappa et al., 2006). Aliphatic C calculated from ^{13}C-NMR and POXC (labile C) showed significant correlations with each other (Fig. 5-9 c) where the mesoaggregate fraction demonstrated a significant strong positive correlation (R^2=0.9).

Summary

In summary, the manure/compost addition enhanced reactive minerals, TOC, and labile C stabilization. No-till management promoted soil C preservation in macroaggregates. Carbon associated with small aggregates is least affected by tillage. Significant correlation between reactive minerals and C were observed indicating chemical stabilization through organo-mineral associations. Large microaggregates showed a strong labile C preservation attributed to physical protection and organo-mineral associations. The NEXAFS (whole soil) and ^{13}C NMR (humic acid frcation) were in agreement with each other to a certain extent, resembling similarities

between the whole C pool and HA. This study supported the current understanding of C preservation brought forward by Schimidt et al. (2011) and strengthens our understanding of the role of agricultural management practices on C sequestration and preservation that can subsequently alter climate change mitigation potential.

References

Abdala, D.B., I.R. da Silva, L. Vergütz and D.L. Sparks. 2015. Long-term manure application effects on phosphorus speciation, kinetics and distribution in highly weathered agricultural soils. Chemosphere 119:504-514.

Albers, C.N., G.T. Banta, O. Jacobsen and P.E. Hansen. 2008. Characterization and structural modelling of humic substances in field soil displaying significant differences from previously proposed structures. Eur. J. Soil Sci. 59:693-705.

Almendros, G., M. Guadalix, F.J. González-Vila and F. Martin. 1996. Preservation of aliphatic macromolecules in soil humins. Org. Geochem. 24:651-659.

Aranda, V. and F. Comino. 2014. Soil organic matter quality in three mediterranean environments (a first barrier against desertification in europe). Journal of Soil Science and Plant Nutrition0-0.

Baldock, J., C. Preston, W. McFee and J. Kelly. 1995. Chemistry of carbon decomposition processes in forests as revealed by solid-state carbon-13 nuclear magnetic resonance. p. 89-117. *In* Chemistry of carbon decomposition processes in forests as revealed by solid-state carbon-13 nuclear magnetic resonance. Carbon forms and functions in forest soils. 1995. Soil Science Society of America Inc.

Balesdent, J., C. Chenu and M. Balabane. 2000. Relationship of soil organic matter dynamics to physical protection and tillage. Soil Tillage Res. 53:215-230.

Beare, M., P. Hendrix, M. Cabrera and D. Coleman. 1994. Aggregate-protected and unprotected organic matter pools in conventional-and no-tillage soils. Soil Sci. Soc. Am. J. 58:787-795.

Berhe, A.A., K.B. Suttle, S.D. Burton and J.F. Banfield. 2012. Contingency in the direction and mechanics of soil organic matter responses to increased rainfall. Plant Soil 358:371-383.

Blair, G.J., R.D. Lefroy and L. Lisle. 1995. Soil carbon fractions based on their degree of oxidation, and the development of a carbon management index for agricultural systems. Crop and Pasture Science 46:1459-1466.

Blume, H., G.W. Brümmer, R. Horn, E. Kandeler, I. Kögel-Knabner, R. Kretzschmar, K. Stahr, B. Wilke, S. Thiele-Bruhn and G. Welp. 2010. scheffer/schachtschabel. Lehrbuch Der 4.

Bossuyt, H., K. Denef, J. Six, S. Frey, R. Merckx and K. Paustian. 2001. Influence of microbial populations and residue quality on aggregate stability. Applied Soil Ecology 16:195-208.

Brandes, J.A., C. Lee, S. Wakeham, M. Peterson, C. Jacobsen, S. Wirick and G. Cody. 2004. Examining marine particulate organic matter at sub-micron scales using scanning transmission X-ray microscopy and carbon X-ray absorption near edge structure spectroscopy. Mar. Chem. 92:107-121.

Brandes, J.A., S. Wirick and C. Jacobsen. 2010. Carbon K-edge spectra of carbonate minerals. Journal of Synchrotron Radiation 17:676-682.

Braun, A., F. Huggins, N. Shah, Y. Chen, S. Wirick, S. Mun, C. Jacobsen and G. Huffman. 2005. Advantages of soft X-ray absorption over TEM-EELS for solid carbon studies—a comparative study on diesel soot with EELS and NEXAFS. Carbon 43:117-124.

Ceccanti, B., G. Masciandaro and C. Macci. 2007. Pyrolysis-gas chromatography to evaluate the organic matter quality of a mulched soil. Soil Tillage Res. 97:71-78.

Chen, Z. and S. Pawluk. 1995. Structural variations of humic acids in two sola of alberta mollisols. Geoderma 65:173-193.

Cheng, L., F.L. Booker, C. Tu, K.O. Burkey, L. Zhou, H.D. Shew, T.W. Rufty and S. Hu. 2012. Arbuscular mycorrhizal fungi increase organic carbon decomposition under elevated CO2. Science 337:1084-1087.

Chenu, C., G. Stotzky, P. Huang, J. Bollag and N. Senesi. 2002. Interactions between microorganisms and soil particles: An overview. Interactions between Soil Particles and Microorganisms: Impact on the Terrestrial Ecosystem.IUPAC.John Wiley & Sons, Ltd., Manchester, UK1-40.

Cody, G., H. Ade, S. Wirick, G. Mitchell and A. Davis. 1998. Determination of chemical-structural changes in vitrinite accompanying luminescence alteration using C-NEXAFS analysis. Org. Geochem. 28:441-455.

Cornelis, G., C.A. Johnson, T. Van Gerven and C. Vandecasteele. 2008. Leaching mechanisms of oxyanionic metalloid and metal species in alkaline solid wastes: A review. Appl. Geochem. 23:955-976.

Cusack, D.F., O.A. Chadwick, W.C. Hockaday and P.M. Vitousek. 2012. Mineralogical controls on soil black carbon preservation. Global Biogeochem. Cycles 26:.

Denef, K., J. Six, H. Bossuyt, S.D. Frey, E.T. Elliott, R. Merckx and K. Paustian. 2001. Influence of dry–wet cycles on the interrelationship between aggregate, particulate organic matter, and microbial community dynamics. Soil Biol. Biochem. 33:1599-1611.

Ding, G., J. Novak, D. Amarasiriwardena, P. Hunt and B. Xing. 2002. Soil organic matter characteristics as affected by tillage management. Soil Sci. Soc. Am. J. 66:421-429.

Elliott, E. 1986. Aggregate structure and carbon, nitrogen, and phosphorus in native and cultivated soils. Soil Sci. Soc. Am. J. 50:627-633.

Gillespie, A., A. Diochon, B. Ma, M. Morrison, L. Kellman, F. Walley, T. Regier, D. Chevrier, J. Dynes and E. Gregorich. 2014. Nitrogen input quality changes the biochemical composition of soil organic matter stabilized in the fine fraction: A long-term study. Biogeochemistry 117:337-350.

Gulde, S., H. Chung, W. Amelung, C. Chang and J. Six. 2008. Soil carbon saturation controls labile and stable carbon pool dynamics. Soil Sci. Soc. Am. J. 72:605-612.

Han, L., K. Sun, J. Jin and B. Xing. 2016. Some concepts of soil organic carbon characteristics and mineral interaction from a review of literature. Soil Biol. Biochem. 94:107-121.

Hitchcock, A. 2008. aXis2000 is written in interactive data language (IDL). It is Available Free for Noncommercial use from Http://unicorn.Mcmaster.ca/aXis2000.Html.

Hitchcock, A.P., H.D. Stöver, L.M. Croll and R.F. Childs. 2005. Chemical mapping of polymer microstructure using soft X-ray spectromicroscopy. Aust. J. Chem. 58:423-432.

Hsu, J. and S. Lo. 1999. Chemical and spectroscopic analysis of organic matter transformations during composting of pig manure. Environmental Pollution 104:189-196.

Intergovernmental Panel on Climate Change (IPCC). 2014. Climate change 2013: The physical science basis: Working group I contribution to the fifth assessment report of the intergovernmental panel on climate change. Cambridge University Press.

Jablonski, E.L., J.L. Lenhart, S. Sambasivan, D.A. Fischer, R.L. Jones, E.K. Lin, W. Wu, D.L. Goldfarb, K. Temple and M. Angelopoulos. 2003. NEXAFS measurements of the surface chemistry of chemically amplified photoresists. p. 439-443. *In* NEXAFS measurements of the surface chemistry of chemically amplified photoresists. AIP conference proceedings, 2003. IOP INSTITUTE OF PHYSICS PUBLISHING LTD.

Jastrow, J., R. Miller and T. Boutton. 1996. Carbon dynamics of aggregate-associated organic matter estimated by carbon-13 natural abundance. Soil Sci. Soc. Am. J. 60:801-807.

Jenkinson, D. and J. Ladd. 1981. Microbial biomass in soil: Measurement and turnover. Soil Biochemistry.

Kleber, M. and M.G. Johnson. 2010. Advances in understanding the molecular structure of soil organic matter: Implications for interactions in the environment. Adv. Agron. 106:77-142.

Kleber, M., C. Mertz, S. Zikeli, H. Knicker and R. Jahn. 2004. Changes in surface reactivity and organic matter composition of clay subfractions with duration of fertilizer deprivation. Eur. J. Soil Sci. 55:381-391.

Kolattukudy, P.E. 1980. Biopolyester membranes of plants: Cutin and suberin. Science 208:990-1000.

Kowalchuk, G.A. 2012. Bad news for soil carbon sequestration. Science 337:1049-1050.

Krull, E.S., J.A. Baldock and J.O. Skjemstad. 2003. Importance of mechanisms and processes of the stabilisation of soil organic matter for modelling carbon turnover. Functional Plant Biology 30:207-222.

Lal, R. 2016. Beyond COP 21: Potential and challenges of the “4 per thousand” initiative. J. Soil Water Conserv. 71:20A-25A.

Lehmann, J. and D. Solomon. 2010. Organic carbon chemistry in soils observed by synchrotron-based spectroscopy. Dev. Soil Sci. 34:289-312.

Lehmann, J., D. Liang, M. Solomon, F. Lerotic, J. Luizão, T. Kinyangi, S. Schäfer, C. Wirick and Jacobsen. 2005. Near-edge X-ray absorption fine structure (NEXAFS) spectroscopy for mapping nano-scale distribution of organic carbon forms in soil: Application to black carbon particles. Global Biogeochem. Cycles 19.

Li, J., G.K. Evanylo, K. Xia and J. Mao. 2013. Soil carbon characterization 10 to 15 years after organic residual application: Carbon (1s) K-edge near-edge X-ray absorption fine-structure spectroscopy study. Soil Sci. 178:453-464.

Loeppert, R. and W. Inskeep. 1996. Iron. P 639-664. Methods of Soil Analysis, Part 3.

Lorenz, K., R. Lal, C.M. Preston and K.G. Nierop. 2007. Strengthening the soil organic carbon pool by increasing contributions from recalcitrant aliphatic bio (macro) molecules. Geoderma 142:1-10.

Lützow, M., I. Kögel-Knabner, K. Ekschmitt, H. Flessa, G. Guggenberger, E. Matzner and B. Marschner. 2007. SOM fractionation methods: Relevance to functional pools and to stabilization mechanisms. Soil Biol. Biochem. 39:2183-2207.

Lynch, J. and E. Bragg. 1985. Microorganisms and soil aggregate stability. p. 133-171. *In* Advances in soil science. Springer.

Margenot, A.J., F.J. Calderón, T.M. Bowles, S.J. Parikh and L.E. Jackson. 2015. Soil organic matter functional group composition in relation to organic carbon, nitrogen, and phosphorus fractions in organically managed tomato fields. Soil Sci. Soc. Am. J. 79:772-782.

Marinari, S., K. Liburdi, G. Masciandaro, B. Ceccanti and S. Grego. 2007. Humification-mineralization pyrolytic indices and carbon fractions of soil under organic and conventional management in central italy. Soil Tillage Res. 92:10-17.

Mathers, N.J., Z. Xu, T.J. Blumfield, S.J. Berners-Price and P.G. Saffigna. 2003. Composition and quality of harvest residues and soil organic matter under windrow residue management in young hoop pine plantations as revealed by solid-state 13C NMR spectroscopy. For. Ecol. Manage. 175:467-488.

McCarthy, J.F., J. Ilavsky, J.D. Jastrow, L.M. Mayer, E. Perfect and J. Zhuang. 2008. Protection of organic carbon in soil microaggregates via restructuring of aggregate porosity and filling of pores with accumulating organic matter. Geochim. Cosmochim. Acta 72:4725-4744.

Mikha, M.M. and C.W. Rice. 2004. Tillage and manure effects on soil and aggregate-associated carbon and nitrogen. Soil Sci. Soc. Am. J. 68:809-816.

Mikha, M.M., C.W. Rice and G.A. Milliken. 2005. Carbon and nitrogen mineralization as affected by drying and wetting cycles. Soil Biol. Biochem. 37:339-347.

Mukome, F.N., A.L. Kilcoyne and S.J. Parikh. 2014. Alteration of biochar carbon chemistry during soil incubations: SR-FTIR and NEXAFS investigation. Soil Sci. Soc. Am. J. 78:1632-1640.

Nicoloso, R. 2009. Soil Organic Carbon Stocks and Stabilization Mechanisms on Temperate and Sub-Tropical Climate Agroecosystems. PhD. DISS. Santa Maria Federal University. Santa Maria.

Oades, J. and A. Waters. 1991. Aggregate hierarchy in soils. Soil Research 29:815-828.

Piccolo, A. and J.S. Mbagwu. 1999. Role of hydrophobic components of soil organic matter in soil aggregate stability. Soil Sci. Soc. Am. J. 63:1801-1810.

Pisani, O., L.H. Lin, O.O. Lun, K. Lajtha, K.J. Nadelhoffer, A.J. Simpson and M.J. Simpson. 2016. Long-term doubling of litter inputs accelerates soil organic matter degradation and reduces soil carbon stocks. Biogeochemistry 127:1-14.

Ravel, B. and M. Newville. 2005. ATHENA, ARTEMIS, HEPHAESTUS: Data analysis for X-ray absorption spectroscopy using IFEFFIT. Journal of Synchrotron Radiation 12:537-541.

Regier, T., J. Krochak, T. Sham, Y. Hu, J. Thompson and R. Blyth. 2007a. Performance and capabilities of the canadian dragon: The SGM beamline at the canadian light source. Nuclear Instruments and Methods in Physics Research Section A: Accelerators, Spectrometers, Detectors and Associated Equipment 582:93-95.

Regier, T., J. Paulsen, G. Wright, I. Coulthard, K. Tan, T. Sham and R. Blyth. 2007b. Commissioning of the spherical grating monochromator soft X-ray spectroscopy beamline at the canadian light source. p. 473-476. *In* Commissioning of the spherical grating monochromator soft X-ray spectroscopy beamline at the canadian light source. SYNCHROTRON RADIATION INSTRUMENTATION: Ninth international conference on synchrotron radiation instrumentation, 2007. AIP Publishing.

Rosenzweig, C. and F.N. Tubiello. 2007. Adaptation and mitigation strategies in agriculture: An analysis of potential synergies. Mitigation Adapt. Strat. Global Change 12:855-873.

Rudrappa, L., T. Purakayastha, D. Singh and S. Bhadraray. 2006. Long-term manuring and fertilization effects on soil organic carbon pools in a typic haplustept of semi-arid sub-tropical india. Soil Tillage Res. 88:180-192.

Schmidt, M.W., M.S. Torn, S. Abiven, T. Dittmar, G. Guggenberger, I.A. Janssens, M. Kleber, I. Kögel-Knabner, J. Lehmann and D.A. Manning. 2011. Persistence of soil organic matter as an ecosystem property. Nature 478:49-56.

Schöning, I., H. Knicker and I. Kögel-Knabner. 2005. Intimate association between O/N-alkyl carbon and iron oxides in clay fractions of forest soils. Org. Geochem. 36:1378-1390.

Schwertmann, U., F. Wagner and H. Knicker. 2005. Ferrihydrite–humic associations. Soil Sci. Soc. Am. J. 69:1009-1015.

Six, J., K. Paustian, E. Elliott and C. Combrink. 2000. Soil structure and organic matter I. distribution of aggregate-size classes and aggregate-associated carbon. Soil Sci. Soc. Am. J. 64:681-689.

Smith, P., M. Bustamante, H. Ahammad, H. Clark, H. Dong, E.A. Elsiddig, H. Haberl, R. Harper, J. House and M. Jafari. 2014. Agriculture, forestry and other land use (AFOLU). Climate Change811-922.

Sollins, P., P. Homann and B.A. Caldwell. 1996. Stabilization and destabilization of soil organic matter: Mechanisms and controls. Geoderma 74:65-105.

Solomon, D., J. Lehmann, J. Harden, J. Wang, J. Kinyangi, K. Heymann, C. Karunakaran, Y. Lu, S. Wirick and C. Jacobsen. 2012. Micro-and nano-environments of carbon sequestration: Multi-element STXM–NEXAFS spectromicroscopy assessment of microbial carbon and mineral associations. Chem. Geol. 329:53-73.

Swift, R.S., D. Sparks, A. Page, P. Helmke, R. Loeppert, P. Soltanpour, M. Tabatabai, C. Johnston and M. Sumner. 1996. Organic matter characterization. Methods of Soil Analysis.Part 3-Chemical Methods.1011-1069.

Tirol-Padre, A. and J. Ladha. 2004. Assessing the reliability of permanganate-oxidizable carbon as an index of soil labile carbon. Soil Sci. Soc. Am. J. 68:969-978.

Weil, R.R., K.R. Islam, M.A. Stine, J.B. Gruver and S.E. Samson-Liebig. 2003. Estimating active carbon for soil quality assessment: A simplified method for laboratory and field use. Am. J. Alternative Agric. 18:3-17.

Wershaw, R.L. 1986. A new model for humic materials and their interactions with hydrophobic organic chemicals in soil-water or sediment-water systems. J. Contam. Hydrol. 1:29-45.

Wiesmeier, M., R. Hübner, P. Spörlein, U. Geuß, E. Hangen, A. Reischl, B. Schilling, M. Lützow and I. Kögel-Knabner. 2014. Carbon sequestration potential of soils in southeast germany derived from stable soil organic carbon saturation. Global Change Biol. 20:653-665.

Woomer, P.L., A. Martin, A. Albrecht, D.V.S. Resck, H. Scharpenseel and M. Swift. 1994. The importance and management of soil organic matter in the tropics. John Wiley & Sons.

Xing, B. and Z. Chen. 1999. Spectroscopic evidence for condensed domains in soil organic matter. Soil Sci. 164:40-47.

Yu, G., M. Wu, G. Wei, Y. Luo, W. Ran, B. Wang, J.c. Zhang and Q. Shen. 2012. Binding of organic ligands with al (III) in dissolved organic matter from soil: Implications for soil organic carbon storage. Environ. Sci. Technol. 46:6102-6109.

Zech, W., N. Senesi, G. Guggenberger, K. Kaiser, J. Lehmann, T.M. Miano, A. Miltner and G. Schroth. 1997. Factors controlling humification and mineralization of soil organic matter in the tropics. Geoderma 79:117-161.

Zhang, J., L. Zhang, P. Wang, Q. Huang, G. Yu, D. Li, Q. Shen and W. Ran. 2013. The role of non-crystalline fe in the increase of SOC after long-term organic manure application to the red soil of southern china. Eur. J. Soil Sci. 64:797-804.

Figures

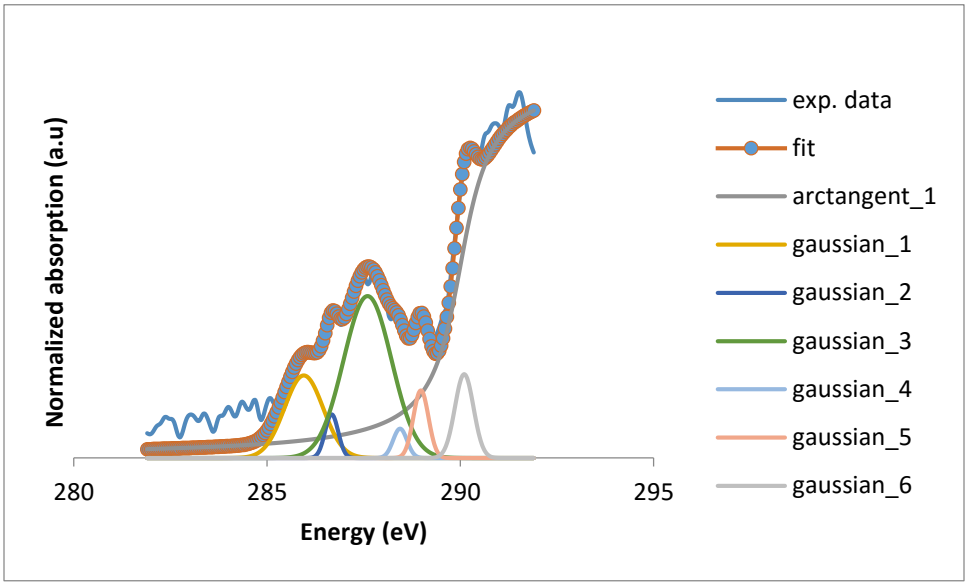

Figure 5-1 An example of Gaussian peak fitting using ATHENA software for near edge x-ray absorption fine structure spectroscopy (NEXAFS) spectra representing large microaggregate fraction (53-250 µm) of no-till control treatment. For the deconvolution, arctangent function was fixed at 290 eV. Full width at half maximum of arctangent function and Gaussian functions were fixed at 1eV and 0.4 eV, respectively. Refer to the Table 5-1 for the C functional group representing each Gaussian curves.

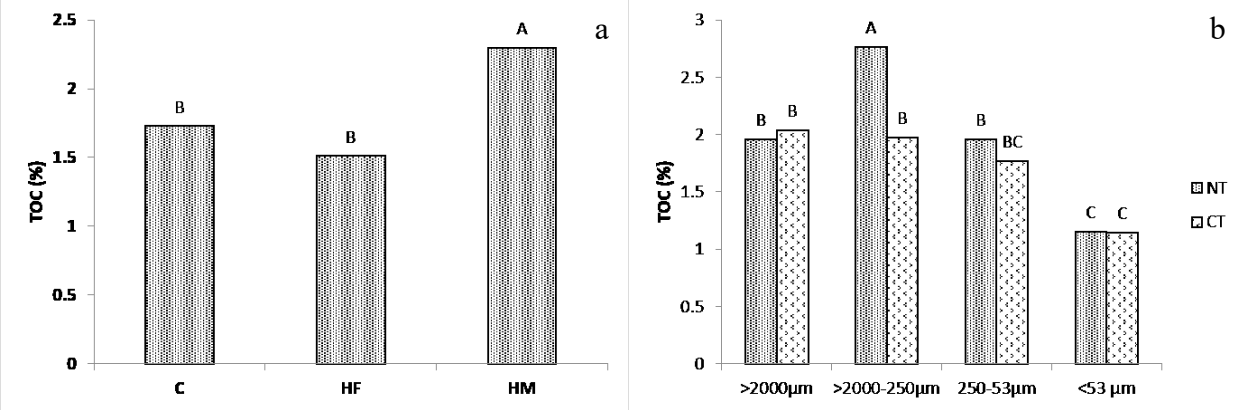

Figure 5-2 Concentration of percentage of TOC representing different fertilizer treatments (a) and level of disturbance and tillage interaction effect (b). Fertilizer treatments: control(C), urea (HF), and manure/compost (HM). Two tillage treatments are no-till/NT and conventional till/CT. Different letters represent the statistical significance at $p<0.05$.

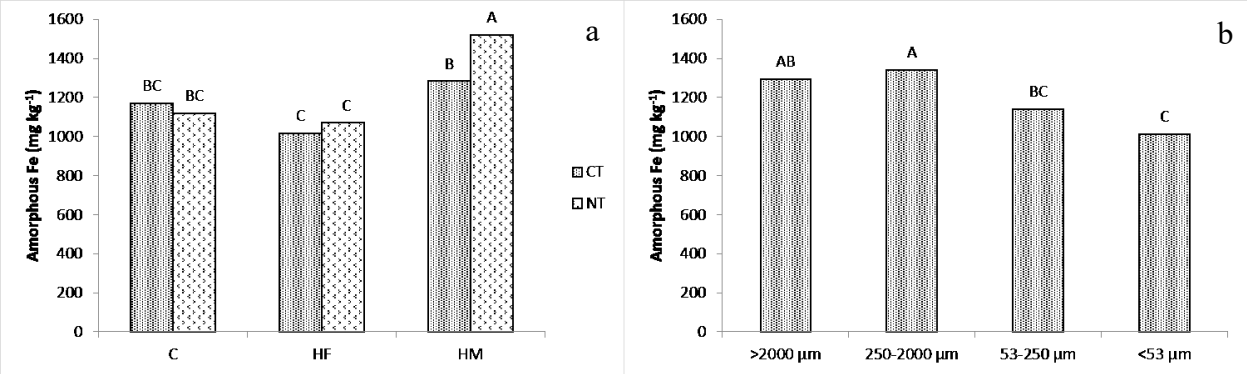

Figure 5-3 Concentration of amorphous iron representing different tillage and fertilizer treatments (a) and aggregate size classes (b) Fertilizer treatments: control(C), urea (HF), and manure/compost (HM). Two tillage treatments are no-till/NT and conventional till/CT. Different letters represent the statistical significance at $p<0.05$)

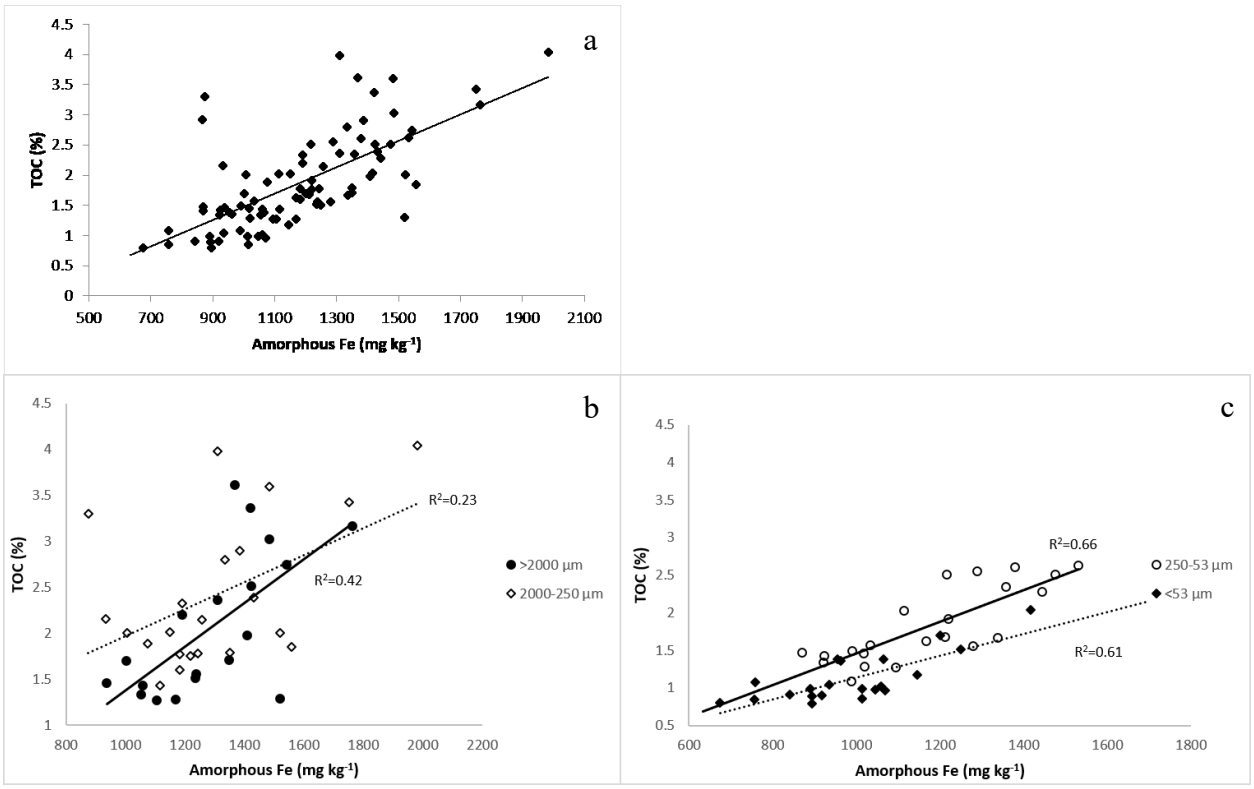

Figure 5-4 Significant correlations between the concentration of amorphous iron and total organic carbon in all the aggregate size fractions (non-composite samples) (a), macro and mesoaggregate fractions (b) and large microaggregate and <53µm fractions (c) representing all the treatment combinations of non-composite samples. Significance of the correlation was determined at p=0.05.

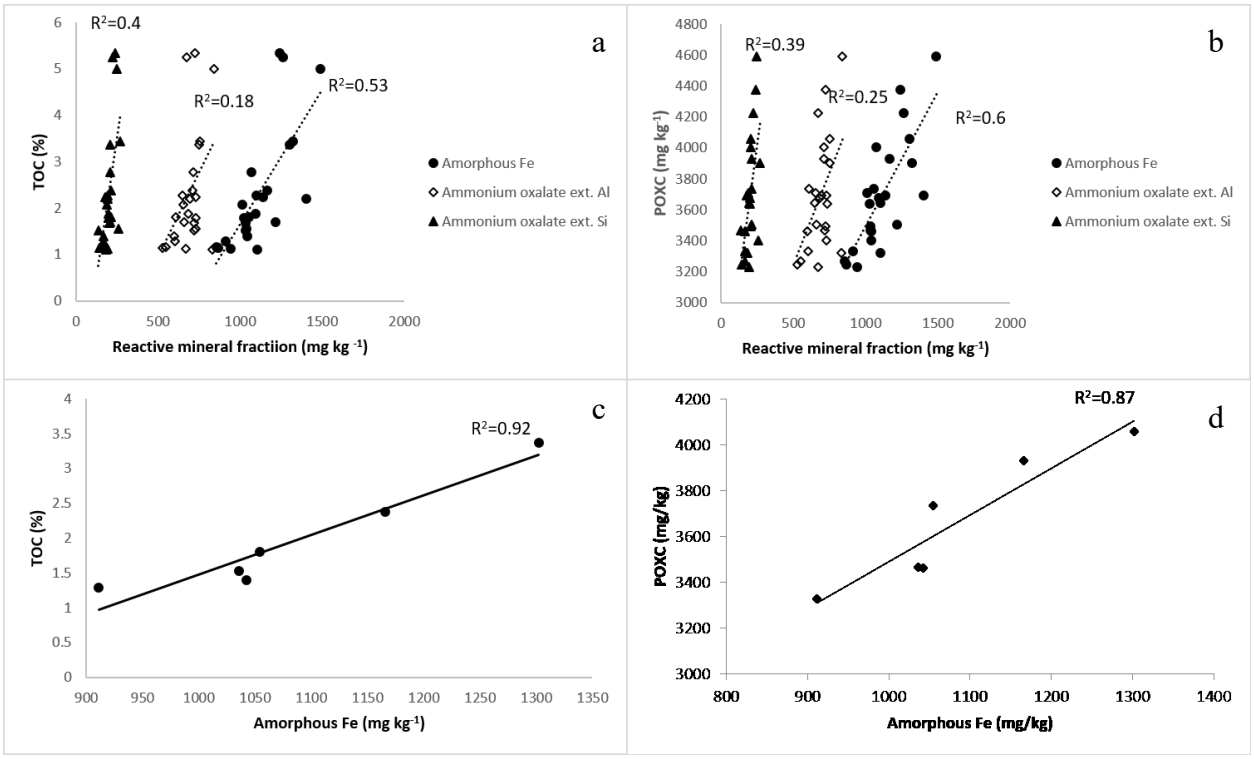

Figure 5-5 Correlation between the concentration of amorphous iron/ammonium oxalate extractable Al/Si and TOC (a) and POXC (b) in all the aggregate fractions of composite samples representing all the treatment combinations. Correlation between the concentration of amorphous iron fraction vs TOC (c) and POXC (d) in large microaggregate fraction. Significance of the correlation was determined at p=0.05. Coefficient of correlations are displayed.

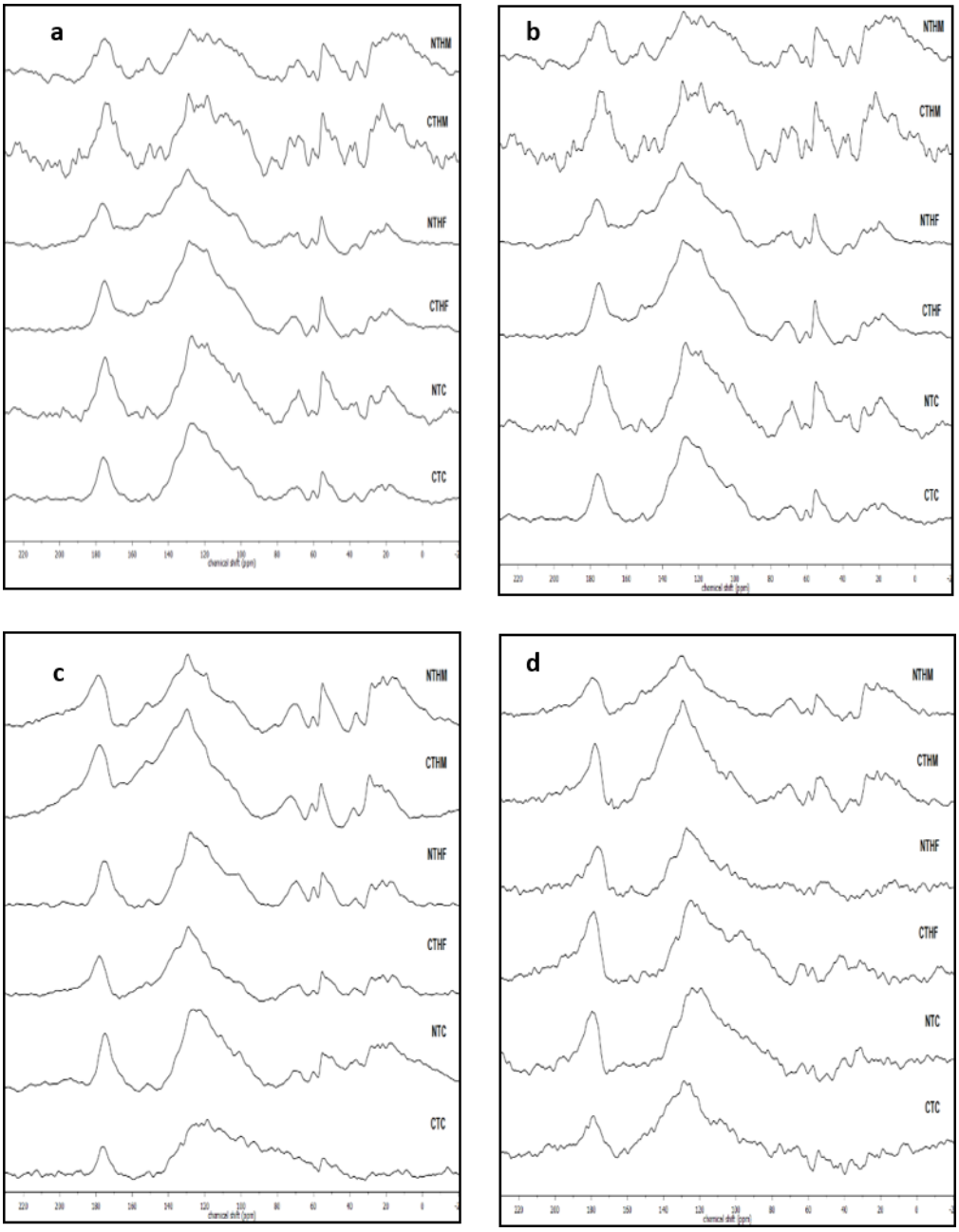

Figure 5-6 Liquid state ^{13}C-NMR data measured on humic acid extracted from composite soil samples representing different treatment combinations (no-till manure/compost/NTHM; conventional till manure/compost/CTHM;no-till urea/NTF; conventional till urea/CTHF; no-till control/NTC; conventional till control/CTC). Different aggregate classes presented are a->2000µm; b-250-2000 µm; c-53-250 µm and d-<53 µm.

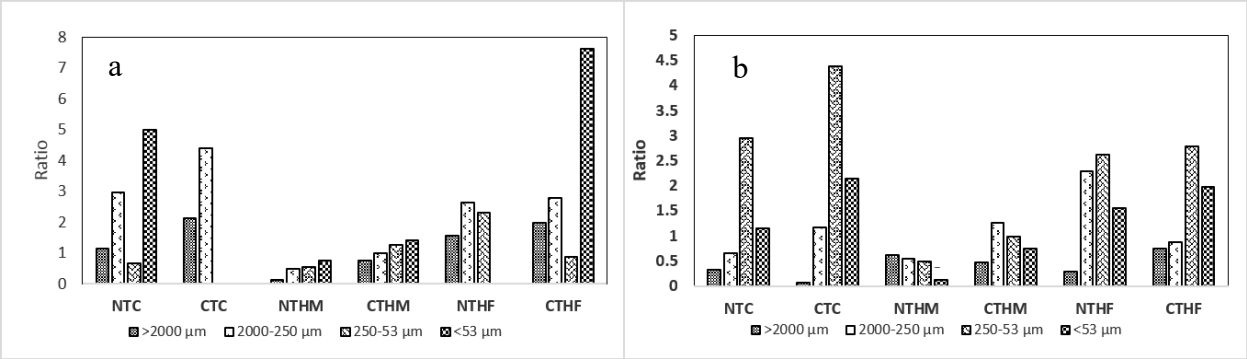

Figure 5-7 Ratio of O-alkyl/alkyl (a) aliphatic:aromatic (AL/AR) (b) of humic acid extracted from composite soil samples representing different treatment combinations (no-till manure/compost/NTHM; conventional till manure/compost/CTHM; no-till urea/NTHF; conventional till urea/CTHF;no-till control/NTC; conventional till control/CTC). Different aggregates classes presented are a->2000 µm; b-250-2000 µm; c-53-250 µm and d-<53 µm. Liquid state ^{13}C-nuclear magnetic resonance spectra presented in Figure 5-6 were integrated in to four regions (Carboxylic, aromatic, alkyl and O-alkyl (Mathers et al., 2003; Zhang et al., 2013)

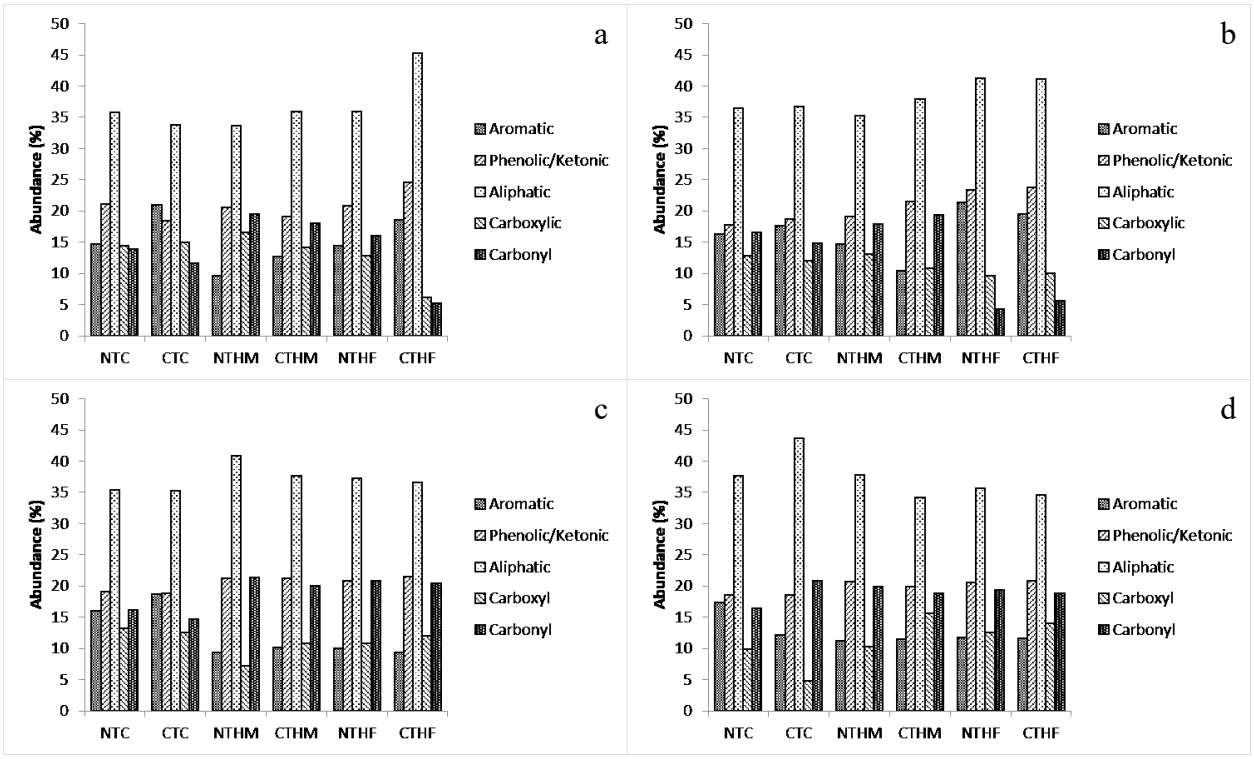

Figure 5-8 Proportions of different C functional groups in composite macroaggregates - >2000 µm (a), mesoaggregates-250-2000 µm (b), large microaggregates - 53-250 µm (c), and <53 µm fraction (d) representing different treatment combinations (no-till manure/compost/NTHM; conventional till manure/compost/CTHM; no-till urea/NTHF; conventional till urea/CTHF; no-till control/NTC; conventional till control/CTC). Proportions were obtained by Gaussian peak fitting using ATHENA software.

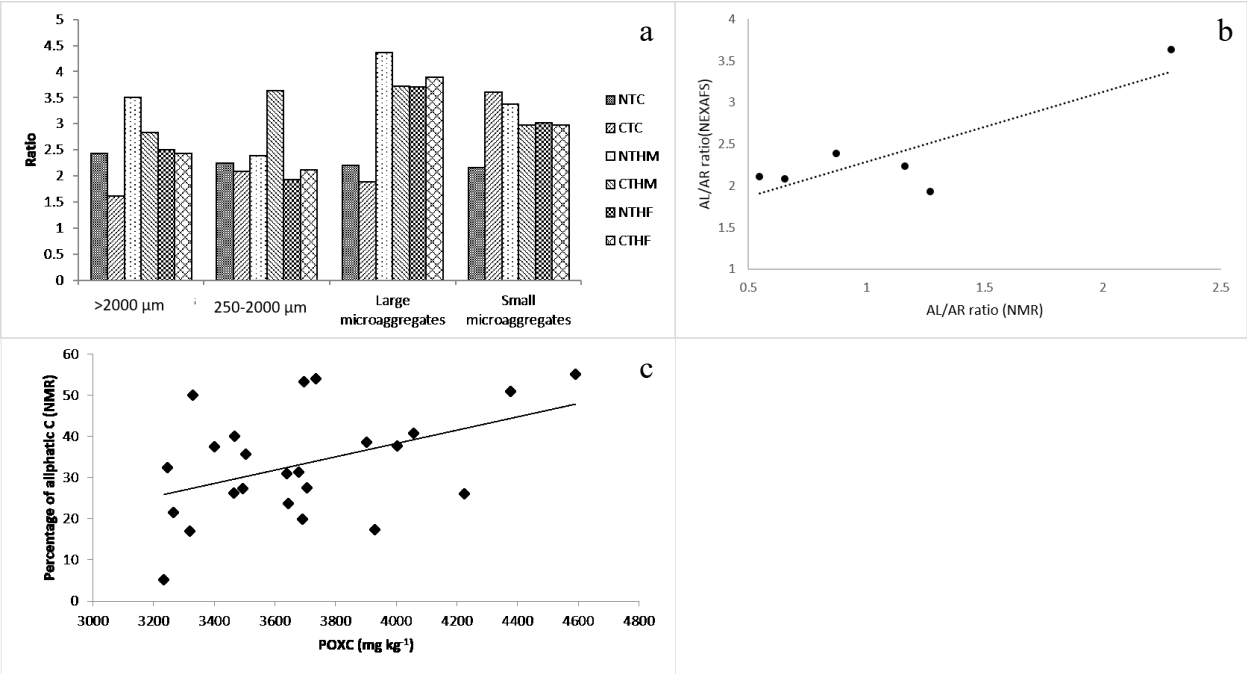

Figure 5-9 Ratio of aliphatic:aromatic (AL/AR) of composite soil samples representing different treatment combinations (a), correlation between aliphatic to aromatic ratio obtained from NEXAFS and NMR approaches in mesoaggregates (b) and correlation between percentage of aliphatic C (NMR approach) and concentration of permanganate oxidizable carbon (POXC). Treatment combinations are no-till manure/compost/NTHM, conventional till manure/compost/CTHM, no-till urea/NTHF, conventional till urea/CTHF, no-till control/NTC), conventional till control/CTC), and aggregate classes. Proportions of each C functional group was obtained from Gaussian peak fitting using ATHENA. Significance of the correlation was determined at p=0.05.

Tables

Table 5-1 Peak assignment for near edge x-ray absorption fine structure spectroscopy

Form of C	Transition	Peak energy (eV)	Gaussian curve	Fit position	References
Quinone C=O, protonated aromatic C	1s-π*	283.7-284.3	-	-	Lehmann et al., 2005
Alkylated to carbonyl-substituted aromatic C	1s-π*	284.9-285.5	-	-	Brandes et al. (2004); Braun et al. (2005)
Unsaturated aromatic C	1s-π*	286-286.5	G1	286	Hitchcock et al. (2005); Lehmann et al. (2005)
Phenolic OH, Ketonic O-C-O		286.5-287.1	G2	286.7	Cody et al. (1998) Hitchcock et al. (2005); Lehmann et al. (2005)
Aliphatic C-H	1s-3p/σ*	287.1-287.8	G3	287.6	Lehmann et al., 2005

Carboxylic C	1s-π*	287.7-288.6	G4	288.4	Lehmann et al., 2005
Carbonyl C	1s-3p, σ *	289.3-289.8	-	-	Hitchcock et al. (2005); Lehmann et al. (2005)
Carboxylic substituted aromatic, carbonyl C=O, carbonates		290-290.5	G5	290.1	Kleber et al., 2010 Brandes et al., 2010

Chapter 6 - Evaluation of Resilience of Sequestered Soil Organic Carbon to Environmental and Anthropogenic Influences

Abstract

The resilience of preserved soil organic carbon (SOC) to changing environmental and anthropogenic influences can ultimately alter the climate change potential. This study was designed as a six-month incubation study to evaluate the dynamics of SOC from four contrasting long-term agroecosystems. Two manure/compost added soils from a temperate climate (Mollisols) were from a continuous corn system which represented no-till (NTM) and conventional-till (CTM). Other two soils from a tropical climate (Oxisols) represented a complex crop rotation with no-till (NTR) and conventional-till (CTR). Soils were subjected to three temperatures (12 ºC, 24 ºC, and 36 ºC), two moistures (field capacity and 80% of the field capacity) and two levels of physical disturbances (intact- <4 mm and crushed- <0.25 mm). Soil C dynamics and changes in soil chemical properties were monitored for six months using an integrated approach. The resilience of SOC was significantly affected by temperature directly and indirectly across both ecosystems. Warming stimulated CO_2-C efflux in all four soils. The crushed fraction of Mollisol showed a relative high CO_2-C efflux, signifying the importance of physical protection on C preservation. This was not observed in Oxisol, indicating the significance of chemical stabilization due to mineral-OC interactions. Cumulative CO_2-C efflux and soil pH was not affected by the level of moisture in Mollisols. The intact fraction of CTM carried a high amount of labile C than the crushed fraction indicating the importance of physical protection. Slow release of C from the intact fraction of NTM enhanced microbial dynamics.

Moreover, high temperature affected the soil acidity and amorphous Fe which ultimately affect organo-mineral associations. The less disturbed nature in soils favored the facilitation of fungi growth leading to a high CO_2-C efflux. Moreover, in temperate agroecosystem, the tilled soils exhibited a relative resistance to changes than no-till during the incubation suggesting strong organo-mineral associations. Soil biological and chemical results were in agreement with each other in most of the instances. It was evident that changes in the macromolecular properties of HA fraction occur even after a short time. Overall, this research strengthens our understanding on how environmental and anthropogenic factors influence on the resislience of SOC even within a short period of time.

Introduction

Rising atmospheric carbon dioxide (CO_2) and climate change have gained the attention of the scientific community worldwide. Soil represents the largest terrestrial organic carbon (C) pool and plays a critical role in C dynamics. Alterations of temperature and/or precipitation patterns can drastically impact soil organic C (SOC) which may further enhance atmospheric CO_2 (Davidson and Janssens, 2006). As stated by Kirschbaum (2000), a modification of 10% of the SOC pool could be comparable to 30 years of anthropogenic CO_2 emission. Climate change is predicted to affect SOC negatively since the effect of warming is greater on SOC decomposition relative to net primary production (Kirshhbaum, 2000; Liski et al., 1999). Emission of CO_2 from soil is mainly due to root respiration and microbial decomposition of SOC and both these processes are temperature and moisture dependent (Davidson and Janssens, 2006). Microorganisms react to temperature variations by producing new enzymes and altering membrane fatty acids (Steinweg et al., 2008). Soil microbial populations and enzymes are significantly affected by soil moisture (Brockett et al., 2012).

The mean residence time of SOC is a major factor that governs the sequestering capacity (Luo et al., 2003). It is highly influenced by decomposer activity and varies with temperature, moisture, pH, and nutrient availability (Jastrow et al., 2007). The heterogeneous and complex nature of SOC complicates information on the kinetic properties associated with intrinsic temperature sensitivity, Q_{10} (Davidson and Janssens, 2006). Both labile and resistant C have been reported to respond similarly to temperature (Fang et al., 2005; Conen et al., 2006).

However, temperature interacts with soil moisture and could have antagonistic effects on mineralization of soil C (Sierra et al., 2015).

Apart from climate change mitigation, SOC sequestration improves soil quality, water quality, and plant productivity. Soil OC is highly reliant on its resilience to changing climate that is uncertain and influenced by a variety of factors. If the combined effects of SOC preservation mechanisms such as biochemical recalcitrance, chemical stabilization, and physical protection (Sollins et al., 1996) are strong, SOC has the potential to withstand the changing climate. A variety of management practices such as agroforestry, the addition of biochar and traditional agroecological strategies such as reduced/no-till, increased cropping intensity, incorporation of soil amendments, cover cropping, and crop rotation (Altieri and Nichollc, 2013; Koide et al., 2015; Mohan et al., 2016; Stavi and Lal, 2013), were identified as best management practices (BMPs) to improve SOC.

Humus decomposition is strongly influenced by moisture and temperature (Stockmann et al., 2013). High temperature enhances respiration where the pCO_2 increases in the soil atmosphere forming carbonic acid (H_2CO_3) (Hinsinger et al., 2003) that can increase soil acidity. Moreover, changes in soil acidity could occur due to microbial-mediated redox reactions. Thermodynamically unstable amorphous ferrihydrite converts to crystalline phases (i.e. goethite and hematite) and the rate and mechanism of transformation are controlled by pH, temperature, Eh, and Fe^{2+}(aq.) (Yee et al., 2006). Therefore, we hypothesize that changing temperature, soil moisture and/or physical protection can influence 1) SOC chemistry, 2) soil pH and 3) soil reactive minerals; and these changes in turn can affect SOC decomposition rates.

The objectives of this study were to 1) evaluate soil CO_2-C efflux in contrasting agroecosystems subjected to different levels of temperature, moisture, and physical disturbance;

2) assess temporal dynamics of SOC over time and to determine the changes in macromolecular chemistry of humic acid (HA), soil pH, and reactive mineral fraction as a response to temperature-moisture regimes and physical disturbance. In addition, microbial community shifts and adaptations were evaluated in a complementary study (Menefee, 2016).

Materials and Methods

Four contrasting soils from long-term temperate (Mollisols) and tropical (Oxisols) agroecosystems were selected for a six-month long laboratory based incubation study. Soils were collected from 0-5 cm depth where a significant amount of C and diversified microbial community structure exists. The top 5 cm of no-till soils has high fungi:bacteria ratios (Beare et al., 1992; Frey et al.,1999) and enzyme activity (Acosta-Martinez et al., 2003; Bergstorm et al., 2000). Sampling from both agroecosystems was done in Fall 2014.

Site description and sample preparation

Two soils were collected from a tropical agroecosystem (established in 1985) located in Cruz Alta, Rio Grande do Sul, Brazil (28º 36'00" S, 53º 40' 21" W). The average precipitation was reported as 1,774 mm with a mean annual temperature of 19.2 ˚C. The soil type is a clayey, kaolinitic, thermic Rhodic Hapludox enriched with kaolinite and iron (Fe) oxides. Two tropical agroecosystems were no-till with a complex crop rotation system (NTR) and conventional till with a complex crop rotation system (CTR). The complex crop rotation was summer and winter crop rotation: wheat/soybean/black oat/soybean/black oat + common vetch/maize/forage radish. To maintain the appropriate pH, soils were amended with dolomitic lime prior to the establishment (1985), and repeated in 1995 and in 2011 at a rate of 5 Mg ha^{-1}. Soil sampling was carried out using a 2-cm diameter soil sampling probe, randomly from several locations to obtain a representative composite sample. Moist soils were packed carefully in polypropylene bags to

minimize physical damage to aggregate structure and shipped to Kansas State University, Manhattan, KS, USA.

The remaining two soils, were collected from a temperate agroecosystem (established in 1990) which was under continuous corn (Zea mays L.). It was located in North Agronomy Farm, Manhattan, Kansas, USA (39º 12'42" N, 96º 35' 39" W). The soil was a moderately well-drained Kennebec silt loam (fine-silty, mixed superactive, mesic Cumulic Hapludolls) and the clay fraction was dominated with 2:1 layer silicates, such as montmorillonite. Soil was sampled from no-till manure/compost (NTM) and conventional till manure/compost (CTM). Fresh cattle manure was added in the first ten years and continued with compost application. They were added on the basis of supplying 168 kg ha^{-1} yr^{-1} of N. Soil sampling was carried out using a 2-cm diameter soil sampling probe, randomly from several locations of each field replicate (four field replicates) to obtain a representative composite sample from each system. Collected soil samples were placed in polypropylene bags and stored at 5 ˚C allowing minimum physical disturbance to aggregates (moist condition).

Moist soils were air dried. Residues were removed carefully, and soils were sieved through a 4 mm sieve. All four soils were separated into two portions. One portion of each soil was gently crushed to disrupt aggregates and sieved through a 250 µm sieve, and the other portion was kept as it is. The two portions which resembled two levels of physical disturbance were intact (<4 mm) and crushed (<0.25 mm).

The aggregates were then incubated at six temperature-moisture treatment combinations. The temperature levels were 12 ºC, 24 ºC, and 36 ºC and the two moisture levels were field capacity (high moisture-M1) and 80% of the field capacity (low moisture-M2). The soils were covered with lids containing circular punctures, and the punctures were shielded with Parafilm®

to facilitate gas exchange. The field capacities of Oxisols and Mollisols were determined using a pressure plate according to the method by Pierzynski et al., (2004). Before the initiation of the incubation, sample cups with moistened soils were kept inside an incubator at 20 ºC for two weeks to equilibrate. The moisture was maintained throughout the experiment. The five destructive sampling times were 7, 30, 60, 120, and 180 days.

Carbon dioxide (CO_2) efflux

A same set of samples from each soil was used for gas sampling until the experiment was terminated. The overall experimental design structure for CO_2 was repeated measures in time. The repeated gas measurements were taken 19 times during the incubation (1, 3, 5, 7, 9, 14, 19, 25, 31, 37, 44, 51, 60, 80, 100, 120, 140, 160, and 180 days). Each sample cup was placed inside a Mason jar with a rubber septa fixed to its lid to collect gas. The Mason jars were tightly sealed, and gas sampling was carried out at 0, 1, 2, and 3 hrs. Before drawing gas, mixing of gas inside the Mason jar was carried out using a syringe. Gas samples (30 mL) were drawn to 12 mL Labco Exetainers (Labco Limited, United Kingdom) with Labco grey butyl rubber septa and stored under a pressurized condition to ensure zero entrance of atmospheric air. After each sampling, the samples were aerated with laboratory air to maintain aerobic conditions throughout the incubation. The analysis of gas was conducted by a Thermal Conductivity Detector (TCD) of automated Bruker Gas Chromatography (SCION 456-GC). The slope of the regression (linear regression) line was determined to get the rate of CO_2-C efflux from soils (CO_2-C g^{-1} hr^{-1}). Cumulative gas emission during incubation was estimated using linear interpolation between sample points and determining the area under the curve. Calculation of temperature sensitivity (Q_{10}) was done according to the Vant's Hoff law as stated in eq. 1. (Dessureault-Rompré et al., 2010).

$$Q_{10}=(Rx/Ry)^{(10/Tx-Ty)} \quad \text{Eq.1}$$

Rx and Ry correspond to the rate of CO_2-C efflux at Tx and Ty temperatures, respectively. The high temperature was represented by Tx and the lower temperature was indicated by Ty. The temperature ranges used for Q_{10} calculations were 12 ºC - 24 ºC (low-temperature range) and 24 ºC - 36 ºC (high-temperature range).

Soil chemical and biological analyses

Basic chemical properties of original soils were determined **(**Error! Reference source not f ound.**).** Permanganate oxidizable C (POXC) and total organic carbon (TOC) were analyzed on three sampling times (7, 60, and 180 days). Soil pH, amorphous iron (Fe), and macromolecular properties of humic acid (HA) were determined at the end of the incubation (180 days). Microbial analysis (PLFA) was conducted at all five sampling times (Menefee, 2016).

Total OC was determined by dry combustion using Carlo Erba C/N analyzer (Carlo Erba instruments, Milan, Italy) (Nelson et al., 1996). Analysis of permanganate oxidizable C was conducted according to the method by Weil et al. (2003). The soils were ground (<0.25 mm) and placed into 50 mL centrifuge tubes. Potassium permanganate (prepared in 0.01 *M* $CaCl_2$) was added to the soil (40 mL) and shaken using an end to end shaker for 2 min (120 strokes /min). Samples were analyzed using a DU 800 by Beckman-Coulter spectrophotometer. Soil pH was determined using a 1:10 soil: deionized water and measured with an Orion star A111 benchtop pH meter (Fisher Scientific, Pittsburgh, PA). Amorphous Fe was determined following ammonium oxalate method in dark (Loeppert and Inskeep, 1996).

To understand the changes in macromolecular C chemistry of HA, ^{13}C nuclear magnetic resonance (^{13}C -NMR) and high performance liquid chromatography (HPLC) were used. Composite soil samples were made by combining equal amounts from each replicate of the same

treatment combination. Humic acid was extracted from composite soil samples according to International Humic Substances Society (IHSS) method with some modifications (Swift et al., 1996). Analyses were only carried out for selected soils from temperate agroecosystem. Methodologies related to ^{13}C-NMR and HPLC are explained in Chapter three.

Statistical analysis

Repeated measure ANOVA was conducted to determine the effect of temperature, moisture, and the level of disturbance on soil CO_2-C efflux and Q_{10}. The effects were estimated by ANOVA using PROC GLIMMIX using SAS 9.4 (SAS Institute Inc., Cary, NC, USA). The statistically significant parameters of CO_2-C efflux were plotted over time, and the best fitted model (linear, quadratic, cubic, exponential, or power) was selected using PROC REG using SAS 9.4 (SAS Institute Inc., Cary, NC, USA). The plots were presented based on the significant best fit and non-significant fits were not shown.

PROC MIXED was used for pH, TOC, POXC, and amorphous Fe. Tukey's HSD multiple comparison method was used to find least square mean differences. The design structure for TOC and POXC was considered as a randomized complete-block design (RCBD), treating three sampling times as fixed blocks. Amorphous Fe and pH were analyzed as a completely randomized design (CRD) and least square means were evaluated using Tukey's HSD. All the statistical comparisons were based at α=0.05 probability level.

Results and Discussion

Each soil from contrasting agroecosystems was different from each other since beginning with respect to a variety of chemical, biological, and physical properties (Table 6-1). Therefore, statistical comparisons were not conducted between soils. Previous studies based on same soils showed a tillage effect on aggregation in Mollisols (Nicoloso, 2009). After 18 years,

macroaggregate fractions (>250 μm) were 52.8% and 75.1% for CTM and NTM, respectively. In contrast, macroaggregate fractions of Oxisols, after 23 years, were 96.9% for CTR and 97.1% for NTR. For the Mollisols, SOC preservation was mainly governed by bio-physical mechanisms whereas the mineral-organo control was the primary mechanism for the Oxisols (Fabrizzi et al., 2009).

Rate of efflux of carbon dioxide (CO_2-C)

All soils had a four-way significant interaction (disturbance x moisture x temperature x date) except CTR (Table 6.2). The rate of CO_2-C efflux was high at 36 ºC due to increased microbial metabolism at high temperature (Fig. 6-1, 6-2). Both aggregate fractions of CTM indicated a decreasing trend in the rate of CO_2-C efflux with time at 36 ºC (Fig. 6-1 **Error! R eference source not found.**a and b). This was related to the decline of readily available OC that was clearly observed in the crushed fraction of CTM (Fig. 6-13 c). In contrast to the observed behavior in CTM, the intact fraction of NTM showed an increasing trend of the rate of CO_2-C efflux at 36ºC, towards the end of the incubation (Fig. 6-1 c). This could be related to high OC and slow release of OC from the intact fraction of NTM (Table 6-1). In NTM, total biomarkers and relative abundance of bacteria were significantly increased in the intact fraction between 7-60 days, and it was the same until the end (Menefee, 2016). The release of OC with time might have enhanced the microbial population resulting in an increased rate of CO_2-C efflux.

Intact and crushed fractions of NTR behaved oppositely. The intact fraction showed a decreasing trend in the rate of CO_2-C efflux with time (Fig. 6-2 a) whereas the crushed fraction exhibited an increased efflux after about 80 days (Fig. 6-2 b). This is an indication of the strength of physical protection in the intact fraction. Crushing eliminated physical protection exposing protected C for microbial decomposition. Furthermore, significantly high bacterial population

was observed in the crushed fraction (Menefee, 2016). A decreasing trend in the rate of CO_2-C efflux was observed with time in both aggregate fractions of CTR. At 36 ºC, the moisture effect was only observed in the intact fraction of CTR (Fig. 6-2 c). Low moisture of intact fraction of CTR had a low rate of CO_2-C efflux signifying the effect of moisture on microbial dynamics (Fig. 6-2 c). High temperature lowers soil moisture hindering the diffusion of solutes and enzymes (Manzoni et al., 2012). Total biomarkers and abundance of bacteria were decreased at low moisture (Menefee, 2016).

Temperature sensitivity of CO_2 efflux (Q_{10})

Temperature sensitivity of soil respiration was reported to be ranging from 0.5 to 300 in laboratory-based experiments (Hamdi et al., 2013) where Q_{10} showed a negative correlation with temperature (below 25 ºC). Arrhenius enzyme kinetic theory elaborated the link between the increased activation energy of substrates and high intrinsic temperature sensitivity. Relatively high activation energy is needed for the decomposition of recalcitrant C (Bosatta and Ågren, 1999). In reality, apparent temperature sensitivity varies in the presence of C preservation mechanisms (Conant et al., 2011).

To better show the variation pattern of Q_{10} with time, polynomial models were plotted. Only the data sets with significant fits were shown. A significant relationship between Q_{10} and incubation time was not found for CTM. The crushed fraction of NTM showed an initial increase followed by a decline towards the end (Fig. 6-3). At both temperature ranges, Q_{10} of the intact fraction of NTM showed an increasing trend with time indicating slow release of substrates from the intact fraction. Moreover, total biomarkers and total bacterial population exhibited an increasing trend with the time in NTM (Menefee, 2016). For the intact fraction of NTM, relatively high Q_{10} was observed throughout the experiment for the high temperature range

compared to the low temperature range (Fig. 6-3). This is in opposition to the general theory which resembled a decrease in Q_{10} as a response to warming (Zhou et al., 2014). A meta-analysis revealed that the decline of Q_{10} in soil OC decomposition was less affected over the range of 25ºC to 50ºC (Hamdi et al., 2013). This was in agreement with the findings from our study.

The intact fraction of CTR exhibited an initial decreasing trend of Q_{10}. Then it showed a slight increase at low moisture (Fig. 6-4 a). Towards the end, a decrease in Q_{10} was observed, indicating lower availability of substrates. Analysis of PLFA supported this observation and showed a decreasing trend in the bacteria and fungi population in the intact fraction of CTR towards the end (Menefee, 2016). The crushed fraction of NTR at higher temperature range showed a mild increase in Q_{10} with time (Fig. 6-4 b). Moreover, Q_{10} of NTR appeared significantly high at low temperature range at low moisture (Fig. 6-4 c). Conversely, Q_{10} was significantly greater at high temperature range at low moisture. With further mineralization, recalcitrant C tends to get concentrated, leading to a subsequent increase in the sensitivity to warming (Wang et al., 2013). Moreover, substrate availability and oxygen diffusivity are enhanced by moisture, resulting increased Q_{10} (Zhou et al., 2009).

Cumulative CO_2-C efflux

Increasing temperatures exhibited a rise in the cumulative CO_2-C efflux in all four soils (Fig. 6-5). The effluxes of CO_2-C in no-till soils (NTM and NTR) were greater than tilled soils (CTM and CTR) due to high SOC in original soils. Moreover, the crushed fraction of CTM demonstrated a high cumulative CO_2-C efflux (Fig. 6-6 a) compared to the intact fraction, implying the significance of physical protection on OC preservation. At 36ºC, the intact fraction of NTM showed high cumulative CO_2-C efflux (Fig. 6-6 b) than the crushed fraction, opposing to the favorable aggregate effect observed in CTM. This could be linked with the facilitation of

fungi growth in less disturbed soils (Helgason et al., 2010). After 60 and 120 days, the fungi community was abundant in the intact fraction of NTM (Menefee, 2016). The high fungi population might have increased CO_2-C efflux accelerating the consumption of both labile and recalcitrant C. At 36 ºC, low cumulative CO_2-C efflux was observed at high moisture in NTR (Fig. 6-7).

Organic C in CTM and NTM seemed not to be affected by moisture level which could be a result of moisture retention due to manure/compost addition. Moreover, NTR was not affected by physical disruption which could be a reflection of strong aggregation due to clay minerals and organo-mineral associations. Temperature and moisture combination is the most significant factor governing the behavior of microbial community (Paul, 2014). The respiration rate of soil microbes increases with rising temperature up to 40 ºC (Chen et al., 2000; Winkler et al., 1996). Even though instantaneous respiration increased with increasing temperature, the fungal and bacterial growth reduced. Fungi are more vulnerable to high temperature than bacteria (Pietikainen et al., 2005). In this study, a reducing trend in microbial population was observed with increasing temperature in all soils (Menefee, 2016).

Soil chemical analysis

Soil pH

With increasing temperature, acidity increased in all four soils (Fig. 6-8). Even though the soils were aerated after each sampling, the concentrations of gaseous CO_2-C in the immediate atmospheres of soils were high throughout the incubation, especially at high temperatures. In NTM, both aggregate fractions did not show any significant difference of pH at each temperature (Fig. 6-8 a). In NTR, pH was significantly high in the crushed fraction at each temperature (Fig.

6-8 d). Even though statistically non-significant, the crushed fraction of NTR had low cumulative CO_2-C efflux.

High moisture in CTM showed a greater acidification indicating facilitated dissolution of gaseous CO_2 (Fig. 6-10 a). In NTR, low moisture led to a decrease in pH (Fig. 6-9 b) which was in agreement with high cumulative CO_2-C efflux at low moisture. Moreover, NTR showed an abundance of bacteria at low moisture (Menefee, 2016) that might have led to high cumulative CO_2-C efflux. In CTR, at high moisture, the crushed fraction exhibited high acidity as a result of facilitated dissolution of CO_2 (Fig. 6-9 c).

Furthermore, cumulative CO_2-C efflux and pH showed significant negative correlations for NTM, CTM, NTR, and CTR with R^2 of 0.9, 0.67, 0.58, and 0.53, respectively (Fig. 6-9). The capability of soil CO_2 in soil acidification is powerful than theoretically predicted because of the displacement of exchangeable base cations (Oh and Richter, 2004). Contrasting pKa values were reported for molecular H_2CO_3 (3.76 at 25ºC) and a mixture of $CO_{2\,(aq)}$ /molecular H_2CO_3 (6.36 at 25ºC) (Oh and Richter, 2004). Apart from high CO_2 concentration, pKa can be increased due to the availability of H^+ scavengers and wide-ranging contact times between phases (soil, water, and gas).

A decrease in pH enhances the anion exchange capacity (AEC) of soil minerals facilitating the sorption of negatively charged C. The amorphous mineral fraction is more prone to develop positive charges on surfaces, increasing AEC (Chichester et al., 1970; Feng et al., 2005). Increasing acidity improves the adsorption of HA to hematite and kaolinite (Hur and Schlautman, 2004; Shaker et al., 2012). Therefore, the Oxisols abundant with kaolinite and Fe oxides should facilitate HA adsorption as a result of low soil pH, ultimately enhancing SOC preservation. Moreover, the formations of organo-mineral associations are promoted through

inner-sphere complexation at low pH (Ramos and Huertas, 2014), enhancing SOC preservation further (Kleber et al., 2015).

Total Organic Carbon (TOC)

The balance between the formation and degradation of microbial by-products governs soil C storage (Six et al., 2004). In CTM, none of the factors were significant (moisture, temperature, sampling time, and level of disturbance) on TOC. Conversely, NTM showed a significant interaction effect of moisture and level of disturbance. At high moisture, TOC was significantly low in the crushed fraction of NTM (Fig. 6-11 a). Over time, a decreasing trend of TOC was observed at both moisture conditions in NTM (Fig. 6-11 b).

In CTR, after 60 days of incubation, a significant reduction of TOC was observed in the intact fraction (Fig. 6-12 a). Moreover, the crushed fraction of NTR showed a reduction of TOC at the end of the incubation. Intact fraction had low TOC at 60 days and increased with time (Fig. 6-12 b). This could be explained by facilitated fungal dominance in less disturbed systems (NTR intact fraction) which incorporate more recalcitrant C as fungi by-products. Fungi metabolites are relatively recalcitrant than bacterial metabolites (Six et al., 2006). In the intact fraction of NTR, there was no any significant change in TOC as affected by temperature and moisture (Fig. 6-12 c). In contrast, the crushed fraction at low moisture exhibited a decreasing trend of TOC with warming (Fig. 6-12 d).

Permanganate oxidizable carbon (POXC)

Permanganate oxidizable C pool is often referred as active/labile C pool in soil (Blair et al., 1995; Rudrappa et al., 2006). Labile C pool is believed to be a representation of readily metabolized components such as carbohydrates, amino acids, peptides, amino sugars, lipids, and

less readily metabolized waxes, fats, resins, lignin, cellulose, hemicellulose (Blair et al., 1995; Tirol-Padre and Ladha, 2004) and some recalcitrant plant materials (Woomer et al., 1994).

In the studied sites, no-till exhibited an abundance of microbial population (Fabrizzi et al., 2009; Menefee, 2016) and TOC (Table 6-1) compared to tilled soils in 0-5 cm depth. No-till and complex crop rotations were identified to be favorable for fungi (Helgason et al., 2010; Six et al., 2006).

A significant effect of temperature was observed on POXC in CTM. At 36 ºC, POXC was significantly reduced, implying high microbial consumption (Fig. 6-13 a). At high moisture, the intact fraction of CTM showed lower POXC when compared to the low moisture treatment (Fig. 6-13 b). This could be a result of less extractability of POXC and an indication of enhanced organo-mineral associations in the intact fraction at high moisture. Moreover, high moisture may have promoted dissolution and re-precipitation of Fe minerals. Relatively high POXC was noticed in crushed soils of CTM in comparison to the original soil, indicating either the addition of microbial byproducts into the system as labile components and/or enhancement of the extractability over time. Moreover, a significant reduction of POXC in crushed fraction of CTM was observed at the end (Fig. 6-13 c). Conversely, the intact fraction persisted its POXC pool without a significant change (Fig. 6-13 c), implying the importance of physical protection. In NTM, a significant moisture effect was observed only at 24 ºC (Fig. 6-13 d). High moisture exhibited a favorable effect on mineralization which led to a low content of POXC (Fig. 6-13 d). At high moisture, no significant effect of temperature was observed. The highest temperature (36 ºC) exhibited a reduction of POXC at low moisture in NTM (Fig. 6-13 e).

Original soils of NTR had twice as much as POXC than CTR (Table 6-1). In Oxisols, POXC was significantly affected by physical disturbance (Fig. 6-14 a). The behaviors of NTR

and CTR were contradictory (Fig. 6-14 a and 6-14 b). Intact aggregates of CTR had more POXC and vice versa for NTR. In NTR, the abundance of fungi and fungi:bacteria ratio were higher for the intact fraction than the crushed fraction and was observed after 120 days. The Bacterial population showed abundance in CTR (Menefee, 2016). This could be related to either the addition of recalcitrant C as microbial by-products or heavy consumption of labile C in a fungi-dominated soil system. In NTR, crushing might have created an adverse effect on fungi. This might have led to a bacteria-dominated environment.

Soil amorphous iron

Ferrihydrite and ferrihydrite like minerals account for the amorphous fraction of Fe minerals in soil. The solubility trends of Fe oxides decrease in the order of $Fe(OH)_3$ amorphous >$Fe(OH)_3$soil >γ-Fe_2O_3 (maghemite) >γ-FeOOH (lepidocrocite) >α-Fe_2O_3 (hematite) > α-FeOOH (goethite). One unit of pH increase results in a thousand-fold decrease in Fe^{3+} activity (Lindsay, 1979). The transformation of ferrihydrite into goethite is unfavorable in Mollisols due to neutral pH (Cornell and Schwertmann, 2003). In acidic and alkaline soils, the transformation is mediated by dissolving ferrihydrite and re-precipitating as goethite (Nagano et al., 1994). In Mollisols, ferrihydrite transforms into hematite by dehydroxylation (Cornell et al., 1989; Schwertmann, 1988; Yee et al., 2006).

A tendency towards the reduction of amorphous Fe with warming was observed in CTM (Fig.6-15 a) and CTR (Fig. 6-16 a) and this could be due to crystallization of amorphous Fe at high temperature. Transformation of amorphous ferrihydrite into relatively less soluble hematite was favored with warming (Das et al., 2010). This can lead to the reductions in the SOC sorbing potential of amorphous Fe minerals.

In NTM, the low moisture had the lowest amorphous Fe (Fig. 6-15 b). At each temperature, there was no effect of the level of disturbance (Fig. 6-15 c). At both moisture levels, the crushed fraction of CTR indicated low amorphous Fe (Fig. 6-16 a). The intact fraction of CTR showed more amorphous Fe than the original soil after six months indicating the formation of amorphous Fe through dissolution and re-precipitation reactions. Iron bearing mineral solubilization varies with soil pH and ionic strength (Colombo et al., 2014) and redox status of soils (Sierra et al., 2015). Moreover, the crushed fraction of CTR indicated low amorphous Fe. Conversely, NTR showed low amorphous Fe in the intact fraction at low moisture (Fig. 6-16 b). Dissolution of Fe^{3+} oxides is facilitated in the presence of acids (i.e., proton induced dissolution), chelate ligands (i.e., ligand promoted dissolution) and Fe^{2+} tends to release much faster than Fe^{3+} due to the bond strength of Fe and O (i.e., reductive dissolution) (Suter et al., 1991). Organic acids (i.e., citrate and HA) produced by microbial activities influence mineral weathering creating acidic environments (Drever and Stillings, 1997; Schwertmann, 2008). Ferrihydrite tends to be highly insoluble at neutral conditions and the transformation into crystalline forms is favored in the presence of Fe^{2+} with a catalytic power (Glasauer et al., 2003; Hansel et al., 2003). Furthermore, the solubility of Fe oxides is enhanced at low E_h (Schwertmann, 2008). There can be anaerobic microsites in aggregates, where the reduction of Fe^{3+} can occur (Sexstone et al., 1985). Dissimilatory Fe reducing bacteria consume both crystalline and amorphous Fe oxides where amorphous Fe oxides serve as terminal electron acceptors (Zachara et al., 2001).

^{13}C Nuclear magnetic resonance (^{13}C-NMR)

Humic substances represent the largest portion of refractory terrestrial OC and are operationally (loosely) defined (Kelleher and Simpson, 2006). The ratio between aliphatic and aromatic C (AL/AR) indicates the proportion labile and stable C. Therefore, it's an indication of

the degree of humification. Further, this ratio is considered as an "energetic reservoir" in extremely poor soils (Ceccanti et al., 2007; Marinari et al., 2007). The ratio of alkyl C to O-alkyl C is another indicator of the relative degree of SOC decomposition (Baldock et al., 1995) and a lower alkyl C to O-alkyl C ratio indicates the preservation of more labile C (Cusack et al., 2012).

The results indicated changes in HA chemistry after six months. In CTM, the ratio of O-alkyl C to alkyl C was high at the end compared to the initial soil, suggesting either an increment of O-alkyl C or a decrement of alkyl C (Fig. 6-17 a). In this soil, POXC was higher at the end of the incubation compared to the original soil and observed high proportion of labile O-alkyl C could be related to the accumulation of POXC. It is also possible that complexation of labile C with HA has occurred during the incubation period, increasing the ratio of O-alkyl C: alkyl C in HA. It has been reported that complexations of monomers, polymers, microbial byproducts, and microbial cellular components with HA reduce the degradability (Sollins et al., 1996). Moreover, the O-alkyl C: alkyl C ratio was decreased with warming in the intact fraction and this effect was clear at both moisture conditions. In the crushed fraction, the ratio did not show a clear change. The ratio of aliphatic: aromatic C was lower than the original soil in all the treatment combinations, except in the T1M2 crushed fraction (Fig. 6-16 c). This can be linked to the increase in the proportion of aromatic C or the consumption of aliphatic C. Microbial derived metabolites (i.e. organic acids, polysaccharides, polyaromatic melanoid pigments, and extracellular enzymes) released as byproducts of microbial metabolic pathways change the C pool qualitatively and quantitatively (Sollins et al., 1996). In NTM, both ratios (AL/AR and O-alkyl C/alkyl C) were consistent with the original soil except for the T1M1 (Fig. 6-17 b and d).

High performance liquid chromatography (HPLC)

Humic acid of CTM increased its hydrophilic nature at 36 ºC relative to 12 ºC, indicating an advanced humification (Fig. 6-18 a) with warming. In NTM, the low moisture seemed to be more favorable for the humification. At each temperature and moisture, the intact fraction of CTM showed relatively more advanced humification as compared to the crushed fraction. Conversely, NTM showed a higher humification of HA in crushed soil at 36 ºC and also for NTM, low moisture appeared to be unfavorable for further humification (Fig. 6-18 b).

Assessment of amorphous iron minerals and soil carbon pools

Overall, there was no significant correlation between amorphous Fe fraction and TOC/POXC in any of the soils. In CTM, only at 36º C, both aggregate fractions showed a positive correlation between amorphous Fe and POXC (intact R^2=0.44 and crushed R^2=0.52). This may be linked to the significant pH reduction observed in this soil at 36º C, because reduction of pH could increase AEC. Also, CTM had the lowest amorphous Fe compared with other soils at the beginning. Other soils might have had excessive Fe oxide sorption sites for OC and the under saturation of Fe oxide-sorption sites might have resulted the poor correlation between amorphous Fe and TOC/POXC.

Summary

Soil OC dynamics is attributed to the additions, removals, and trasfomations that are influenced by temperature, moisture, and physical disturbance. The resilience to environmental and anthropogenic influences vary depending on the ecosystem properties. A large array of processes involving in soil C dynamics control soil C, the most complex piece in soil.

In this study, the resilience of SOC was significantly affected by temperature directly and indirectly, across both ecosystems. High temperature influenced CO_2-C efflux as well as soil

acidity and amorphous Fe ultimately affecting organo-mineral associations. Cumulative CO_2-C efflux, pH, and Q_{10} for the low temperature range were resilient to moisture effect in Mollisol. This could be an indication that the used moisture levels were not distinct enough. In Oxisols, the moisture effect was significant except for POXC and Q_{10} at low temperature range. The Mollisols were added with manure/compost which could have enhanced the moisture holding capacity, resulting in lack of sensitivity to moisture levels used in this study. Tilled Mollisols (CTM) showed more resilence than no-till soils (NTM) in preserving soil C. Tilled Mollisols soils that are being tilled over 25 years could be possessing strong chemical stabilization mechanisms in preserving C. Intact fraction of CTM had more POXC (labile C) indicating the significance of physical protection. The intact fraction of NTM released C slowly but showed increased microbial activities at the latter stages of the incubation. The crushed fraction showed high C emission in CTM. Moreover, the less disturbance of Mollisols facilitated the fungi growth ultimately leading to a high CO_2-C efflux.

The release of substrates due to crushing of Oxisols showed high CO_2-C efflux towards the latter stages of incubation. No-till Oxisol (NTR) was not affected either by physical disturbance or moisture differences indicating strong organo-mineral associations. In general, soil biological and chemical results were in agreement with each other. It was evident that changes in the macromolecular propeties of HA fraction occurred within a period of six months.

The integrated approach of this research study showed different environmental and anthropogenic factors could influence the resilience of SOC. Long-term studies mimicking real environment scenarios through fluctuating the temperature-moisture regimes will be useful to determine the explicit observations on C dynamics, changes of soil chemical properties, organo-mineral associations, microbial responses, and microbial community struture changes.

References

Acosta-Martinez, V., T. Zobeck, T. Gill and A. Kennedy. 2003. Enzyme activities and microbial community structure in semiarid agricultural soils. Biol. Fertility Soils. 38:216-227.

Altieri, M.A. and C.I. Nicholls. 2013. The adaptation and mitigation potential of traditional agriculture in a changing climate. Clim. Change. 1-13.

Baldock, J., C. Preston, W. McFee and J. Kelly. 1995. Chemistry of carbon decomposition processes in forests as revealed by solid-state carbon-13 nuclear magnetic resonance. p. 89-117. *In* Chemistry of carbon decomposition processes in forests as revealed by solid-state carbon-13 nuclear magnetic resonance. Carbon forms and functions in forest soils. 1995. Soil Science Society of America Inc.

Beare, M.H., R.W. Parmelee, P.F. Hendrix, W. Cheng, D.C. Coleman and D. Crossley Jr. 1992. Microbial and faunal interactions and effects on litter nitrogen and decomposition in agroecosystems. Ecol. Monogr. 569-591.

Bergstrom, D., C. Monreal, A. Tomlin and J. Miller. 2000. Interpretation of soil enzyme activities in a comparison of tillage practices along a topographic and textural gradient. Can. J. Soil Sci. 80:71-79.

Blair, G.J., R.D. Lefroy and L. Lisle. 1995. Soil carbon fractions based on their degree of oxidation, and the development of a carbon management index for agricultural systems. Crop and Pasture Science. 46:1459-1466.

Bosatta, E. and G.I. Ågren. 1999. Soil organic matter quality interpreted thermodynamically. Soil Biol. Biochem. 31:1889-1891.

Brockett, B.F., C.E. Prescott and S.J. Grayston. 2012. Soil moisture is the major factor influencing microbial community structure and enzyme activities across seven biogeoclimatic zones in western canada. Soil Biol. Biochem. 44:9-20.

Ceccanti, B., G. Masciandaro and C. Macci. 2007. Pyrolysis-gas chromatography to evaluate the organic matter quality of a mulched soil. Soil Tillage Res. 97:71-78.

Chen, H., M.E. Harmon, R.P. Griffiths and W. Hicks. 2000. Effects of temperature and moisture on carbon respired from decomposing woody roots. For. Ecol. Manage. 138:51-64.

Chichester, F., M. Harward and C. Youngberg. 1970. pH dependent ion exchange properties of soils and clays from mazama pumice. Clays Clay Miner. 18:81-90.

Colombo, C., G. Palumbo, J. He, R. Pinton and S. Cesco. 2014. Review on iron availability in soil: Interaction of fe minerals, plants, and microbes. Journal of Soils and Sediments. 14:538-548.

Conant, R.T., M.G. Ryan, G.I. Ågren, H.E. Birge, E.A. Davidson, P.E. Eliasson, S.E. Evans, S.D. Frey, C.P. Giardina and F.M. Hopkins. 2011. Temperature and soil organic matter decomposition rates–synthesis of current knowledge and a way forward. Global Change Biol. 17:3392-3404.

Conen, F., J. Leifeld, B. Seth and C. Alewell. 2006. Warming mineralizes young and old soil carbon equally. Biogeosciences. 3:515-519.

Cornell, R.M. and U. Schwertmann. 2003. The iron oxides: Structure, properties, reactions, occurrences and uses. John Wiley & Sons.

Cornell, R.M., R. Giovanoli and W. Schneider. 1989. Review of the hydrolysis of iron (III) and the crystallization of amorphous iron (III) hydroxide hydrate. Journal of Chemical Technology and Biotechnology 46:115-134.

Cusack, D.F., O.A. Chadwick, W.C. Hockaday and P.M. Vitousek. 2012. Mineralogical controls on soil black carbon preservation. Global Biogeochem Cycles. 26.

Das, S., M.J. Hendry and J. Essilfie-Dughan. 2010. Transformation of two-line ferrihydrite to goethite and hematite as a function of pH and temperature. Environ. Sci. Technol. 45:268-275.

Davidson, E.A. and I.A. Janssens. 2006. Temperature sensitivity of soil carbon decomposition and feedbacks to climate change. Nature. 440:165-173.

Dessureault-Rompré, J., B.J. Zebarth, A. Georgallas, D.L. Burton, C.A. Grant and C.F. Drury. 2010. Temperature dependence of soil nitrogen mineralization rate: Comparison of mathematical models, reference temperatures and origin of the soils. Geoderma. 157:97-108.

Drever, J. and L. Stillings. 1997. The role of organic acids in mineral weathering. Colloids Surf. Physicochem. Eng. Aspects. 120:167-181.

Fabrizzi, K.P., C.W. Rice, T.J. Amado, J. Fiorin, P. Barbagelata and R. Melchiori. 2009. Protection of soil organic C and N in temperate and tropical soils: Effect of native and agroecosystems. Biogeochemistry. 92:129-143.

Fang, C., P. Smith, J.B. Moncrieff and J.U. Smith. 2005. Similar response of labile and resistant soil organic matter pools to changes in temperature. Nature. 433:57-59.

Feng, X., A.J. Simpson and M.J. Simpson. 2005. Chemical and mineralogical controls on humic acid sorption to clay mineral surfaces. Org. Geochem. 36:1553-1566.

Frey, S., E. Elliott and K. Paustian. 1999. Bacterial and fungal abundance and biomass in conventional and no-tillage agroecosystems along two climatic gradients. Soil Biol. Biochem. 31:573-585.

Glasauer, S., P.G. Weidler, S. Langley and T.J. Beveridge. 2003. Controls on fe reduction and mineral formation by a subsurface bacterium. Geochim. Cosmochim. Acta. 67:1277-1288.

Hamdi, S., F. Moyano, S. Sall, M. Bernoux and T. Chevallier. 2013. Synthesis analysis of the temperature sensitivity of soil respiration from laboratory studies in relation to incubation methods and soil conditions. Soil Biol. Biochem. 58:115-126.

Hansel, C.M., S.G. Benner, J. Neiss, A. Dohnalkova, R.K. Kukkadapu and S. Fendorf. 2003. Secondary mineralization pathways induced by dissimilatory iron reduction of ferrihydrite under advective flow. Geochim. Cosmochim. Acta. 67:2977-2992.

Helgason, B., F. Walley and J. Germida. 2010. No-till soil management increases microbial biomass and alters community profiles in soil aggregates. Applied Soil Ecology. 46:390-397.

Hinsinger, P., C. Plassard, C. Tang and B. Jaillard. 2003. Origins of root-mediated pH changes in the rhizosphere and their responses to environmental constraints: A review. Plant Soil. 248:43-59.

Hur, J. and M.A. Schlautman. 2004. Effects of pH and phosphate on the adsorptive fractionation of purified aldrich humic acid on kaolinite and hematite. J. Colloid Interface Sci. 277:264-270.

Jastrow, J.D., J.E. Amonette and V.L. Bailey. 2007. Mechanisms controlling soil carbon turnover and their potential application for enhancing carbon sequestration. Clim. Change. 80:5-23.

Kelleher, B.P. and A.J. Simpson. 2006. Humic substances in soils: Are they really chemically distinct? Environ. Sci. Technol. 40:4605-4611.

Kirschbaum, M.U. 2000. Will changes in soil organic carbon act as a positive or negative feedback on global warming? Biogeochemistry. 48:21-51.

Kleber, M., K. Eusterhues, M. Keiluweit, C. Mikutta, R. Mikutta and P.S. Nico. 2015. Chapter one-Mineral–Organic associations: Formation, properties, and relevance in soil environments. Adv. Agron. 130:1-140.

Koide, R.T., B.T. Nguyen, R.H. Skinner, C.J. Dell, M.S. Peoples, P.R. Adler and P.J. Drohan. 2015. Biochar amendment of soil improves resilience to climate change. GCB Bioenergy. 7:1084-1091.

Lindsay, W.L. 1979. Chemical equilibria in soils. John Wiley and Sons Ltd.

Liski, J., H. Ilvesniemi, A. Mäkelä and C.J. Westman. 1999. CO_2 emissions from soil in response to climatic warming are overestimated: The decomposition of old soil organic matter is tolerant of temperature. Ambio. 171-174.

Loeppert, R. and W. Inskeep. 1996. Iron. P 639-664. Methods of Soil Analysis, Part 3.

Luo, Y., L.W. White, J.G. Canadell, E.H. DeLucia, D.S. Ellsworth, A. Finzi, J. Lichter and W.H. Schlesinger. 2003. Sustainability of terrestrial carbon sequestration: A case study in duke forest with inversion approach. Global Biogeochem. Cycles. 17.

Manzoni, S., J.P. Schimel and A. Porporato. 2012. Responses of soil microbial communities to water stress: Results from a meta-analysis. Ecology. 93:930-938.

Marinari, S., K. Liburdi, G. Masciandaro, B. Ceccanti and S. Grego. 2007. Humification-mineralization pyrolytic indices and carbon fractions of soil under organic and conventional management in central Italy. Soil Tillage Res. 92:10-17.

Menefee, D. 2016. Anthropogenic Influences on Soil Microbial Properties. MS Thesis. Kansas State University. Manhattan.

Mohan, D., A. Kumar and C.U. Pittman. 2016. Sustainable biochar-A tool for climate change mitigation, soil management and water and wastewater treatment. p. 949-952. *In* Geostatistical and geospatial approaches for the characterization of natural resources in the environment. Springer.

Nagano, T., S. Nakashima, S. Nakayama and M. Senoo. 1994. The use of color to quantify the effects of pH and temperature on the crystallization kinetics of goethite under highly alkaline conditions. Clays Clay Miner. 42:226-234.

Nelson, D.W., L.E. Sommers, D. Sparks, A. Page, P. Helmke, R. Loeppert, P. Soltanpour, M. Tabatabai, C. Johnston and M. Sumner. 1996. Total carbon, organic carbon, and organic matter. Methods of Soil Analysis.Part 3-Chemical Methods.961-1010.

Nicoloso, R. 2009. Soil Organic Carbon Stocks and Stabilization Mechanisms on Temperate and Sub-Tropical Climate Agroecosystems. PhD. DISS. Santa Maria Federal University. Santa Maria.

Oh, N. and D.D. Richter. 2004. Soil acidification induced by elevated atmospheric CO2. Global Change Biol. 10:1936-1946.

Paul, E.A. 2014. Soil microbiology, ecology and biochemistry. Academic press.

Pierzynski, G.M., J.L. Heitman, P.A. Kulakow, G.J. Kluitenberg and J. Carlson. 2004. Revegetation of waste fly ash landfills in a semiarid environment. Rangeland Ecology & Management. 57:312-319.

Pietikainen, J., M. Pettersson and E. Baath. 2005. Comparison of temperature effects on soil respiration and bacterial and fungal growth rates. FEMS Microbiol. Ecol. 52:49-58.

Ramos, M.E. and F.J. Huertas. 2014. Adsorption of lactate and citrate on montmorillonite in aqueous solutions. Appl. Clay. Sci. 90:27-34.

Rudrappa, L., T. Purakayastha, D. Singh and S. Bhadraray. 2006. Long-term manuring and fertilization effects on soil organic carbon pools in a typic haplustept of semi-arid sub-tropical india. Soil Tillage Res. 88:180-192.

Schwertmann, U. 1988. Occurrence and formation of iron oxides in various pedoenvironments. p. 267-308. *In* Iron in soils and clay minerals. Springer.

Schwertmann, U. 2008. Iron oxides. p. 363-369. *In* Encyclopedia of soil science. Springer.

Sexstone, A.J., N.P. Revsbech, T.B. Parkin and J.M. Tiedje. 1985. Direct measurement of oxygen profiles and denitrification rates in soil aggregates. Soil Sci. Soc. Am. J. 49:645-651.

Shaker, A.M., Z.R. Komy, S.E. Heggy and M.E. El-Sayed. 2012. Kinetic study for adsorption humic acid on soil minerals. The Journal of Physical Chemistry A 116:10889-10896.

Sierra, C.A., S.E. Trumbore, E.A. Davidson, S. Vicca and I. Janssens. 2015. Sensitivity of decomposition rates of soil organic matter with respect to simultaneous changes in temperature and moisture. Journal of Advances in Modeling Earth Systems. 7:335-356.

Six, J., H. Bossuyt, S. Degryze and K. Denef. 2004. A history of research on the link between (micro) aggregates, soil biota, and soil organic matter dynamics. Soil Tillage Res. 79:7-31.

Six, J., S. Frey, R. Thiet and K. Batten. 2006. Bacterial and fungal contributions to carbon sequestration in agroecosystems. Soil Sci. Soc. Am. J. 70:555-569.

Sollins, P., P. Homann and B.A. Caldwell. 1996. Stabilization and destabilization of soil organic matter: Mechanisms and controls. Geoderma. 74:65-105.

Stavi, I. and R. Lal. 2013. Agroforestry and biochar to offset climate change: A review. Agronomy for Sustainable Development. 33:81-96.

Steinweg, J.M., A.F. Plante, R.T. Conant, E.A. Paul and D.L. Tanaka. 2008. Patterns of substrate utilization during long-term incubations at different temperatures. Soil Biol. Biochem. 40:2722-2728.

Stockmann, U., M.A. Adams, J.W. Crawford, D.J. Field, N. Henakaarchchi, M. Jenkins, B. Minasny, A.B. McBratney, de Courcelles, Vivien de Remy and K. Singh. 2013. The knowns, known unknowns and unknowns of sequestration of soil organic carbon. Agric. , Ecosyst. Environ. 164:80-99.

Suter, D., S. Banwart and W. Stumm. 1991. Dissolution of hydrous iron (III) oxides by reductive mechanisms. Langmuir. 7:809-813.

Swift, R.S., D. Sparks, A. Page, P. Helmke, R. Loeppert, P. Soltanpour, M. Tabatabai, C. Johnston and M. Sumner. 1996. Organic matter characterization. Methods of Soil Analysis.Part 3-Chemical Methods.1011-1069.

Tirol-Padre, A. and J. Ladha. 2004. Assessing the reliability of permanganate-oxidizable carbon as an index of soil labile carbon. Soil Sci. Soc. Am. J. 68:969-978.

Wang, G., Y. Zhou, X. Xu, H. Ruan and J. Wang. 2013. Temperature sensitivity of soil organic carbon mineralization along an elevation gradient in the wuyi mountains, china. PloS One. 8:e53914.

Weil, R.R., K.R. Islam, M.A. Stine, J.B. Gruver and S.E. Samson-Liebig. 2003. Estimating active carbon for soil quality assessment: A simplified method for laboratory and field use. Am. J. Alternative Agric. 18:3-17.

Winkler, J.P., R.S. Cherry and W.H. Schlesinger. 1996. The Q 10 relationship of microbial respiration in a temperate forest soil. Soil Biol. Biochem. 28:1067-1072.

Woomer, P.L., A. Martin, A. Albrecht, D.V.S. Resck, H. Scharpenseel and M. Swift. 1994. The importance and management of soil organic matter in the tropics. John Wiley & Sons.

Yee, N., S. Shaw, L.G. Benning and T.H. Nguyen. 2006. The rate of ferrihydrite transformation to goethite via the fe (II) pathway. Am. Mineral. 91:92-96.

Zachara, J.M., J.K. Fredrickson, S.C. Smith and P.L. Gassman. 2001. Solubilization of fe (III) oxide-bound trace metals by a dissimilatory fe (III) reducing bacterium. Geochim. Cosmochim. Acta. 65:75-93.

Zhou, T., P. Shi, D. Hui and Y. Luo. 2009. Global pattern of temperature sensitivity of soil heterotrophic respiration (Q10) and its implications for carbon-climate feedback. Journal of Geophysical Research: Biogeosciences. 114.

Zhou, W., D. Hui and W. Shen. 2014. Effects of soil moisture on the temperature sensitivity of soil heterotrophic respiration: A laboratory incubation study. PloS One. 9:e92531.

Figures

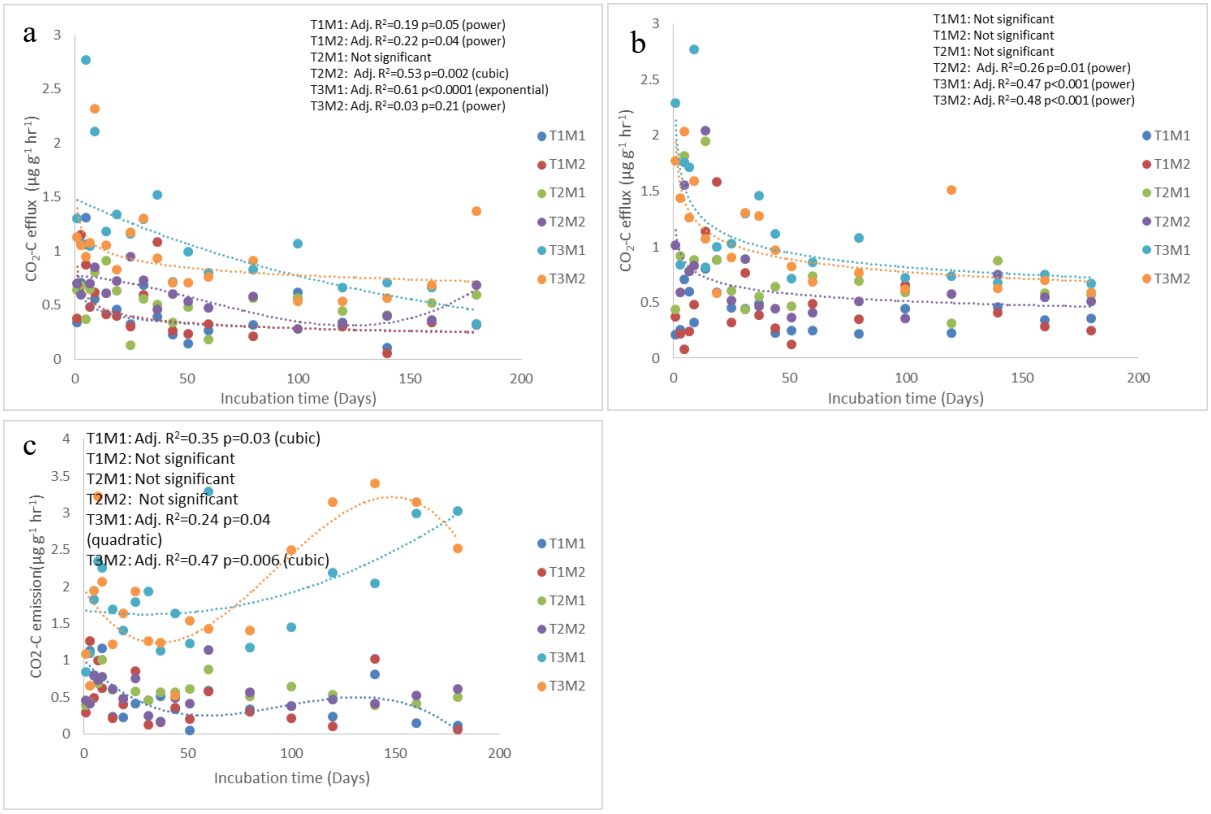

Figure 6-1 Efflux of carbon dioxide (CO_2-C) over the time from CTM_intact (a), CTM_crushed (b) and NTM_intact (c) representing different temperature and moisture combinations. T1, T2, and T3 were 12°C, 24°C, and 36°C, respectively. M1 and M2 were field capacity (high moisture) and 80% field capacity (low moisture), respectively. Intact and crushed fractions were <4 mm and <0.25 mm, respectively. Significance of each model was determined at p=0.05. Trends are displayed only for significant models.

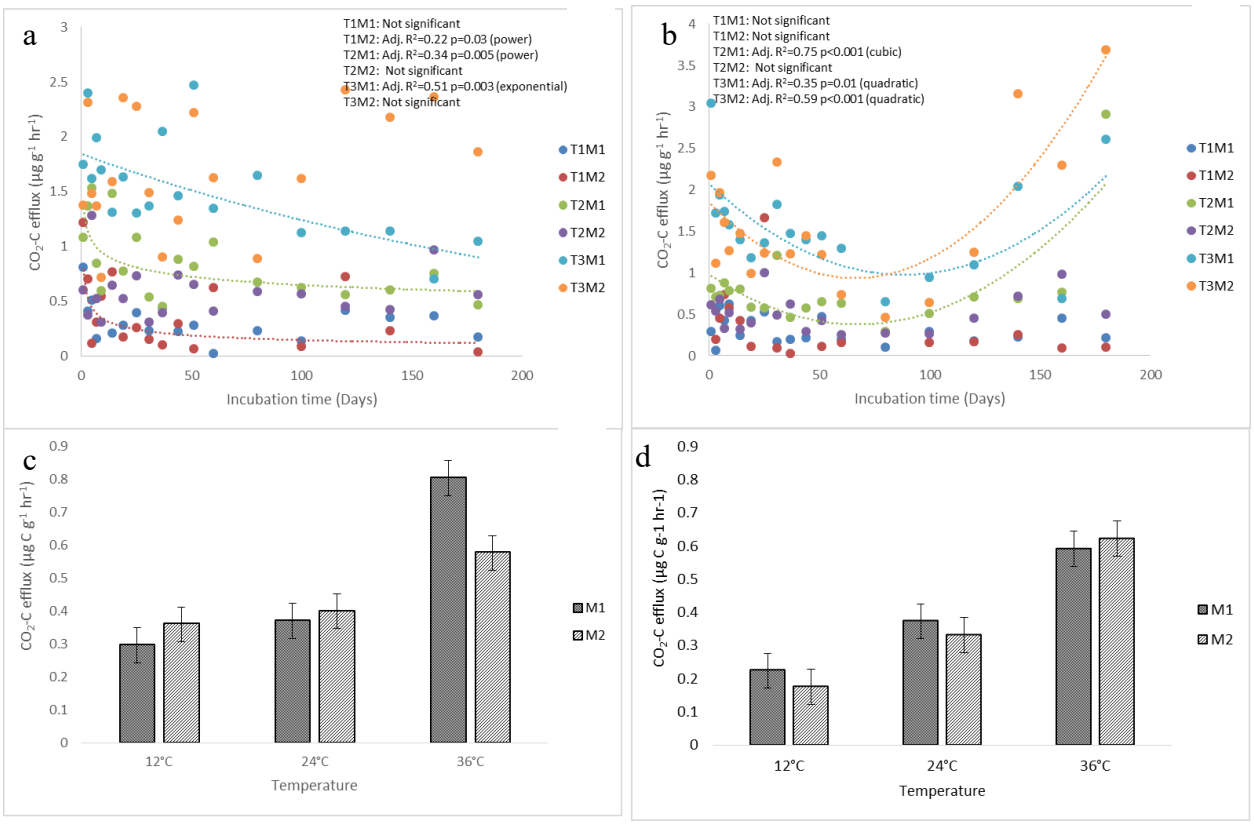

Figure 6-2 Efflux of carbon dioxide (CO_2-C) over the time period from the NTR_intact (a), NTR_crushed (b) and efflux of CO_2-C of CTR_intact (c) and CTR_crushed(d) representing different temperature and moisture interaction. T1, T2, and T3 were 12°C, 24°C, and 36°C, respectively. M1 and M2 were field capacity (high moisture) and 80% field capacity (low moisture), respectively. Intact and crushed fractions were <4 mm and <0.25 mm, respectively. Significance of each model were determined at p=0.05. Trends are displayed only for significant models.

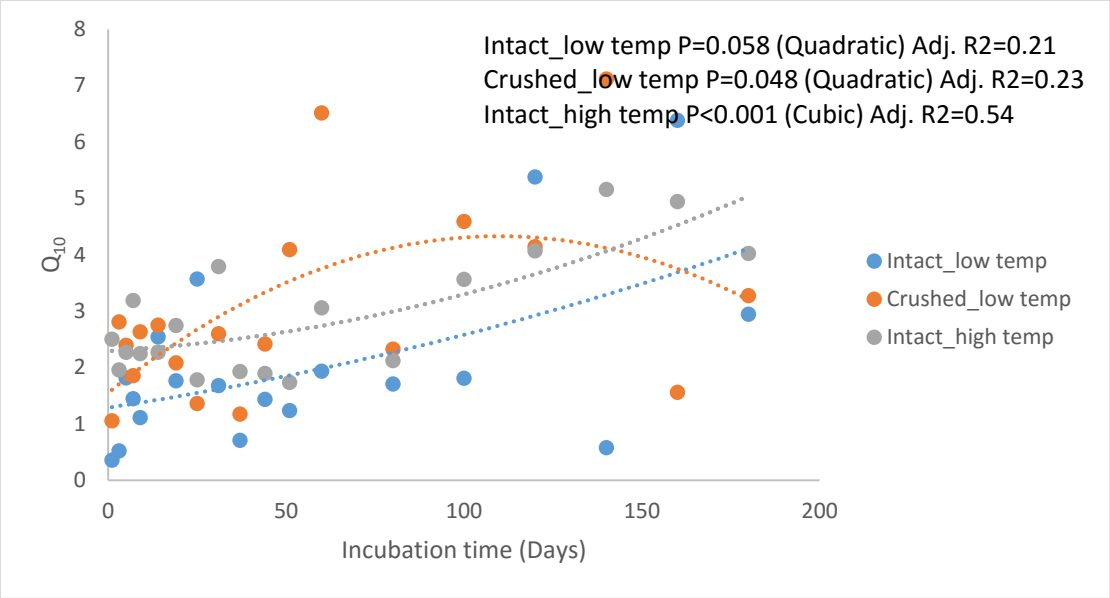

Figure 6-3 Effect of temperature range and level of disturbance on variation of temperature sensitivity (Q_{10}) over time in NTM. Low temperature and high temperature ranges were 12ºC-24ºC and 24ºC-36ºC. Intact and crushed fractions were <4 mm and <0.25 mm, respectively. Significance of each model was determined at p=0.05. Trends are displayed only for significant models.

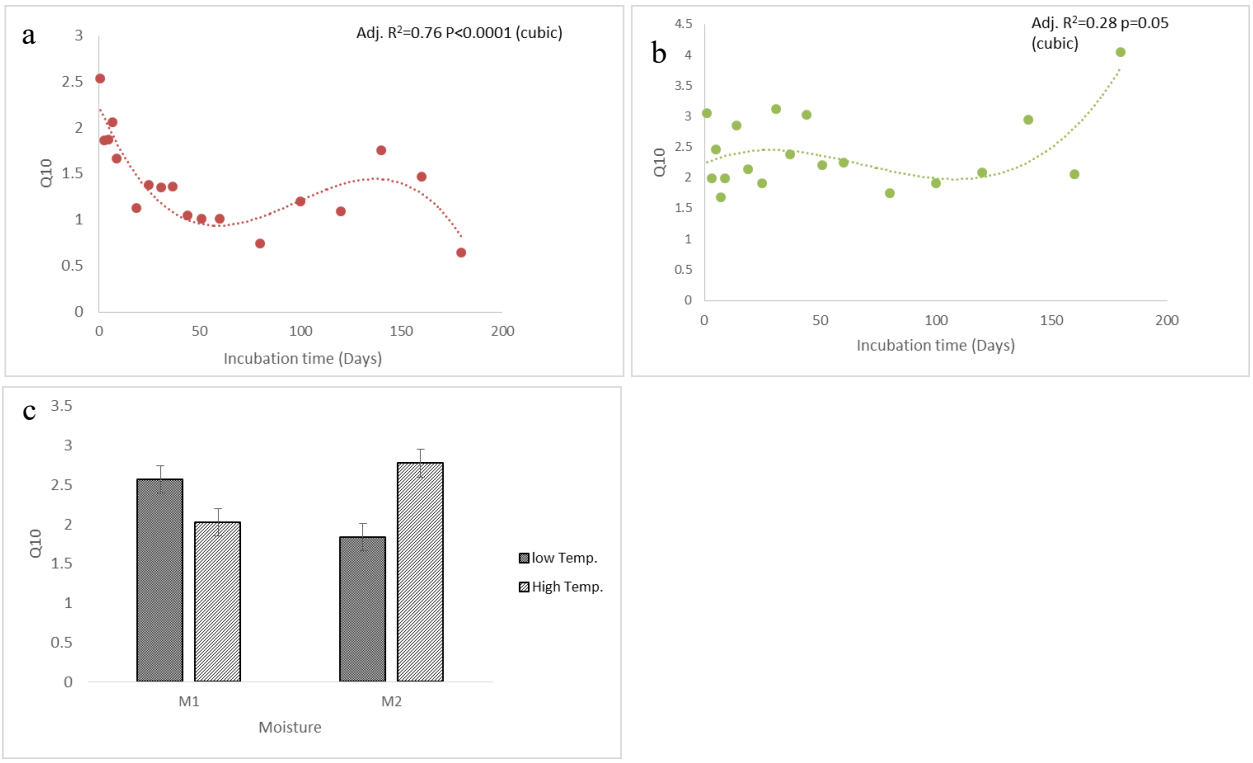

Figure 6-4 Variation of temperature sensitivity (Q_{10}) of CTR_intact fraction at M2 (a), NTR_crushed at high temperature range (24 ºC-36 ºC) (b), and the interaction effect of moisture and temperature ranges of NTR (c). Low temperature and high temperature ranges were 12ºC-24ºC and 24ºC-36ºC, respectively. M2 represented 80% field capacity. Intact and crushed fractions were <4 mm and <0.25 mm, respectively. Significance of each model was determined at p=0.05. Trends are displayed only for significant models.

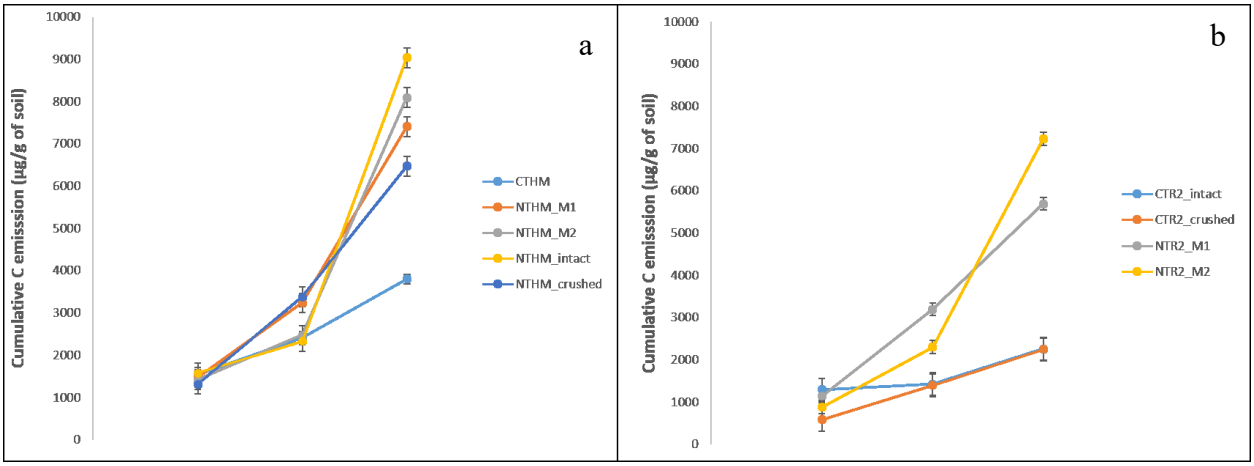

Figure 6-5 Cumulative carbon dioxide (CO_2-C) efflux in temperate (a) and tropical (b) agroecosystems. T1, T2, and T3 were 12ºC, 24ºC, and 36ºC, respectively. M1 and M2 were field capacity (high moisture) and 80% field capacity (low moisture), respectively. Intact and crushed fractions were <4 mm and <0.25 mm, respectively. Only the significant factors (p=0.05) were drawn.

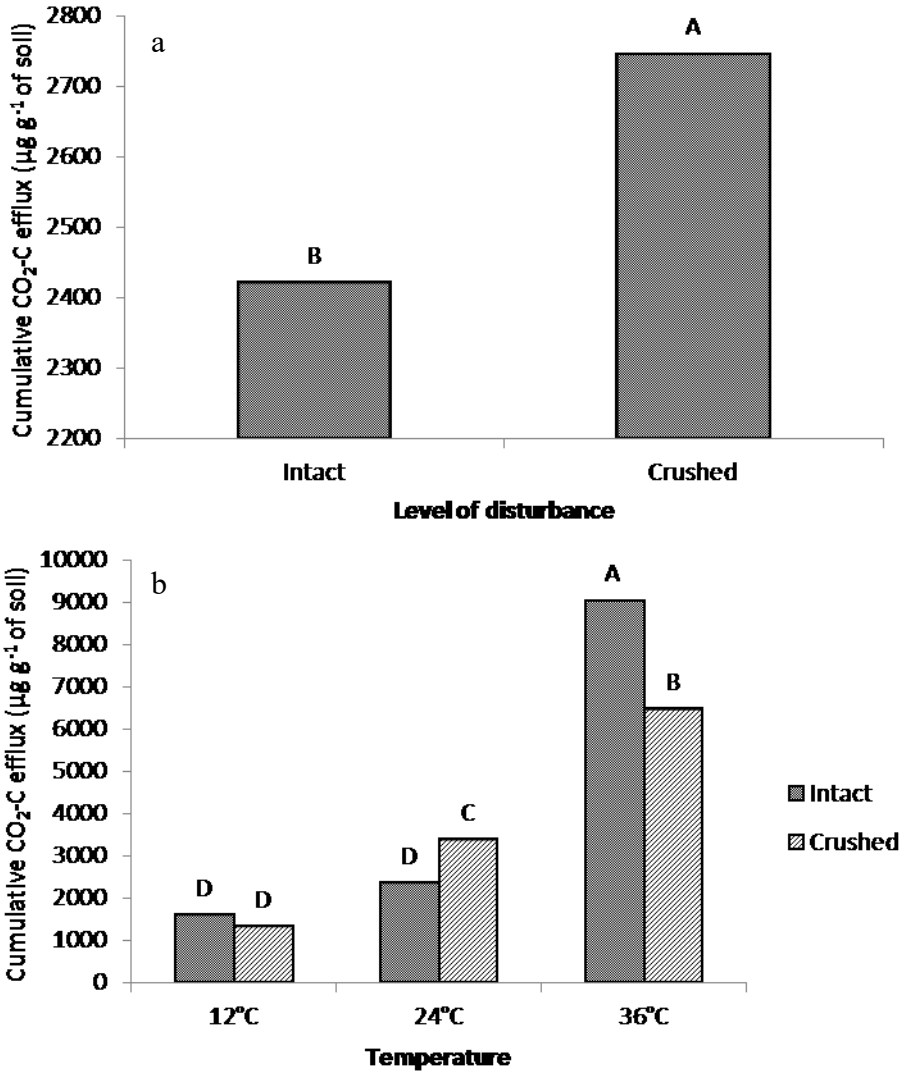

Figure 6-6 Effect of level of disturbance on cumulative carbon dioxide (CO_2-C) efflux of CTM (a) and interaction effect of level of disturbance and temperature of NTM. Intact and crushed fractions were <4 mm and <0.25 mm, respectively. Different letters indicated significant difference at 0.05 probability level.

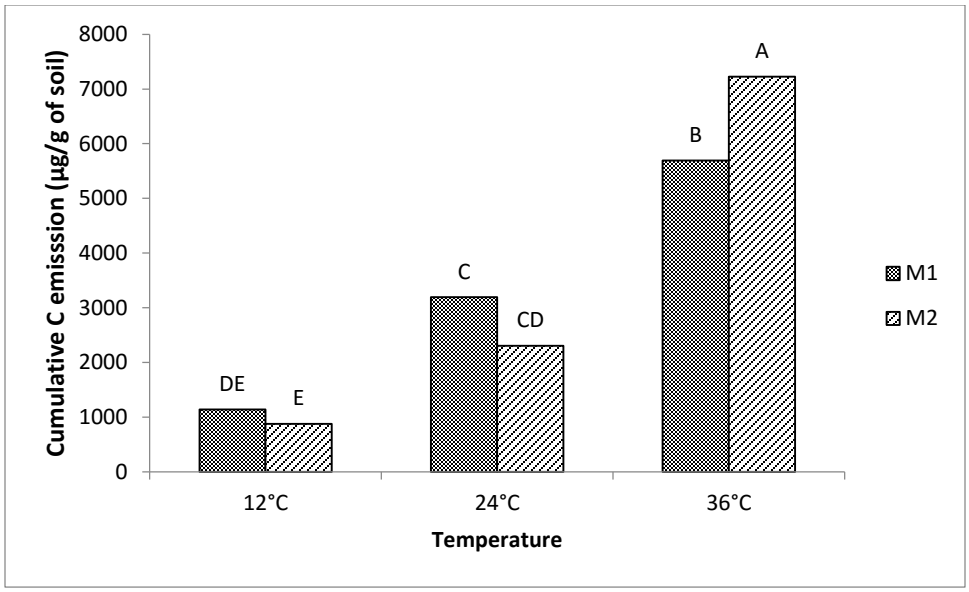

Figure 6-7 Effect of temperature and moisture on cumulative carbon dioxide (CO_2-C) efflux of NTR. M1 and M2 were field capacity (high moisture) and 80% field capacity (low moisture), respectively. Different letters indicate significant difference at 0.05 probability level.

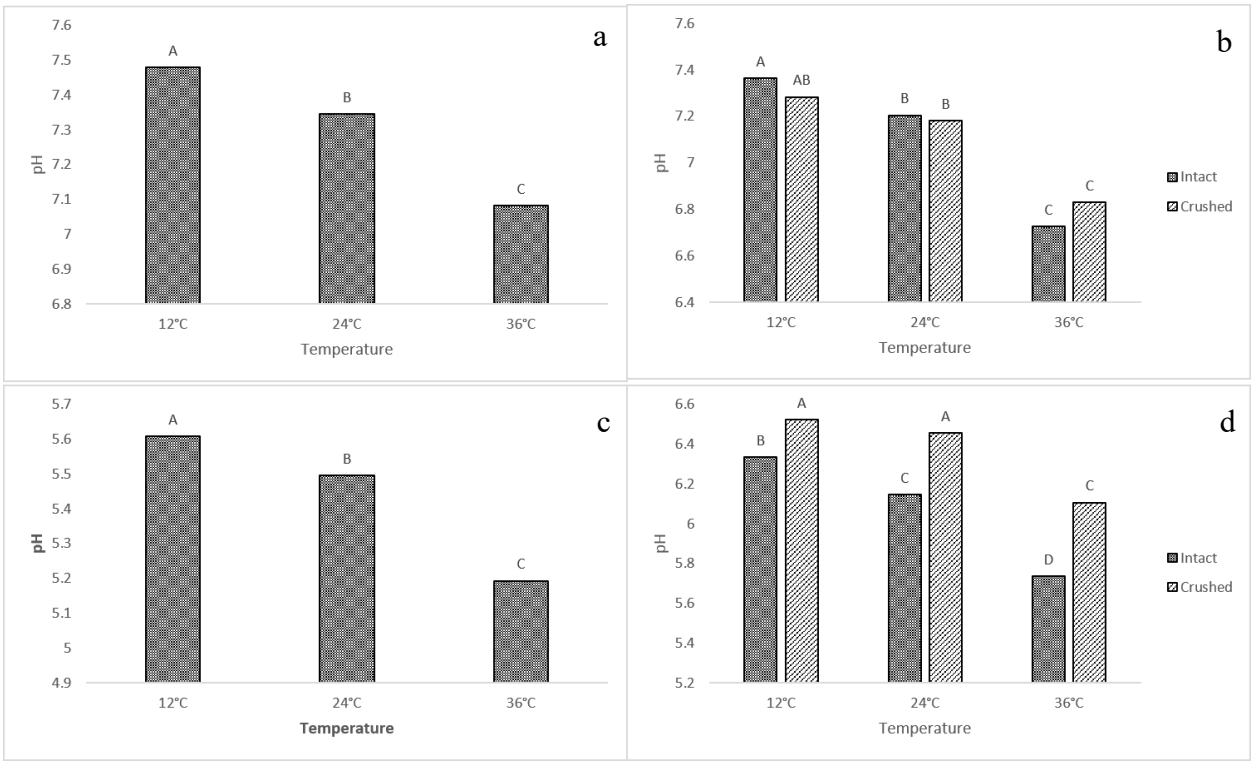

Figure 6-8 Significant effects of temperature and level of disturbance on pH of CTM (a), NTM (b), CTR (c) and NTR (d). Intact and crushed fractions were <4 mm and <0.25 mm, respectively. Different letters represent significance at 0.05 probability level.

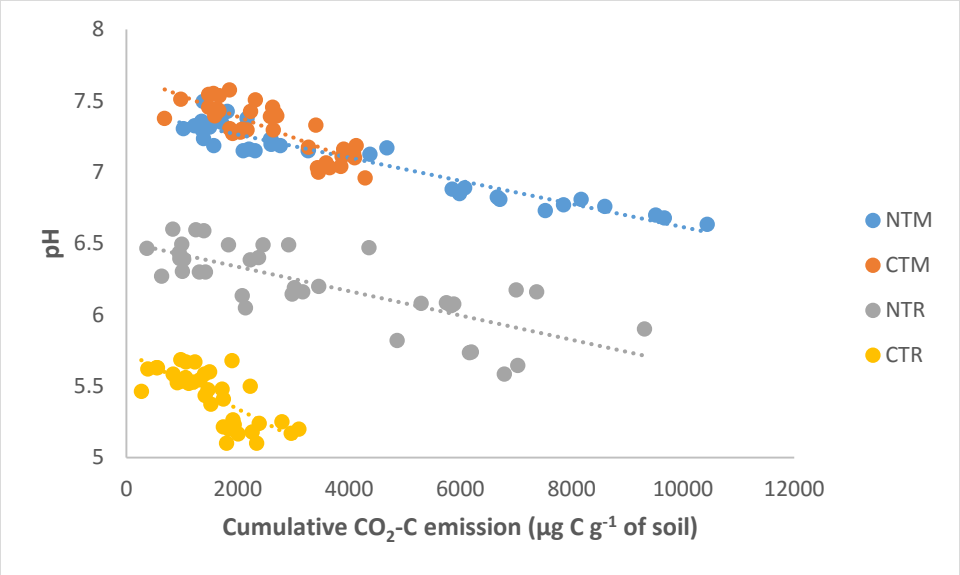

Figure 6-9 Correlation between cumulative CO_2-C efflux and pH of soils. All correlations were significant at 0.05 probability level. R^2 for NTM, CTM, NTR, and CTR were 0.90, 0.67, 0.58 and 0.53, respectively.

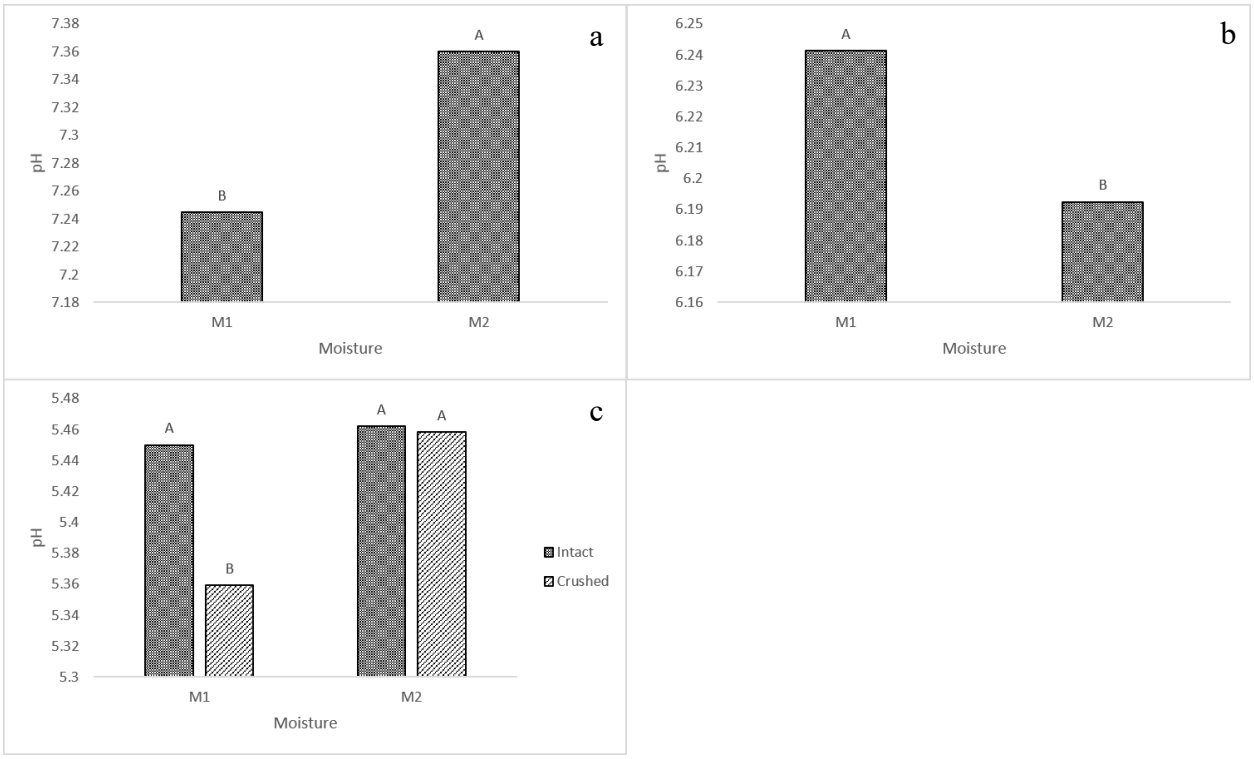

Figure 6-10 Effect of moisture on pH of CTM (a), NTR (b) and interaction effect of moisture and the level of disturbance in CTR (c). M1 and M2 were field capacity (high moisture) and 80% field capacity (low moisture), respectively. Intact and crushed fractions were <4 mm and <0.25 mm, respectively. Different letters represent significance at 0.05 probability level.

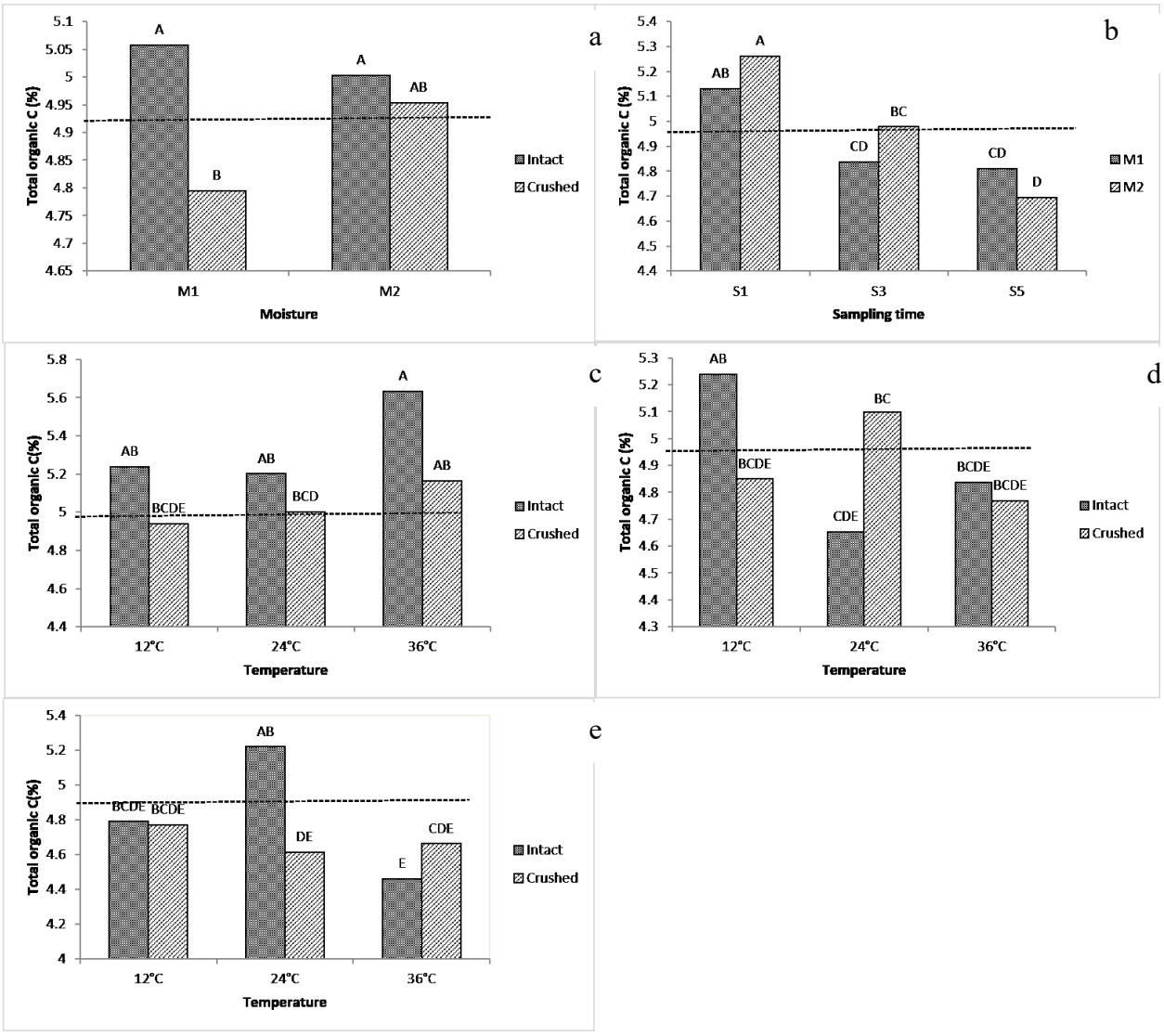

Figure 6-11 Significant interaction effects on concentration of total organic carbon (TOC) in NTM. Effect of moisture and disturbance (a), moisture and sampling time (b) temperature and disturbance at 7 days (c), 60 days (d) and 180 (e) of sampling. M1 and M2 represents field capacity (high moisture) and 80% of the field capacity (low moisture). S1, S3, and S5 represent 7 days, 60 days and 180 days of sampling, respectively. Intact and crushed fractions were <4 mm and <0.25 mm, respectively. Different letters represent significance at 0.05 probability level. Dotted line indicates the TOC of original soils.

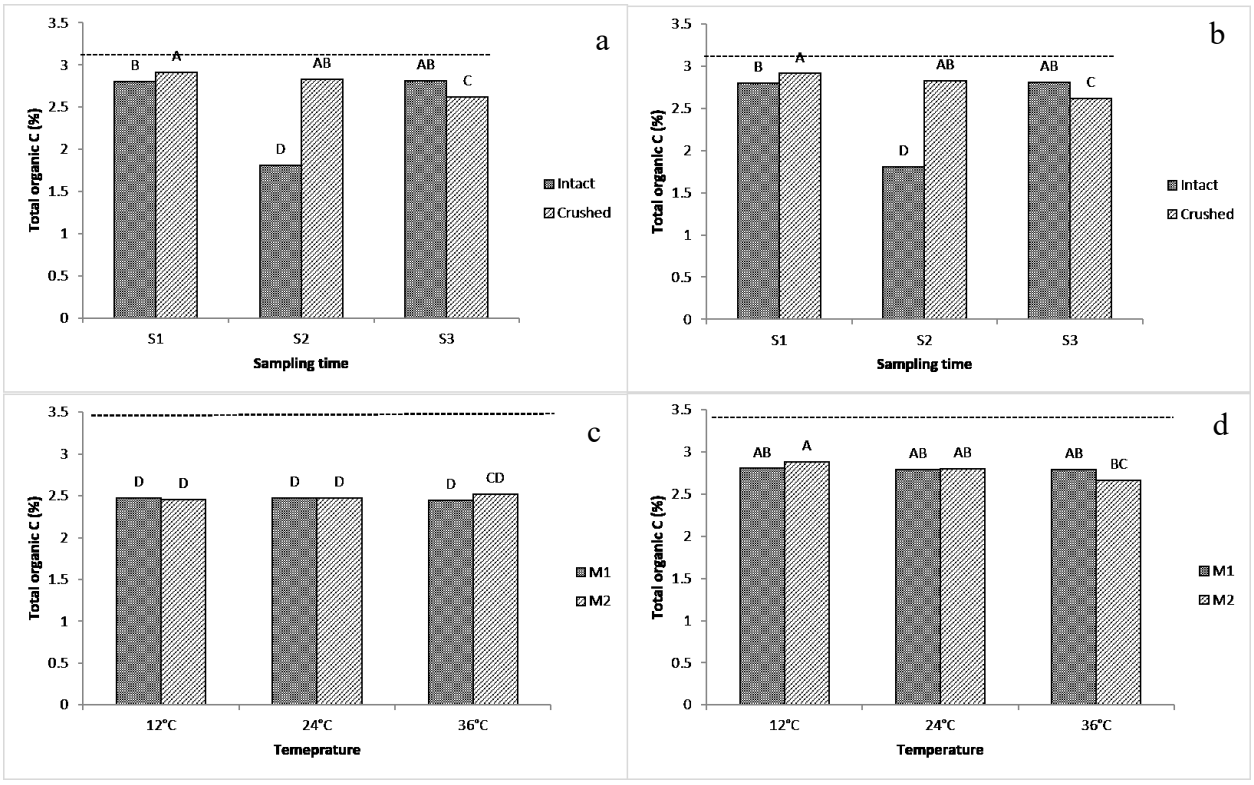

Figure 6-12 Interaction effects of level of disturbance and sampling time on the concentration of total organic carbon (TOC) of CTR (a) and NTR (b). Interaction effect of temperature and moisture of NTR_intact (c) and NTR_crushed (d). S1, S3, and S5 represent 7 days, 60 days and 180 days, respectively. M1 and M2 represented field capacity (high moisture) and 80% of the field capacity (low moisture). Intact and crushed fractions were <4 mm and <0.25 mm, respectively. Different letters represent significance at 0.05 probability level. Dotted line indicates the TOC of original soils. Different letters represent significance at 0.05 probability level. Dotted line indicates TOC of the original soils.

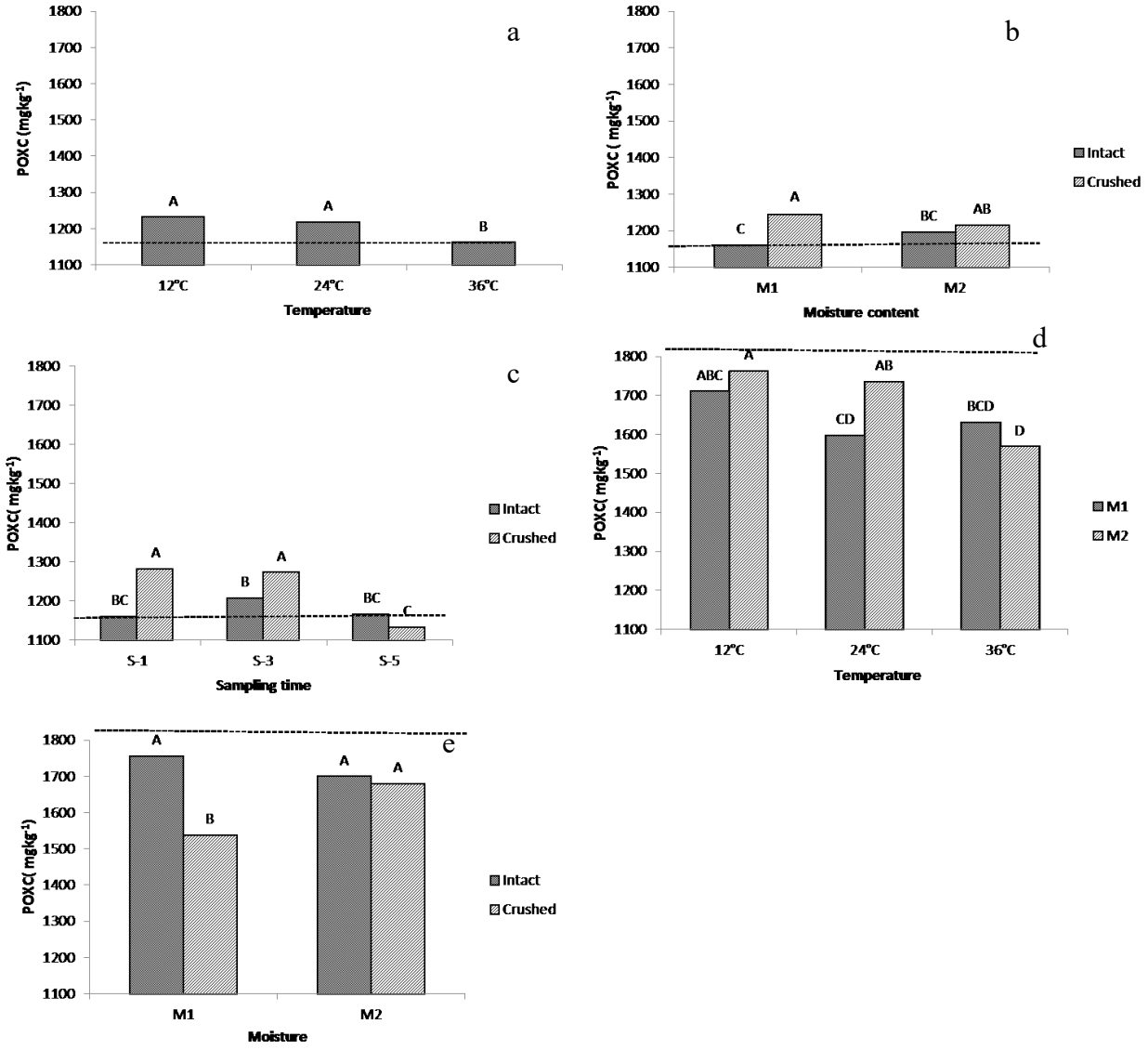

Figure 6-13 Effect temperature (a), interaction effect of moisture and the level of disturbance (b) sampling time and the level of disturbance (c) on POXC of CTM. Interaction effects of temperature and moisture (d) and moisture and level of disturbance (e) on POXC of NTM. M1 and M2 were field capacity (high moisture) and 80% of the field capacity (low moisture). Intact and crushed fractions were <4 mm and <0.25 mm, respectively. Different letters represent significance at 0.05 probability level. Dotted line indicates the POXC of original soils.

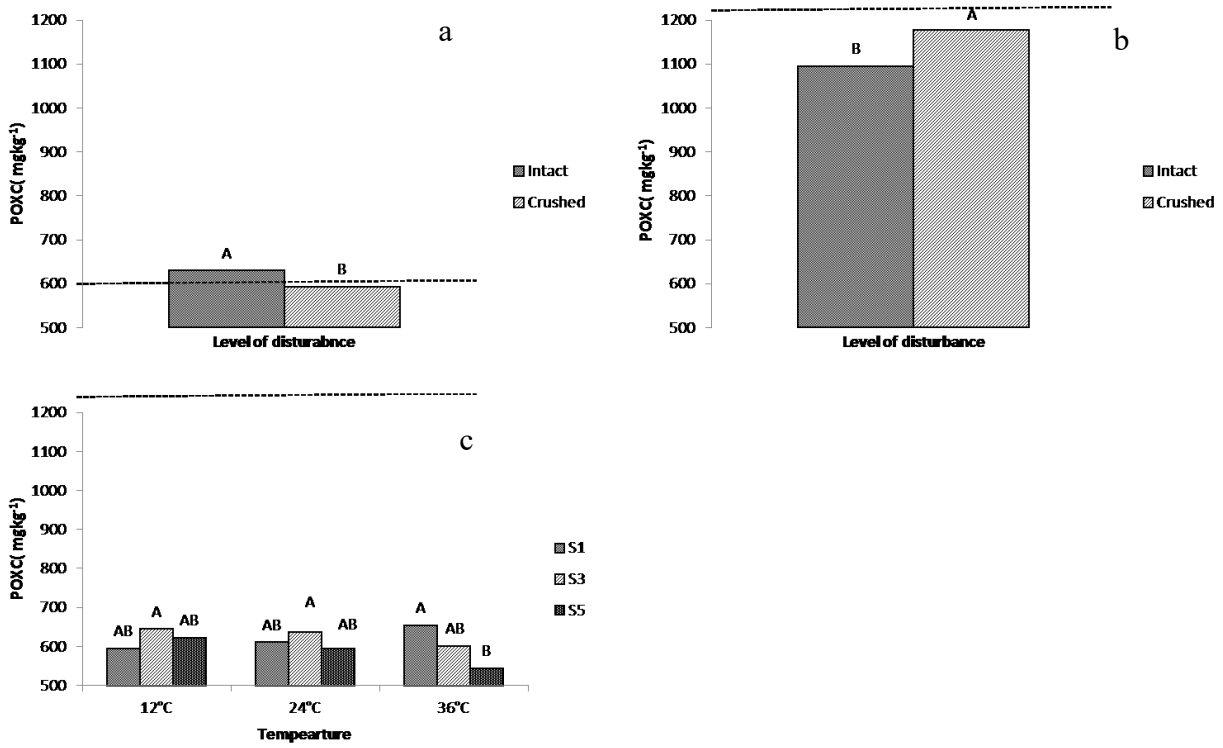

Figure 6-14Effect of level of disturbance of CTR (a) and NTR (b), interaction effect of sampling time and temperature (c) of NTR on POXC. M1 and M2 were field capacity (high moisture) and 80% of the field capacity (low moisture). S1, S3, and S5 were 7 days, 60 days and 180 days, respectively. Intact and crushed fractions were <4 mm and <0.25 mm, respectively. Different letters represent significance at 0.05 probability level. Dotted line indicates POXC of original soils.

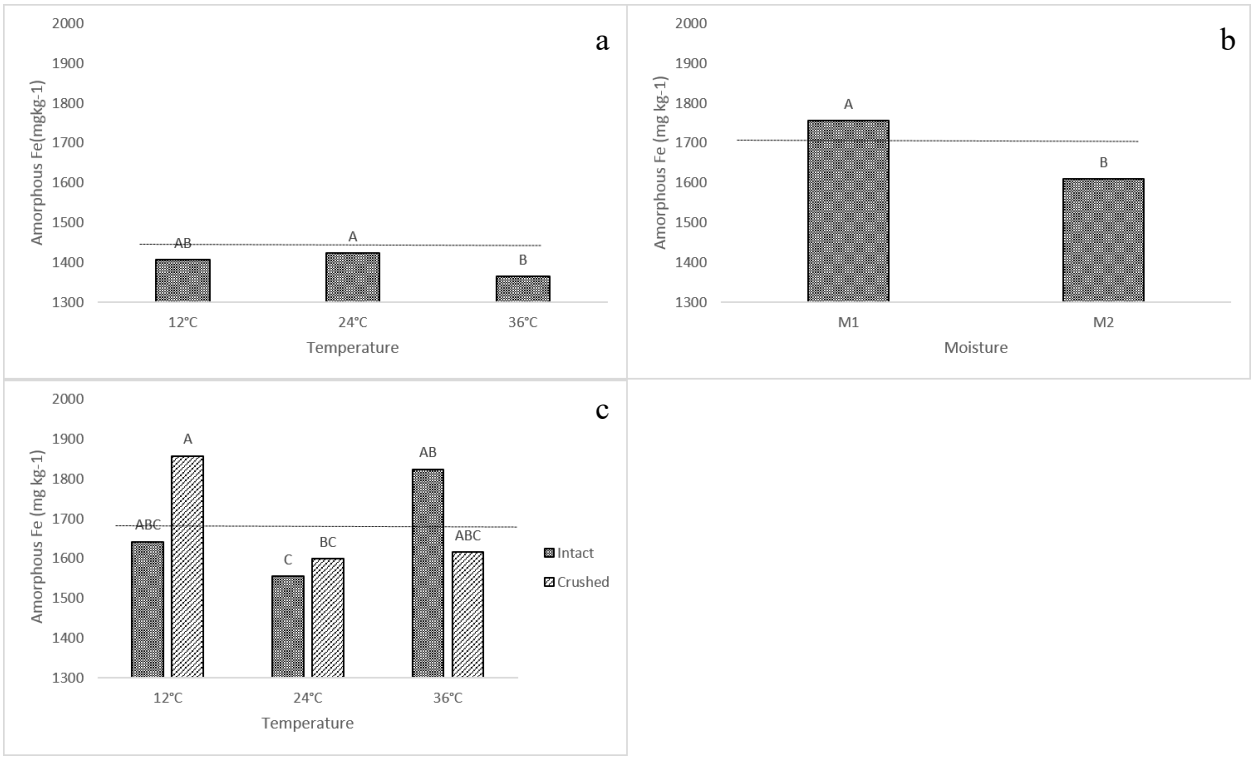

Figure 6-15 Effect of temperature of CTM (a), effect of moisture in NTM (b) and interaction effect of temperature and the level of disturbance in NTM (c). M1 and M2 were field capacity (high moisture) and 80% of the field capacity (low moisture). Intact and crushed fractions were <4 mm and <0.25 mm, respectively. Different letters represent significance at 0.05 probability level. Dotted line indicates amorphous Fe of original soils.

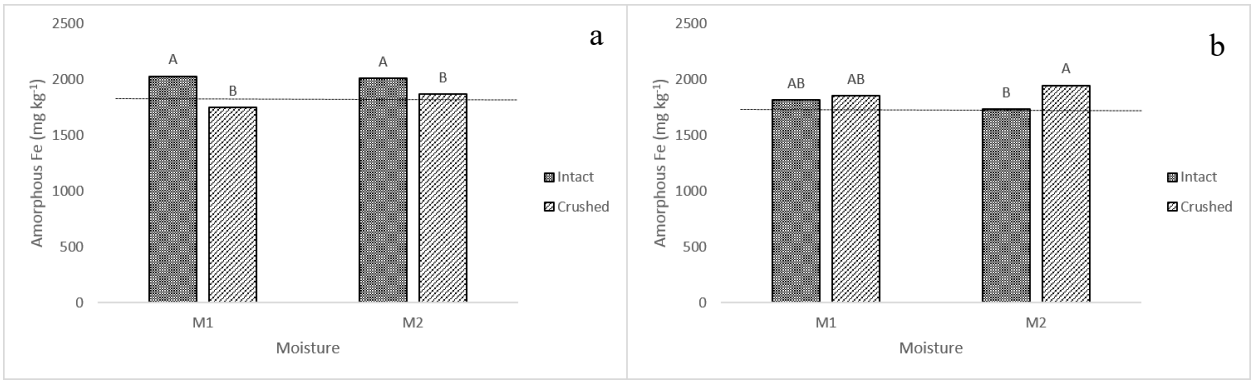

Figure 6-16 Interaction effect of moisture and the level of disturbance on amorphous Fe in CTR (a) and NTR (b). M1 and M2 were field capacity (high moisture) and 80% of the field capacity (low moisture). Intact and crushed fractions were <4 mm and <0.25 mm, respectively. Different letters represent significance at 0.05 probability level. Dotted line indicates the initial level of amorphous Fe.

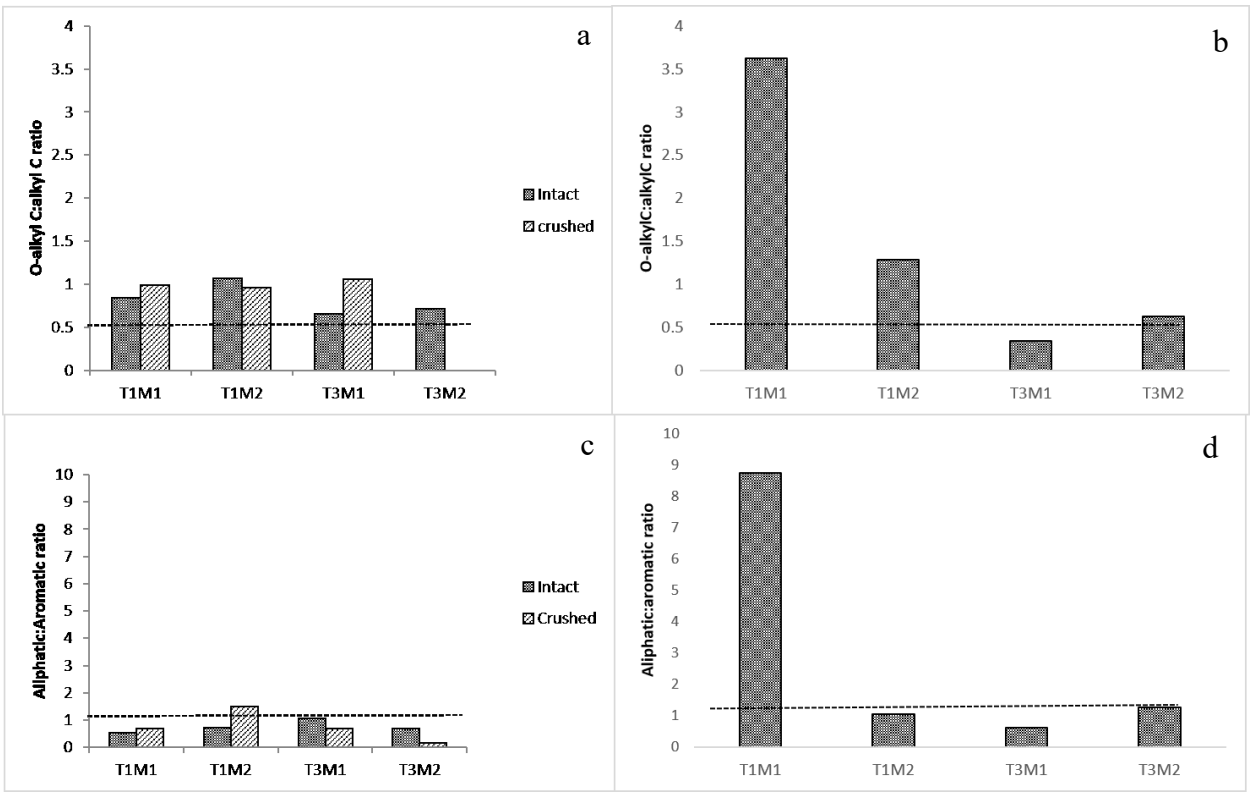

Figure 6-17 Ratio between O-alkyl C and alkyl C in CTM (a) and NTM (b). Ratio between aliphatic:aromatic C in CTM (c) and NTM (d). Obtained from integrating ^{13}C-NMR spectra. T1, T2, and T3 were 12ºC, 24ºC, and 36ºC, respectively. M1 and M2 were field capacity (high moisture) and 80% of the field capacity (low moisture). Intact and crushed fractions were <4 mm and <0.25 mm, respectively. Dotted line indicates the ratio of original soils.

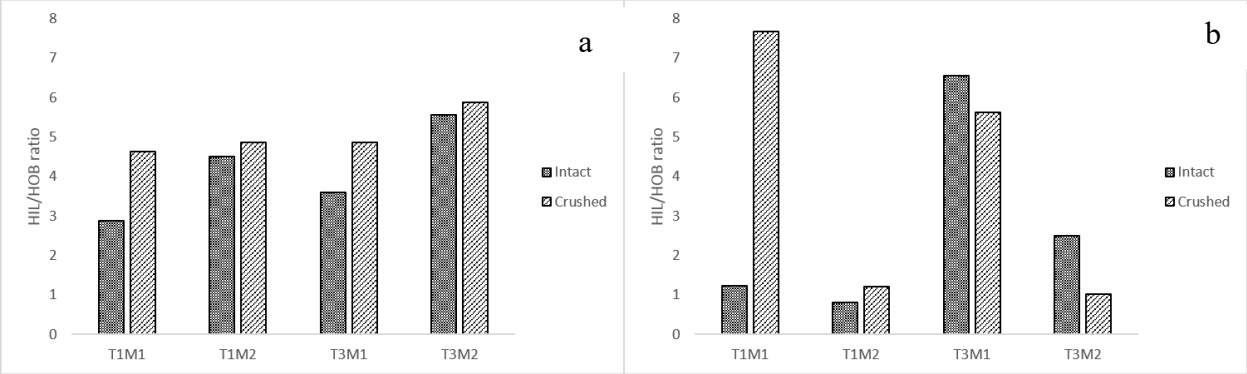

Figure 6-18 Ratio between hydrophilic to hydrophobic ratios (obtained from HPLC) of CTM (a) and NTM (b). T1, T2, and T3 were 12ºC, 24ºC, and 36ºC, respectively. M1 and M2 were field capacity (high moisture) and 80% of the field capacity (low moisture). Intact and crushed fractions were <4 mm and <0.25 mm, respectively. Dotted line indicates the hydrophilic to hydrophobic ratio of original soils.

Tables

Table 6-1 Basic soil properties of the native soil prior to the incubation

	pH	¶TOC (%)	#POXC (mg kg^{-1})	Amorphous Fe (mg kg^{-1})	ǂHOB/HIL ratio	¥AL:AR ratio	$O-alkyl:alkyl ratio
CTM	7.58	3.05	1142	1434	6.0	1.22	0.52
NTM	7.46	4.93	1843	1697	4.8	1.19	0.62
CTR	5.58	1.92	604	1859	5.9	1.2	0.62
NTR	6.44	3.1	1261	1809	4.3	1.23	0.75

¶Total organic carbon

#Permanganate oxidizable carbon

ǂ Hydrophobic to hydrophilic ratio obtained from high performance liquid chromatography (HPLC)

¥Ratio of aliphatic carbon to aromatic carbon obtained by integrating ^{13}C-nuclear magnetic resonance spectra (^{13}C-NMR)

$ratio of O-alkyl carbon to alkyl carbon obtained by integrating ^{13}C-nuclear magnetic resonance spectra (^{13}C-NMR)

Table 6-2 ANOVA table for the carbon dioxide-carbon (CO_2-C) efflux

	Interactions
CTM	DatexMxAgxT***
NTM	DatexMxAgxT***
CTR	DatexAgxT***, AgxTxM*, DatexTxM**
NTR	DatexMxAgxT*

Significant interactions and main effects: 0.05-*, 0.01-** and <0.001-***

Level of disturbance: Ag; Temperature: T; Moisture: M; Sampling time: ST

Table 6-3 ANOVA table for the temperature sensitivity (Q_{10}) at lower (12 ºC-24 ºC) and higher temperature (24 ºC-36 ºC) ranges

	High-temperature range	Low-temperature range
CTM	DatexAgxM**	Date*
NTM	DatexAgxM***	Date***
CTR	DatexAgxM***	DatexAgxM**
NTR	DatexM***	DatexAg*
	DatexAg***	
	M***	

Significant interactions and main effects: 0.05-*, 0.01-** and <0.001-***

Level of disturbance: Ag; Moisture: M

Table 6-4 ANOVA table for the cumulative efflux of carbon dioxide (CO_2-C)

	Significant effects
CTM	T***, Ag*
NTM	TxAg***
CTR	AgxTxM*
NTR	TxM***

Significant interactions and main effects: 0.05-*, 0.01-** and <0.001-***

Level of disturbance: Ag; Temperature: T; Moisture: M; Sampling time: ST

Table 6-5 ANOVA table for chemical analysis

	CTM	NTM	CTR	NTR
Amorphous iron	T*	TxAg*	T**	MxAg*
		M*	MxAg *	
pH	T***	TxAg**	T***	M*
	Ag***		MxAg*	TxAg*
[#]POXC	STxAg***	TxSTxAg***	Ag*	Ag
	MxAg**	MxAg***	TempxST*	TxM*ST
	Temp***	TxM**		
[¶]TOC	-	MxST*	TxMxSTxAg**	TxMxAg*
		MxAg*		STxAg***

Significant interactions and main effects: 0.05-*, 0.01-** and <0.001-***

Level of disturbance: Ag; Temperature: T; Moisture: M; Sampling time: ST

[¶]Total organic carbon

[#]Permanganate oxidizable carbon

Chapter 7 - Summary and Recommendations

This study was designed to explore in depth information of soil carbon (C) sequestration in two long-term contrasting agroecosystems, representing temperate (Mollisol) and tropical (Oxisol) climates. New generation cutting-edge stereomicroscopy techniques, new to study soil C were employed for these studies. The complexity and heterogeneity of soil organic C (SOC) led to challenges in data acquisition, analysis and interpretation. To overcome the associated challenges and to gain a better picture, these studied were assisted with both new generation and traditional laboratory-based techniques.

The spectromicroscopy studies performed on intact soil microaggregates from both Oxisols and Mollisols (Chapter 03 and 04) showed submicron level information on soil C preservation. Results indicated biotic and abiotic involvement on C dynamics. Preservation of organic C structures with original morphology indicated that the preservation is not purely related to substrate chemistry. Spetromicroscopy investigations also revealed organo-mineral associations. Bulk analyses of microaggregates from Mollisol highlighted the importance of manure/compost addition on enhancing organic C, reactive minerals, and the preservation of macromolecular C in humic acid. Moreover, amorphous Fe and organic C in microaggregates from Mollisol showed a strong correlation. We propose, direct preservation of C sources inside pore spaces as one of the primary mechanisms of C sequestration in these soils. Soil C appeared to be protected due to both inaccessibility to microbiota and the formation of organo-mineral associations. The findings of these studies supported the concepts brought forward by Schimidt et al. (2011) and Lehmann and Kleber (2015) by providing direct evidence.

The study on temperate agroecosystem (Chapter 05) indicated that manure/compost addition enhanced reactive minerals, organic C, and labile C preservation. No-till enhanced the soil C preservation in macroaggregates. Carbon preserved in smaller microaggregates was not affected by tillage. The significant correlation that was observed between reactive minerals and C, indicated the chemical stabilization through organo-mineral associations. Large microaggregates preseved higher labile C than other aggregates and this was attributed to strong physical protection and organo-mineral associations. This study further supported the current understanding of C preservation brought forward by Schimidt et al. (2011), which suggested soil C preservation as an ecosystem property.

In the six-month long incubation study (Chapter 06), the resilience of SOC was significantly affected by temperature directly and indirectly across the soils from both temperate and tropical ecosystems. High temperature influenced the efflux of carbon dioxide (CO_2-C) as well as soil acidity and amorphous iron, ultimately affecting organo-mineral associations. Cumulative CO_2-C efflux, pH, and temperature sensitivity (Q_{10}) at the low-temperature range were resilient to moisture effect in Mollisol. Manure/compost addition in Mollisol could have enhanced the moisture holding capacity, resulting in the lack of sensitivity to moisture levels used in this study. In Oxisol, the moisture effect was significant except for labile C and Q_{10} at the low-temperature range.Tilled Mollisol showed greater resilience than no-till soils to the conditions used in the incubation. Macromolecular properties of humic acid showed changes after six months of incubation. In general, soil biological (Menefee, 2016) and chemical results were in agreement with each other. The integrated approach of this research showed how the resileince of SOC was influenced by different environmental and anthropogenic influences.

Understanding the relative importance of chemical and mineralogical contribution on C preservation is needed to develop process-based soil C models. Therefore, findings from this research could be useful in building mechanistic models on soil C preservation with a better certainty. Direct evidence from the spectromicroscopy study supported new theory on soil C preservation. Moreover, this research showed the significance of employing the best management practices on soil C sequestration and preservation. It was clear that the no-till promotes soil C preservation and aggregation. Additions of organic fertilizers directly and indirectly were involved in sequestering and preserving soil C. Organo-mineral associations and aggregation were prominent in organic fertilizer added systems.

We recommend long-term incubation studies, mimicking real environment scenarios, fluctuating temperatures and moisture regimes to address seasonal variations to determine the explicit observations on C dynamics, changes of soil chemical properties, organo-mineral associations, microbial responses, and microbial community structure changes. Moreover, we also recommend expanding research focus towards understanding C sequestration in deep soils.

References

Schmidt, M.W., M.S. Torn, S. Abiven, T. Dittmar, G. Guggenberger, I.A. Janssens, M. Kleber, I. Kögel-Knabner, J. Lehmann and D.A. Manning. 2011. Persistence of soil organic matter as an ecosystem property. Nature 478:49-56.

Lehmann, J. and M. Kleber. 2015. The contentious nature of soil organic matter. Nature 528:60-68.

Menefee, D. 2016. Anthropogenic Influences on Soil Microbial Properties. MS diss. Kansas State University, Manhattan.

Appendix A - Supporting Information: Chapter 03

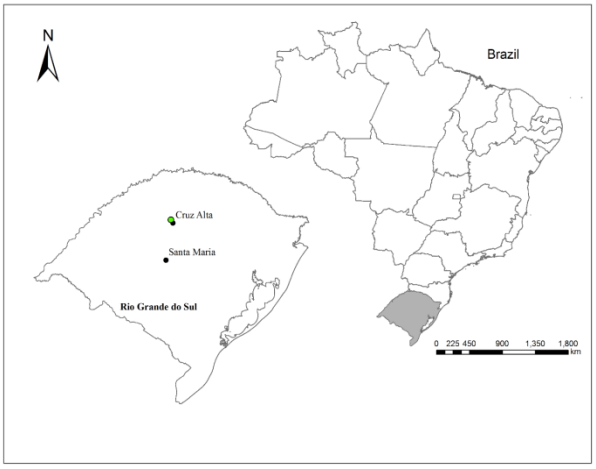

Figure A- 1 Map of the site in Cruz Alta, Brazil

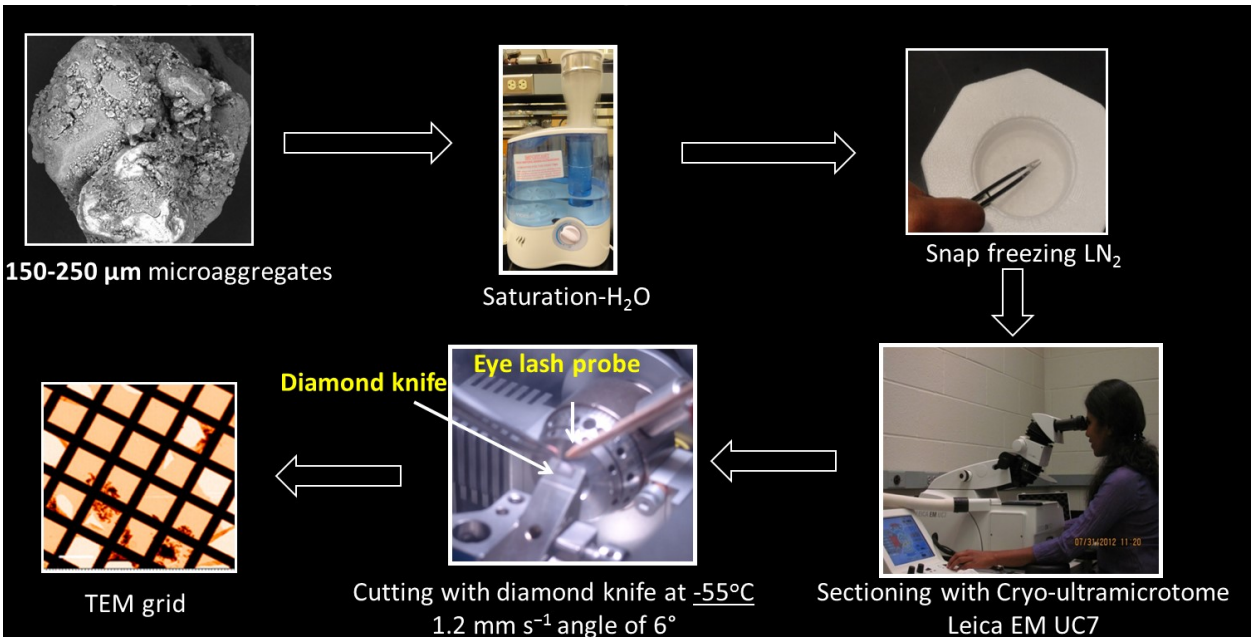

Figure A- 2 Preparation of intact microaggregate thin sections

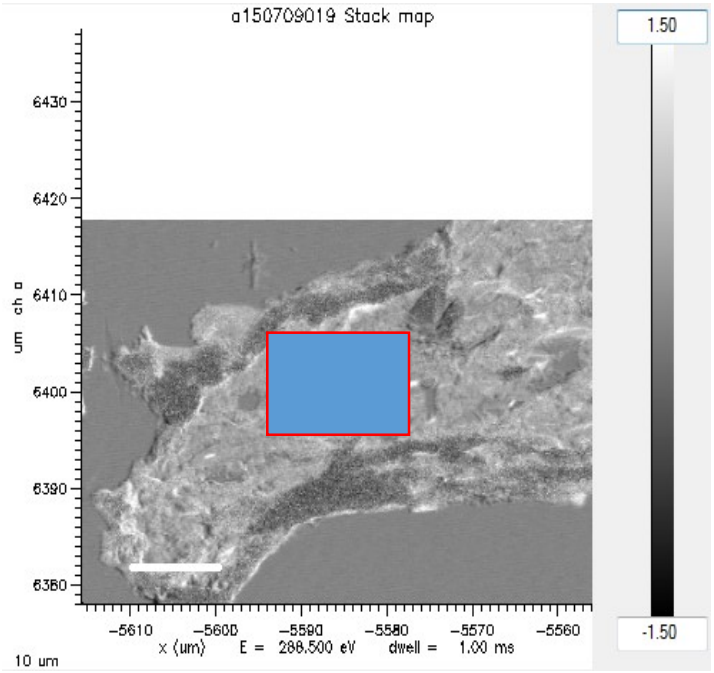

Figure A- 3 Area of the selected thin section representing NTR2 (No till complex crop rotation). Scanned at 288.8 eV to generate a contrast map. Selected area (15µmx20µm) for the data collection is denoted with a red color box.

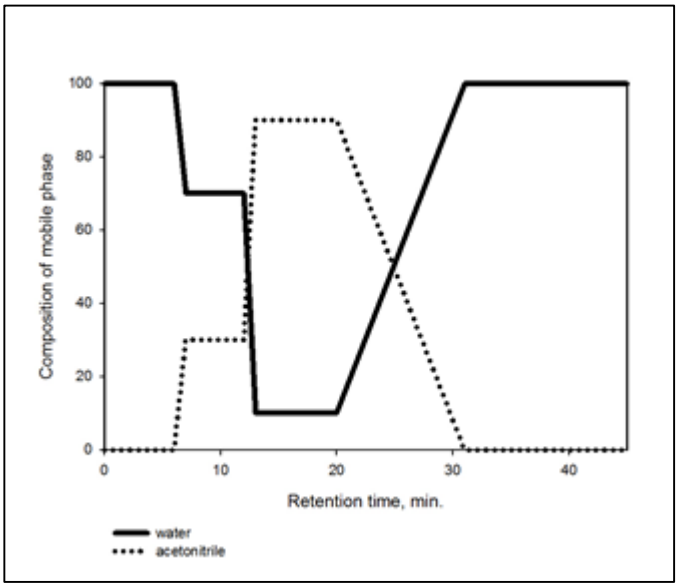

Figure A- 4 Gradient program for the humic acid fractionation (high performance liquid chromatography)

Appendix B - Supporting Information: Chapter 04

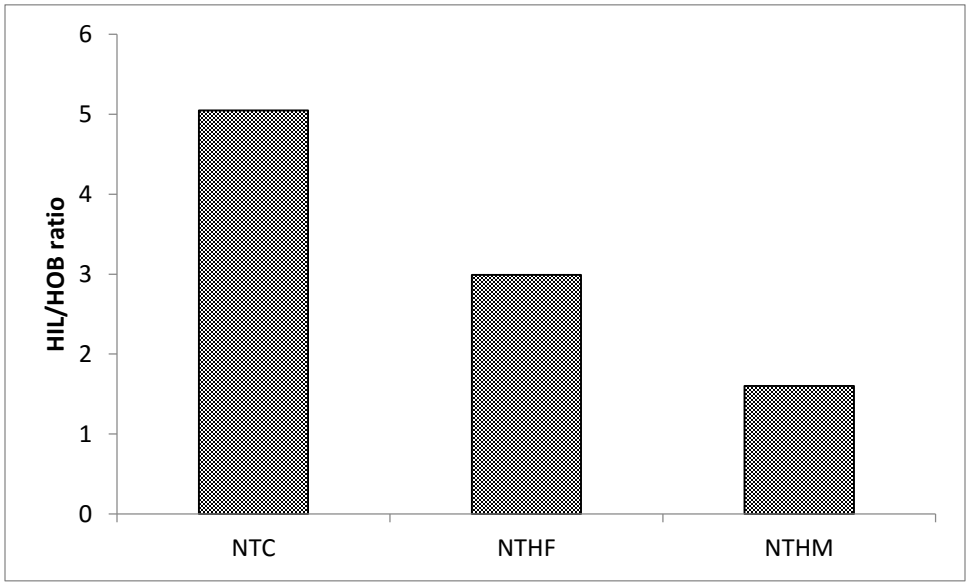

Figure B-1 Ratio of hydrophilic C to hydrophobic C (HPLC) representing different treatments

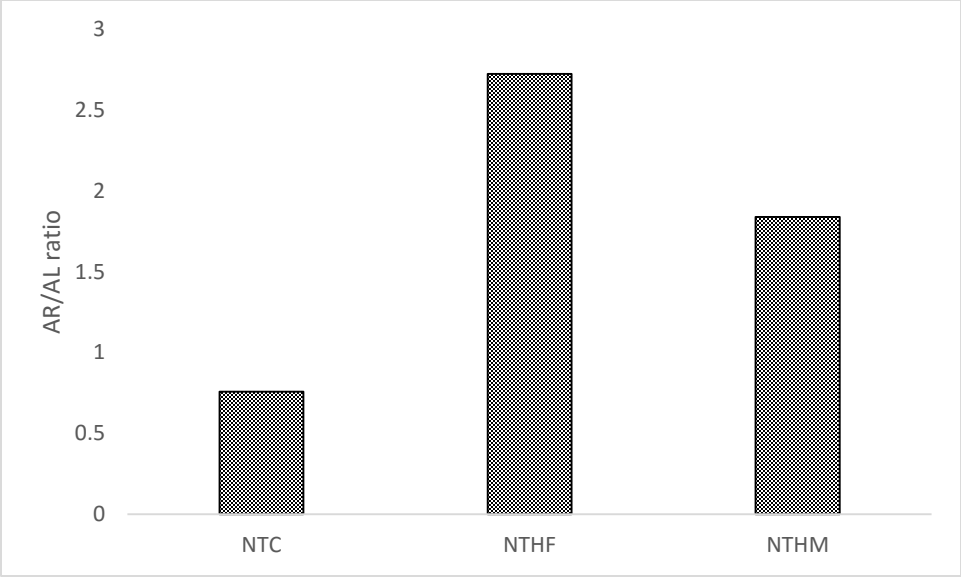

Figure B-2 Ratio of aliphatic to aromatic C representing different treatments (^{13}C NMR)